3. USED FUEL CHARACTERISTICS

3.1 Used Fuel Description

3.1.1 Used Fuel Type and Amount

The used fuel waste form is a post-discharge natural uranium UO_2 CANDU fuel bundle.

The hypothetical repository is assumed to contain 4.6×10^6 bundles, which is the total reference used fuel inventory projected over the expected lifetime of the current fleet of Canadian CANDU power reactors (Garamszeghy 2012)[1].

There are a few variant CANDU fuel bundle designs, in particular the 28-element bundle, the 37-element standard bundle, the 37-element long length bundle, and the 37m bundle[2]. Some older bundles do not have CANLUB, which is a thin graphite coating between the fuel pellet and the fuel sheath. Sensitivity studies by Tait et al. (2000) indicate that the radionuclide inventory per unit mass of fuel is not sensitive to these different designs, and so the standard 37-element (Bruce) fuel bundle is selected as the reference as it will be the most common bundle.

The age of the fuel when placed in the repository will vary. Because the earliest bundles date back to 1970 and because the repository is unlikely to open before 2035, some fuel will be over 60 years old. The older the fuel, the lower the residual thermal power and the lower the radiation fields. For this pre-project review, all fuel bundles are assumed to have an out-of-reactor decay time of 30 years.

Table 3-1 summarizes the characteristics of the reference used fuel. These are further discussed below.

---

[1] Includes refurbishment of Bruce A, Darlington, Point Lepreau and Gentilly-2. No further refurbishment of Pickering or Bruce B. No new build reactors. Because Gentilly-2 has decided to not proceed with refurbishment, the projected used fuel inventory is reduced to about 4.4×10^6 bundles.

[2] A modified 37-element bundle (37m) will be entering service in some stations; however, the changes are minor and do not significantly affect inventory.

Table 3-1: Used Fuel Parameters

Parameter	Value	Comment
Waste Form	37-element UO_2 fuel bundle	Standard fuel bundle from Bruce and Darlington stations
Mass U/bundle	19.25 kg	Initial mass (before irradiation)
Mass Zircaloy/ bundle	2.2 kg	Includes cladding, spacers, end plates
Initial U-235	0.72 wt%	Natural uranium is used in OPG CANDU fuel
Burnup	220 MWh/kgU	Highest OPG station-average burnup in Tait et al. (2000). More recent data indicate this exceeds the median value recorded for each station for each decade of operation (Wilk 2013)
Power Rating	455 kW/bundle	Nominal mid-range value
Fuel Age (when placed in repository)	30 years	e.g., 10 years in pools, 20 years in dry storage
Fuel Pellet Geometric Surface Area	8.47 cm^2	Surface area of undamaged pellet (37 element design)

Note: From Tait et al. (2000).

3.1.2 Geometry

Fuel pellets formed from natural uranium UO_2 are placed inside a fuel sheath made of a zirconium-tin alloy (Zircaloy-4) with a thin CANLUB graphite coating on the inside. The ends of the sheath are closed by a welded zirconium alloy plug to produce a sealed fuel element. Fuel elements are welded to zirconium alloy end plates to form a fuel bundle as shown in Figure 3-1.

The number of pellets in a fuel element, and the number and dimensions of the fuel elements in a fuel bundle depend on the particular CANDU reactor. The most common bundle contains 37 fuel elements, each of which is 13.1 mm diameter and 486 mm long. This fuel bundle weighs 23.9 kg, of which 21.7 kg is UO_2 and 2.2 kg is Zircaloy (Tait et al. 2000).

Upon discharge, less than 0.1% of the bundles have minor damage or defects (such as pinhole failures in the fuel sheaths) (Tait et al. 2000). Analysis of the integrity of used fuel bundles indicates that they are unlikely to fail during storage (Freire-Canosa 2011). A small percentage may have increased susceptibility to integrity failure during subsequent transport to permanent storage. While the specific value may be relevant to the packaging plant design, the postclosure safety assessment is not sensitive to this value since no credit is taken for fuel integrity.

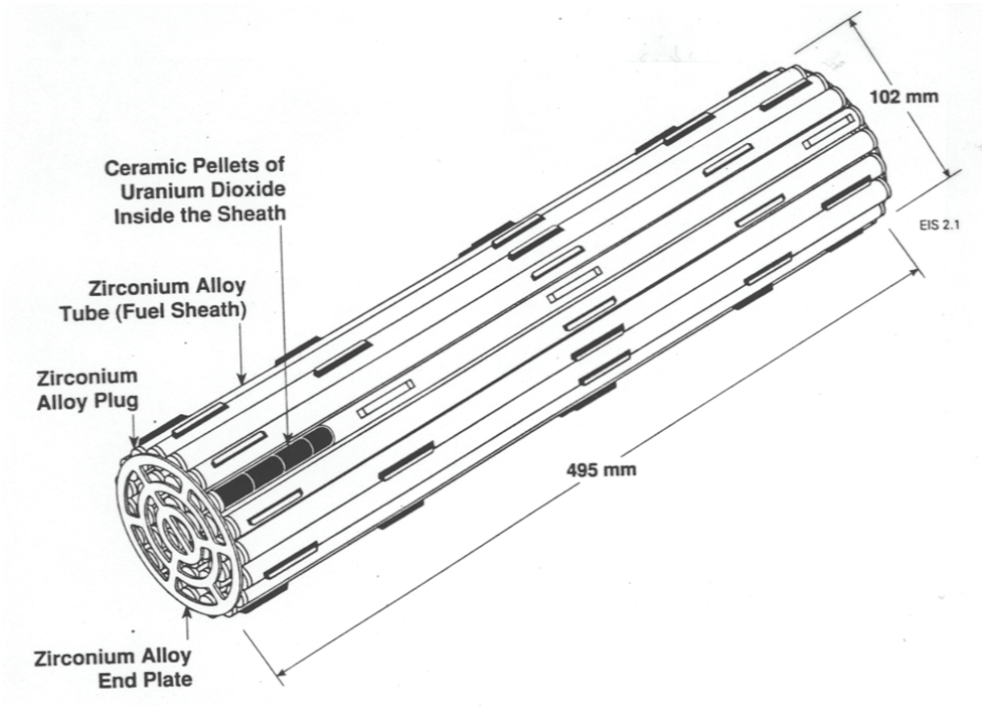

Figure 3-1: Typical CANDU Fuel Bundle

3.1.3 Burnup and Linear Power

The radioactivity level, heat generation rate, and bundle composition are all affected by the fuel burnup. This in turn depends on many factors including the type of reactor, the location of the bundle in the core, the bundle residence time, and bundle shifts that occur during fuelling operations. Although each bundle has a unique irradiation history, used fuel from all CANDU reactors is similar enough that it is not necessary to know individual detailed characteristics to assess the overall behaviour of the used fuel assemblies in the repository.

The aggregate 95th percentile burnup value for CANDU fuel is 254 MWh/kgU with some exceptional fuel elements experiencing burnups as high as 706 MWh/kgU (Wilk 2013). On a per station per decade basis, the 95th percentile values vary between 224 MWh/kgU and 286 MWh/kgU (Wilk 2013). A 220 MWh/kgU burnup exceeds the median value recorded for all stations for all decades and is well above the aggregate median value of about 190 MWh/kgU (Wilk 2013). At this level, about 2% of the initial uranium is converted into other elements.

The other major irradiation parameter that characterizes used fuel is linear power, which is the energy production rate per unit length. Tait et al. (2000) considered a power range of 200 to 900 kW/bundle (10-50 kW/m) as typical for the power range within which most CANDU bundles operate during their reactor lifetimes. The power level primarily affects the operating temperatures, which typically range from around 400^{o}C on the outside of the fuel sheath to between 800^{o}C and 1700^{o}C in the fuel centreline, well below the melting temperature of 2800^{o}C.

Tait et al. (2000) have calculated that the differences in radionuclide inventories between typical minimum and maximum power levels (200 and 900 kW/bundle) are generally less than about 2% for the same burnup. Tait et al. (2000) therefore used a mid-range value of 455 kW/bundle for reference inventory calculations.

In summary, a burnup level of 220 MWh/kgU and a power level of 455 kW/bundle are used to calculate radionuclide inventories.

3.1.4 Effect of Irradiation

The fuel undergoes a number of microstructural changes during irradiation, as illustrated by the sequence of photographs in Figure 3-2. Unirradiated fuel has a cohesive, interlocking microstructure and many grains have some internal sintering porosity from the fuel fabrication process. During irradiation, the sintering porosity is largely eliminated, boundaries between individual grains become more distinct, and some volatile elements diffuse out of the fuel grains to form fission gas bubbles at the interfaces between grains. At linear power ratings higher than approximately 50 kW/m (i.e., higher than achieved in most CANDU bundles), the fission gas bubbles enlarge and begin to coalesce, leading in some cases to the formation of gas tunnels along grain boundaries.

Unirradiated fuel pellets are very fine-grained, but at linear power ratings higher than approximately 50 kW/m equiaxial grain growth occurs in the pellet interior where temperatures are highest (Figure 3-3). Grain growth is typically accompanied by the diffusion and segregation of non-volatile fission products, some of which form small metallic particles at grain boundaries as shown in Figure 3-4.

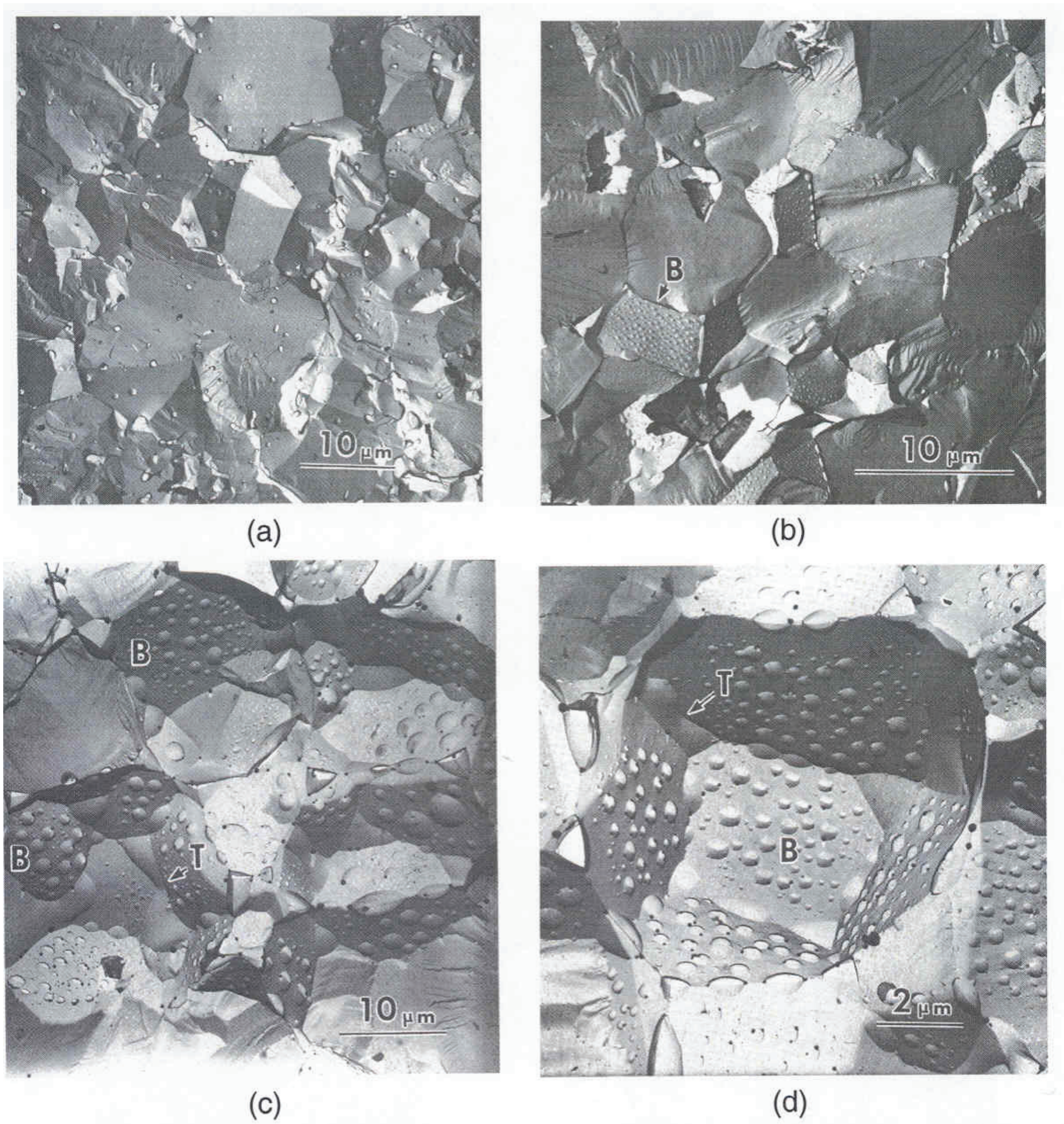

Notes:
a) Typical microstructure of unirradiated UO_2. Small inclusions = sintering porosity.
b) Irradiated at low power (< 45 kW/m). Note loss of sintering porosity and development of small intergranular fission gas bubbles (B).
c) Irradiated at higher power (≥ 50 kW/m), showing growth of fission gas bubbles (B) and initiation of tunnels (T).
d) Magnified view of irradiated higher power fuel. Note the grain-edge tunnels (T) and the development of fission gas bubbles (B) on all faces of the "pull-out" of a single grain.

Ref.: Hastings (1982).

Figure 3-2: Typical Microstructure of Unirradiated and Irradiated UO_2 Fuel

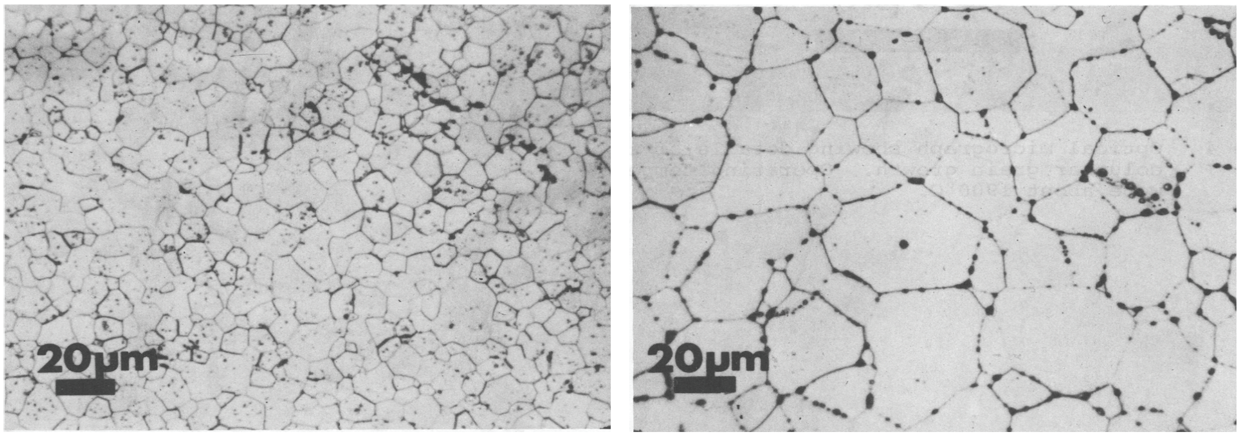

(a) (b)

Notes: a) Unirradiated UO_2. Note sintering porosity in grain interiors.
b) Irradiated UO_2 at low burnup and high power (20 MWh/kgU at 50 kW/m). Note increase in grain size, loss of sintering porosity, and formation of fission gas bubbles and tunnels along boundaries.
Ref.: Hastings (1982).

Figure 3-3: Grain Growth in Irradiated UO_2 Fuel

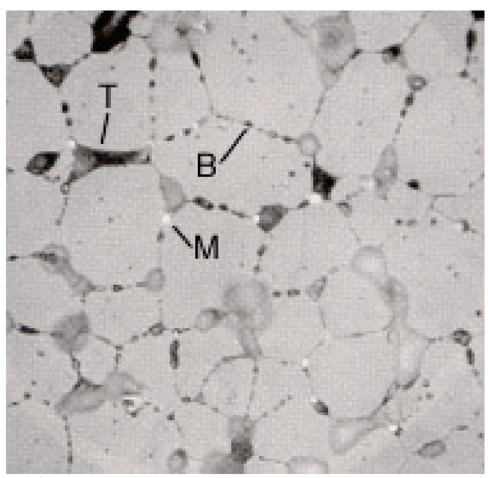

Ref: Novak and Hastings (1991)

Notes: Optical micrograph of polished and etched UO_2 fuel irradiated to very high burnup (770 MWh/kgU at 52 kW/m), showing small white particles at grain boundaries (M) that are formed from incompatible metals such as Mo, Ru, and Pd that have diffused out of the UO_2 grains. Well-developed fission gas bubbles (B) and tunnels (T) are also present at grain boundaries. Scale is approximately same as shown for Figure 3-3.

Figure 3-4: Segregation of Metallic Fission Products from UO_2 Fuel

Compared to fresh bundles, used bundles contain new elements (approximately 2% by mass), including fission products, activation products and actinides other than uranium. Of these, more than ~95% remain within the UO_2 lattice very close to the location of their formation (Gobien et al. 2013, and references therein).

As indicated in Figure 3-5, the species produced can be grouped according to their chemical behaviour into the following categories (Kleykamp 1985):

1. Species such as He, Kr, Ar, Cs and I that are gaseous or somewhat volatile at fuel operating temperatures (i.e., 400-1700^{o}C). Due to their relatively high diffusion coefficients, during reactor operation a small fraction of each species migrates out of the fuel grains and into fuel element void spaces (i.e., into the fuel sheath gap and into cracks in the fuel pellets). At the same time, another small fraction moves to the grain boundaries within the fuel pellets and forms fission gas bubbles. The remainder (roughly 95%) of the fission gases are held in the UO_2 crystal lattice.

2. Species such as the metals Mo, Ru, and Pd that are non-volatile but have a low solubility in UO_2. At high in-reactor temperatures, small quantities of these species can diffuse from the fuel grains and segregate as metallic alloy phases at grain boundaries, particularly in areas of UO_2 grain growth. The majority of incompatible species remain trapped within the fuel grains due to their low diffusion coefficients in UO_2 at fuel operating temperatures.

3. Species that are compatible with UO_2, including the lanthanide elements and actinides such as Pu, Am, Np. These elements can substitute chemically for uranium in UO_2, and the atoms are then structurally bound as trace elements in the UO_2 crystal lattice.

The Zircaloy-4 fuel sheath consists of more than 98 wt% Zr and approximately 1.5 wt% Sn, with a number of other elements present as impurities (Tait et al. 2000). During irradiation, the cladding receives a neutron fluence of around 10^{25} n/m^2 (Truant 1983). The irradiated metal cladding is a fine-grained material (grain size typically 10 μm, thickness typically 0.4 mm) with neutron activation products, such as C-14, Ni-59 and Ni-63, present at concentrations less than 1 mg/kg Zr. Due to the low temperature of the cladding during irradiation (< 400^{o}C), activation products in the Zircaloy cannot diffuse any significant distance from the site of their formation, and they are therefore likely to be distributed uniformly throughout the metal. While in-reactor, coolant pressure causes the fuel cladding to collapse onto the fuel pellets, the heat generated in the fuel causes the pellets to expand slightly into an hourglass shape, which leads to the formation of minor cylindrical ridges in the cladding. This effect is more pronounced at high linear power and when fuel is in the reactor for long times.

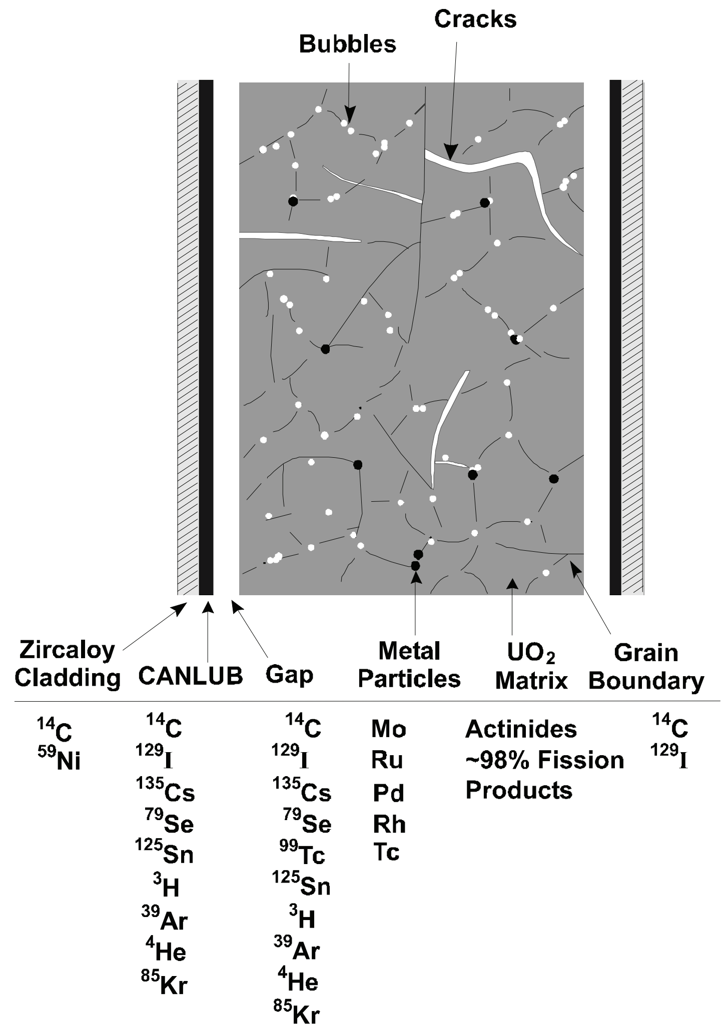

Figure 3-5: Illustrative Distribution of Some Fission Products and Actinides within a Used-Fuel Element

3.2 Radionuclide and Chemical Element Inventory

At the time of discharge the used fuel contains hundreds of different radionuclides; however, following placement in a deep geological repository only a small fraction poses a potential radiological risk to humans or the environment. The subset of radionuclides of potential concern for safety assessment is identified via a screening analysis.

The screening analysis for the groundwater-transport scenarios, described in Chapter 7, analysis identifies 31 radionuclides from the UO_2 fuel as potentially important. The gas-transport scenario, described in Chapter 8, considers C-14, Cl-36 Se-79, and I-129 as potentially important, with C-14 releases from both the UO_2 fuel and the Zircaloy included. Parents and progeny of the screened in radionuclides are also included to ensure ingrowth is properly accounted for. In all, a total of 38 radionuclides are represented.

Table 3-2 shows the included radionuclides and their associated decay chains.

Table 3-2: Radionuclides Included in the Radiological Assessment

Fuel	
Single Nuclides	C-14, I-129, Cl-36, Cs-135, Pd-107, Se-79, Sm-147, Tc-99
Chains	
Neptunium Series	Am-241 → Np-237 → Pa-233 → U-233 → Th-229 → Ra-225 → Ac-225
Uranium Series	Pu-242 → U-238 → Th-234 → U-234 → Th-230 → Ra-226 → Rn-222 → Pb-210 → Bi-210 → Po-210
Actinium Series	Pu-239 → U-235 → Th-231 → Pa-231 → Ac-227 → Th-227 → Ra-223
Thorium Series	Pu-240 → U-236 → Th-232 → Ra-228 → Th-228 → Ra-224

At the time of discharge the used fuel also contains essentially the entire periodic table of elements from hydrogen to californium; however, only a small fraction of these could pose a non-radiological hazard to humans or to the environment. As is the case for radionuclides, the subset of chemical elements of potential concern is identified via a screening analysis.

This screening analysis is also described in Chapter 7. The analysis identifies 26 elements of potential concern arising from the fuel, where multiple isotopes of an element (i.e., U, Pb, and Ba) are considered as one element. To ensure that ingrowth is properly accounted for in the system model, an additional 33 radionuclides are also included. The analysis also shows seven elements of potential concern arising from the Zircaloy sheath, to which an additional three parent radionuclides have been added due to include ingrowth.

Table 3-3 shows the included chemical elements and their associated decay chains.

Table 3-3: List of Potentially Significant Chemically Hazardous Elements and Associated Radionuclide Decay Chains Included in the Hazardous Substance Assessment

Fuel	
Elements	Al, Cd, Ce, Co, Cr, Cu*, Hg, La, Mo, Nd, Ni, P, Pr, Sb, Se, Sm, V, Y
Chains	
Neptunium Series	Am-241 → Np-237 → Pa-233 → U-233 → Th-229 → Ra-225 → Ac-225 → Bi
Uranium Series	Pu-242 → U-238 → Th-234 → U-234 → Th-230 → Ra-226 → Rn-222 → Pb-210 → Bi-210 → Po-210 → Pb
Actinium Series	Pu-239 → U-235 → Th-231 → Pa-231 → Ac-227 → Th-227 → Ra-223 → Pb
Thorium Series	Pu-240 → U-236 → Th-232 → Ra-228 → Th-228 → Ra-224 → Pb
Misc	Sn-126 → Sb-126 → Te Sr-90 → Y-90 → Zr Cs-135 → Ba Cs-137 → Ba Pd-107 → Ag Sm-151 → Eu
Zircaloy	
Elements	Be, Cr, Cd, Sb, V
Chains	Pd-107 → Ag Sr-90 → Y-90 →Zr

Note: * Cu arising from the fuel is screened out in Chapter 7. It is included here because of the copper containers.

Note that it is the total concentration of a potentially chemically hazardous element that is important for the hazardous substance assessment. For example, the total uranium concentration in a particular biosphere medium is the sum of the concentrations of all the uranium isotopes.

Table 3-4 and Table 3-5 list all the radionuclides included in either Table 3-2 or Table 3-3 together with their half lives, their inventories at the assumed time of placement in the repository, and various uncertainties associated with the inventories. The inventories are taken from Tait and Hanna (2001); however, corrections were made to account for the difference in the bundle average and "ring sum[3]" inventories if differences exceeded +1%, as described in Gobien et al. (2013).

It should be emphasized that what is important for the safety assessment is the uncertainty in the total radionuclide inventory in a container with 360 fuel bundles which (based on the central limit theorem) would be much smaller than the uncertainly in the inventory of a single fuel bundle. Thus, it is the uncertainties in total inventory in the container that are shown in Table 3-4.

---

[3] "Ring sum" refers to a separate radionuclide inventory calculation performed with different burnup assumptions in the individual fuel bundle 'rings'

Uncertainty arises due to the accuracy of the ORIGEN-S calculations when compared against measurements (σ_{OR}), and due to the use of an average power rating (σ_{PR}) in the calculation of initial radionuclide inventories. The latter uncertainty is small for the radionuclides of interest except for Cs-135 (Gobien et al. 2013).

There is no need to account for the uncertainty arising from calculating the inventories at a burnup of 220 MWh/kgU because this burnup is greater than the average burnup from any of the generating stations (Wilk 2013). Thus, since inventories generally increase with burnup (Tait et al. 2000), the calculated inventories are conservative.

Validation studies (Tait et al. 1995) indicate that ORIGEN-S predictions generally agree with measured actinide and fission product inventories, with the residual uncertainty in many cases related more to the accuracy of the measurements. A comparison of measured and predicted values for a Pickering fuel bundle is shown in Table 3-6. Pickering is used because more comprehensive data are available.

More recent comparisons by SKB (2010) for PWR fuel, indicates that the ratio of measured to ORIGEN calculated inventories is 1.01 for U and Pu isotopes, 1.01 for fission products and 1.11 for actinides other than U and Pu. Again, the agreement is good and within the uncertainty of the measured data.

Further information on the derivation of the uncertainties is available in Gobien et al. (2013).

Table 3-7 and Table 3-8 list the chemical elements included in Table 3-3 together with their inventories, at the assumed time of placement in the repository, and with the various uncertainties associated with the inventories. The inventory of an element shown in Table 3-7 excludes the concentration of all short-lived isotopes of the element as well as the concentrations of the long-lived isotopes of the element shown in Table 3-4.

The inventories are from Tait and Hanna (2001). However, corrections to the inventories were made to account for the difference in the bundle average and “ring sum” inventories if differences exceeded +1%, as described in Gobien et al. (2013). Also, for Eu, the inventory includes the inventory of a short-lived precursor (Sm-151).

Table 3-4: Inventories of Radionuclides of Interest in UO_2 Fuel for 220 MWh/kgU Burnup and 30 Years Decay Time

Nuclide	Half-life* [a]	Inventory [moles/kgU initial]	σ_{OR} [%]	σ_{PR} [%]	σ_{Total} [%]
Ac-225	2.738E-02	1.662E-14	-	-	NA1
Ac-227	2.177E+01	1.573E-11	2.5	-	2.5
Am-241	4.326E+02	1.155E-03[&]	15	-	15
Bi-210	1.372E-02	5.296E-18	-	-	NA1
C-14	5.700E+03	5.60E-06	-	-	NA2
Cl-36	3.010E+05	5.42E-06	-	-	NA2
Cs-135	2.300E+06	2.675E-04	7	3	7.6
Cs-137	3.008E+01	1.287E-03	5	-	5.0
I-129	1.570E+07	4.228E-04	7	-	7.0
Np-237	2.144E+06	1.708E-04	20	-	20
Pa-231	3.276E+04	3.820E-08	2.5	-	2.5
Pa-233	7.385E-02	5.901E-12	-	-	NA1
Pb-210	2.220E+01	8.604E-15	55	-	55
Pd-107	6.500E+06	6.901E-04	7	-	7
Po-210	3.789E-01	1.463E-16	-	-	NA1
Pu-239	2.411E+04	1.123E-02	3	-	3
Pu-240	6.561E+03	5.339E-03	4	-	4.0
Pu-242	3.735E+05	4.257E-04	7	-	7.0
Ra-223	3.129E-02	2.243E-14	-	-	NA1
Ra-224	1.002E-02	1.099E-12	-	-	NA1
Ra-225	4.079E-02	2.460E-14	-	-	NA1
Ra-226	1.600E+03	2.354E-12	55	-	55
Ra-228	5.750E+00	8.370E-13	-	-	NA1
Rn-222	1.047E-02	1.541E-17	-	-	NA1
Sb-126	3.381E-02	2.462E-12	-	-	NA1
Se-79	2.950E+05	1.762E-05	7	-	7.0
Sm-147	1.060E+11	6.551E-04	7	-	7.0
Sm-151	9.000E+01	1.455E-05	7	-	7.0
Sn-126	2.300E+05	5.182E-05	7	-	7.0
Sr-90	2.879E+01	7.561E-04	4	-	4.0
Tc-99	2.111E+05	2.409E-03	10	-	10
Th-227	5.114E-02	3.620E-14	-	-	NA1
Th-228	1.912E+00	2.097E-10	-	-	NA1
Th-229	7.340E+03	4.783E-09	20	-	20

Nuclide	Half-life* [a]	Inventory [moles/kgU initial]	σ_{OR} [%]	σ_{PR} [%]	σ_{Total} [%]
Th-230	7.538E+04	1.636E-08	55	-	55
Th-231	2.911E-03	2.944E-14	-	-	NA1
Th-232	1.405E+10	2.095E-03	4	-	4
Th-234	6.598E-02	6.091E-11	-	-	NA1
U-233	1.592E+05	3.608E-05	20	-	20
U-234	2.455E+05	2.089E-04[&]	50	-	50
U-235	7.038E+08	7.238E-03	2.5	-	2.5
U-236	2.342E+07	3.501E-03	4	-	4
U-238	4.468E+09	4.125E+00	0	-	0
Y-90	7.301E-03	1.965E-07	-	-	NA1

Notes:
NA1 = Nuclide assigned a constant inventory because it has a short half-life.
NA2 = Nuclide inventory is assigned a uniform distribution. For C-14, the inventory is between 2.45×10^{-6} and 8.75×10^{-6} moles/kgU and for Cl-36 the inventory is between 9.86×10^{-7} and 9.86×10^{-6} moles/kgU. Table shows the median value, which is not from Tait et al. (2000).
NA3 = Nuclide assigned a constant inventory because it is formed by activation of impurity in the fuel, and impurity levels were assigned high values in Tait et al. (2000).
*Half-life from ENDF/B VII.1 (Chadwick et al. 2011) and converted as required using 365.25 days = 1 year.
[&]Includes inventory of short-lived precursor: Am-241 (Pu-241, 2.737E-4 mol/kgU) and U-234 (Pu-238, 2.259E-5 mol/kgU). Since the uncertainty is expressed as a percentage, it is affected by addition of the precursor inventory.

Table 3-5: Inventories of Radionuclides of Interest in Zircaloy for 220 MWh/kgU Burnup and 30 Years Decay Time

Nuclide	Half-life* [a]	Inventory [moles/kgZr initial]	σ_{OR} [%]	σ_{PR} [%]	σ_{Total} [%]
C-14	5.700E+03	1.903E-05			NA2
Pd-107	6.500E+06	6.222E-08	7	-	7.0
Sr-90	2.879E+01	4.776E-11	4	-	4.0
Y-90	7.301E-03	1.241E-14	-	-	NA1

Notes:
NA1 = Nuclide assigned a constant inventory because it has a short half-life.
NA2 = Nuclide assigned a constant inventory because it is formed by activation of impurity in Zircaloy, and impurity levels were assigned high values in Tait et al. (2000).
*Half-life from ENDF/B VII.1 (Chadwick et al. 2011) and converted as required using 365.25 days = 1 year.

Table 3-6: ORIGEN-S: Pickering Fuel Inventory Comparison

Isotope	Measured[1] (Bq/kgU)	ORIGEN-S (Bq/kgU)	Ratio (meas/calc)
Cm-244	7.12E+08 ± 15%	7.44E+08	0.96 ± 0.14
Am-241	1.86E+10 ± 20%	1.92E+10	0.97 ± 0.19
Np-237	1.00E+05 ± 20%	8.51E+05	1.17 ± 0.23
H-3	2.07E+09 ± 7%	2.23E+09	0.92 ± 0.06
Sr-90	4.86E+11 ± 4%	5.03E+11	0.97 ± 0.04
Tc-99	1.08E+08 ± 10%	1.50E+08	0.72 ± 0.07
Ru-106	8.72E+07 ± 5%	2.52E+08	0.35 ± 0.02
Sb-125	2.20E+09 ± 18%	2.56E+09	0.86 ± 0.16
I-129	2.44E+05	3.62E+05	0.67
Cs-134	4.16E+09 ± 7%	4.03E+09	1.03 ± 0.07
Cs-137	8.05E+11 ± 5%	7.88E+11	1.02 ± 0.05
Eu-154	8.14E+09 ± 5%	9.07E+09	0.90 ± 0.04
Eu-155	3.35E+09 ± 8%	3.13E+09	1.07 ± 0.09
Isotope	**Measured (g/kgU)**	**ORIGEN-S (g/kgU)**	**Ratio (meas/calc)**
U-233	< 0.01	2.22E-07	--
U-234	0.0339 ± 55%	0.0423	0.8 ± 0.44
U-235	1.64 ± 2.4%	1.64	1.00 ± 0.02
U-236	0.802 ± 3.7%	0.813	0.99 ± 0.04
U-238	983.5 ± 0.01%	983.5	1.00 ± 0.0
Pu-238	0.0058 ± 5.6%	0.0053	1.10 ± 0.06
Pu-239	2.69 ± 2.5%	2.72	0.99 ± 0.03
Pu-240	1.22 ± 37%	1.25	0.98 ± 0.04
Pu-241	0.134 ± 9%	0.142	0.95 ± 0.09
Pu-242	0.094 ± 6.8%	0.0972	0.97 ± 0.07

Notes:

From Tait et al. (1995), Pickering fuel bundle with average burnup of 221 MWh/kgU and average outer-element linear power of 43 kW/m.

[1] Analytical uncertainty expressed as a percentage.

Table 3-7: Inventories of Chemical Elements of Interest in UO_2 Fuel for 220 MWh/kgU Burnup and 30 Years Decay Time

Element	Main Source[1]	Inventory* [moles/kgU initial]	σ_{OR} [%]	σ_{PR} [%]	σ_{Total}[2] [%]
Ag	FP	3.348E-4	7	-	7.0
Al	Imp	3.702E-3	-	-	NA1
Ba	FP	4.738E-3	7	-	7.0
Bi	Imp	9.595E-5	-	-	NA1
Cd	FP	1.928E-4	7	-	7.0
Ce	FP	4.766E-3	7	-	7.0
Co	Imp	3.099E-4	-	-	NA1
Cr	Imp	9.635E-4	-	-	NA1
Cu	Imp	3.121E-4	-	-	NA1
Eu	FP	1.895E-4	6.5	-	6.5
Hg	Imp	6.719E-6	-	-	NA1
La	FP	2.459E-3	7	-	7.0
Mo	FP	9.488E-3	7	-	7.0
Nd	FP	7.562E-3	7	-	7.0
Ni	Imp	1.044E-3	-	-	NA1
P	Imp	1.935E-3	-	-	NA1
Pr	FP	2.181E-3	7	-	7.0
Pb	Imp	4.824E-4	-	-	NA1
Pr	FP	2.181E-3	7	-	7.0
Sb	FP	2.977E-5	7	-	7.0
Se	Imp	4.185E-4	-	-	NA1
Sm	FP	1.063E-3	7	-	7.0
Te	FP	1.048E-3	7	-	7.0
V	Imp	3.892E-4	-	-	NA1
Y	FP	1.327E-3	7	-	7.0
Zr	FP	1.021E-2	7	-	7.0

Notes:

*The inventories shown here exclude the concentrations of all short-lived isotopes of the element and the concentrations of the long-lived radionuclides in Table 3-4.

[1] Source of chemical element in fuel is either fission product (FP) or impurity in fuel (Imp).

[2] NA1 = Nuclide assigned a constant inventory because it is formed by activation of impurity in the fuel, and impurity levels were assigned high values in Tait et al. (2000).

Table 3-8: Inventories of Chemical Elements of Interest in Zircaloy for 220 MWh/kgU Burnup and 30 Years Decay Time

Element	Main Source[1]	Inventory [moles/kgZr initial]	σ_{OR} [%]	σ_{PR} [%]	σ_{Total} [%]
Ag	Imp	7.644E-5	-	-	NA1[2]
Be	Imp	1.111E-2	-	-	NA1[2]
Cd	Act	2.327E-5	7	-	7.0
Cr	Imp	2.495E-2	-	-	NA1[2]
Sb	Imp	1.098E-4	-	-	NA1[2]
V	Imp	1.008E-3	-	-	NA1[2]
Zr	MM	1.064E+1	-	-	NA2[3]

Notes:

[1] Source of chemical element in Zircaloy is either an activation product (Act) or impurity in Zircaloy (Imp) or the matrix material (MM).

[2] NA1 = Nuclide assigned a constant inventory because it is formed by activation of impurity in the fuel, and impurity levels were assigned high values in Tait et al. (2000).

[2] NA2 = Zr assigned a constant inventory because the inventory of the matrix material is well known.

3.3 References for Chapter 3

Chadwick, M.B., M. Herman, P. Obložinský, M.E. Dunn, Y. Danon, A.C. Kahler, D.L. Smith, B. Pritychenko, G. Arbanas, R. Arcilla, R. Brewer, D.A. Brown, R. Capote, A.D. Carlson, Y.S. Cho, H. Derrien, K. Guber, G.M. Hale, S. Hoblit, S. Holloway, T.D. Johnson, T. Kawano, B.C. Kiedrowski, H. Kim, S. Kunieda, N.M. Larson, L. Leal, J.P. Lestone, R.C. Little, E.A. McCutchan, R.E. MacFarlane, M. MacInnes, C.M. Mattoon, R.D. McKnight, S.F. Mughabghab, G.P.A. Nobre, G. Palmiotti, A. Palumbo, M.T. Pigni, V.G. Pronyaev, R.O. Sayer, A.A. Sonzogni, N.C. Summers, P. Talou, I.J. Thompson, A. Trkov, R.L. Vogt, S.C. van der Marck, A. Wallner, M.C. White, D. Wiarda, P.G. Young. 2011. ENDF/B-VII.1 Nuclear data for science and technology: Cross section, covariances, fission product yields, and decay data. *Nuclear Data Sheets*: 112-12, 2887-2996 (2011).

Freire-Canosa, J. 2011. Used Fuel Integrity Program: Summary Report. Nuclear Waste Management Organization Report NWMO TR-2011-04. Toronto, Canada.

Garamszeghy, M. 2012. Nuclear Fuel Waste Projections in Canada - 2012 Update. Nuclear Waste Management Organization Report NWMO TR-2012-13. Toronto, Canada.

Gobien, M., F. Garisto, E. Kremer and C. Medri. 2013. Fifth Case Study: Reference Data and Codes. Nuclear Waste Management Organization Report NWMO TR-2013-05. Toronto, Canada.

Hastings, I.J. 1982. Structures in Irradiated UO_2 Fuel from Canadian Reactors. Atomic Energy of Canada Limited Report AECL-MISC-249. Chalk River, Canada.

Kleykamp, H. 1985. The chemical state of the fission products in oxide fuels. Journal of Nuclear Materials 131, 221-246.

Novak, J. and I.J. Hastings. 1991. Ontario Hydro Experience with Extended Burnup Power Reactor Fuel. Atomic Energy of Canada Limited Report AECL-10388. Chalk River, Canada.

SKB. 2010. Spent nuclear fuel for disposal in the KBS-3 repository. Swedish Nuclear Fuel and Waste Management Company Report SKB TR-10-13. Stockholm, Sweden.

Tait, J.C., I.C. Gauld and A.H. Kerr. 1995. Validation of the ORIGEN-S code for predicting radionuclide inventories in used CANDU fuel. Journal of Nuclear Materials 223, 109-121.

Tait, J.C. and S. Hanna. 2001. Characteristics and radionuclide inventories of used fuel from OPG nuclear generating stations, Volume 3 - Radionuclide inventory data. Ontario Power Generation Report 06819-REP-01200-10029-R00. Toronto, Canada.

Tait, J.C., H. Roman and C.A. Morrison. 2000. Characteristics and Radionuclide Inventories of Used Fuel from OPG Nuclear Generating Stations, Volumes 1 and 2. Ontario Power Generation Report 06819-REP-01200-10029. Toronto, Canada.

Truant, P.T. 1983. CANDU Fuel Performance: Power Reactor Experience. Atomic Energy of Canada Limited Report AECL-MISC-250, Rev. 1. Chalk River, Canada.

Wilk, L. 2013. CANDU Fuel Burnup and Power Rating – 2012 Update. Nuclear Waste Management Organization Report NWMO-TR-2013-02. Toronto, Canada.

THIS PAGE HAS BEEN LEFT BLANK INTENTIONALLY

4. REPOSITORY FACILITY – CONCEPTUAL DESIGN

4.1 General Description

The APM facility is a self-contained complex that includes an underground repository for used CANDU fuel and a number of surface facilities designed to support the construction and operation of the repository. The primary function of the surface facilities is to receive used fuel that is shipped from reactor-site storage facilities, place it in durable used fuel containers and transfer the containers to the underground repository. The reference used fuel container is designed with a corrosion-resistant copper barrier and an inner supporting steel vessel to provide long-term containment of the fuel in the repository (SNC Lavalin 2011).

Since a repository site has not been selected, the assumptions made for development of the site model reflect the properties of typical sedimentary rock found in Canada. Therefore, a generic repository design is described here for the purpose of preparing an illustrative postclosure safety assessment for a hypothetical APM facility in sedimentary rock. Two key safety concepts on which the repository design is based are the multiple barrier system for containment of the fuel, and passive safety. In this case, passive safety means that once the operational phase is complete and the repository is backfilled and sealed, no further actions will be required to ensure its safety.

For the purpose of this study, the repository is assumed to be constructed in sedimentary rock at a depth of 500 m. In the repository, the used fuel containers will be surrounded by an engineered barrier consisting of clay-based sealing materials that will provide protection against mechanical, chemical and biological agents that could cause container damage. The function of the repository engineered barriers also includes creating both a chemical and physical environment that would limit the mobility of contaminants. The used fuel container, the sealing systems surrounding the container and the rock mass in which the repository is constructed constitute a multiple barrier system that is capable of containing and isolating the used fuel indefinitely.

The underground repository consists of several panels of used fuel container placement rooms, which are connected to the surface via a network of access tunnels and three vertical shafts. The containers are placed horizontally, supported by a compacted bentonite pedestal, along the axis of the placement room.

An illustration of an APM facility in sedimentary rock is shown in Figure 4-1.

Monitoring systems for verification of safety performance are provided as part of the repository system design. Retrievability of the fuel containers is another design feature of the APM repository. These two capabilities of the repository design are discussed further by SNC Lavalin (2011) and Villagran (2012).

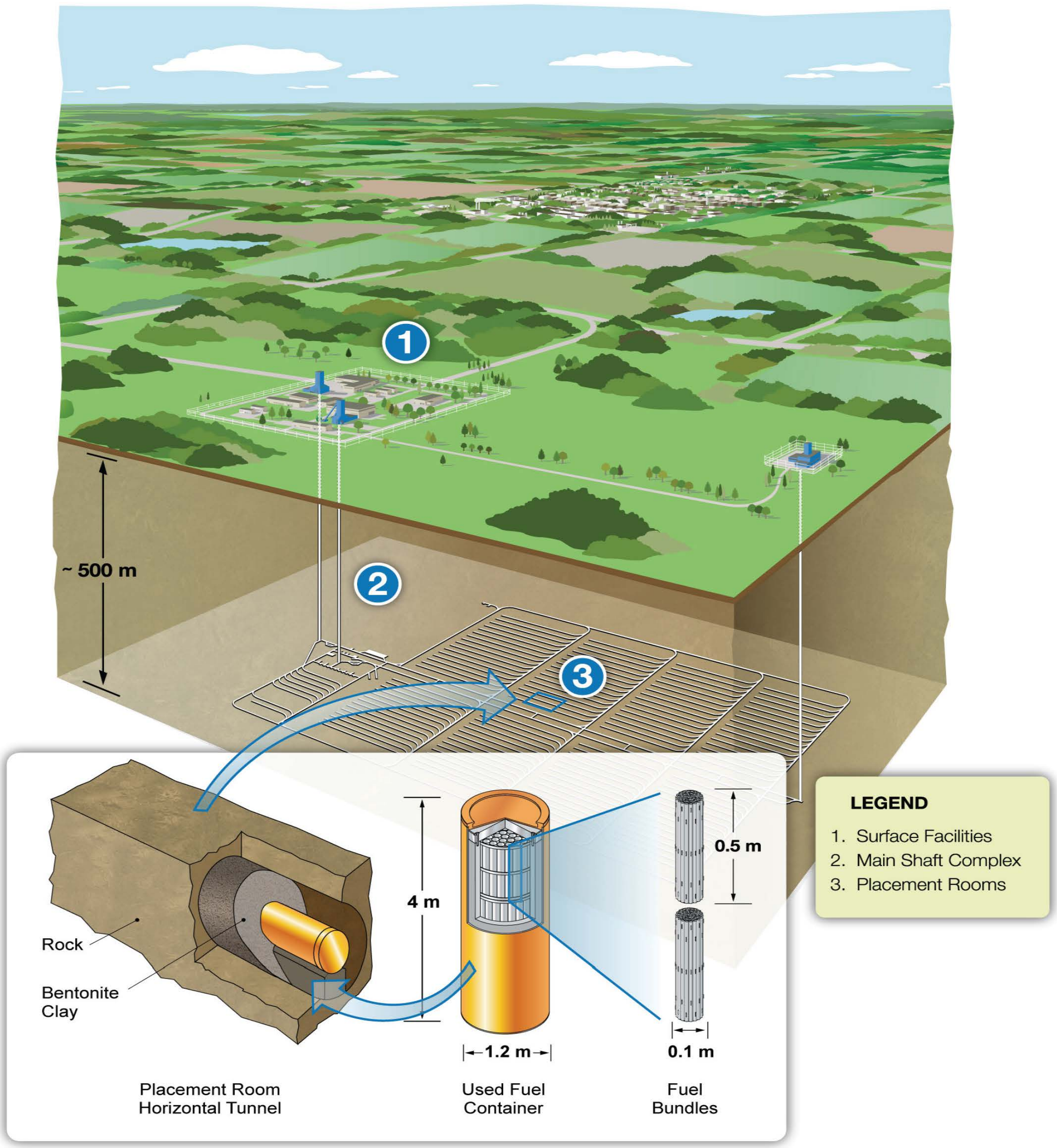

Figure 4-1: Illustration of an APM Facility in Sedimentary Rock

4.2 Surface Facilities

The APM facility requires a dedicated surface area of about 600 m by 550 m for the surface buildings and about 100 m by 100 m for the ventilation exhaust shaft located about 2 kilometres from the main facility. The APM facility also requires an off-site storage area of about 700 m by 700 m for the excavated rock; its location would be selected in consultation with the community and surrounding region. The surface water run-off from the excavated rock will be monitored and appropriate effluent control procedures will be implemented based on the monitoring results.

The site layout is shown in Figure 4-2; individual buildings and other surface facilities are listed Table 4-1. The site is surrounded by a perimeter fence; and the facilities within this perimeter are arranged into two areas:

1. The Protected Area, which is a high-security zone; and
2. The Balance of Site, a zone which includes facilities that do not require high security.

The main facilities included in the Protected Area are the Used Fuel Packaging Plant (UFPP), the main shaft and service shaft buildings as well as the auxiliary building, quality control offices, laboratory, radioactive waste handling facilities, switchyard, transformer area and powerhouse. All activities pertaining to handling and storage of used nuclear fuel are conducted in the UFPP. A detailed description of the UFPP and its operation is given in Section 4.4.

The Balance of Site zone includes the administration building, the fire hall, the ventilation shaft building, as well as ancillary facilities such as the cafeteria, garage, warehouse, water and sewage treatment plants, and helicopter pad. Fuel and water storage tanks and an air compressor building are also found in the Balance of Site, as well as the aggregate plant, concrete batch plant and the sealing materials compaction plant.

The aggregate plant will produce material for the concrete batching plant and sealing materials compaction plant. The concrete batching plant will produce the concrete mixes required for specific functions in the repository, including the Low-Heat, High-Performance Concrete (LHHPC) required for the bulkheads used for closing the filled container placement rooms and as components of other repository seals. At the sealing materials compaction plant, raw materials from the aggregate plant and externally sourced lake clay and bentonite will be mixed to produce dense backfill blocks, light backfill, compacted bentonite blocks and gap-fill material required for used fuel container placement and for sealing of the placement rooms.

A number of other support buildings and structures including offices, laboratory facilities and the common services required in a self-sufficient industrial site are also included in the site; a complete list is given in Table 4-1.

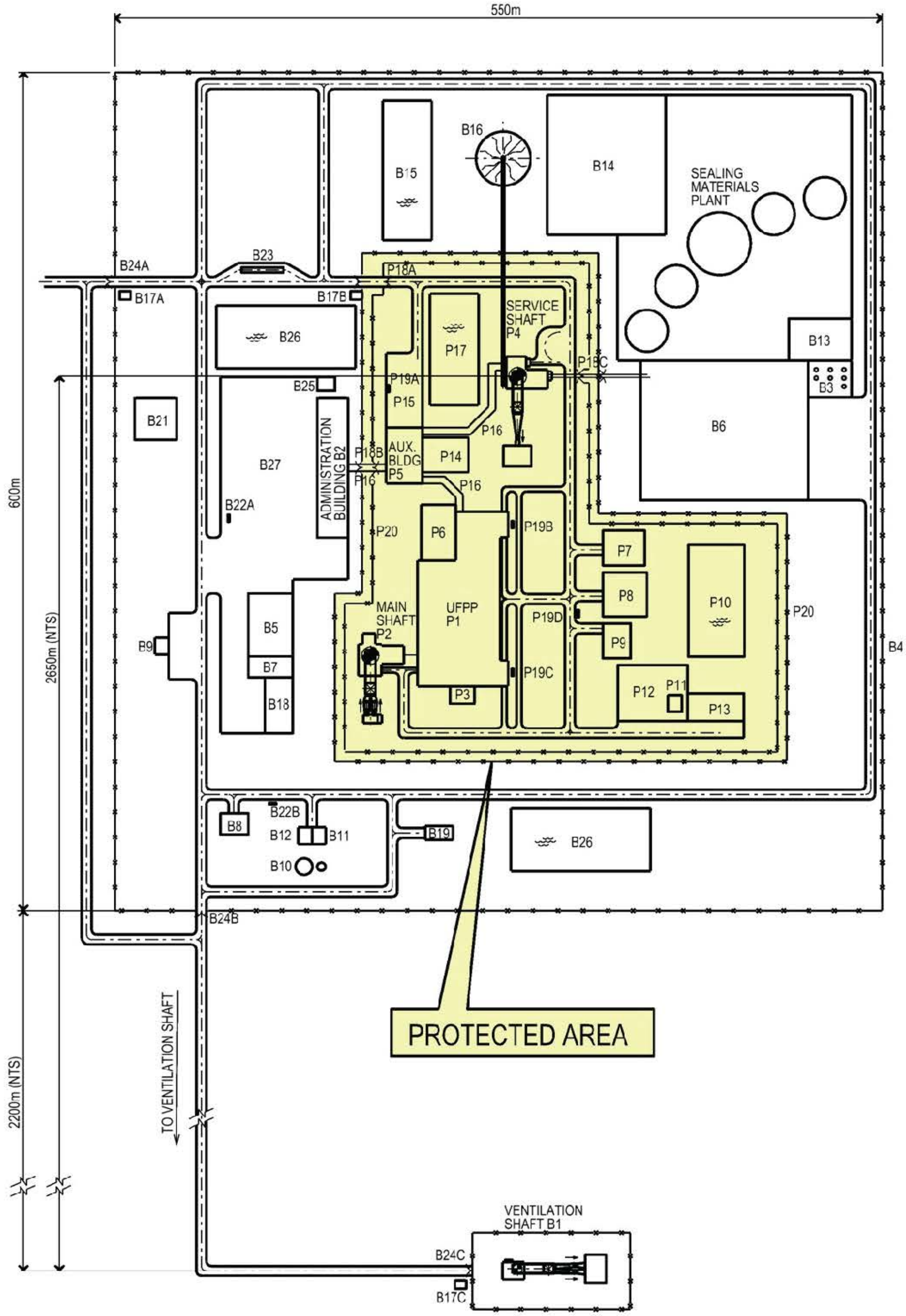

Figure 4-2: APM Surface Facilities Layout

Table 4-1: APM Facility Number and Description

Area	Protected Area	Area	Balance of Site
P1	Used Fuel Packaging Plant	B1	Ventilation Shaft Complex
P2	Main Shaft Complex	B2	Administration Building including Firehall and Cafeteria
P3	Stack	B3	Sealing Material Storage Bins
P4	Service Shaft Complex	B4	Perimeter Fence
P5	Auxiliary Building	B5	Garage
P6	Active Solid Waste Handling Facility	B6	Sealing Materials Compaction Plant
P7	Waste Management Area	B7	Warehouse and Hazardous Materials Storage Building
P8	Active Liquid Waste Treatment Building	B8	Air Compressor Building
P9	Low-Level Liquid Waste Storage Area	B9	Fuel Storage Tanks
P10	Stormwater Retention Pond	B10	Water Storage Tanks
P11	Switchyard	B11	Water Treatment Plant
P12	Transformer Area	B12	Pump House
P13	Powerhouse	B13	Concrete Batch Plant
P14	Quality Control Offices and Laboratory	B14	Aggregate (Rock Crushing) Plant
P15	Parking Area	B15	Process Water Settling Pond
P16	Covered Corridor / Pedestrian Routes	B16	Waste Rock Stockpile
P17	Mine Dewatering Settling Pond	B17	Guardhouse
P18	Security Checkpoint	B18	Storage Yard
P19	Bus Shelters	B19	Sewage Treatment Plant
P20	Double Security Fence	B20	Not Used
		B21	Helicopter Pad
		B22	Bus Shelters
		B23	Weigh Scale
		B24	Security Checkpoints
		B25	Security Monitoring Room
		B26	Storm water Retention Ponds
		B27	Parking Area

4.3 Used Fuel Container

The reference used fuel container design used for this study is the IV-25 copper container. It consists essentially of two vessels: an inner carbon-steel vessel that provides the required mechanical strength and outer copper vessel that provides a durable corrosion barrier. The capacity of the IV-25 copper container is 360 used CANDU fuel bundles with a mass of 8,640 kg. The inner vessel wall thickness is 102.5 mm and it is designed to sustain a maximum external isotropic pressure of 45 MPa, which is a conservative estimate of the maximum load the container would experience in the repository during a glaciation cycle, as a result of a 3 km thick ice sheet above the repository site.

The IV-25 container has been designed with a 25 mm thick outer copper shell for corrosion, fabrication and handling purposes. Under repository conditions, corrosion of the copper barrier is predicted to be less than 2 mm over a period of one million years (Kwong 2011), which is approximately the time required for the radioactivity of the used CANDU fuel to decay to levels comparable to those of natural uranium deposits.

The used fuel bundles are arranged inside the container in six layers of 60 bundles each. They are loaded into the container in three baskets holding two layers of 60 fuel bundles. The container and basket are illustrated in Figure 4-3. The design parameters of the copper and the steel vessels are given in Table 4-2 and Table 4-3, respectively. The total mass of a loaded used fuel container is approximately 26,700 kg.

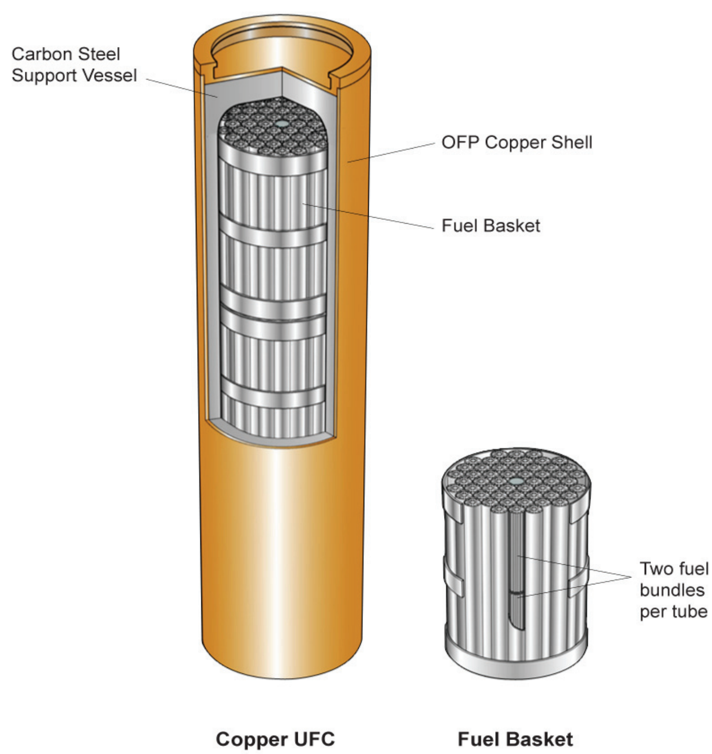

Figure 4-3: Copper Used-fuel Container and Fuel Basket

Table 4-2: Reference Copper Vessel Parameters

IV-25 Outer Copper Vessel	
Material	Oxygen-free, phosphorus-doped, high purity copper
Height	3,842 mm
Outside diameter	1,247 mm
Thickness (minimum)	25 mm
Mass of copper vessel	4,170 kg

Table 4-3: Reference Steel Vessel Parameters

IV-25 Inner Steel Vessel	
Material	ASTM[1] A516 Gr 70 steel
Height	3,700 mm
Outside diameter	1,195 mm
Thickness (minimum)	102.5 mm
Mass of steel vessel	12,650 kg
Mass of 3 fuel baskets	1,240 kg

4.4 Used Fuel Packaging Plant

The Used Fuel Packaging Plant (UFPP) is a multi-storey building designed to receive the used fuel shipped from interim storage facilities, transfer the fuel bundles into long-lived used fuel containers, seal and inspect the containers for subsequent transfer to the underground repository. The UFPP concrete structure contains a number of cells where specialized operations requiring shielding and containment capability are conducted. The plant conceptual design is illustrated in a cross-section and two layout plans inserted towards the end of this section. These drawings are useful to visualize both fuel handling operations, and the loading and processing of used fuel containers.

[1] American Society for Testing and Materials.

The used fuel containers are assumed to be manufactured at a dedicated plant, separate from the APM facility and shipped to the UFPP, where they will be received at a dedicated receiving hall for empty used fuel containers.

The used nuclear fuel is assumed to be shipped from interim storage facilities at the reactor sites in a used fuel transportation package (UFTP). The reference UFTP has a capacity of 192 fuel bundles, held in two used fuel storage modules containing 96 bundles each (NWMO 2013). The casks are received at the dedicated UFTP receiving and shipping hall. The process for transferring the used fuel from transport casks and placing it into used fuel containers consists of several major steps:

1. Receiving, unloading, decontamination and return of the UFTP;
2. Moving the received used fuel storage modules to the module handling cell and then to the fuel handling cell or, alternatively, placing them in a module storage pool;
3. Receiving and preparing new used fuel containers for loading;
4. Transferring the used fuel bundles from fuel storage modules to used fuel baskets;
5. Loading the fuel baskets into new used fuel containers;
6. Sealing and machining the container closure seal;
7. Inspecting the quality of the container closure seal; and
8. Placing used fuel container in a shielded transfer cask for transfer to the underground repository.

These operations and the associated features of the UFPP are described in the following sub-sections of this report.

4.4.1 Transport Cask Receiving and Unloading

The transport cask receiving and shipping hall is a dedicated area for transport cask handling and temporary storage provided with an overhead crane, which is initially used to unload the cask from the transport vehicle. Subsequently the transport cask impact limiter is removed and the cask is placed on a transfer pallet, which will move the cask along one of two processing lines. These two processing lines are identical and allow parallel unloading of casks and transfer of the used fuel storage modules either directly to the fuel handling cell or into a wet storage pool.

Transfer pallets that move on rails are used to move the transport casks from the cask receiving and shipping hall to a cask vent cell, and then to a docking position below the module handling cell (Figure 4-10 through to Figure 4-12). The transfer pallets are equipped with a scissors lift that enables the cask to be raised and docked at the module handling cell port.

The cask vent cell permits safe removal of the lid bolts and venting of the transport casks in a containment space. The vent cells are used also during dispatch of empty casks for replacing and fastening lid bolts, pressure testing lid seals and monitoring the cask surface for contamination. If necessary the transport casks can be decontaminated at the cask vent cell.

4.4.2 Module Handling Cells

From the vent cell the transport cask is moved to a cask docking cell, where it is connected to one of the two (parallel) module handling cells. Once docked, the cask lid is removed and placed on the cell floor. The module handling cells are equipped with lead glass windows and remotely-operated manipulators. They provide the required radiation shielding and containment to safely unload the fuel storage modules from the transport cask. An overhead crane is used in each module handling cell for lifting and transferring modules between different positions in the cell.

A module drying booth is included in the fuel processing line to permit drying of the used fuel before it is transferred to the fuel handling cell, where the fuel is placed into used fuel baskets. Alternatively, a fuel storage module in either of the two module handling cells can be moved into a module storage pool for interim storage before processing. The module storage pool provides buffer storage so that the fuel transfer and container loading operations can proceed without interruption.

4.4.3 Empty Used Fuel Container Receiving

Receiving and storage of new, empty used fuel containers takes place in a dedicated receiving hall located at ground floor level that includes storage positions for 40 empty used fuel containers and 126 empty fuel baskets. The receiving hall has a dedicated truck bay for unloading the new used fuel containers arriving at the UFPP.

The hall is equipped with a 30 tonne crane and a used fuel container preparation platform. The platform contains two parallel positions for inspection, installation of used fuel containers into sleeves, required to load the used fuel container into a shielded frame. Adjacent to the preparation platform are eight storage positions for sleeves, eight positions for empty baskets and four positions for pallets with empty used fuel containers in sleeves. The pallets are moved within the hall using an air-cushion transporter. Three new used fuel baskets are placed inside each fuel container prior to placing it in its docking position under the Fuel Handling Cell port.

4.4.4 Used Fuel Container Transport within the Plant

Both empty and full used fuel containers are moved in a Shielded Frame consisting essentially of a steel frame holding two telescopic, cylindrical shields vertically mounted on a steel platform. The bottom shield section can be raised and lowered by screw jacks, enabling a used fuel container to be raised and docked at the processing stations docking ports.

The top section is equipped with a gamma gate and is designed for airtight docking to the container ports at the used fuel container loading and processing stations. The shielded frame provides the required radiation shielding and effective isolation of the Fuel Handling Cell and the container processing stations from the used fuel container transfer area.

The shielded frames are moved between stations using an air-cushion transporter. The air-cushion transporter is equipped with steering wheels that remain in contact with the floor while the transporter is in the raised position, and can be controlled both manually and remotely. This technology is routinely used in industry as a safe and efficient means of moving heavy equipment. A shielded frame on an air-cushion transporter being used at SKB's Canister Laboratory in Sweden is shown in Figure 4-4.

Figure 4-4: Shielded Frame and Air-cushion Transporter

Using air-cushion technology for moving the shielded frames allows the containers to be transported independently of each other and allows simultaneous, independent operation of all the processing stations. Other operational advantages of this used fuel container transport method include easy maintenance and faster recovery from equipment failure, minimizing the risk of production stops.

4.4.5 Fuel Handling Operations

The fuel handling cell is a shielded containment cell used for transferring used fuel bundles from storage modules into fuel baskets and for loading the filled fuel baskets into used fuel containers. To fulfill these tasks the cell is equipped with three fuel handling machines, lead glass windows, remote manipulators and vacuum cleaners. All equipment in the fuel handling cell is remotely operated. To enable loading of filled baskets into a container, the fuel handling cell has a docking port that connects it to the used fuel container transfer area.

During the fuel transfer operation from a module to a basket, the fuel bundle serial number is recorded for safeguard purposes. Damaged bundles can be placed in cans and/or loaded into baskets specially designed to accommodate damaged fuel.

The cell is also equipped with a crane for lifting used fuel modules and baskets. Within the cell, there are four positions for the temporary storage of modules, and one position for parking the containment door and inner vessel lid. The cell also has a dedicated area for the temporary storage of up to 12 filled or empty baskets. In the floor of the fuel handling cell, there is a port with a gamma gate leading to a waste management facility, which includes provisions for the decontamination and compaction of empty fuel storage modules.

4.4.6 Used Fuel Container Processing

Once three fuel baskets are loaded into the used fuel container, the container inner lid is bolted on and the container is moved to other processing stations where a sequence of operations takes place to seal and test the container prior to its transfer to the underground repository. These operations, which take place at four separate processing stations, include backfilling the container with an inert gas, welding of the outer copper lid, machining the weld surface and non-destructive testing (NDT) of the weld. These processing stations are described below.

4.4.6.1 Inerting Station

The inerting station is a radiation shielded cell that contains provisions for remotely bolting the inner vessel lid to the inner steel vessel. The station also houses equipment for removing the air contained in the inner vessel and backfilling the volume with an inert gas. This process is done via a valve in the inner vessel lid that can also be used for testing the leak-tightness of the lid. Containers are docked to the station in the same manner as described for the fuel handling cell. The inerting station is also equipped with a hatch and a crane for importing and moving container lids and any required equipment. Figure 4-5 shows a conceptual illustration of the inerting station.

After its inner volume is backfilled with an inert gas the container is moved to the welding station, illustrated in Figure 4-6, which has the required equipment for placing the copper lid on the container and welding it to the copper shell.

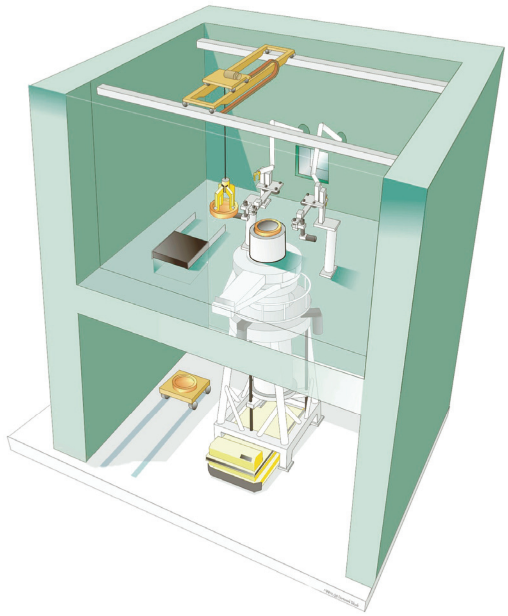

Figure 4-5: Inerting Station

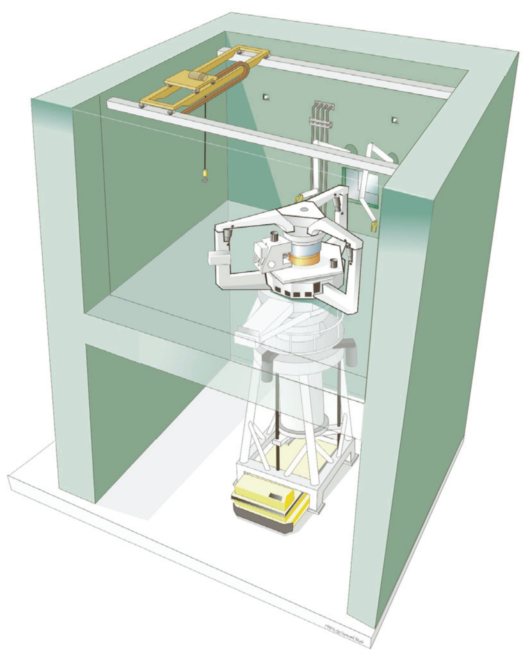

Figure 4-6: Welding Station

4.4.6.2 Welding Station

The selected method for welding the container copper lid to the container is Friction-Stir Welding (FSW). This method was originally developed for various industrial applications by The Welding Institute (TWI) in the United Kingdom, and adapted to this specific use by SKB. The process essentially consists of inserting a rotating metal tool in the lid-body joint at a perpendicular angle to the container surface and moving the tool along the circumference of the joint (Figure 4-7). The rotation of the welding tool around its own axis generates heat that effectively joins the lid and body of the container without melting of the metal. To execute this operation the container is held in a fixed position while the welding head assembly rotates around the container axis. Non-destructive testing (NDT) methods will be used to examine and verify the quality of the welds.

FSW has been extensively tested at SKB's Canister Laboratory and selected as the reference welding method for the Swedish spent fuel canisters after a thorough comparison with Electron-Beam Welding (EBW). FSW was found to be a more reliable process resulting in more uniform weld quality, and the properties of the resulting weld material were very close to those of the original OFP copper material. The FSW development program and the assessment results are documented in SKB 2007 and SKB 2008.

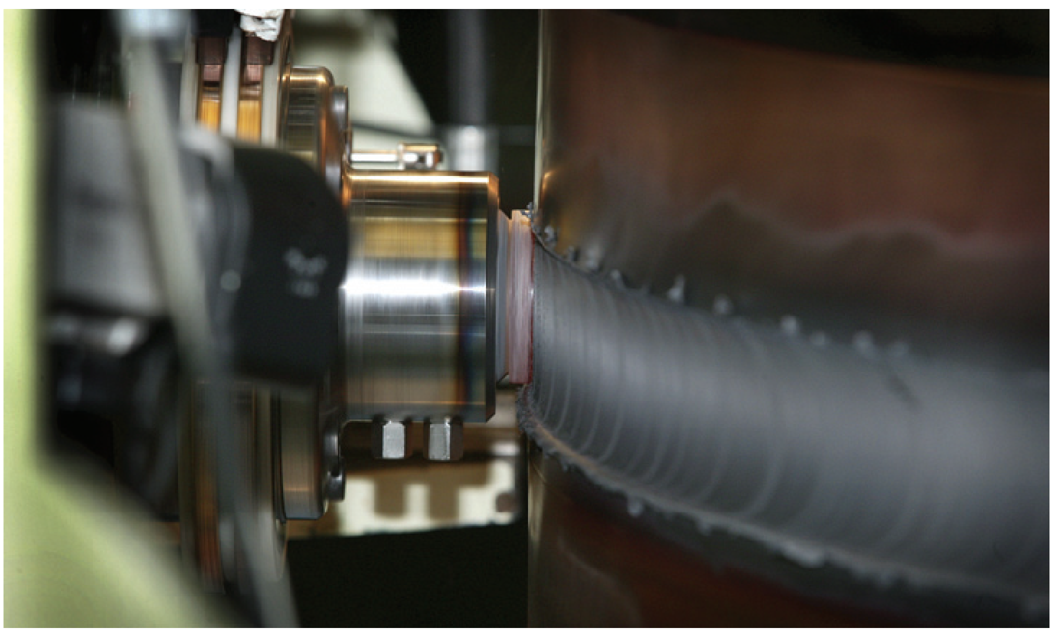

Figure 4-7: Friction Stir Welding of a Copper Lid

4.4.6.3 Machining and NDT Stations

Following welding of the copper lid, the used fuel container is moved to a station where the weld surface is machined to achieve a finish similar to that of the rest of the container surface. This is required to ensure that the weld surface has a corrosion behaviour consistent with the rest of the copper shell as well as to facilitate non-destructive testing of the weld.

During machining, the equipment is rotated and the used fuel container is held in a fixed position (see Figure 4-8). The docking arrangements in the machining station are similar to those in the welding station (see Figure 4-9). After this operation the container is moved to the non-destructive testing station, which contains equipment to conduct a visual examination of the weld plus two other independent NDT examinations using different testing methods. Two methods being considered are radiography (tomography) and ultrasonic testing. High-energy X-ray sources with very small focal spots and fast detectors with good time and spatial resolution allow the construction of good 3-D images in practical times. These weld examination methods are currently being assessed by Posiva (Finland) and SKB (Sweden), whose spent fuel container designs include a thick copper shell as corrosion barrier.

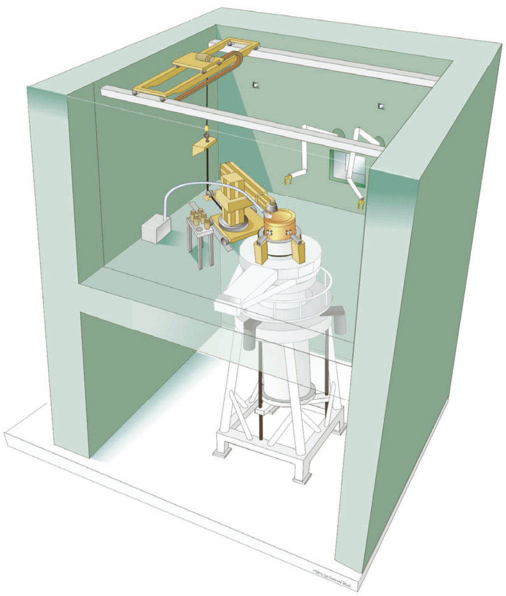

Figure 4-8: Machining Station

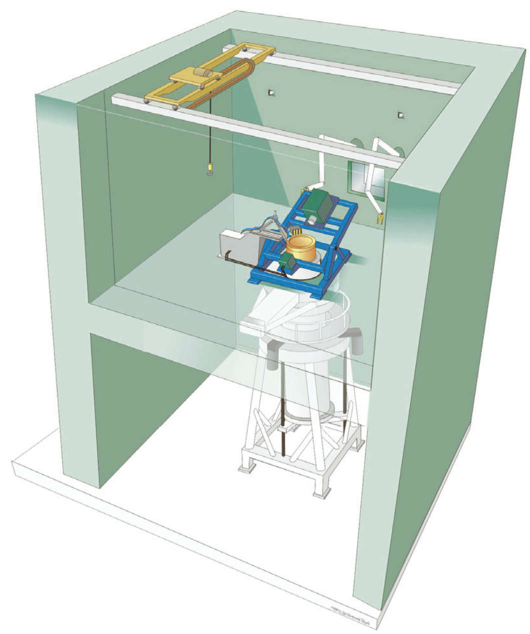

Figure 4-9: Non-destructive Testing Station

Both the stereoscopic radiography and ultrasound testing methods appear to provide satisfactory results (Sandlin 2010a, 2010b, 2010c). The stereographic radiography method has some limitations for detection of thin, planar defects; in this case ultrasonic testing is used to overcome the radiographic method's limitations. Further tests on a larger sample of welds will be needed to achieve the required level of precision. Both SKB and Posiva are continuing work in the testing of full-scale container welds (Pitkanen 2010).

For design (logistics) purposes, it is assumed that one out of 100 containers are found to not meet the specified weld quality requirements during non-destructive testing in the UFPP (SNC Lavalin 2011). The handling of defective containers is outlined below.

For postclosure safety assessment, it is assumed that one out of 5,000 containers placed in the repository have <u>undetected</u> through-wall defects. Effectively, this requires that both a substantive defect exists <u>and</u> that it is not detected by three NDT examinations using different methods. This rate is based on a review of failure statistics for other nuclear components (Maak et al. 2001). The assumed undetected weld defect rate is considered to be conservative for safety assessment purposes, although a lower probability of undetected defects could likely be achieved. The achievable failure rate would need to be confirmed by studies and testing of prototype containers.

Recently, an International Review Team was established by the Nuclear Energy Agency (NEA) to review SKB's postclosure safety case for a used fuel repository in Sweden (NEA 2012). The review was conducted by the NEA Secretariat on behalf of the Swedish Government. The International Review Team reviewed the methods developed by SKB for non-destructive testing of the container and the weld, and concluded that those methods have been verified to be able to detect inconsistencies and failures below the design limits of the safety case.

4.4.6.4 Handling of Defective Containers

Upon detecting a defect in a sealed used fuel container, the container processing at the UFPP is stopped and two separate actions are taken:

1. The cause for the weld defects is investigated and resolved before loading and processing of new containers is allowed to proceed; and
2. Depending on the nature of the defect, the defective container is either repaired and re-inspected or the defective container is opened (copper shell cut open only), the loaded steel core is retrieved and put into a new copper shell, which is then welded and inspected. The original (defective) copper shell is decontaminated and returned to the container factory for recycling of the materials.

To implement this second action, the container with the defective weld is moved from the NDT station back to the machining station where the container weld is cut. Subsequently the copper lid is removed and the container is docked at the module handling cell where the three fuel baskets are extracted from the container, then both the lid and the container body are decontaminated and returned to the container factory for recycling.

After the cause for the weld defect is identified and the problem corrected, used fuel container processing is allowed to resume. As data is acquired through both development and implementation of the weld examination process, more sophisticated methods can be used to improve the statistics of the NDT data (Holmberg and Kuusela 2011).

4.4.7 Filled Used Fuel Container Storage Cell

At the end of the used fuel container processing area opposite to the module handling cell there is a shielded area where full used fuel containers can be monitored and placed in temporary storage. This cell has 40 storage positions and is located above the container transfer area; it is equipped with four ports and a 30 tonne overhead crane capable of handling both empty and full used fuel containers.

Containers that have been successfully loaded, welded and inspected are then brought to an entrance port dedicated to the import/export of full containers. After a container is brought into the storage area it is either placed in a storage spot or monitored, decontaminated if required, and then transferred to the filled container dispatch cell. Containers requiring decontamination can be lowered using the overhead crane into a decontamination cell located below the floor level of the storage area.

4.4.8 Used Fuel Container Dispatch Hall

Adjacent to the loaded used fuel container storage cell is a dispatch hall, where the filled used fuel containers are placed into a shielded transfer cask for transfer to the repository. In the dispatch hall there is an airlock for the transfer casks arriving and departing on a rail wagon.

The used fuel container dispatch hall is equipped with an 80 tonne overhead crane and a working platform for inspection and cask preparation operations. The hall is also equipped with an air-cushion transporter and pallet for the transfer of a cask between the working platform and the filled used fuel container dispatch hall (see Figure 4-10 and Figure 4-12).

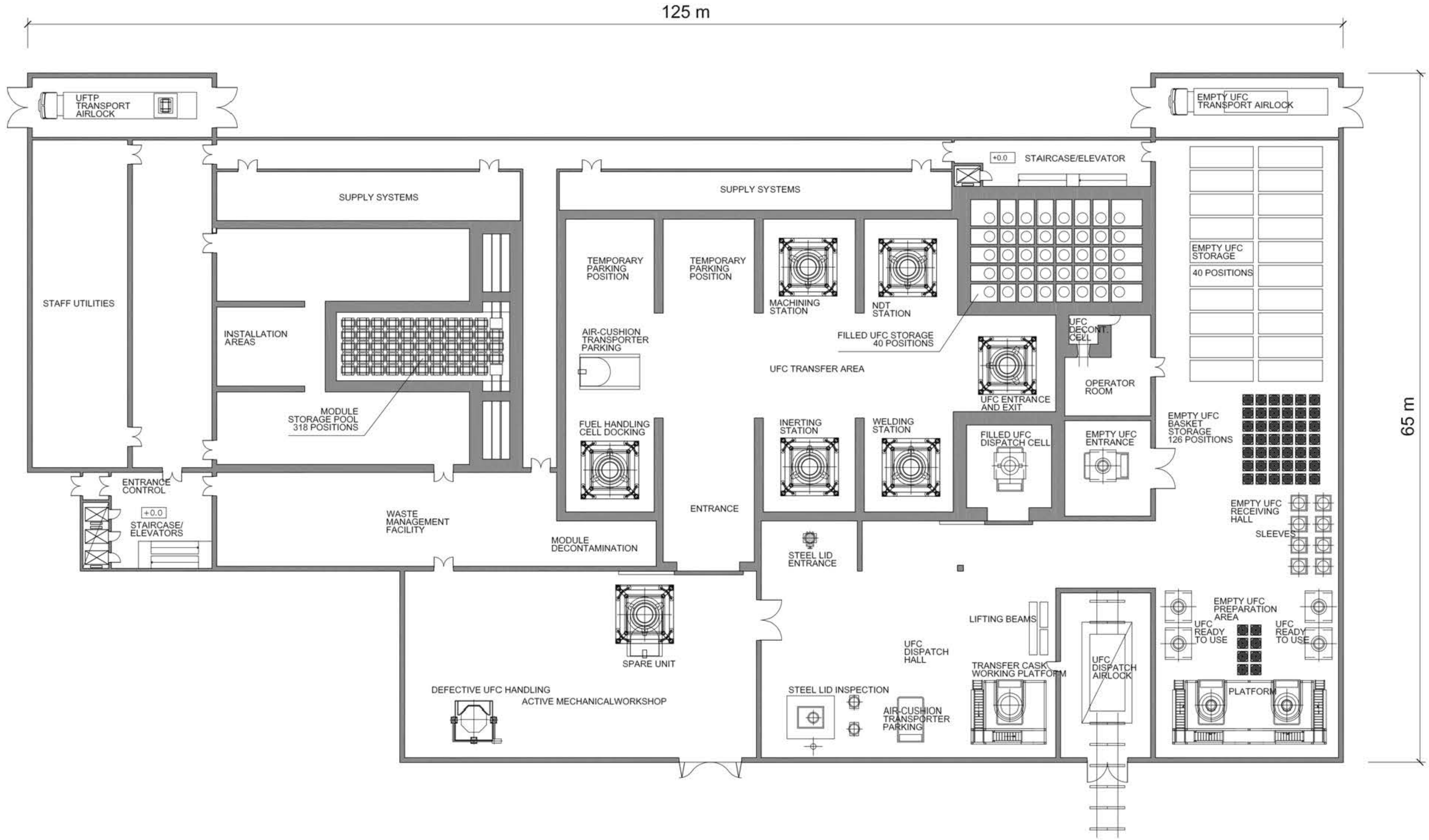

Figure 4-10: Used Fuel Packaging Plant – Container Transfer Level

THIS PAGE HAS BEEN LEFT BLANK INTENTIONALLY

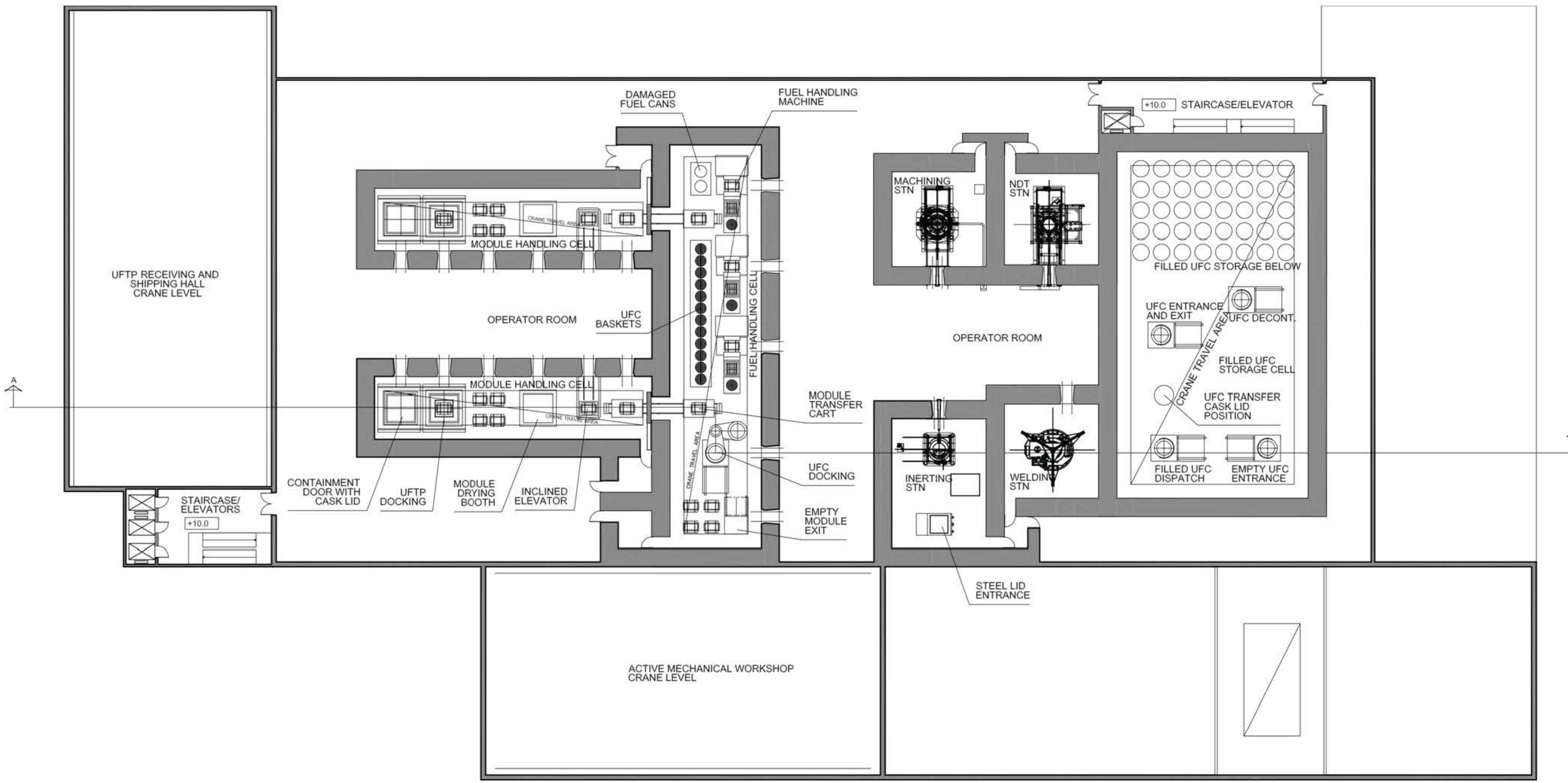

Figure 4-11: Used Fuel Packaging Plant – Operation Level

THIS PAGE HAS BEEN LEFT BLANK INTENTIONALLY

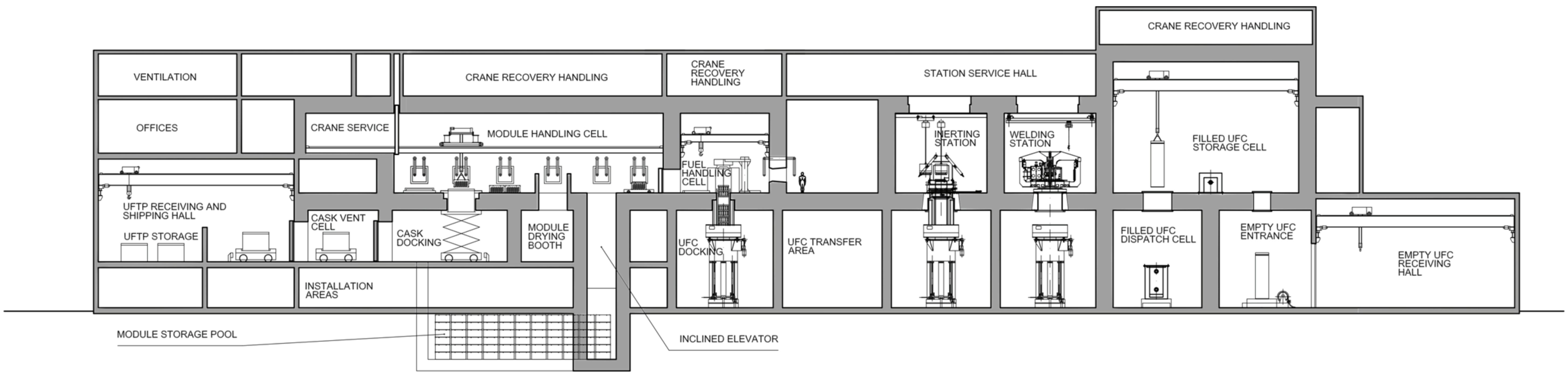

Figure 4-12: Used Fuel Packaging Plant – Cross-Section

THIS PAGE HAS BEEN LEFT BLANK INTENTIONALLY

4.5 Seals and Sealing Materials

4.5.1 General Description

The engineered barriers system concept presented in this report is based on previous Canadian and international studies. This concept uses a highly compacted bentonite (HCB) pedestal to support the used fuel container in its assigned position and bentonite pellets, placed by pneumatic methods, to fill all the remaining voids in the container placement room.

After a placement room has been filled, it will be closed off by means of a Low-Heat High-Performance Concrete (LHHPC) bulkhead. The concrete bulkhead will counteract the swelling pressure of the bentonite components and keep the tunnel backfill materials in their intended position. The room closure would also provide physical isolation of the filled container placement rooms from the ongoing operations in the rest of the repository.

The use of compacted bentonite blocks and in-situ compacted bentonite in tunnel and shaft sealing applications has been demonstrated during the past several years in various repository programs (Dixon et al. 2009, 2012 and Pusch et al. 2004). Research is currently underway on the manufacturing and installation methods of bentonite pellets in order to optimize both the as-placed and final density of the material when used as backfill in horizontal tunnels (Kim et al. 2012).

Other sealing materials of potential use in the repository include grouts that may be used to seal possible rock fractures or any areas of higher rock permeability that may intersect tunnels, and compacted bentonite blocks that may be used as a component of placement room closure seals or shaft seals. Concrete may also be used as a component of repository seals.

After the repository operational period, during decommissioning, the access tunnels and shafts also would be backfilled and sealed. Seals will be required at locations where tunnels or shafts intersect hydraulically active regions in the rock and also along the shafts, to interrupt potential transport paths to the surface.

Shaft seals designs would use durable, well understood materials, and proven placement methodologies. The shaft seals would likely consist of multiple components placed in series that may include a column of in-situ compacted bentonite/sand mixture, or pre-compacted bentonite blocks, and/or an asphalt column. The intent will be to suit the configuration and rock characteristics of the geological layers intersected by the shaft and provide redundant, low permeability sealing components to prevent water movement. Concrete bulkheads could be used to provide structural support and confinement to the column of shaft sealing materials (Dixon et al. 2009, 2012).

Siting, construction, and operation of a repository would require the drilling of exploratory and monitoring boreholes, including those drilled from the surface as well as boreholes drilled from tunnels and shafts into the adjacent rock. As part of repository closure, these boreholes will eventually be decommissioned and sealed. Composite seals made of similar materials as those used for the sealing of tunnels and shafts would be used for this purpose.

4.5.2 Placement Room Backfill Materials

The materials used in the container placement room consist of a highly-compacted bentonite (HCB) pedestal designed to support the used fuel container, and bentonite pellets, which will be pneumatically placed to fill the remaining spaces surrounding the containers. Both the pedestal and the pelletized backfill are made of 100% bentonite and have properties as described in Dixon et al. (2009, 2012). The main mineral phase in bentonite is montmorillonite, a smectitic clay mineral that has expandable layers when allowed access to free water, as well as a high cation-exchange capacity. As a consequence, bentonite can significantly increase its original volume when it becomes in contact with water. When compacted bentonite placed in a confined space comes in contact with water it will incorporate water and develop a substantial swelling pressure. This makes it an excellent material to seal fractures and produce tight contacts with interfacing materials. Bentonite-based materials also have the advantage of having a very low permeability, reducing advective transport, and, when placed at high density, bentonite also has the capability of limiting microbial activity. For the purposes of this design it is assumed that the pneumatically placed bentonite pellets backfill will achieve the required density to inhibit bacterial life (Kim et al. 2012).

4.5.3 Placement Room Configuration

The placement rooms are essentially circular cross-section tunnels 2.5 m in diameter. The used fuel containers are positioned horizontally, supported by the HCB pedestal, in a coaxial configuration with the placement tunnel. The container configuration in the tunnel is shown in Figure 4-13.

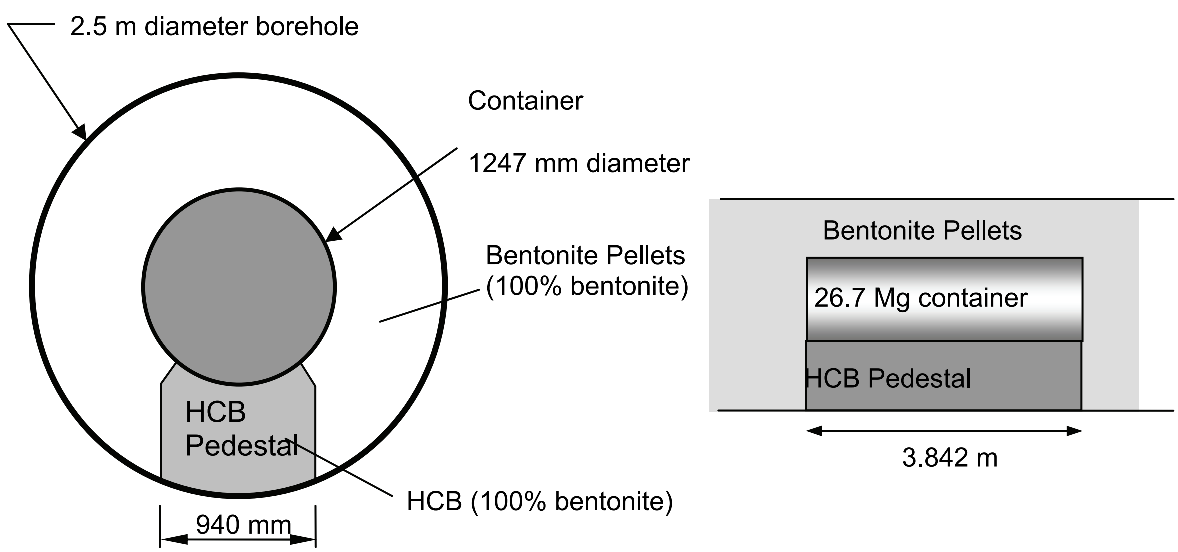

Figure 4-13: Container and Pedestal Configuration

The functions of the bentonite components in the container placement tunnel include:

- Maintaining the container position and geometry in the tunnel;
- Providing mechanical protection by acting as a buffer between the container and the rock;
- Providing a counter pressure that will tend to close EDZ fractures and reduce their transmissivity
- Facilitating heat transfer between the container and the rock;
- Limiting the container corrosion rate by inhibiting the movement of corrosion agents and influencing the chemistry of groundwater around the container; and
- Inhibiting the viability of bacteria near the container, reducing the potential for microbially induced corrosion of the container surface.

In the event of a breach of the container barrier, the bentonite components would also:

- Limit the solubility of certain contaminants by maintaining the pH of the groundwater around neutral conditions; and
- Retard or prevent the migration of dissolved contaminants by restricting their movement to diffusion transport, and to a lesser extent, by sorption. In this case study, only a few elements are assumed to be retained by sorption in the sealing materials because of the assumed high salinity of the groundwater.

4.5.4 Access Tunnels Backfill

Man and Martino (2009) identify two types of backfill that are used in the repository tunnels: dense backfill and light backfill, which are manufactured in the form of pre-compacted blocks. These materials will be used for backfilling the repository longitudinal drifts, as well as the cross-cuts that provide access to the placement rooms. However, these materials will not be used as backfill in the container placement rooms. The general composition and properties of materials considered at this preliminary design stage are given in Table 4-4. In order to provide a method for comparison of sealing materials performance, their properties are expressed in terms of their “effective montmorillonite dry density”, a parameter that normalizes bentonites and bentonite-sand mixtures based of the content of montmorillonite clay.

Dense backfill as formulated in Table 4-4 is a mixture of crushed rock, naturally-occurring glacial lake clay, and bentonite. It is manufactured and installed in the form of pre-compacted blocks to fill the majority of the tunnel volume. Important functions of the dense backfill are to provide load-bearing support to the rock openings by filling most of the excavated space in tunnels, and to slow the movement of groundwater within the repository excavated spaces.

Light backfill has similar functions to dense backfill, but it contains less crushed rock and more bentonite than dense backfill, as indicated in Table 4-4. Light backfill blocks are also made of different shapes in order to fill the sides and upper (crown) regions of tunnels where for geometric reasons it is not possible to place dense backfill blocks. Depending on the application, light backfill can also be compacted in-situ.

Table 4-4: Composition and As-Placed Properties of Clay-Based Sealing System Components

	Dry density [kg/m^3]	Saturation [%]	Porosity [%]	Bulk density [kg/m^3]	Water content [kg/kg]	Effective montmorillonite dry density [kg/m^3]
HCB (100% bentonite)	1,610	65	41.3	1,880	0.167	1,470
Gap Fill (100% bentonite)	1,410	6	48.6	1,439	0.021	1,260
Light backfill (50:50 bentonite/ sand)	1,240	33	53.7	1,418	0.143	692
70% bentonite (70:30 bentonite/ sand)	1,600	80	41.1	1,930	0.205	1,220
Dense backfill (5:25:70 bentonite/clay/crushed rock aggregate)	2,120	80	19.4	2,276	0.074	376

Note: Dry densities and saturations of the clay-based sealing materials are taken from SNC Lavalin (2011); other properties are determined using calculations illustrated in Baumgartner (2006).

4.5.5 Concrete

Concrete is used throughout the repository for sealing components and tunnel closure bulkheads and in the concrete components of repository seals. It is also used for tunnel floors where required. The concrete used to support tracks in the placement rooms will be removed as container placement progresses. The concrete floors installed in drifts and cross-cuts will be removed as a part of the repository decommissioning process. The only concrete that will remain in the repository is the concrete used in repository seals.

Interactions between concrete and water in a repository have the potential to produce alkaline chemical conditions that are detrimental to the swelling properties of bentonite, therefore LHHPC (Dixon et al. 2009, 2012) will be used, in repository seal components. LHHPC has a lower lime content than regular concrete, which results in a lower pH in reactions with water. The lower alkalinity limits the potential for adverse chemical reactions within the repository. In addition, the LHHPC generates less heat than regular concrete during the curing process, so the poured concrete is less likely to develop cracks during curing.

4.5.6 Grout

Grouting will be used during excavation and construction in any localized areas with higher rock permeability, or in order to limit seepage around engineered structures. Clay-based grouting materials may be an option under some conditions in a repository, but cement or silica-based grouts are more likely to be used. A sample grout specification for use in a repository environment is included in Table 4-5 (Dixon et al. 2009).

Table 4-5: Composition and Properties of a Cement Grout for Repository Use

Mix Composition	
Solids	90% Canadian Type HS* cement, 10% Silica fume by dry mass
	The cement Blaine fineness needs to be specified for the specific application (e.g., 600 m^2/kg).
Water/cement ratio	0.4 to 0.6 by mass
Superplasticizer	Sodium sulphonate naphthalene formaldehyde
Selected Properties	
Viscosity	Modified by water/cement ratio and superplasticizer content
Setting time	Initial: varies with temperature 10 to 16 hours
	Final: varies with temperature 12 to 20 hours
Strength	Varies with water to cement ratio, time and temperature: 20 to 60 MPa at 28 days
Hydraulic Conductivity	< 10^{-12} m/s

Note: * Type HS cement is the designation for sulphate resistant cement in Canada.

4.5.7 Asphalt

An asphalt column may form part of the shaft seals. Asphalt has the ability to flow and make good contact with host rock, and will create an effective barrier to water flow immediately upon placement. The reference asphalt mixture is based on a mix of asphalt compounds and combined aggregates with a small porosity fraction to ensure low permeability, including also lime to reduce microbial activity.

4.6 Sealing Materials Production Plants

A number of engineered barriers are used as part of the repository system to isolate the used fuel containers from the rock and to inhibit the mobility of water and contaminants within the repository. These engineered barriers are manufactured on site, using bentonite clay, sand and crushed rock as their main components, and are globally referred to as sealing materials. The primary barriers placed around the used fuel container consist of: a) a pedestal made of compacted bentonite that is placed on the tunnel floor and supports the used fuel container in its designated position, and b) placement tunnel backfill, in the form of bentonite pellets, that fills the remaining spaces in the placement room, including the space between the containers and the rock and the space between containers.

Other sealing materials used to construct seals at strategic points in the repository or used as backfill for the repository access tunnels include highly-compacted bentonite (HCB) blocks, used to construct tunnel and shaft seals, and backfill blocks used to fill the repository excavated spaces (other than the container placement rooms) at the time of repository decommissioning.

The backfill blocks are of two general types, dense backfill, and light backfill. Their composition is given in Table 4-6. The concrete components of repository seals are made of LHHPC, described by Dixon et al. (2009).

Table 4-6: Sealing Materials Attributes

Material	Attributes
Pedestal Composition and Density	Monolithic blocks, made from 100% bentonite clay (MX-80 or equivalent) and compacted to 1,610 kg/m^3 dry density
Dense Backfill Composition and Density	5% bentonite, 25% lake clay, 70% crushed rock aggregate, 2,120 kg/m^3 dry density
Light Backfill Composition and Density	50/50 bentonite clay/ sand, compacted in-situ to 1,240 kg/m^3 dry density
Tunnel and Shaft Seals Composition and Density	70:30 bentonite clay/sand, either in pre-compacted blocks, or in-situ compacted to1,600 kg/m^3 dry density
Concrete	Low-heat high-performance concrete (LHHPC)

The repository surface facilities used to produce sealing materials include an aggregate plant and rock crushing plant (Area B14), a concrete batch plant (Area B13) and a sealing material compaction plant with associated material storage bins (Areas B6 and B3), as shown in Figure 4-2.

The aggregate plant uses a portion of the excavated rock to manufacture products suitable for the concrete batch plant, including sand and stone. Modified granular A (a graded crushed stone commonly used on roads) and fine sand for the compaction plant are also produced in the aggregate plant and used as a component of the sealing materials. Externally sourced raw materials required in the production of the various sealing materials include binders (Type 50 cement, silica fume and flour) as well as bentonite and glacial lake clay. The concrete batch plant produces two different types of LHHPC mixes, one for the placement room floor and the other for the placement room closure bulkhead.

During decommissioning, the plant will produce the bentonite shaft seal materials. Asphalt seal mixes that may be required for sealing of shafts are assumed to be produced externally.

4.7 Shafts and Hoists

Access to the repository is via shafts serviced by hoisting facilities. Three shafts will be constructed: the main shaft, the service shaft, and the ventilation shaft (Figure 4-14); each serving specific functions during construction, operations and decommissioning of the repository facility. Their primary functions are the transport of materials and personnel, and providing ventilation to the repository. The shafts will be constructed using techniques that minimize host rock damage, to enhance the effectiveness of postclosure repository seals. The finished diameter of each shaft is: main shaft 7.0 metres, service shaft 6.5 metres; and ventilation shaft 6.5 metres.

The headframes for the three shafts will be of slip-formed concrete construction for a durable and easily maintainable structure. All the shafts will be concrete lined; the lining will be removed during decommissioning and closure of the facility. The three shaft structures (including head frames and hoisting plants) provide a number of support functions during underground development, repository operation and decommissioning:

- The main shaft serves as the exclusive means for transfer of used fuel containers from the surface to the underground repository. It could also be used for transfer of a retrieved used fuel container from the repository to the surface, if this was required. The main shaft also provides the fresh air supply to the underground.
- The service shaft serves as the principal conveyance for personnel, materials and equipment to the underground as well as for transport of excavated rock to the surface. It also provides some ventilation exhaust.
- The ventilation shaft, located about 2 km outside the main surface facilities fence is the primary exhaust shaft and serves also as emergency exit from the repository.

4.8 Underground Facility Design

For the purpose of preliminary design and safety studies for a hypothetical site in sedimentary rock, the used fuel repository is assumed to be developed on a single level, at a depth of approximately 500 m. A possible layout of a repository designed to accommodate a reference inventory of 4.6 million used fuel bundles is shown in Figure 4-14. The actual layout for a selected repository site will be adapted to suit the specific site conditions. The geology of the hypothetical site used in this study is described in Chapter 2.

The layout of the repository reference design, shown in Figure 4-14, has a rectangular configuration, with two central access drifts and two perimeter access drifts connected by perpendicular tunnels (cross-cuts) that provide access to the used fuel container placement rooms.

The container placement rooms are a series of parallel tunnels arranged in ten panels. Within each panel, the placement rooms have a centre-to-centre spacing of 20 m, and each room has a single access from the corresponding cross-cut tunnel. The entrance to the room has a 50 m turning radius to facilitate the movement of the container transfer cask and related systems. The length of the rooms in the reference design is specified as 412 m and the used fuel containers are placed along the tunnel axis with a center-to-center spacing of 8.0 m. The longitudinal section of a container placement room is illustrated in Figure 4-15.

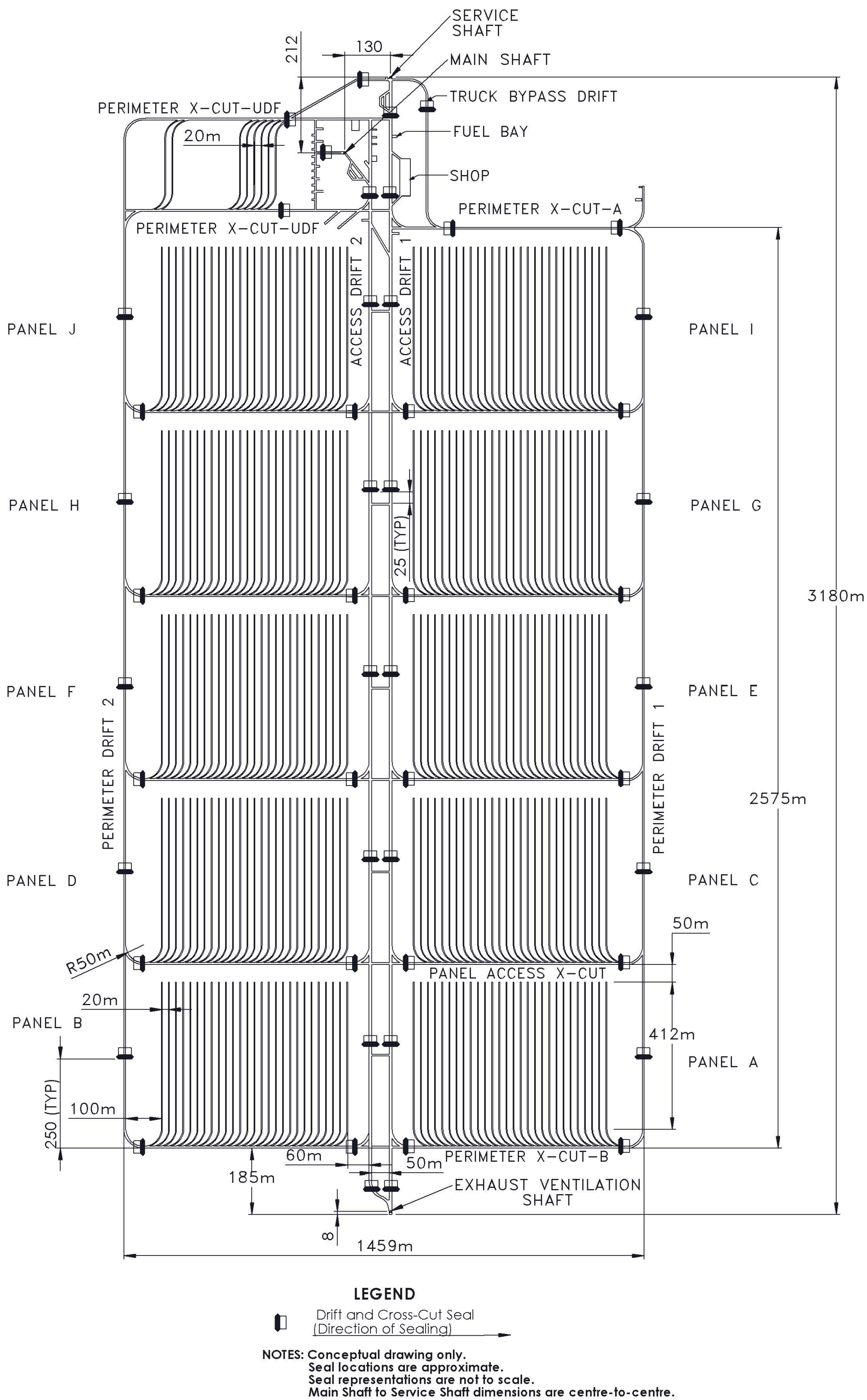

Figure 4-14: Underground Repository Layout

The used fuel container density is designed to minimize the repository underground footprint while satisfying thermal design requirements as described in Chapter 5. The repository includes provision for an underground demonstration facility located near the main and service shafts. This facility may be used to support long-term testing and demonstration of repository technology.

In each placement room, as used fuel container placement operations advance, the rails and concrete floor are removed and the room is backfilled with pneumatically placed bentonite pellets. The pellets will fill the spaces between the container and the tunnel wall as well as the space between containers. After a placement room is full, a 12 m concrete bulkhead will be placed to seal the entrance to the room. The major components of a placement room are illustrated in Figure 4-15 (SNC Lavalin 2011).

Both repository development (excavation) and used fuel container placement will be conducted on a panel by panel basis and, in a sequence that will provide suitable separation of these two major activities. The repository development/operation strategy will optimize efficiency while considering both, safety and operating factors (e.g., vehicle traffic and ventilation) as well as the potential interactions between repository development and operations.

4.8.1 Ventilation System

The repository ventilation system utilizes the three shafts and a combination of parallel airways for intake and exhaust. Underground booster fans, ventilation doors and dampers are used to control the airflow distribution. Since the primary repository ventilation system consists of relatively large airways, the overall circuit has relatively low resistance characteristics in a push-pull type network. Two parallel, surface fresh air fans supply air (heated as required) to the main shaft. The fresh air supply reaches the repository level at the main shaft station and is split to the underground demonstration facility and the main repository itself. A portion of the exhaust air flow is routed to the service shaft by an exhaust booster fan.

Exhaust air from the repository area is routed to the ventilation shaft by two exhaust booster fans, installed underground in a parallel configuration at the shaft station. Return air is exhausted to atmosphere by two parallel exhaust fans installed on the surface in the ventilation shaft area. Air distribution in the repository is promoted through the use of fans and regulators. Fresh air will be distributed to the individual panels through axial flow fans. Individual placement rooms will also be ventilated by axial flow fans that will remove air from the rooms and direct it into the exhaust circuit.

The ventilation fans will work with a duct network to provide a design flow of 37.8 m^3/s of air to the room during excavation. During used fuel container placement activities, the required supply flow per room will be 14 m^3/s. The exhaust air flow from these ventilation fans will be routed to the panel exhaust drift, and then to underground booster exhaust fans (SNC Lavalin 2011).

The system will be operated to ensure that the underground work is performed in a fresh air supply stream with the exhaust being directed through unoccupied areas. High-efficiency particulate air (HEPA) filtration systems could be installed in the service shaft and ventilation shaft stations as stand-by systems that would be activated as required. Subsurface ventilation systems could also be equipped with air filtration systems if required. For the purpose of this conceptual design, stand-by HEPA filtration systems are assumed to be installed at the service shaft and ventilation shaft stations.

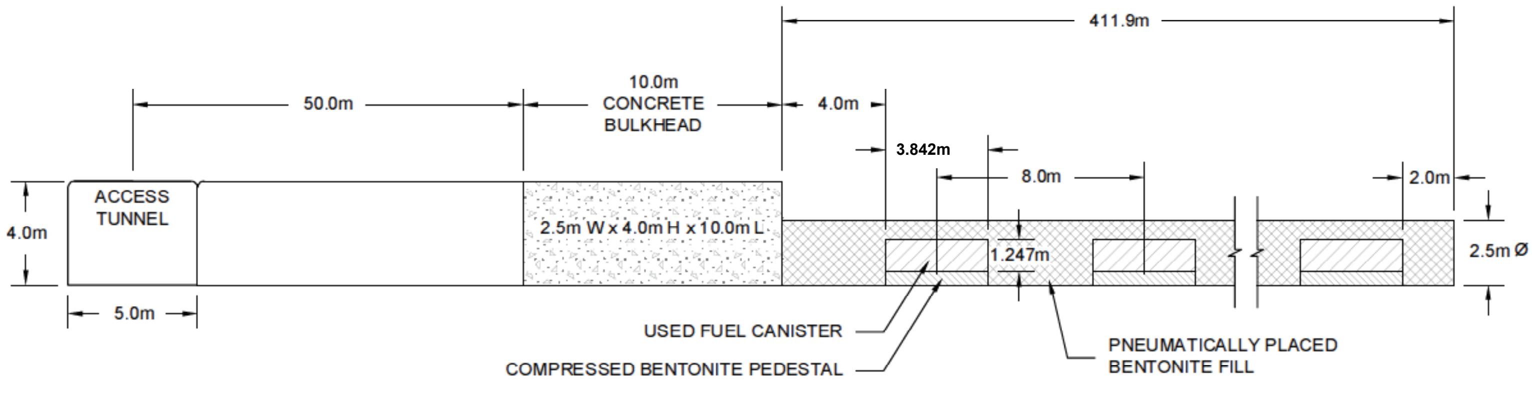

Figure 4-15: Longitudinal Section of Placement Room

4.9 Repository Construction

Repository construction will be initiated after both a safety assessment and an environmental assessment have been completed and a construction licence has been obtained for the site. Initial site preparation activities, including clearing and grading, establishing access roads and the installation of basic infrastructure systems may be conducted in advance under a site preparation licence. The site infrastructure required to support excavation, such as electrical systems, headframes, ventilation and excavated rock management systems would follow after the construction licence is obtained.

Controlled construction methods will be used to minimize disturbances to the area surrounding the facility. The three shafts will be developed using a controlled drill and blast shaft sinking approach specifically designed to minimize the excavation damage zone (EDZ).

Conventional blasting operations include drilling blast holes in a converging pattern designed to minimize the quantity of detonated explosive per volume of rock. In order to reduce damage to the perimeter of the opening, a larger number of blast holes with smaller explosive charges will be used in the outer region of the shaft. This method, usually referred to as contour wall blasting, will be used to minimize the thickness of the excavation damage zone. Between the blasting cycles, fumes will be vented, scaling will be done to remove loose rock and ground support is applied as required. This excavation method is expected to result in a rate of advance of approximately 2.5 m to 3.5 m per day.

Upon completion of the three shafts, the perimeter drifts will be excavated, defining the outline of the underground facility. The underground development required as support infrastructure will precede the development of used fuel container placement rooms. Then, development of placement room panels will be initiated along the cross-cut near the ventilation shaft and will continue in a retreating fashion towards the main shaft end of the repository. This strategy is designed to minimize any possible effects of the excavation activities on container placement operations.

Both, panel development and used fuel placement operations will move from the ventilation shaft end towards the main shaft end of the repository. Retreating towards the main shaft will minimize the need for personnel to enter or pass by completed repository areas and will ensure that all ventilation air from operating areas is routed directly to the exhaust shaft. Each placement room panel will require about 3 years for development to be completed. Placement activities in each panel are expected to require from 3.5 to 4 years. Since development and container placement operations (in different panels) will largely overlap the estimated duration of the repository operating phase is expected to be of the order of 40 years.

4.10 Repository Operation

The first step of the used fuel container placement operation will be the installation of a concrete floor and tracks that will be used to move on rails heavy equipment such as the container transfer cask. It is envisaged that the track system will be modular, consisting in rail segments pre-mounted on a steel bottom plate that will be bolted to the concrete floor. The equipment required for the container placement operations is schematically illustrated in Figure 4-16, and the sequence of operations is shown in Figure 4-17. Note that in these figures and in the description below “used fuel container” is abbreviated as UFC and highly-compacted bentonite is abbreviated as HCB.

4.10.1 Container Placement

A thin layer of bentonite will be placed at the pedestal location and compacted into place to fill any irregularities left by the excavation process. For the purpose of this description, the pedestal is considered to be a monolithic block of HCB. In practice handling requirements may require that the pedestal be made of three monolithic HCB segments. In either case, the pedestal will be transported into the placement room by rail and installed in place using a specially designed crane, which is part of the Pedestal Placement trolley.

Once the first pedestal is installed, the UFC placement cart and the shielding barrier are moved into place. A loaded UFC transfer cask will then be brought by rail from the Main Shaft area to the placement room and coupled to the shielding barrier. The doors of the transfer cask and the shielding barrier will then be opened and the UFC will be pushed, using a ram, from the transfer cask onto the UFC placement cart, which is equipped with a set of roller beds that can be adjusted to receive, raise or lower the UFC as required.

The placement cart holding the UFC will then be moved into place over the pedestal and the UFC will be lowered onto its designated position. The ram will then be retracted, the shield doors and transfer cask doors will be closed, and the empty UFC transfer cask will be returned to the shaft area. The outer shielding door will subsequently be moved into place to allow the safe backfilling of the tunnel around the UFC (see Figure 4-17, Phase 20). The current logistics for the container placement operation require that the pedestal for the next UFC be installed before the backfill is placed around the last placed UFC. The step-by-step UFC placement operation is graphically described in Figure 4-17.

4.10.2 Backfilling Operation

Once a UFC has been placed and the placement equipment removed, a segment of the bottom plate and rails will be removed to allow placement of the next pedestal. The next pedestal will then be transported to the placement room and lowered into place. Following this, the bentonite blowing equipment will be moved into the placement room and connected to services. A locomotive will be attached to the UFC placement barrier, pedestal shielding barrier and UFC placement frame. Bentonite will be continuously blown to the far end of the placement room, retreating towards the entry of the room. As bentonite injection retreats, the locomotive will retreat the shielding barrier and placement frame. These operations are described step by step in Figure 4-17.

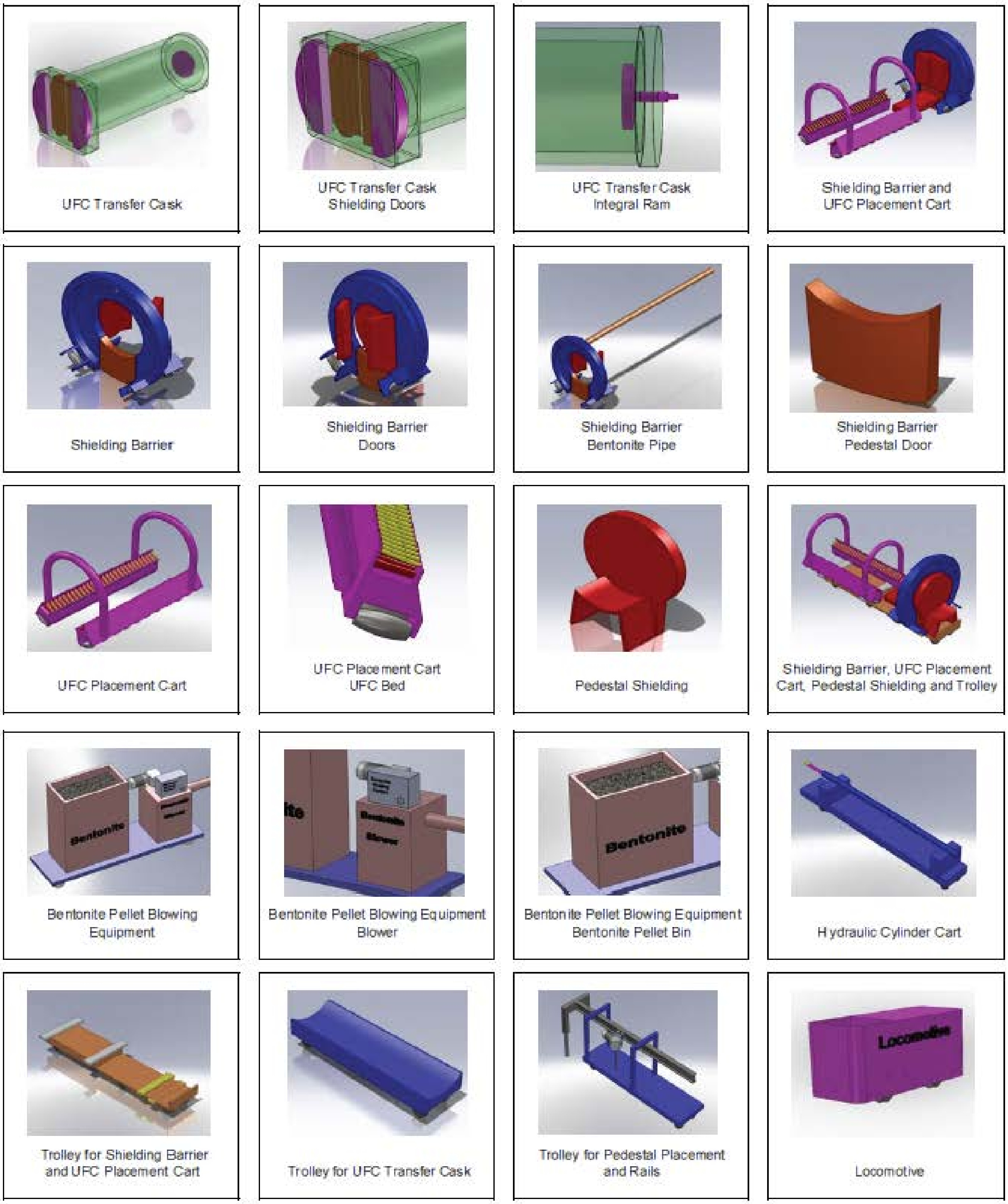

Figure 4-16: Legend for Container Placement Equipment

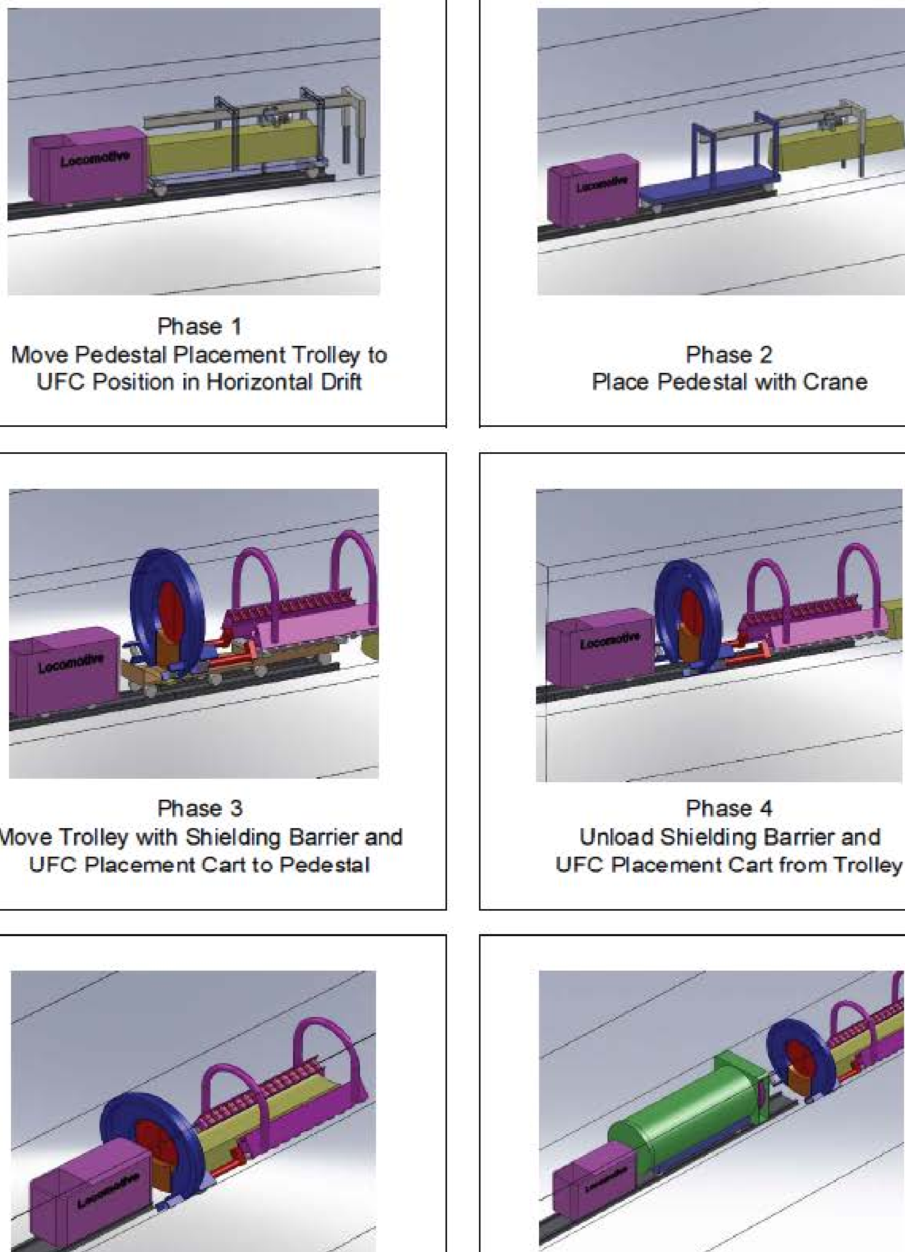

Figure 4-17: Container Placement – Sequence of Operations

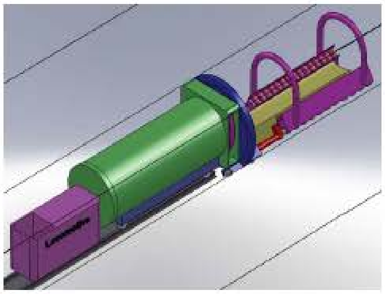

Phase 7
Connect UFC Transfer
Cask to Shielding Barrier

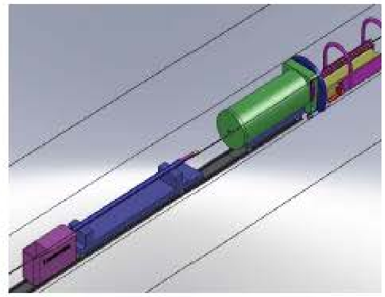

Phase 8
Move Hydraulic Cylinder Cart
to UFC Transfer Cask

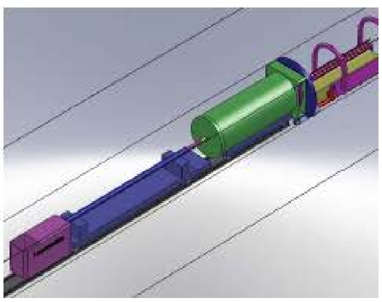

Phase 9
Connect Hydraulic Cylinder
Cart and Ram to UFC Transfer Cask

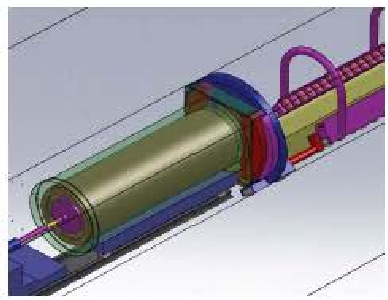

Phase 10
Open Shielding Doors on Shielding
Barrier and UFC Transfer Cask

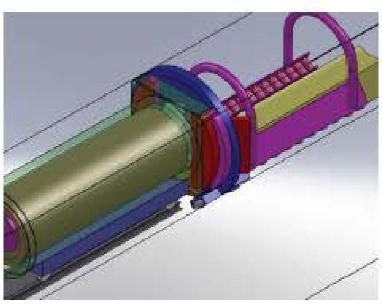

Phase 11
Postion Bed on Placement Cart
to Shielding Door and lock in place

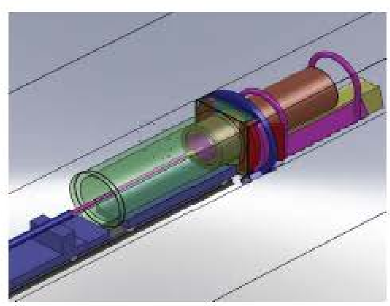

Phase 12
Use Cylinder to
push UFC onto Bed

Figure 4-17: Container Placement – Sequence of Operations (Continued)

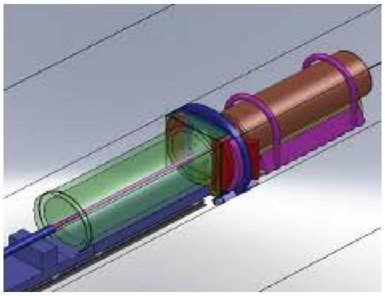

Phase 13
Unlock Placement Cart Bed and push UFC and Bed into position over Pedestal

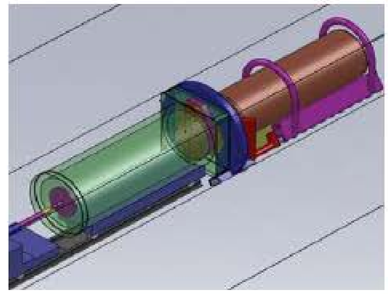

Phase 14
Retract Cylinder and close Shielding Doors on Barrier and UFC Transfer Cask

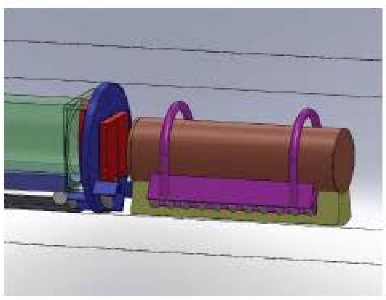

Phase 15
Lower Placement Cart Bed so UFC is placed on Pedestal

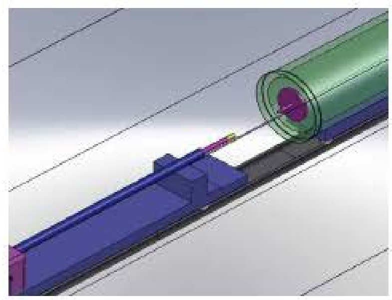

Phase 16
Remove Coupling between Cylinder and Ram

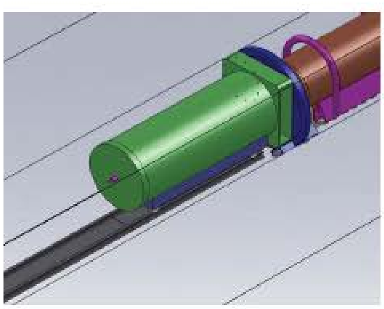

Phase 17
Remove Hydraulic Cylinder Cart

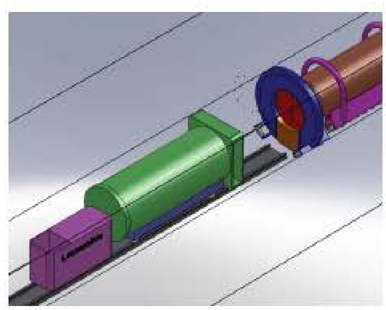

Phase 18
Disconnect UFC Transfer Cask from Shielding Barrier

Figure 4-17: Container Placement – Sequence of Operations (Continued)

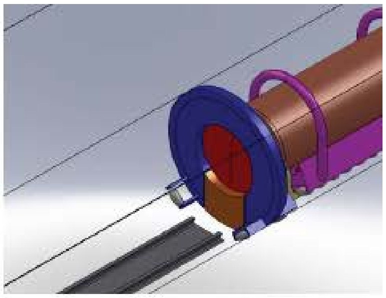

Phase 19
Move UFC Transfer Cask
and Trolley to Storage

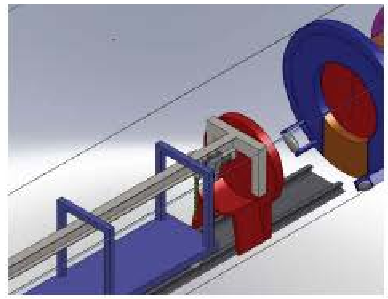

Phase 20
Using Pedestal Placement Trolley move
Outer Shielding Door to Shielding Barrier

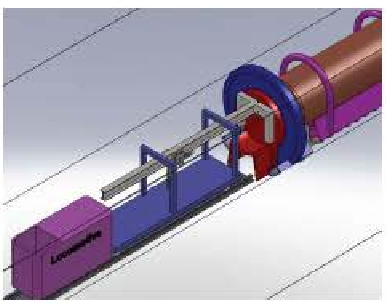

Phase 21
Attach Outer Shielding
Door to Shielding Barrier

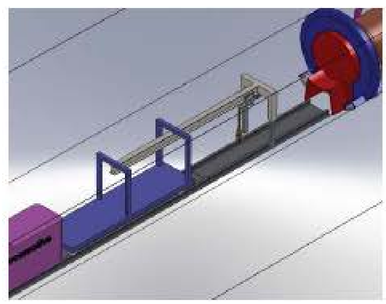

Phase 22
Position Pedestal Placement Trolley
to remove Rails and Bottom Plate

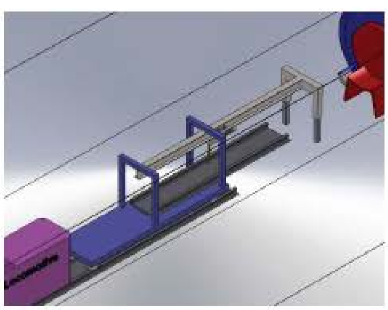

Phase 23
Lift Rails and Bottom Plate
into Cart and transfer to Storage

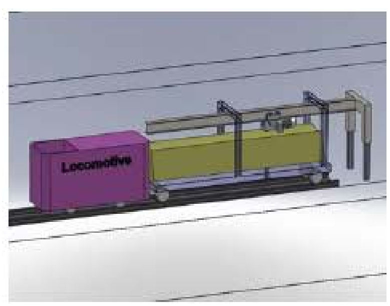

Phase 24
Move Pedestal Placement Trolley to
next UFC Position in Horizontal Drift

Figure 4-17: Container Placement – Sequence of Operations (Continued)

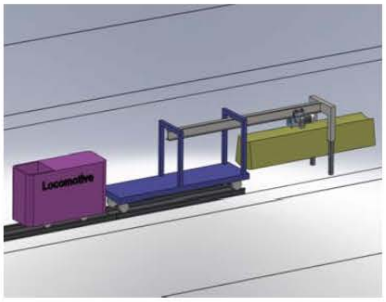

Phase 25
Place Pedestal with Crane and move
Pedestal Placement Trolley to Storage

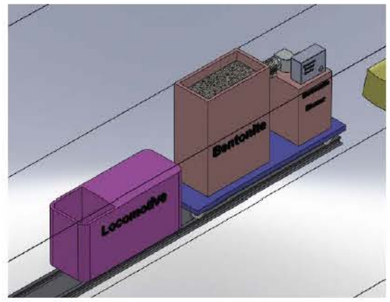

Phase 26
Move Bentonite Blowing Equipment
Cart to Shielding Barrier

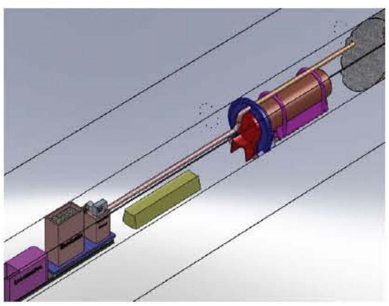

Phase 27
Connect Bentonite Blowing Equipment to
Services and blow in Bentonite Pellets

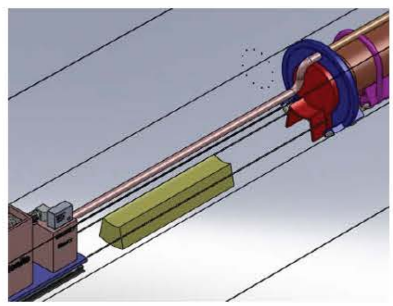

Phase 28
Connect Locomotive to
Shielding Barrier with Cable

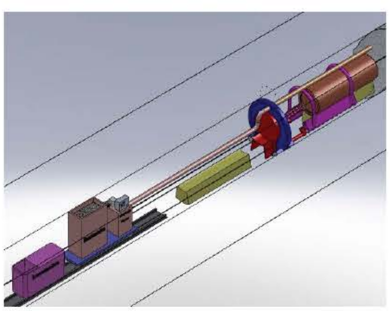

Phase 29
Move Barrier and Placement
Cart to Pedestal with Locomotive

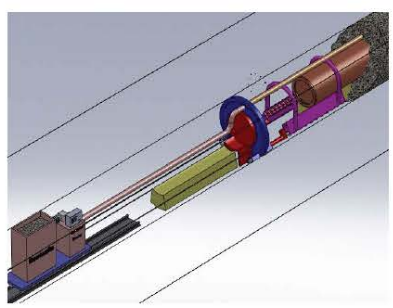

Phase 30
Continue Blowing Bentonite Pellets

Figure 4-17: Container Placement – Sequence of Operations (Continued)

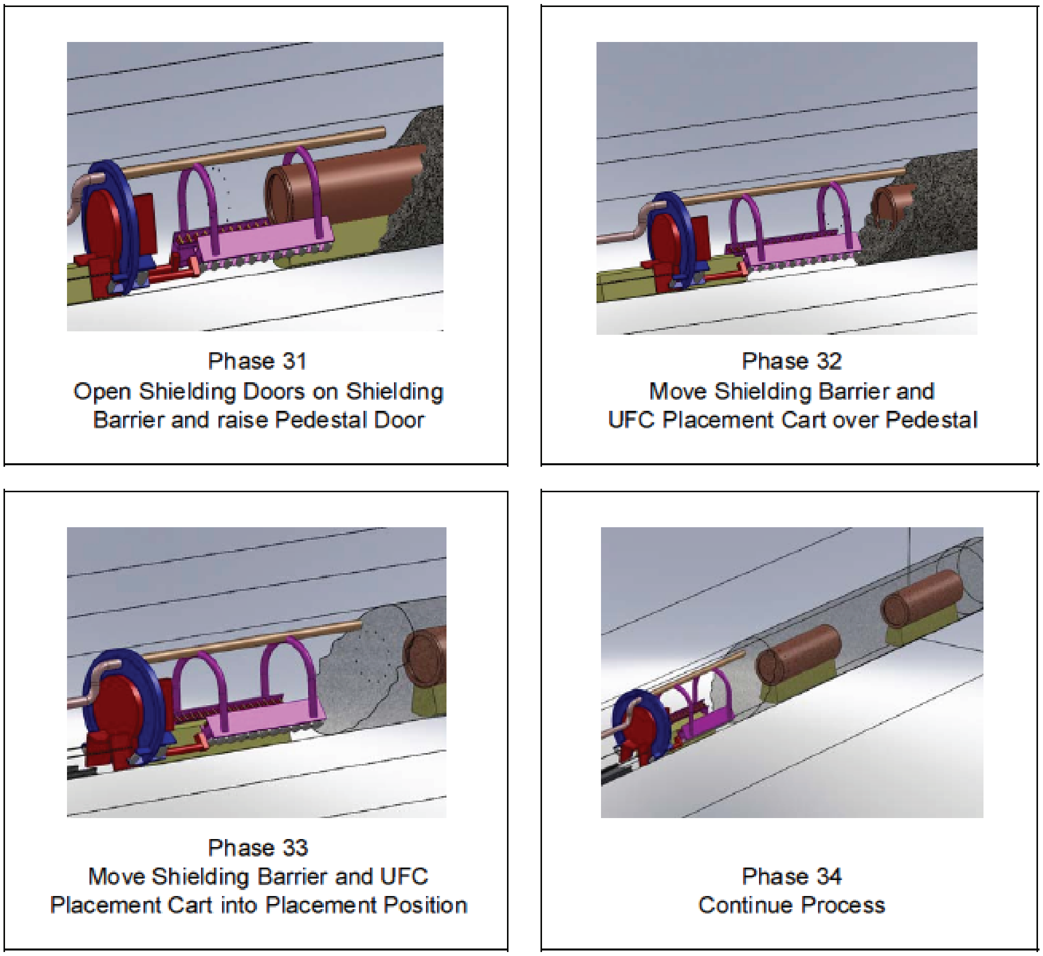

Figure 4-17: Container Placement – Sequence of Operations (Continued)

The repository operations will continue until all used fuel has been repackaged in used fuel containers, all used fuel containers are placed into placement rooms and all placement rooms sealed. The duration of the repository operational phase is expected to be approximately 40 years.

4.11 Extended Monitoring

Upon completion of all used fuel container placement activities, all placement rooms will have been sealed and closed, but the access tunnels and shafts will remain open. The facility will be placed in an extended care and maintenance program during which monitoring of the repository and surrounding geosphere will continue to confirm the performance of the repository system. The extended monitoring period could have a duration of several decades.

4.12 Decommissioning

Once the extended monitoring period has been completed, the facility will formally enter a decommissioning phase where the underground facilities will be prepared for backfilling and then backfilled and sealed from the surface. Subsequently, the surface facilities will be decommissioned and the site will be returned to a green-field condition. The repository decommissioning phase is discussed below.

4.12.1 Sealing of Underground Horizontal Openings

The sealing of underground horizontal openings consists of closing off access drifts and ancillary facilities. Such activities will commence with the preparation of exposed rock surfaces by removing loose rock before backfilling and sealing. This will be followed by removal of all remaining equipment and installations. Cross-cuts access drifts will then be backfilled, with sealing bulkheads installed at strategic locations.

The tunnels and underground openings will be backfilled using a combination of dense backfill blocks and light backfill, as specified in Section 4.6 and Table 4-6. The clay-based backfill will be complemented by strategically placed composite seals consisting of a concrete bulkhead and a clay component consisting of highly-compacted bentonite blocks (see Table 4-6) to provide a barrier to groundwater movement.

The sequence for the closure of tunnels will see first the sealing of cross-cuts and perimeter tunnels in a retreating manner from the ventilation shaft to the service shaft while maintaining open a central access tunnel. Bulkheads will be installed near access drift intersections and also near intersections with significant zones (as appropriate). The purpose of the bulkheads is to provide mechanical restraint against the forces exerted by swelling clay seals and other repository sealing systems. The bulkheads will further act to keep the sealing materials isolated in their intended positions.

4.12.2 Sealing of Shafts

Sealing of the shafts will be the last step in the decommissioning of the underground repository. This activity will start when the sealing of underground tunnels and ancillary areas is complete. At that time, the following activities will take place:

- Removal of shaft services including compressed air lines, water lines, power supply, lighting and communication cables;
- Removal of instruments and sealing from any impacted geological investigation boreholes;
- Removal of furnishings including all of the shaft guides and sets, steel support brackets, brattice and lower crash beam assemblies from bottom to top while backfilling; and
- Reaming of the shafts (as required) to remove the concrete linings and any degraded wall rock.

It is assumed that approximately 0.5 m of rock will be removed from the shaft walls to expose the sound rock. After this operation, each shaft will be re-equipped with services and staging, and backfilling will be initiated with sealing bulkheads installed at strategic locations. The proposed design for a shaft seal system is described in Table 4-7. The final design for the shaft seals will depend on the geological conditions of the site.

The purpose of removing monitoring wells and then sealing the geological borehole is to inhibit groundwater movement and contaminant transport. A combination of cement-based materials and clay-based materials with low permeability and a high swelling potential will be used as required to isolate fractured and highly permeable zones and prevent the geological boreholes from becoming preferential transport paths.

Table 4-7: Proposed Sealing System for Shafts

Depth from Surface	Material
0 – 20 m	Low-heat high-performance concrete– concrete cap at surface
20 – 150 m	70/30 bentonite / sand shaft seal compacted in-situ
150 – 170 m	Low-heat high-performance concrete for concrete bulkhead keyed into rock / overburden to a distance of 0.5 times the original radius of the shaft
170 – 330 m	70/30 bentonite / sand shaft seal compacted in-situ
330 – 380 m	Asphalt or highly-compacted bentonite seal
380 – 480 m	70/30 bentonite / sand shaft seal compacted in-situ
480 – 500 m	Concrete monolith – Low-heat high-performance concrete

4.12.3 Decommissioning of Monitoring Wells and Sealing of Geological Boreholes

A minimized administration area will be maintained during the end of decommissioning to support the post-decommissioning monitoring systems. If at that time it is felt that permanent facilities are no longer required, the monitoring systems could be supported by small enclosures for the electrical equipment, and all other remaining facilities could be removed and the site fully returned to greenfield conditions.

The facility's environmental monitoring carried out during the operational and extended monitoring periods as well as throughout the decommissioning stage may be continued following decommissioning and closure. The scope and duration of such tasks will be decided at the appropriate time by both regulatory entities and society at large.

4.13 References for Chapter 4

Baumgartner, P. 2006. Generic Thermal-Mechanical-Hydraulic (THM) Data for Sealing Materials – Volume 1: Soil-water Relationships. Ontario Power Generation Report 06819-REP-01300-10122-R00. Toronto, Canada.

Dixon, D.A., J.B. Martino and D.P. Onagi. 2009. Enhanced Sealing Project (ESP): Design, Construction and Instrumentation Plan. Nuclear Waste Management Organization Report APM-REP-01601-0001. Toronto, Canada.

Dixon, D.A., D.G. Priyanto and J.B. Martino. 2012. Enhanced Sealing Project (ESP): Project Status and Data Report for Period Ending 31 December 2011. Nuclear Waste Management Organization Report APM-REP-01601-0005. Toronto, Canada.

Holmberg, Jan-Erik, and P. Kuusela. 2011. Analysis of Probability of Defects in the Disposal Canisters. Posiva Working Reprt 2011-36. Posiva Oy, Eurajoki, Finland.

Kim, C.S., A. Man, D. Dixon, E. Holt and A. Fritzell. 2012. Clay-based Pellets for use in tunnel backfill and as gap fill in a deep geological repository: characterization of therma-mechanical properties. Nuclear Waste Management Organization Report NWMO TR-2012-05. Toronto, Canada.

Kwong, G. 2011. Status of Corrosion Studies for Copper Used Fuel Containers under Low Salinity Conditions. Nuclear Waste Management Organization Report NWMO TR-2011-14. Toronto, Canada.

Maak, P., P. Gierszewski and M. Saiedfar. 2001. Early Failure Probability of Used-Fuel Containers in a Deep Geological Repository. Ontario Power Generation Report 06819-REP-01300-10022-R00, Toronto, Canada.

Man, A. and J.B. Martino. 2009. Thermal, Hydraulic and Mechanical Properties of Sealing Materials. Nuclear Waste Management Organization Report NWMO TR-2009-20. Toronto, Canada.

NEA. 2012. The Post-Closure Radiological Safety Case for a Spent Fuel Repository in Sweden. An International Peer Review of the SKB License-Application Study of March 2011 (Final report). Nuclear Energy Agency Report NEA/RWM/PEER(2012)2. Paris, France.

NWMO. 2013. Used Fuel Transportation Package Safety Analysis Report. Nuclear Waste Management Report APM-SR-00531-0001 R000. Toronto, Canada.

Pitkänen, Jorma. 2010. Inspection of Bottom and Lid Welds for Disposal Canisters. Posiva Report 2010-04. Posiva Oy Olkiluoto, Finland.

Pusch, R. L. Börgesson and C. Svemar. 2004. Prototype Repository - Final Report (Deliverable D36). Svensk Kärnbränslehantering AB, International Progress Report IPR-04-27. Stockholm, Sweden

Sandlin, S. 2010a. X-Ray Inspection Setups for the Disposal Canister Welds. Posiva Oy Report 2009-98. Olkiluotto, Finland.

Sandlin, S. 2010b. High-Energy Radiography for Inspection of the Lid Weld in Disposal Canisters. Posiva Oy Report 2009-82. Olkiluoto, Finland.

Sandlin, S. 2010c. Defect Detectability in the Disposal Canister Lid-Weld using the 9 MeV Linear Accelerator. Posiva Oy Report 2009-84. Olkiluoto, Finland.

SKB. 2007. RD&D Programme 2007. Programme for Research, Development and Demonstration of Methods for the Management and Disposal of Nuclear Waste. Swedish Nuclear Fuel and Waste Management Company Report SKB TR-07-12. Stockholm, Sweden.

SKB. 2008. Inspection of Copper Canister for Spent Nuclear Fuel by means of Ultrasound. FSW Monitoring with Emission, Copper Characterization and Ultrasonic Imaging. Swedish Nuclear Fuel and Waste Management Company Report SKB TR-08-12. Stockholm, Sweden.

SNC Lavalin. 2011. Deep Geological Repository Design Report Sedimentary Rock Environment Copper Used Fuel Container. SNC Lavalin Nuclear Report APM-REP-00440-0002. Toronto, Canada.

Villagran, J. 2012. Used Fuel Container Retrieval from a Deep Geological Repository in Sedimentary Rock. Horizontal Tunnel Configuration. Nuclear Waste Management Organization Report NWMO TR-2012-17. Toronto, Canada.

THIS PAGE HAS BEEN LEFT BLANK INTENTIONALLY

5. LONG-TERM EVOLUTION OF THE MULTIPLE BARRIER SYSTEM

Chapters 2, 3, and 4 of this report describe aspects of the hypothetical sedimentary site, the used fuel waste form and the engineered repository design sufficient to support the presentation of an illustrative postclosure safety assessment. This chapter considers how these multi-barrier components of the system are expected to interact with each other and with the environment in the long term, consistent with CNSC Guide G-320 (CNSC 2006). Additional Features, Events and Processes (FEPs) were assessed and excluded for the reasons outlined in the FEPs report (Garisto 2013) and thus are not part of the expected evolution described in this chapter.

As noted in Chapter 1, a geosynthesis will be required as part of a safety case for a repository at a selected site. The geosynthesis provides a description of the site's past geologic evolution, its current state and potential future evolution as influenced by repository construction and external perturbations (i.e., glaciations and earthquakes). In this respect, the geosynthesis provides evidence to support an understanding of the natural geologic barriers and, in particular, their function and long-term integrity at timeframes relevant to demonstrating repository safety. In the absence of a real site and therefore a geosynthesis, a number of assumptions have been made in this report to illustrate the safety assessment approach and methodology.

The evolution of certain site parameters and conditions are presented herein to allow illustration of the type of considerations that would be given to specific aspects of the site. Table 5-1 presents general information for the key repository components, many of which were described in Chapters 2, 3, and 4. The evolution of these components are discussed in separate sections of this chapter.

The preparation of this report is consistent with the expectations of CNSC Guide G-320, which states:

> *"Early in the licensing lifecycle, it may be necessary to rely on design specifications, waste acceptance criteria, generic or default data, and assumptions to describe the waste management system in sufficient detail that its performance can be predicted. At later stages in the facility's development, as-built information and operational data should be used to refine the model of the system for assessment purposes. As with the site model, the model of the waste management system should evolve to become more realistic, and less conservative, based on real data."*

The NWMO continues technical work in a number of areas that are summarized in the NWMO's research, development and demonstration program as detailed in Crowe et al. (2013) and Villagran et al. (2011). The technical program's objectives include increasing knowledge and reducing uncertainties associated with components described in this chapter.

Table 5-1: General Parameters

PROPERTY	REFERENCE VALUE
Used Fuel	
Waste form	Used CANDU fuel bundles
Bundle	37-element standard bundle length of 495 mm (e.g., Bruce, Darlington)
Initial mass U	19.25 kg/bundle
Initial mass Zircaloy	2.2 kg/bundle
Average burnup	220 MWh/kgU
Average bundle power rating	455 kW/bundle
Minimum fuel age at placement	30 years (out of reactor)
Container	
Design	Copper outer vessel, with steel load-bearing inner vessel, bundles held in steel sleeves
Outer shell material	Oxygen-free, phosphorus-doped high-purity copper
Inner shell material	Carbon steel
Container fill gas	Inert gas installed at atmospheric pressure
Container capacity	360 bundles
Container dimensions	1.25 m outer diameter x 3.84 m long
Outer shell thickness	25 mm
Container mass	26.7 Mg loaded
Thermal output	1270 W at 30 years, 220 MWh/kgU
Temperature (outer surface)	Up to 120^{o}C
Buffer/Backfill	
Buffer design	UFC is placed on a 0.63 m high, 0.94 m wide Highly Compacted Bentonite (HCB) buffer pedestal, with the remainder of placement tunnel backfilled with 100 % bentonite gap fill (GF) pellets
Buffer material	100% bentonite clay, MX-80 or equivalent
HCB buffer density	1,610 kg/m^3 dry density
Gap fill buffer density	1,410 kg/m^3 dry density
Backfill design	Backfill is used to fill access drifts and perimeter drifts. It is primarily a dense backfill material, with gap fill used to fill remaining gaps
Dense backfill material	5% bentonite, 25% lake clay, 70% granite aggregate, 2,120 kg/m^3 dry density
Concrete	Low-heat, high-performance concrete
Buffer temperature	At a minimum, 0.3 m of buffer under 100°C
Repository	
Depth	500 m
Footprint	~6 km^2
General design	Horizontal tunnel placement, single row of containers along room centre

PROPERTY	REFERENCE VALUE
Total number of bundles	4.6 million
Total number containers	12,800
Operation phase	40 years
Extended monitoring phase	Up to 70 years (following placement of all containers)
Geosphere	
Predominant rock type	Sedimentary
Rock structure at depth	Limestone/Shale
Geothermal gradient	14°C/km
Temperature at depth	12°C (assuming land surface temperature of 5°C)
Hydraulic conductivity	$2x10^{-14}$ m/s horizontally and with $2x10^{-15}$ m/s vertically at repository horizon
Porosity	0.015 at repository horizon
Total Dissolved Solids	275 g/L at repository horizon
Surface/Biosphere	
Land surface temperature	+5°C annual average (present)
Air surface temperature	+5°C annual average (present)
Ecosystem	Temperate deciduous (present)

5.1 Long-Term Evolution of Used Fuel

A detailed description of the used fuel waste form when placed in the repository is provided in Chapter 3. The used fuel assemblies remain isolated and dry within the container. The main long-term process is radioactive decay, as long as there is no container failure, as outlined in Table 5-2. The processes in a failed container are described later.

Table 5-2: Processes with a Potential Influence on the Evolution of Used Fuel Bundles

PROCESS	POTENTIAL INFLUENCE
RADIATION	
Radioactive decay	• Production of heat, radiation and helium • Decay of radionuclides
THERMAL	
Heat transfer from fuel to container	• Change in fuel temperature
HYDRAULIC & PNEUMATIC	
None	• None
MECHANICAL	
None	• None
CHEMICAL	
None	• None
BIOLOGICAL	
None	• None

Notes: Processes listed are those that are most likely to have a notable effect on the used fuel bundles, over a time scale of one million years.

5.1.1 Radioactive Decay

When the used fuel is first removed from the reactor it is highly radioactive. This activity decreases rapidly over the first year and more slowly thereafter as shown in Figure 5-1.

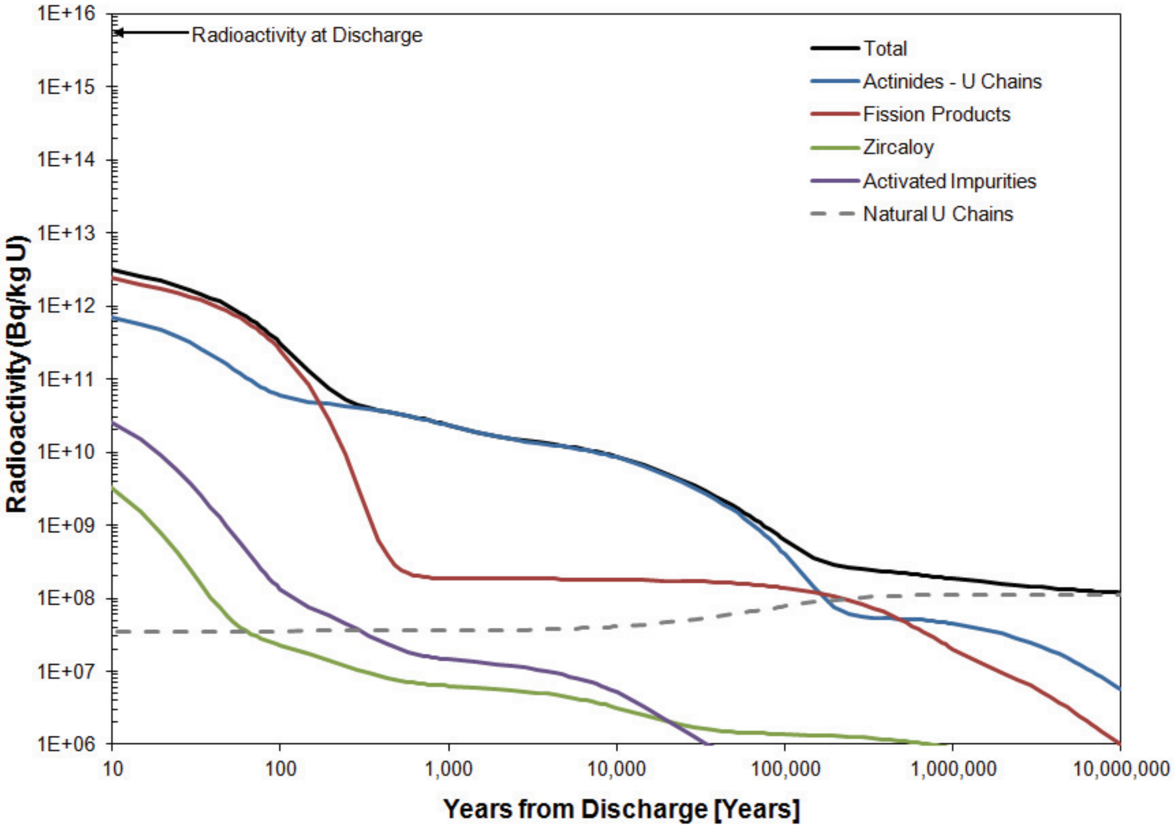

Note: U Chains represents radioactivity from uranium in fuel, including all progeny.

Figure 5-1: Radioactivity of Used CANDU Fuel (220 MWh/kgU burnup)

During the first year out of the reactor, the overall radioactivity decreases to about 1% of its initial value, and after about 100 years it decreases to 0.01% of its initial value. For the first 500 years, the total radioactivity of the fuel would be dominated by numerous short-lived fission products, most of which are gamma emitters; thereafter, it would be dominated by long-lived actinides, including uranium, many of which decay by emission of alpha particles. After about a million years, the total radioactivity in fuel would have declined to levels that are equivalent to that found in naturally occurring uranium.

Radioactive decay would gradually change the radionuclide composition of the used fuel. The radionuclide inventory, radiation output and heat output can be calculated as a function of time, as illustrated in Figure 5-2 for the radionuclide inventory. The greatest change in the composition of the used fuel is a pronounced decrease in fission products after about 500 years. Nevertheless, over a million-year timeframe all of the changes resulting from radioactive decay would represent only a modest change in the composition of the fuel, of which about 98% would persist as uranium and oxygen.

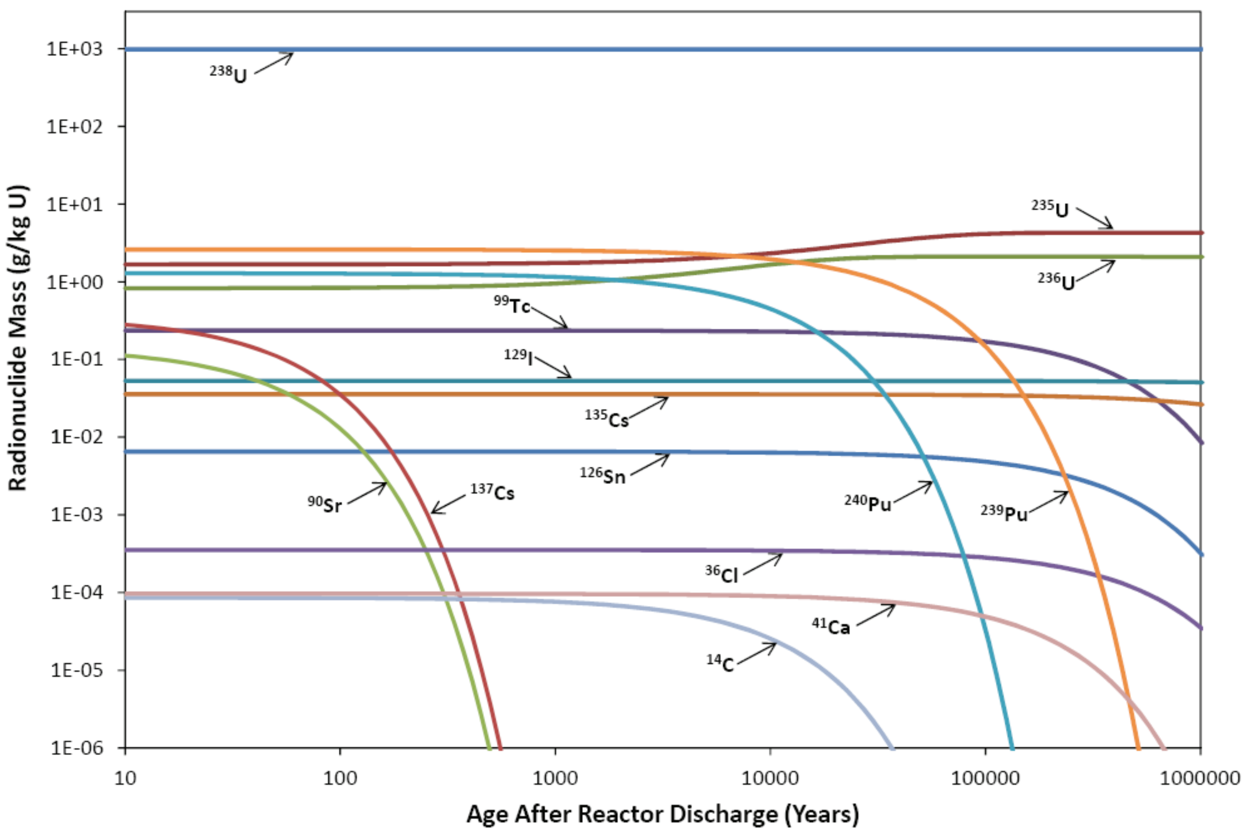

Note: Figure is based on data taken from Tait et al. (2000).

Figure 5-2: Amounts of Key Long-Lived Radionuclides in Used Fuel (220 MWh/kg U burnup)

5.1.2 Changes in Temperature

Radioactive decay of the fuel is accompanied by alpha, beta and gamma radiation that is largely absorbed by the fuel itself and converted to heat. Immediately after being removed from a power reactor, a reference used fuel bundle would release about 27,000 watts of heat. This heat output rapidly decreases. After 10 years, the thermal output has decreased to 5.4 watts and after 30 years about 3.5 watts. The minimum used fuel age at the time of placement is 30 years out of reactor.

Figure 5-3 illustrates the time dependence of thermal power for a container with 360 fuel bundles. Around 10,000 years after placement, the heat output of the entire container would be approximately that of a single 60-watt light bulb. It may be noted that the heat output of the used fuel after 10 years is low enough that the containers can be passively cooled; that is, they do not require active water cooling.

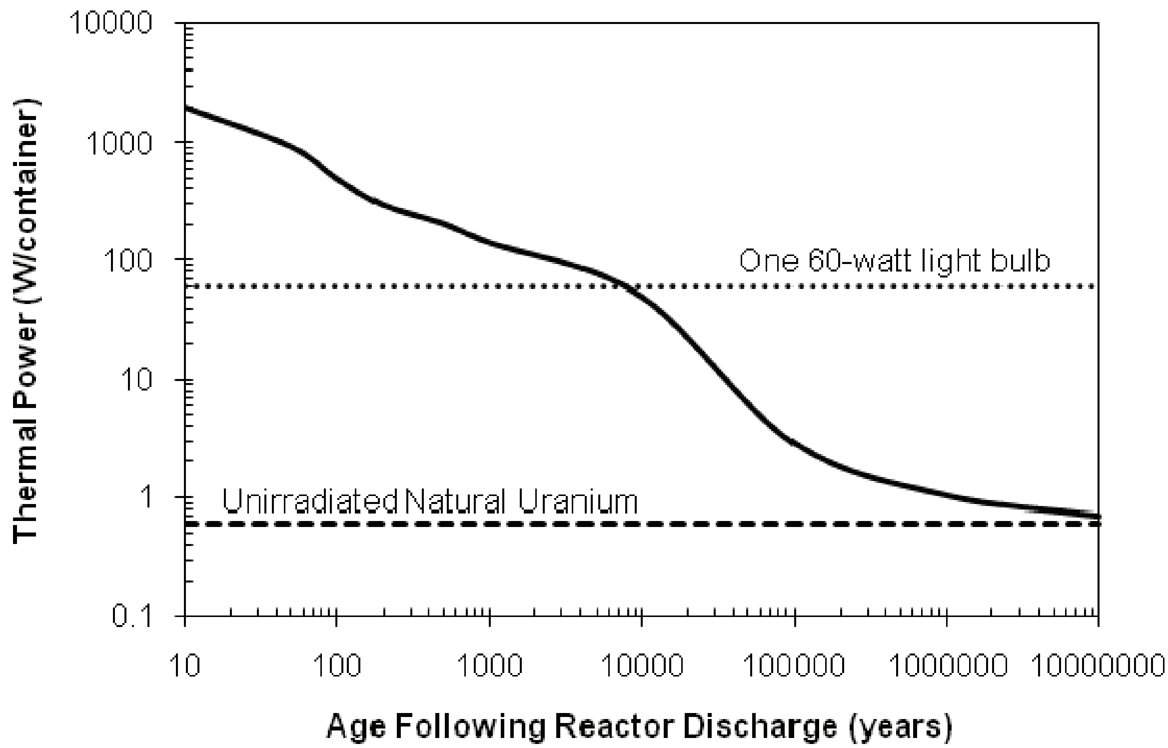

Figure 5-3: Heat Output of a Used Fuel Container with 360 Used Fuel Bundles

The temperature of the container's outer surface will increase up to 120°C after placement (see Section 5.2.4). The temperature of the used fuel bundles inside the container is determined largely by the internal container design, which transfers heat from the bundles to the container surface. The used fuel temperature inside the reference container, loaded with 30-year-cooled used CANDU fuel, would not exceed 200°C. Temperature measurements of used fuel inside concrete storage containers suggest that, more likely, the interior temperature would be less than about 150°C. The maximum temperature of the used fuel bundles would be attained within about 30 years after placement in the repository.

5.1.3 Changes in the UO_2

In the dry, inert gas environment inside the sealed containers, there are few processes that would significantly alter the condition of the used fuel assemblies, even over long times.

5.1.3.1 Radionuclide Diffusion

The crystalline structure of the UO_2 would experience radiation damage due to alpha-recoil during storage and after placement in a repository, and temperatures would not be high enough to ensure annealing of the damage. Radiation damage has the potential to increase the rate at which gaseous species diffuse through the UO_2 fuel; however, theoretical and experimental assessments (Ferry et al. 2008) indicate that this effect is small and there is little redistribution of radionuclides within the fuel under repository conditions.

5.1.3.2 Changes in the Oxidation State of Fuel

In some cases, radioactive decay results in the formation of an element with a higher oxidation valence than that of the parent radionuclide. In principle this could modify the oxygen potential and oxidation state of the UO_2 matrix, in turn affecting diffusion coefficients for radionuclides. Thermal diffusion coefficients of radionuclides are small at repository temperatures, but increase as the oxygen/metal (O/M) ratio of the fuel increases. However, any changes in CANDU fuel are expected to be quite small, from O/M ~ 2.001 to 2.010 or less, and this would not significantly affect thermal diffusion coefficients.

The oxidation state of the fuel potentially could also be changed by the reaction of UO_2 and Zr to produce ZrO_2, which is more stable thermodynamically than UO_2. Where the cladding and UO_2 are in direct contact, the Zr eventually would reduce UO_2 to U by solid-state diffusion of oxygen atoms. This process is unlikely to be significant for used fuel due to the small amount of Zr present (10% of UO_2) and very slow solid-state diffusion rates at repository temperatures (McMurry et al. 2003).

5.1.3.3 Build-Up of He Gas

Alpha decay results in the formation of helium (He) atoms in the used fuel. Because helium is stable (non-radioactive) and unreactive with other elements, the total amount of helium gas in the fuel elements would increase over time. Figure 5-4 compares the effective volume of helium gas that would be produced in a CANDU fuel element with the volume of fission gases (essentially the radionuclides of the noble gases Kr and Xe) present in the same element, assuming that none of the gases are retained in the UO_2 matrix. The fission gases formed during irradiation in the nuclear reactor, and their amount (except for radioactive decay) would be constant over time. In contrast, after about 30,000 years, the amount of helium would be equal to that of the fission gases, so that the total amount of gas present would be double that of the initial conditions. After about one million years, the rate at which helium was being produced in the fuel would slow to a value corresponding to the decay of natural uranium and its progeny, but the total amount of helium within the fuel element would continue to increase.

Under repository temperatures, He release from the UO_2 grains to the grain boundaries would be relatively low, so that helium would accumulate within the grains. For low burnup fuel (like CANDU fuel), the quantity of He produced is not sufficient to induce micro-cracking of grains (Ferry et al. 2008), which is the first step before any significant He release to grain boundaries occurs. Thus, the microstructure of CANDU fuel should not significantly evolve with He accumulation, and build-up of He gas within the void volume of the fuel element would not occur (see also Section 5.1.4.1).

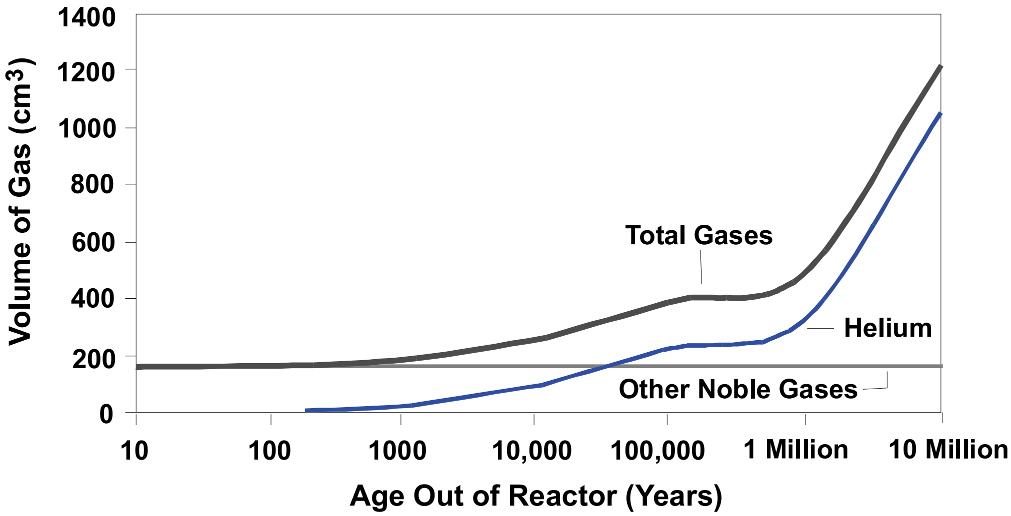

Note: Figure from McMurry et al. (2003).

Figure 5-4: Equivalent Volume of Gas at Standard Temperature and Pressure Produced in a CANDU Fuel Element (220 MWh/kgU burnup)

5.1.3.4 Alpha Radiation Damage

During radioactive decay, the crystalline matrix of the used fuel would experience localized damage to the crystal lattice from the emission of alpha particles, which travel only short distances from the nucleus but have high energy and a relatively large mass. The implications for radionuclide diffusion have been discussed above.

Natural analogue evidence suggests that alpha irradiation damage would not cause used fuel to crumble, even after extremely long times. At Oklo in western Africa, uraninite (UO_2) ore deposits underwent spontaneous nuclear fission reactions more than two billion years ago. Although affected by brecciation during fission and by subsequent hydrothermal alteration in some cases, the uraninite is still granular and massive (Jensen and Ewing 2001).

5.1.4 Changes in the Zircaloy Cladding

Intact cladding would provide a further barrier to water contacting the fuel or to radionuclide release. A summary of relevant work associated with changes in the Zircaloy cladding is presented below. Some of the changes could lead to cracking or rupture of the cladding. However, even if it occurred, the cracking or rupture of the cladding inside a sealed container would have few consequences. Helium from alpha decay and fission gases would, for example, merely be released into the larger volume of the container interior, and the fuel pellets would be exposed to the inert gas atmosphere inside the container. Although cracked, the cladding itself would continue to provide physical support to most of the used fuel pellets in the fuel element.

5.1.4.1 Zircaloy Creep and Rupture

The most significant physical process potentially affecting the cladding over time is likely to be long-term creep of the Zircaloy, as caused by stresses created by pressure build up inside the sealed fuel elements due to the decay-related production of helium gas. The mechanisms and extent of creep processes in Zircaloy are uncertain. Most creep data for cladding are from high stress, short-term experiments (McMurry et al. 2003).

Conservative calculations, assuming the He gas migrates to the fuel-cladding gap, suggest that given sufficient time, the gas pressure inside the sealed fuel element would increase to the point that the Zircaloy cladding would rupture. However, as indicated in Section 5.1.3.3, it is unlikely that the He would escape from the fuel grains and increase the pressure within the cladding. Hence, He generation should not lead to rupture of the Zircaloy cladding on relevant time scales.

5.1.4.2 Uniform Corrosion (Oxidation) of Cladding

The corrosion properties of Zircaloy cladding have been determined from almost 50 years of experience with reactor operation, pool storage, and dry storage of used fuel. When Zircaloy is exposed to air, a thin passive zirconium oxide film forms rapidly on its surface which then inhibits further corrosion. Experiments were conducted that examined the condition of used CANDU fuel under dry storage conditions over several decades. It was found that the average outer and inner surface zirconium oxide thickness, after 19 years of dry air storage at seasonally varying temperatures, was about 6 μm, slightly more than an average pre-storage oxide layer thickness of about 4 μm. Therefore, most of the uniform corrosion of the Zircaloy would have occurred prior to placement (McMurry et al. 2003). Shoesmith and Zagidulin (2010) also indicate that passive corrosion rates of Zircaloy would be very low.

The fuel containers are filled with an inert gas. In the absence of oxygen, further growth of a uniform oxidation film on the cladding cannot occur.

5.1.4.3 Hydrogen Absorption and Zircaloy Embrittlement

As-fabricated Zircaloy cladding has a residual hydrogen concentration of about 25 μg/g. After use in a CANDU reactor, the cladding also contains up to about 100 μg/g of deuterium, absorbed in-reactor from the heavy water coolant, in addition to trace amounts of tritium. The hydrogen precipitates as zirconium hydrides in the Zircaloy after the fuel is removed from the reactor and cools. The hydrides result in a less ductile (more brittle) Zircaloy that is more susceptible to fracturing (McMurry et al. 2003).

In intact used fuel containers that had been dried and backfilled with an inert gas prior to sealing, little or no hydrogen would be available for reaction with the cladding after placement. Small amounts of H_2O may be present as residual humidity or as liquid water (e.g., in defected fuel elements). Hydrogen would be released from this water via radiolysis or as the water was consumed by corrosion of the steel interior of the container, which could be absorbed by the Zircaloy and also increase the amount of hydrides present.

5.1.4.4 Delayed Hydride Cracking

The main factors required for delayed hydride cracking are sufficient tensile stress, a defect site to concentrate the stress, and sufficient hydrogen in the metal. Even where hydrogen is distributed in relatively low concentrations in Zircaloy, under certain conditions of stress and temperature the hydrogen can diffuse through the metal to form locally high hydrogen concentrations that lead to the precipitation of zirconium hydrides. These hydrides are brittle and tend to crack.

Detailed examination of used CANDU fuel stored in dry air at 150°C for 15 years indicates that highly stressed areas in the cladding must be present for delayed hydride cracking to occur. Generally, the most stressed areas in cladding are the heat-affected zones at and near welds. The timing and extent of delayed hydride cracking in a repository would be controlled by diffusion of hydrogen to the crack tip. The susceptibility of cladding to delayed hydride cracking is unlikely to be significant at temperatures inside the container (Freire-Canosa 2011).

5.1.4.5 Stress Corrosion Cracking

Stress corrosion cracking of zirconium metal occurs in oxidizing environments, in strongly oxidizing neutral saline solutions, and in the presence of some metals and gases such as cesium and iodine. Little work has been directed towards the study of stress corrosion cracking of Zircaloy under conditions such as would occur in a deep geological repository. However, the dry environment inside an unbreached container would not contain sufficient quantities of strongly oxidizing agents (such as nitric acid or hydrogen peroxide) or of iodine gas from fuel elements to induce stress corrosion cracking (McMurry et al. 2003). Moreover, CANLUB inhibits the diffusion of iodine into the Zircaloy. In addition, in CANDU fuel almost all of the iodine in the fuel gap is present as cesium iodide (CsI) and so is unable to form the zirconium iodides that are thought to be the chemical precursors of stress corrosion cracking (OPG 2002).

5.1.4.6 Pellet Swelling and Cladding "Unzipping"

Cladding "unzipping" is driven by the expansion of a fuel pellet (pellet swelling) in proximity to a defect in the cladding, causing a strain in the cladding that extends the size of the defect. If the two processes (i.e., swelling and rupture) perpetuate each other, the deformation would propagate in increments over time ("unzipping"). One example of this phenomenon occurs when water enters a fuel element through a pinhole defect and reacts with the fuel, transforming the UO_2 into the less-dense phase U_3O_8. The additional stress exerted on the defect site by the expansion in the volume of the pellet then leads to further cracking of the cladding. More water is then able to enter the fuel element, which in turn leads to more alteration, more swelling, and further deformation of the cladding. In intact containers, there would be no source of water to initiate pellet swelling, so unzipping by this process can be disregarded.

5.1.5 Other Processes

Several other processes expected to have minimal or no effects on the evolution of the used fuel are indicated below.

5.1.5.1 Criticality

Criticality is not an issue for several reasons, the most important of which is that CANDU fuel cannot become critical without the presence of heavy water, regardless of the density or age of the fuel. Ordinary water is insufficient to induce criticality. Moreover, water would have no access to the used fuel in intact containers and so it could not act as a moderator.

5.1.5.2 Hydraulic Processes

As long as the containers remain intact, there are no hydraulic processes affecting the used fuel assemblies.

5.1.5.3 Mechanical Stresses

As long as the fuel bundles are supported by baskets in intact containers, they are not subjected to significant load-bearing stresses. If tremors associated with earthquakes caused the fuel bundles to vibrate sufficiently, presumably some of the fuel pellets or the cladding could be damaged. The damaged material would remain in an intact container, and the overall evolution of the used fuel bundles would not be significantly changed.

5.1.5.4 Biological Processes

No changes arising from biological processes are expected because the combination of high temperatures, significant radiation fields, and the absence of water and organic carbon would exclude any biological reactions inside a container.

5.1.6 Confidence

At the time of placement in a deep geological repository, the physical properties of the used fuel and the inventory of radionuclides would be well characterized. Radionuclide decay constants are generally well defined, and so the changes in the inventory and the related changes in decay heat over time can be calculated with a high degree of confidence.

The rates of several processes, such as the diffusion of helium in UO_2 and of hydrogen in Zircaloy, are influenced by temperature. These rates would be low since the temperature inside the container would be at most several tens of degrees hotter than the exterior container surface, which would only increase up to 120°C, and drop to ambient host rock temperatures on a 100,000 year timeframe.

In the dry and closed-system environment provided by an intact and load-bearing container, the physical condition of the fuel is not expected to change significantly over long periods of time. The only significant factor would be container failure, which is discussed later.

5.2 Long-Term Evolution of the Repository Environment

5.2.1 Repository-Induced Disturbances

Disturbances to the geosphere as a result of construction and operation of a repository include those induced by excavation (damage to surrounding host rock and development of unsaturated conditions within the host rock) and due to placement of the waste and engineered systems, including temperature changes, changes to near-field chemistry and potential gas generation. These processes are summarized in Table 5-3.

Table 5-3: Processes with a Potential Influence on the Near-Field Geosphere

PROCESS	POTENTIAL INFLUENCE
RADIATION	
None	• None
THERMAL	
Heat transport from repository	• Increased porewater pressure in rock around repository • Altered hydraulic conductivity around repository
HYDRAULIC & PNEUMATIC	
Excavation-related drawdown along shaft and access tunnels	• Temporary desaturated, oxygenated zone around vault
Groundwater flow	• Saturation of repository • Mass transfer of aqueous chemical species at repository interface
MECHANICAL	
Excavation of shaft and rooms	• Formation of higher permeability excavation damaged zone in shaft and rooms
Thermal stresses	• Microcracking
CHEMICAL	
Reactions with redox-sensitive minerals	• Initial partial oxidation of some minerals • Long-term maintenance of reducing conditions at repository depth
Reactions with repository porewater	• Precipitation of secondary minerals near interface • Steel corrosion and gas generation
BIOLOGICAL	
Microbial activity	• Maintenance of redox conditions at repository depth

Notes: Processes listed are those that are most likely to have a notable effect on the near-field geosphere, over a time scale of one million years.

5.2.2 Excavation Damaged Zone

The zone of rock immediately surrounding the placement rooms, tunnels, shafts and other underground openings that is mechanically disturbed during excavation is referred to as the excavation damaged zone (EDZ). This zone is characterized by structural changes in the rock, such as the formation of microcracks, along with a potential increased permeability. The shape, extent and properties of this zone depend on factors such as the nature of the host rock, the ground stress regime, the geometry of the excavation, the excavation method and the strength of the rock. A summary of EDZ classification and in-situ observations in sedimentary rock is described in a literature review conducted by Fracture Systems (2011).

In tunnels constructed using drill-and-blast techniques, the explosive charge density has been shown to influence the extent and severity of damage in the near-field. There is evidence to suggest that connected permeability associated with blast-induced damage may not be continuous across blast rounds in environments with a high strength to stress ratio (Fracture Systems 2011, Simmons 1992). This is also supported by recent in-situ work in crystalline rock (Posiva 2010). Because the EDZ behaves hydraulically as a serial system, a local increase in EDZ permeability does not translate to a continuous zone of connected high permeability along the axes of shafts and tunnels.

For the sedimentary sequence considered in this report (Chapter 2), the maximum EDZ is expected to occur in the weak Cabot Head shale and is anticipated to be about a half of the shaft excavation diameter (NWMO 2011). Fracture Systems (2011) found that regardless of the damage mechanism, the extent of EDZ measured around underground openings is typically less than 1.5 times the radius of the openings. Smaller EDZ extent would occur around the emplacement rooms within the stronger host rock of the Cobourg Formation.

Perturbations to the geosphere, such as glaciation and earthquakes (see Section 5.5), are not expected to have any major structural effects on the long-term behaviour of the EDZ due the confining pressure of the backfill materials. The EDZ may also have some tendency to seal itself over time in rock formations with high clay content - several mechanisms, including the impact of increased stress on the EDZ due to swelling of backfill materials, are discussed in Bock et al. (2010). These mechanisms would be assessed for a specific site.

5.2.3 Repository Saturation

During the construction and operational phases, groundwater inflows into the excavations will be managed through pumping. At a depth of 500 m below the surface, the hydrostatic pressure within a water-saturated rock mass is about 6 MPa. A sharply defined hydraulic gradient would exist between the geosphere at repository depth and the excavated openings (rooms, cross-cuts and drifts), which would be at atmospheric pressure. This difference would tend to draw porewater through the host rock into the open spaces of the repository. However, porewater movement through the low permeability, low porosity host rock considered in this study is expected to be extremely slow.

Any groundwater seeping into the repository from the surrounding rock will be pumped away to maintain dry conditions within excavated openings. Evaporation would tend to keep the rock surfaces in the excavated openings dry, and may induce partial desaturation of the rock immediately adjacent to the openings (i.e., within the excavation damaged zone and host rock near the repository). Any dewatering during operation and monitoring of the repository will be of relatively short duration and will result in groundwater flow(s) toward the repository until pumping activities cease following repository closure. In the postclosure phase, water will move towards the repository and the near-field will slowly resaturate.

The process of saturation may require a long time, as ingress of water may be restricted because of low host rock permeabilities and the use of grouting and seals. Furthermore, the rate of resaturation will likely vary at different locations within the repository. In particular, local heating from the containers, swelling of buffer materials, and local gas generation could delay resaturation. A "pre-saturated period" can be defined, which covers the time period from when the containers are first placed in a repository until their exterior surface comes in contact with fully saturated sealing materials. In low permeability sedimentary rock, it is likely that this pre-saturated period would last at least 10,000 years (see Section 5.4.1).

At the time that the placement rooms are backfilled and sealed, they would contain partially saturated buffer. Voids (porosity) in the sealing materials would contain trapped air. Heat from the container would cause the nearby buffer to dry out, and condensation of the water vapour would occur in cooler portions of the buffer near the rock. The relative humidity of the trapped air in the sealing materials near a container is of interest because corrosion of copper and iron in air is observed to be slow or nonexistent at relative humidities of less than about 60%.

5.2.4 Temperature

Among the first changes to occur in a repository after container placement is an increase in temperature of the sealing materials around the containers. The exact distribution and time dependence of temperatures in a repository depends on design details and site-specific conditions.

Figure 5-5 shows an example of thermal profiles for a region around a used fuel container placed in a limestone setting (horizontal tunnel placement). A range of points from the exterior surface of a container out through the buffer and into the near-field rock is illustrated.

Key points to note in Figure 5-5 are:

- The temperature of sealing materials adjacent to the surface of the container increases rapidly at first, within days or weeks of placement.
- The maximum temperature of the buffer occurs within the first 30 years and remains below 120°C. More than 0.3 m of the buffer remains below 100°C.
- Within about one hundred years, reflecting in part the decay of the heat source, there is an appreciable reduction in peak temperatures.
- After several thousand years, the thermal evolution is marked by a slow, steady cooling. Temperatures return to near-ambient conditions within about 100,000 years.

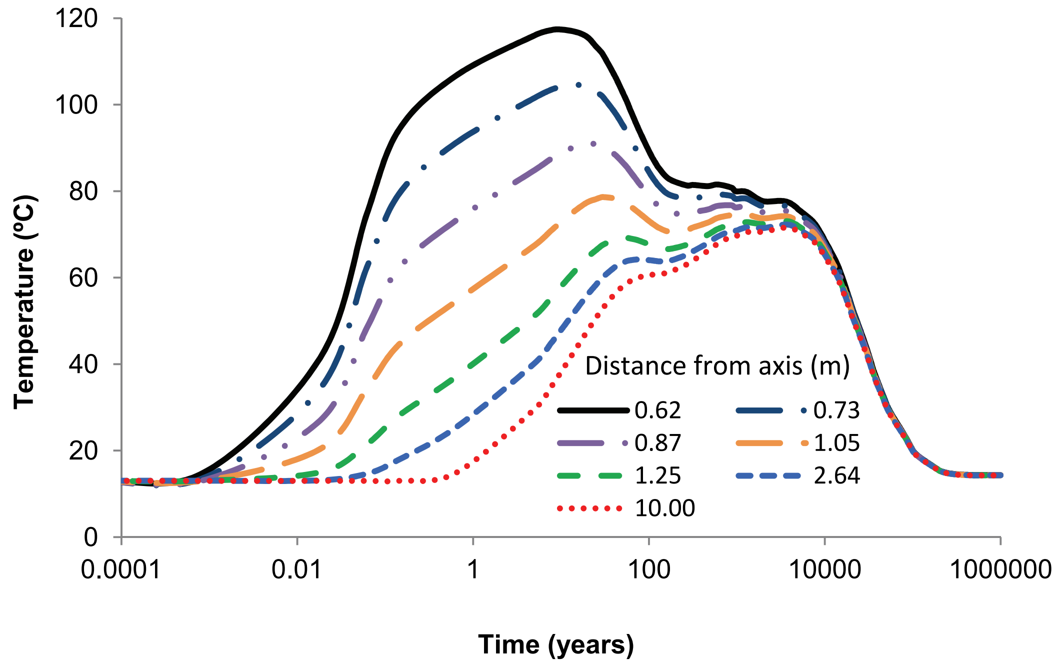

Note: Figure from Guo (2010). The solid black line is the container surface and the dashed green line is the rock wall.

Figure 5-5: Illustrative Example of the Range of Temperature Variation over Time in a Placement Room

5.2.5 Near-Field Chemistry

During repository excavation and operations, oxidizing conditions would develop in the porewaters of the adjacent rock due to exposure to the air in the repository. This could result in some oxidizing reactions, such as partial conversion of sulphides in the rock into sulphates.

However, after the rooms are closed and sealed, the redox conditions within the near-field will evolve back to an anaerobic state. Oxygen is consumed by a number of reactions, including reactions with residual iron in the rooms (e.g., rock bolts) and with copper on the containers (Reaction (5-1)), as well as by reactions with microbes and with redox-sensitive materials throughout the buffer.

$$Cu + Air \rightarrow Cu_2O, CuO \qquad (5\text{-}1)$$

Most of the repository-related changes in groundwater chemistry would occur at or near the interface between the geosphere and the sealing materials. The diffusion of porewater components, or the mixing of fluids at the repository-geosphere interface, may result in the precipitation of secondary mineral phases at the interface or in nearby fractures in the geosphere. A broader effect would be due to heat from the repository, which would raise the temperature of water in the geosphere. This could result in a slightly greater dissolution rate for some minerals. Later, as the waters cool, the precipitation of secondary phases, such as amorphous silica and calcite, would occur. The extent and significance of the precipitation would depend on site-specific characteristics, such as the distribution and dimensions of the fractures. In the long term, the geosphere, as a whole, would act as a strong buffer in response to chemical and thermal perturbations from a repository. As the pore fluids in the repository evolve to a composition more similar to that of the surrounding groundwater, and as temperatures in the geosphere gradually return to ambient levels, the chemical conditions in the geosphere would be diminishingly affected by the presence of a repository.

5.2.6 Steel Corrosion and Gas Generation

In principle, corrosion of carbon steel (C steel) in underground facilities has a number of potential impacts on the performance of the repository system. Dissolved ferrous species produced as a result of corrosion reactions can interact with bentonite and convert swelling smectite clays to non-swelling illitic forms, resulting in a partial loss of swelling capacity (Wersin et al. 2007). Anaerobic corrosion will result in the generation of hydrogen that may form a gaseous H_2 phase in the repository, which will affect repository pressures and may impact the migration of radionuclides. This latter effect may impact the viability of some microbial species, favouring anaerobic species that can use hydrogen as an energy source.

Accordingly, this section is focussed primarily on the estimation of the rate of H_2 generation due to corrosion of the carbon steel in the repository. In the normal evolution of a repository, this process is relevant because of the presence of steel structures such as rock bolts, supports or other infrastructure that is necessary for the safe construction of a repository; clearly, this presumes that such steel is left behind after used fuel container placement.

Owing to the very low gas transport that can occur in Canadian sedimentary environments, the steel corrosion processes have been examined in great detail below. The volume of steel available for corrosion within the normal evolution scenario is sufficiently small that the relatively small quantiy of hydrogen gas produced does not have the potential to alter the repository characteristics. However, because of the use of carbon steel as a container material, the impact of hydrogen generation on the repository is considered within the All Containers Fail scenario in Chapter 8.

The corrosion behaviour of the steel components will change with time as the environment in the repository evolves. From a corrosion perspective, the most important environmental factors are the temperature, the redox conditions, the degree of saturation of the repository material, and the composition of the pore water in contact with the steel components. For a DGR in low-permeability sedimentary host rock, saturation of the DGR may take tens of thousands of years. This slow saturation has led to the definition of four phases in the evolution of the environment, as described below, as well as in detail within other NWMO references (Suckling et al. 2012 and King 2013).

Phase 1

An early aerobic period prior to the onset of aqueous corrosion. Immediately following closure of the repository, it is assumed that saturation of the Engineered Barrier System (EBS) has not yet occurred, that no liquid water is available for corrosion, and that the EBS near the UFCs remains unsaturated due to high temperatures and gas generation. Oxygen is initially present in the in the unsaturated pore space when the EBS is emplaced. If relative humidity is also low, corrosion will be limited to slow air oxidation. This unsaturated aerobic corrosion is modelled as follows:

$$4Fe + 3O_2 \rightarrow 2Fe_2O_3 \quad (5\text{-}2)$$

$$R_1 = \frac{A_1 \exp\left(-\frac{5864}{T}\right)}{t^{1/2}} \ \mu m \cdot a^{-1} \quad (5\text{-}3)$$

where R_1 is the rate of corrosion in microns per year, T is the Kelvin temperature, and t is the time in years and the pre-exponential term A_1 is assigned a best-estimate value, as well as lower and upper bounds. Although there are relatively few data available, it is not unreasonable to expect that the lower and upper bound corrosion rates might differ by a factor of ten. In the absence of other information, it is assumed here that the best-estimate value is the (geometric) mean of the lower and upper bound values. Thus, the values of A_1 for the lower and upper bound estimates are 4.279×10^5 μm/a and 4.279×10^6 μm/a, respectively (King 2013). Aqueous corrosion is possible above a critical or threshold relative humidity (RH) that is determined by the nature of the surface and the presence of surface contaminants. As relative humidity increases above a lower threshold value, the consumption of carbon steel by Phase 1 corrosion will decrease until an upper RH threshold is reached, upon which Phase 1 corrosion stops. For this work, the lower RH threshold was set to 60% and the upper RH threshold was 80% (Suckling et al. 2012).

Phase 2

An unsaturated aerobic phase following the condensation of liquid water on the steel surface. During Phase 1, if relative humidity rises above 60-80%, aerobic aqueous corrosion may instead proceed according to the following relationships:

$$4Fe + 3O_2 + 2H_2O \rightarrow 4FeOOH \quad (5\text{-}4)$$

$$R_2 = A_2 \exp\left(-\frac{1340}{T}\right) \ \mu m \cdot a^{-1} \quad (5\text{-}5)$$

where A_2 has a best-estimate value of 4,168 μm/a, and values of 1,042 μm/a and 10,420 μm/a for the lower and upper bound fits, respectively. As relative humidity increases above a lower threshold value (60%), the consumption of carbon steel by Phase 2 corrosion will gradually increase until an upper RH threshold is reached (80%), at which point full Phase 2 corrosion is calculated. Note that Phase 1 and Phase 2 corrosion overlap as the relative humidity increases from 60% to 80%.

Phase 3

An unsaturated anaerobic phase will occur following the consumption of the oxygen and prior to the full resaturation of the repository; the gaseous phase will be predominantly N_2, H_2 and H_2O vapour. Corrosion during this period is supported by the cathodic reduction of water accompanied by the evolution of hydrogen. Detailed surface analysis indicates that corrosion under unsaturated anaerobic conditions forms magnetite as the predominant corrosion product, which is represented in the model as follows:

$$3Fe + 4H_2O \rightarrow Fe_3O_4 + 4H_2 \quad (5\text{-}6)$$

$$R_3 = A_3 \exp\left(-\frac{5332}{T}\right) \ \mu m \cdot a^{-1} \quad (5\text{-}7)$$

where the pre-exponential term A_3 is assigned a best-estimate value, as well as lower and upper bounds. The best-estimate value for the pre-exponential term A_3 is equal to 8.89×10^6 µm/a. Although there are relatively few data available, it is not unreasonable to expect that the lower and upper bound corrosion rates under anaerobic unsaturated conditions might differ by a factor of ten. In the absence of other information, it is assumed here that the best-estimate value is the (geometric) mean of the lower and upper bound values. Thus, the values of A_3 for the lower and upper bound estimates are 2.81×10^6 µm/a and 2.81×10^7 µm/a, respectively (King 2013).

The rate of reaction is affected by relative humidity (RH), which has upper and lower bounding conditions, $RH_{CRIT,U}$ and $RH_{CRIT,L}$:

for $RH \le RH_{CRIT,L}$ $\quad$ Rate = 0 $\quad$ (5-8)

for $RH_{CRIT,L} < RH \le RH_{CRIT,U}$ $\quad$ $Rate = R_3 \left(\frac{RH - RH_{CRIT,L}}{RH_{CRIT,U} - RH_{CRIT,L}}\right)$ $\quad$ (5-9)

and

for $RH > RH_{CRIT,U}$ $\quad$ Rate = R_3 $\quad$ (5-10)

where the values of best-estimate and upper- and lower-bound values for $RH_{CRIT,L}$ and $RH_{CRIT,U}$ are dependent on the cationic content of the buffer system, but may be as low as 0.1 and 0.2, respectively, for highly saline systems. Thus, for RHs as low as 20%, the reaction could proceed at its maximum rate.

Phase 4

A long-term saturated anaerobic phase once the EBS material has become completely saturated by groundwater. As with Phase 3, corrosion during Phase 4 is supported by the cathodic reduction of water accompanied by the evolution of hydrogen. In the presence of compacted bentonite under saturated conditions, in addition to the reaction shown in (5-6), where magnetite (Fe_3O_4) is the corrosion product, carbon steel corrodes with the formation of a carbonate-containing corrosion product. The source of carbonate is calcite and other carbonate minerals assumed to be present in the EBS material. The overall stoichiometry of the corrosion reaction and the corrosion rate for Phase 4 are modelled according to the following relationships:

$$\mathrm{Fe} + \mathrm{CO_3}^{2-} + \mathrm{H_2O} \rightarrow \mathrm{FeCO_3} + \mathrm{H_2} + 2\mathrm{OH}^- \qquad (5\text{-}11)$$

$$R_4 = A_4 \exp\left(-\frac{2435}{T}\right) \ \mu m \cdot a^{-1} \qquad (5\text{-}12)$$

For the best-estimate corrosion rate, A_4 = 8,200 µm/a; A_4 = 16,400 µm/a for the upper bound and A_4 = 2,050 µm/a for the lower bound (King 2013).

It is important to note that these four phases do not necessarily occur sequentially. Phases 1 and 2 both occur under aerobic conditions and the degree to which the Phase 1 and Phase 2 corrosion processes are active depends on the relative humidity. The Phase 3 and 4 corrosion processes proceed under anaerobic conditions after Phase 1 and Phase 2. The degree to which the Phase 3 and Phase 4 corrosion processes are active depends on whether or not liquid water has moved through to the steel components or not. As noted above, the Phase 3 process also depends on relative humidity.

The vast majority of H_2 that will be produced in the repository will result from the uniform corrosion of C steel during the (unsaturated and saturated) anaerobic phase. Hydrogen can be produced under aerobic conditions due to the reduction of H^+ in acidic environments in pits, crevices, or porous corrosion products formed as a result of the hydrolysis of Fe(III) species (Akiyama et al. 2010, Tsuru et al. 2005). Local reduction of H^+ may lead to enhanced hydrogen absorption and environmentally assisted cracking (King 2009a) but will not lead to the generation of significant H_2 and is not considered further here.

Hydrogen generated by corrosion can undergo a number of subsequent processes. The H_2 that is evolved could be consumed by microbes (Pedersen 2000) in those parts of the near- and far-fields in which the environment is conducive to microbial activity (namely a water activity greater than 0.96, Stroes-Gascoyne et al. 2006, Stroes-Gascoyne and Hamon 2008). Another fraction of the hydrogen will be absorbed by the C steel as atomic H, either from adsorbed H atoms prior to their evolution as H_2 or via the dissociative absorption of gaseous H_2; however, eventually this hydrogen will be released as the steel continues to corrode.

In addition to the evolution of the redox conditions and the degree of saturation, the temperature will also change during these different phases. The precise time dependence of the repository temperature will depend on the rate of saturation, which is not known a priori. However, in general, it is clear that Phases 1 and 2 will be warmer than Phase 3 and 4, with Phase 3 and 4 encompassing the period of long-term ambient conditions.

The rate of oxidation of carbon steel in dry air (Phase 1) is low at the temperatures of interest (maximum of approximately 120°C) and will result in only a few microns of corrosion. Although the rate of aerobic corrosion in the presence of moisture under unsaturated conditions (Phase 2) is higher, the extent of corrosion is limited by the initial inventory of trapped oxygen in the repository. Therefore, upon the establishment of high humidity Phase 2 conditions, the duration of aerobic corrosion is predicted to be less than 1 year. This has been confirmed in all model results to date.

Of most interest is the rate of anaerobic corrosion under first unsaturated (Phase 3) and subsequently saturated (Phase 4) conditions. Based on the review of published corrosion studies, these rates are temperature dependent; the corrosion rate decreases with time as the container cools.

A number of other environmental parameters, in addition to the temperature, relative humidity, and redox conditions, also affect the uniform corrosion behaviour, including:

Pore-water chemistry:	Under saturated conditions, the steel will be in contact with EBS pore water. At least initially, the composition of the pore water may differ from that of the groundwater. Eventually, however, the pore water will equilibrate with the ground water.
pH:	Calcite minerals in the bentonite may effectively buffer the pH in the range pH 7-8.
Mass transport:	During the aerobic phase, the rate of corrosion may be limited by the rate of transport of O_2 to the steel surface through low permeable EBS materials.
Radiation:	Gamma radiolysis of water will produce oxidizing and reducing radiolysis products. However, the maximum surface absorbed dose rate for a 10-cm-thick C steel UFC will be <1 Gy/a, for which there is no significant effect on the corrosion rate (Shoesmith and King 1999). Steel components more distant from the UFC will certainly see no effect of radiation/radiolysis.
Microbial activity:	Microbial activity is suppressed by the presence of saline solutions in compacted bentonite (Stroes-Gascoyne et al. 2006, Stroes-Gascoyne and Hamon 2008). However, since rock bolts and other steel components will reside outside the UFC engineered barrier system, it is possible that halophilic microbial species may accelerate corrosion versus a non-microbially active region of the engineered barrier system.
Stress:	Applied and residual stresses affect the environmentally assisted cracking behaviour of the steel but have no effect on uniform corrosion.
Mineral impurities:	Mineral impurities in the host rock (e.g., pyrite) will have an insignificant effect on the uniform corrosion behaviour of the container.

As described above, for a repository with intact containers, the only steel available for reaction is material from repository construction and operations, such as rock bolts, that remain in the placement rooms after closure. Little hydrogen would be produced by corrosion of these metals. A quantitative discussion of the effects of gas generation for the All Containers Fail scenario appears in Chapter 8.

5.2.7 Confidence

Excavation Damaged Zone: Estimates of the extent and permeability of the excavation damaged zone are based on investigative findings for other sedimentary rocks; however, actual repository specific data will not be known until in-situ measurements are obtained. Once available, these data will be incorporated into the various assessments together with appropriate allowances for residual uncertainties.

Sensitivity studies indicate that long-term repository performance is not especially sensitive to reasonable variations in EDZ assumptions.

Repository Saturation: The resaturation rate depends on properties of the host rock and engineered barrier materials, temperature, hydraulic gradients, and gas or vapour transport, and so requires coupled models. The modelling would be supported in part through engineering demonstration tests or monitoring of early placement rooms. While there is some inherent uncertainty, long-term repository performance is not particularly sensitive to the actual time of resaturation.

Additional discussion on repository saturation is provided in Section 5.4.1.

Temperature: There is good confidence in results obtained from thermal models over long periods of time and in conservative estimates at shorter times. Some uncertainties exist in temperature predictions for pre-saturation conditions due to varying physical parameters (such as shrinkage or cracks) and moisture content (affecting thermal conductivity) of the material surrounding the container.

Additional discussion on temperature effects is provided in Section 5.1.2, Section 5.3.1.2 and Section 5.4.2.

Near-Field Chemistry: The time at which reducing conditions will be re-established following repository closure is uncertain due to specifics of the complex interactions between groundwater, repository components, and microbial processes.

Regardless of the amount of time required, the total amount of oxygen is limited and it is a given that reducing conditions will be re-established at some point in the postclosure period. Conservative assumptions can be applied in the repository design and analysis process to bound the associated uncertainties to ensure appropriate conclusions concerning repository performance are made.

Additional discussion on chemistry is provided in Section 5.3.1.4, Section 5.3.1.5 and Section 5.4.3.

Steel Corrosion and Gas Generation: Gas generation and migration depends upon host rock properties, the rate at which water enters the repository, the quantity of organic material present, the number and distribution of rock bolts, the degree to which radiolysis of water occurs, the timing and number of container failures, and the corrosion rates. For the bounding case considered in Chapter 8, gas generation from corrosion of all steel inner containers far exceeds that from other sources, so that some of the related uncertainties are not of special concern.

Confidence in the predictions is gained through modelling, comparison of models with international experience and the use of bounding assumptions. The remaining uncertainties can be reduced through the use of improved modelling codes and the adoption of repository designs that cater to gas migration. Research and model development activities continue in Canada and elsewhere with this objective in mind.

5.3 Long-Term Evolution of a Used Fuel Container

As described in Chapter 1, the design of the reference container is consistent with lifetimes in excess of 100,000 years. To achieve such lifetimes, a container must be able to withstand the expected geological evolution from hot, dry and aerobic, to cool, water saturated anaerobic conditions. Within this context, specific effects have been examined as they pertain to the evolution of the used fuel container in a deep geological repository; these are summarized in Section 5.3.1, below. In addition, and in keeping with the safety arguments described in Chapter 1, specific conditions that pertain to a breached container are described in Section 5.3.2, below.

5.3.1 Evolution of Intact Containers

As described in Section 4.3, the reference copper container design for sedimentary rock consists of a copper outer vessel that encloses a steel inner vessel. Upon placement in the repository, the copper outer vessel protects the inner steel vessel from corrosion. The copper outer vessel is not designed to be load-bearing. When the normal 7 MPa load from hydrostatic and swelling pressures is applied to the container, the copper shell would compress onto the steel inner vessel, transferring the external load to the steel inner vessel (Poon et al. 2001). The container is designed to withstand an external isotropic pressure of 45 MPa at 50°C; this value indicates that the container could withstand the additional hydrostatic load exerted at repository depth by a 3,800 m glacier above the repository connecting the container's surface to the top of the glacier by a continuous column of water. Thus, in the analysis of intact containers, many of the specific effects of placement of the containers within the repository are limited to processes that affect the outer copper shell and inner steel vessel. The main processes experienced by the container over time are listed in Table 5-4 and discussed in the succeeding sections.

Table 5-4: Processes with a Potential Influence on the Evolution of Containers

PROCESS	POTENTIAL INFLUENCE
RADIATION	
None	• None
THERMAL	
Heat transfer from fuel to container	• Change in container temperature
HYDRAULIC & PNEUMATIC	
Saturation of repository	• Pressure applied to container • Initiation of aqueous corrosion on container surface
MECHANICAL	
Hydrostatic load and swelling of the buffer	• Stresses on container
Glacial loading	• Stresses on container
Creep	• Deformation of copper shell onto steel inner vessel
CHEMICAL	
Reactions with water and oxygen in sealing materials or chlorides/sulphides in water	• Thin layer of corrosion products on container surface • Corrosion of container
BIOLOGICAL	
Aerobic microbial activity in vault	• Consumption of oxygen • Production of sulphide

Notes: Processes listed are those that are most likely to have a notable effect on the containers, over a time scale of one million years.

5.3.1.1 Irradiation of Container Materials

The radioactivity inside the container is at its maximum value when the fuel is first loaded. The radiation field around the container is dominated by the gamma emission from short-lived fission products, which decay almost completely within the first 500 years after placement (see Figure 5-1). Thereafter, the residual radiation field would be very low because most of the remaining radioactivity would be from the alpha emission of long-lived actinides. Alpha particles do not penetrate beyond the fuel cladding.

High levels of neutron radiation, as found in nuclear reactors, can lead to hardening and embrittlement of reactor parts. The neutron flux inside a reactor is on the order of $4x10^{13}$ $n/cm^2 \cdot s$ (neutron per centimetre squared, per second). In comparison, the neutron flux from used fuel is much smaller (~10^2 - 10^3 $n/cm^2 \cdot s$ initially in a container of used CANDU fuel) and is mainly lower-energy neutrons. Over a million-year timeframe, the total neutron fluence experienced by the container would be less than 10^{15} n/cm^2 (based on Tait et al. 2000), whereas a neutron fluence greater than 10^{22} n/cm^2 would be required to produce measurable displacement effects in metal. Defect formation from thermal neutrons would require neutron fluences of 10^{19} - 10^{21} n/cm^2 in copper and iron at 70 - 80°C to result in significant hardening. Consequently, it is unlikely that the container metals would be significantly affected by radiation over a million year exposure to used fuel (McMurry et al. 2003).

Radiation would be more likely to have a small indirect influence on container properties, in terms of changes to the chemical environment that would result from the decomposition (radiolysis) of air and water in the vicinity of the container.

5.3.1.2 Changes in Container Temperature

Thermal analyses are performed to determine thermally acceptable layouts of a repository using computer codes such as CODE_BRIGHT (Guo 2010). Various heated field experiments have been conducted and modelled (e.g., the full-scale Canister Retrieval Test at the Äspö Hard Rock Laboratory in Sweden, Guo 2009). The findings indicate that thermal responses were successfully modelled. There is good confidence that the evolution of temperatures of the container surface and surrounding bentonite buffer materials can be well estimated by existing computer models.

In this case study, the exterior surface temperature of the reference copper container after placement reaches a maximum value of 120°C (see Figure 5-5), considering the reference horizontal tunnel placement concept at a depth of 500 m in sedimentary rock and the repository layout presented in Chapter 4. This is higher than the 100°C value reached in crystalline rock because of the slightly lower thermal conductivity of sedimentary rock, as well as the horizontal placement adopted in the present study. Both temperature values are ensured by the container spacing within the repository such that the heat can be conducted away through the buffer and rock.

The purpose of determining the maximum temperature value is to understand the effect of elevated temperatures on the physical properties of the buffer sealing material surrounding the container. Only a fraction of the containers in a repository (those with the youngest fuel and / or the highest burnup values) would approach this maximum temperature. In the case of containers that otherwise are identical, those near the edges of a repository would have lower maximum temperatures than those in the centre of a repository because they would be less affected by heat from adjacent containers as illustrated in Figure 5-6.

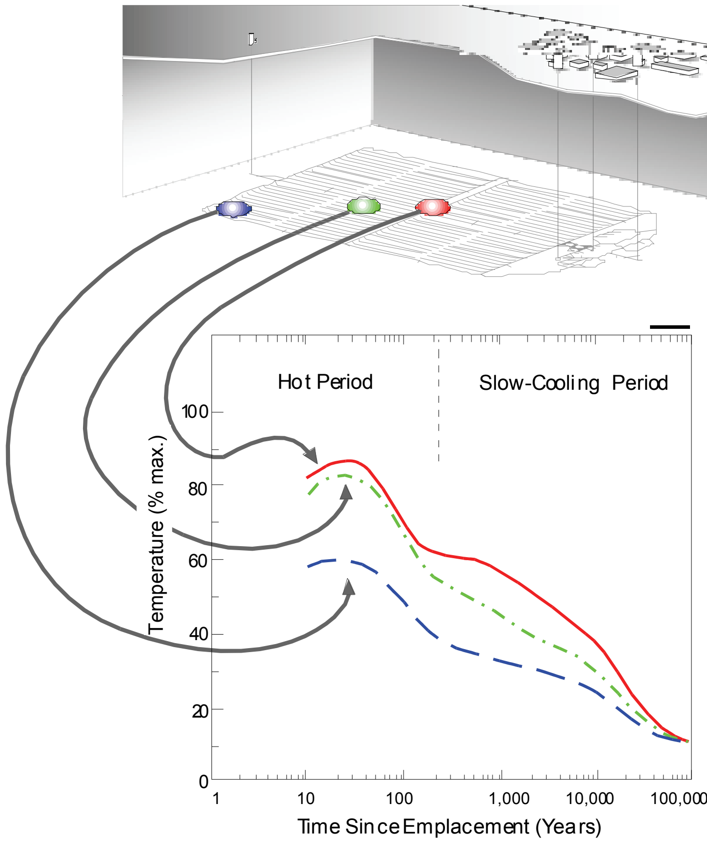

Notes: Figure is adapted from McMurry et al. (2003). Although otherwise identical, containers near the repository margin would remain cooler than those near the centre. The maximum temperature reached is 117°C, as shown in Figure 5-5.

Figure 5-6: Illustrative Container Temperature Profiles at Three Generalized Locations within a Repository

The thermal profile for a reference container near the centre of the repository (red position in Figure 5-6) is shown in Figure 5-5. Some key points are:

1. The maximum container surface temperature is reached relatively soon after placement (i.e., within 30 years). In general, the greater the heat flux for the container, the sooner the peak temperature is attained.
2. There is a subsequent plateau or slow decline in the container temperature. The specific shape of this region is influenced by repository design and site conditions.
3. The containers cool to near-ambient conditions after approximately 100,000 years.

5.3.1.3 Changes to Mechanical Integrity

Containers would experience a range of stress conditions over time. The structural design of the container is determined largely by the requirement to provide adequate mechanical strength throughout its design life.

5.3.1.3.1 Early Conditions

As soon as the steel lid is bolted onto the steel vessel, heat from the used fuel bundles would increase the pressure of the inert gas inside the vessel. For example, at a temperature of 120°C inside the container, the internal gas pressure would increase by about 40%. This internal pressure would have a negligible effect on container stresses and would decrease with time as the container cooled.

Another early heat-related stress effect would be the differential expansion of the metals in the container. The coefficient of thermal expansion of steel is about $3.7x10^{-6}$ mm/mm/°C at 100°C, whereas that of copper is about $5.4x10^{-6}$ mm/mm/°C. Over a period of hours to days after the used fuel bundles are loaded, the temperature increase would result in a slight differential thermal expansion of the two container materials, causing the small gap between the outer and inner vessels to increase by less than a tenth of a millimetre. This effect would not be significant.

After the containers are loaded and sealed, they would be transferred from the fuel loading and container assembly area to a placement room in the repository. Depending on the facility design, the transportation and placement process would involve multiple stages of handling of the containers, possibly including several rotations from vertical to horizontal orientations during transfer from the surface facilities to a final position in a placement room. This handling would impose various short-term loads on the container that would be within its design basis.

5.3.1.3.2 Effects of Hydrostatic and Buffer Swelling Pressures

After placement, the external load on the containers initially would consist of little more than the weight of the overlying sealing materials. The load would gradually increase during saturation of the repository. The swelling of the bentonite in the sealing materials is likely to occur unevenly on a local scale because the swelling would be controlled by the supply of water from the rock, by the shape of the room, and by the pathway of water along interfaces. The heterogeneous development of swelling pressures would result initially in non-uniform external loads on the containers, an effect that is expected to diminish as full saturation is achieved. The container design is robust enough to account for this.

By the time a repository is fully saturated, the hydrostatic pressure would have increased to about 6 MPa at the repository depth of 500 m. Buffer swelling pressures would contribute up to another 0.4 to 1 MPa to the load on the containers, depending on groundwater salinity and buffer density. Under these loading conditions the copper shell would be expected to compress onto the steel load-bearing inner vessel. The resulting load is within the container design basis.

5.3.1.3.3 Effects of Glacial Loading

Additional compressive stresses would be applied to the container by glaciation. It is unlikely that an ice sheet would develop over the repository until at least several tens of thousands of years had elapsed. By this time, the buffer saturation-related pressure loads would be fully applied. The increased stresses associated with glacial loading are likely to recur several times over a million-year timeframe because of successive glaciation events (Figure 5-7).

The container is designed to withstand a load of 45 MPa. In this case study, the container could withstand an increase in hydrostatic pressure of 38 MPa from glacial loading (in addition to the 7 MPa due to pre-glaciation hydrostatic and swelling pressures), a value that corresponds to a loading from a 3,800-metre thick ice sheet above the repository location. Recent studies have indicated that a glacial loading estimate of 38 MPa is likely to be conservative, i.e., the additional hydrostatic pressure at repository depth is likely to be considerably less than this (see Chapter 2).

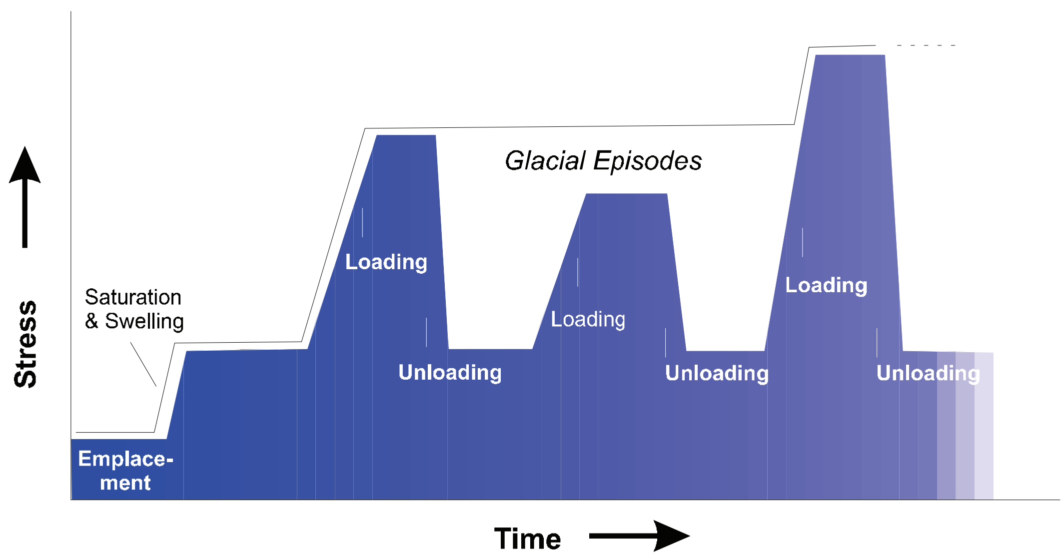

Figure 5-7: Schematic Representation of the Loading History in a Repository

5.3.1.3.4 Effect of Seismic Stresses

In general, the Michigan Basin is characterized by low levels of seismic activity as it is located within the tectonically stable center of the stable North America continent (Hayek et al. 2010). Most earthquakes in the regional area, although rare, are deep and occur in pre-existing faults within the Precambrian basement. Seismic events with focal depths in the Paleozoic sequence are not known to occur. During glaciation, an increase in the frequency of earthquakes is expected during a glacial retreat, however the magnitude of these events is expected to remain low. Within the sedimentary rock in the Michigan Basin below the Bruce nuclear site, this is supported by the lack of apparent evidence for cross formational mixing of groundwaters and the lack of neotectonic deformation (NWMO 2011).

To further improve confidence in long-term stability regarding seismic hazards, there is a considerable body of evidence to show that earthquakes, in general, are less destructive at depth than at the surface, diminishing the impact of any seismic activity (including proximal events) on a deep geological repository (Bäckblom and Munier 2002, Atkinson and Kraeva 2011). In addition, an analysis conducted for an in-floor placement in crystalline rock design by the Swedish repository program (Raiko et al. 2010) concluded that there would be no significant effect on containers even if an earthquake resulted in shearing over a distance of 0.05 m in the rock directly across the container location.

5.3.1.3.5 Effect of Creep

Creep is the slow deformation of a material under an applied stress that results in a permanent change in shape. The process of creep in copper is governed by properties of the metal (e.g., grain size, impurities at grain boundaries, crystallographic structure), temperature, stress level, and time. To maintain the mechanical integrity of the copper shell, the container is designed so that the total of the elastic, plastic, and creep strains developed in the metal does not exceed its creep-rupture strain over the design lifetime. A number of research and development studies have been carried out in the Canadian, Swedish, and Finnish nuclear fuel waste management programs to assess the creep lifetime of dual-vessel containers that have a copper outer shell. These studies have included the development of oxygen-free phosphorus-doped (OFP) copper materials with improved creep ductility, and container designs that limit the amount of creep deformation. While recent analysis of this data has revealed some uncertainty in the long-term creep fracture performance of OFP copper (SSM 2012a), as well as a need to supplement modelling capability with respect to creep ductility (SSM 2012b), a long-term study is ongoing to improve confidence in these areas. The upper bound of the creep rates for a copper vessel in a deep geological repository is presently estimated to be in the range of $3x10^{-13}$ to $1x10^{-10}$ /s.

During the saturation period, when hydrostatic and swelling pressures begin to apply stress to the container, the copper shell would have a surface temperature of about 120°C at most. The copper would compress onto the steel vessel, closing the small assembly gap (1 mm) that was initially present between the two parts of the container. At the expected temperature and pressure, the main process by which this deformation takes place is creep, since the maximum stresses that develop in the copper shell would be below the yield stress limit of the copper, preventing plastic yielding from taking place.

In certain areas (e.g., around the lid), some gap is likely to remain between the copper and steel, and localized creep of copper would be likely to continue. First-order analyses have suggested that the additional creep strain developed in these areas would be negligible because of the low stresses and low temperatures at long times (Saiedfar and Maak 2002).

Under isotropic loading, independent creep of the copper would cease after the copper compresses against the steel vessel. If any further creep of copper were to occur, it would be in response to deformation of the steel vessel. However, the thick-walled steel vessel would be designed to remain load-bearing over the design lifetime for a container (Werme 1998, Saiedfar and Maak 2002). For example the maximum stresses developed in the reference steel vessel are only about 30% of its yield strength under saturation-related pressures, and approaches the yield strength under peak design-basis glaciation pressures. The creep rate of steel under the anticipated loading conditions (20% of its ultimate tensile strength under saturation-related pressures) and temperature (20% of melting temperature) is insignificant. The exact rate is uncertain, but it is expected that it would take at least 100,000 years for any appreciable amount of creep deformation to develop in the steel vessel (Dutton 2006).

5.3.1.4 Effect of Chemical Processes Inside the Container

The containers remain intact throughout the timeframe of the study. Chemical changes over time involving those processes that affect the interior of the container (a closed system) may therefore be considered separately from those that affect its exterior surface.

At the time of packaging, the container interior is dry, as are the used fuel assemblies. Most water vapour is eliminated from the container interior during packaging operations because the air inside the container is replaced by an inert gas before the container is sealed. The small amount of residual air and water vapour would provide some oxygen to react with the metals in the container interior, and the irradiation of any air present would produce small quantities of nitrogen oxides by radiolysis. For the anticipated "dry" conditions inside the container, aggressive corrosive agents such as nitric acid would not form (McMurry et al. 2003).

The zirconium alloy in the fuel bundles would already have a surface film of ZrO_2 that formed at high temperatures in a reactor. This resistant ZrO_2 surface layer on the cladding would inhibit any further reaction with the small amount of air initially available inside the container. In contrast, the more porous iron oxide layer on steel would slow but not prevent further reaction. Thermodynamic arguments predict that reaction between the iron and oxygen would occur even at a very low oxygen partial pressure. The steel inner vessel and the steel baskets holding the fuel bundles would tend to react rapidly with any available oxygen, forming iron oxides/hydroxides as corrosion products. Corrosion of the steel would effectively remove any gaseous oxygen from the interior of the container, so that conditions in the interior would become anoxic. An upper bound on the amount of corrosion from residual air can be obtained by assuming that the container is filled with air instead of with an inert gas. For a container design as indicated in Table 5-1, the total internal void volume is about 1.58 m^3. The total consumption of oxygen from air trapped in this space would result in 0.01 mm of corrosion of the steel basket walls. This indicates that there would be more than enough iron present to consume any oxygen.

Fuel elements with defective cladding would release some fission gases to the container interior, particularly if the cladding fails after the container is sealed. Iodine, which assists stress corrosion cracking of metals under some conditions, is the most noteworthy of these gases. The partial pressure and total quantities of any released gases would be small, (e.g., $<10^{-40}$ MPa for oxygen and $<10^{-17}$ MPa for iodine), and the CANLUB coating within the fuel element would tend to absorb any gaseous iodine. Most of the other released gases would be adsorbed onto the internal surfaces of the steel structure, or they would be distributed among the exposed iron, zirconium and copper surfaces, not resulting in any significant changes to the interior of the container (McMurry et al. 2003).

In summary, the scarcity of oxygen and water inside the inert gas-filled sealed containers would greatly limit the chemical changes that would take place there. Water radiolysis, accompanied by reactions with the metal interior of the container, would quickly consume the small amount of gaseous oxygen that would be present (SKB 2011). The interior of the container thereafter would have a dry, reducing chemical environment that would persist as long as the container remains intact.

5.3.1.5 Effect of Chemical Processes Outside the Container

This section summarizes the current understanding of the corrosion behaviour of copper used fuel containers in a deep geological repository. This understanding has been developed on the basis of an extensive experimental program carried out in Canada and elsewhere over the past 30 years and on the results of mechanistically based mathematical modelling of various corrosion processes.

The corrosion behaviour of copper depends on the nature of the environmental conditions. For this discussion, the following attributes of the container and reference repository design are important:

- The container corrosion barrier is manufactured from an oxygen-free grade of copper;
- The container is placed in the room and sealed immediately afterwards;
- The containers are surrounded by a buffer material comprising dense bentonite pellets with an average dry density of at least 1.4 Mg/m^3;
- The groundwater is a Ca-Na-Cl solution, with small amounts of sulphate and low levels of carbonate;
- The available O_2 is limited to that trapped initially in the pores of the buffer and backfill materials, the groundwater itself is O_2-free;
- The container includes a thick inner steel vessel resulting in a maximum surface absorbed dose rate of <1 Gy/a;
- The container surface temperature will reach a value of up to 120°C;
- There is a period of unsaturated conditions immediately following container placement and prior to saturation of the repository;
- There is no sulphide (HS^-) present in the groundwater; and
- The container is subject to external loading from a combination of the hydrostatic load and bentonite swelling pressure, assuming that the relaxation of the surrounding rock has completed prior to container placement.

Experimental research and modelling has considered uniform corrosion, pitting corrosion, stress corrosion cracking (SCC) and microbial-induced corrosion (MIC). A list of studies conducted in the Canadian copper corrosion program is tabulated in Kwong (2011), and reviewed in Scully and Edwards (2013).

Overall, these studies conclude that a copper-shelled used fuel container in a deep geological repository will be primarily subject to general corrosion. The degree of localized attack (pitting), MIC and SCC will be negligible and can be controlled using standard engineering design and practice. All forms of corrosion will be stifled as the repository environment becomes anoxic. The various corrosion mechanisms are discussed in more detail in the following sections.

The important characteristics of the corrosion of copper containers in a deep geological repository are:

- The corrosion behaviour changes with time, largely as a result of the evolution of the repository environment (King and Shoesmith 2010). This environment evolves from an initial period of warm, aerobic conditions to an indefinite period of cool, anoxic conditions. From a corrosion perspective, this environmental evolution means that localized corrosion processes are limited to the early period, with corrosion becoming more uniform in nature as time progresses;

- The nature of the environment at the container surface determines the corrosion behaviour. The surface environment can be different from that in the host rock as a result of the chemical conditioning of the groundwater by the bentonite clay and the slow mass transport of reactants to, and of corrosion products away, from the container surface due to the presence of the bentonite;

- In general, groundwater chloride promotes the uniform dissolution of copper and suppresses localized corrosion and SCC (King et al. 2010, 2011a); and

- The dense bentonite clay buffer and high groundwater salinity around the container suppresses microbial activity.

5.3.1.5.1 Uniform Corrosion

The uniform corrosion of copper in the environment expected in a deep geological repository has been extensively studied and the corrosion mechanism is well understood and summarized in Kwong (2011). Figure 5-8 illustrates the mechanism developed to describe the uniform corrosion of copper in compacted bentonite saturated with oxygen (O_2)-containing chloride (Cl^-) porewaters. The mechanism couples the interfacial electrochemical reactions that occur on the container surface to various processes occurring at or within the bentonite. These processes include: the diffusive mass-transport of species to and from the corroding interface (denoted by the wavy arrows in Figure 5-8); the adsorption and desorption of Cu(II) on the clay; redox reactions involving dissolved O_2, Fe(II), and Cu(I) and Cu(II) species; the dissolution and precipitation of various solid mineral phases and corrosion products; the partitioning of O_2 between the gaseous and aqueous phases, and, in a simplistic manner, the microbial consumption of dissolved O_2. This reaction scheme applies equally to both the buffer and backfill materials, as well as the host rock, and further details are included in this section.

Copper can react in dry air as shown in Reaction (5-13). The rate of copper oxidation in dry air at temperatures below 150°C is of the order of nm/a, and, therefore, effectively negligible.

$$2\mathrm{Cu} + \tfrac{1}{2}\mathrm{O_2} \rightleftarrows \mathrm{Cu_2O} \qquad (5\text{-}13)$$

The corrosion behaviour of copper in O_2-containing Cl^- solution has been well studied. A detailed reaction mechanism exists that accounts for the various electrochemical, chemical, redox, adsorption/desorption, precipitation/dissolution, and mass transport processes involved in the corrosion process in compacted bentonite. The behaviour of copper over a range of chloride concentrations has also been experimentally evaluated. Kinetic rate constants, equilibrium constants and other thermodynamic parameters required for modelling are available, as summarized in Kwong (2011).

Copper will corrode in solutions containing O_2 and Cl^- and under atmospheric conditions providing the relative humidity is above that required to form a thin surface water film, i.e., approximately 50 to 70% relative humidity. The rate of corrosion will depend on the presence of atmospheric contaminants, such as SO_2, NO_2, and CO_2. The ion-containing water film acts as an electrolyte to support electrochemical reactions and the dissolved impurities will further enhance the corrosion process. For instance, the SO_2 forms H^+ and HSO_3^-; the latter species can be oxidized to sulphate by oxidants in the air, and NO_2 can be absorbed in the water film as HNO_3, which dissociates to H^+ and NO_3^-.

Copper dissolves in Cl^--containing solutions as the cuprous (Cu(I)) complex ion $CuCl_2^-$; this process is of particular importance for the expected high salinity of the Canadian sedimentary environment, see Table 2-4. The anodic dissolution is coupled to the cathodic reduction of an oxidant, either dissolved O_2 or Cu^{2+}. Cupric species are produced by homogeneous oxidation of Cu(I) by O_2 (Reaction (5-14)).

$$4Cu(I) + O_2 + 2H_2O \rightarrow 4Cu(II) + 4OH^- \tag{5-14}$$

Both Cu(I) and Cu(II) can precipitate as Cu_2O and $CuCl_2{\cdot}3Cu(OH)_2$, respectively (Reactions (5-15) and (5-16)). Such a duplex corrosion product layer would comprise an inner layer of Cu_2O and an outer layer of basic Cu(II) salts such as $CuCl_2{\cdot}3Cu(OH)_2$) or $Cu_2CO_3(OH)_2$, depending on the specific composition of the porewater.

$$2CuCl_2^- + H_2O \rightleftarrows Cu_2O + 2H^+ + 4Cl^- \tag{5-15}$$

$$2Cu_2O + O_2 + 2Cl^- + 4H_2O \rightleftarrows CuCl_2 \cdot 3Cu(OH)_2 + 2OH^- \tag{5-16}$$

The precipitated surface film blocks surface electrochemical reactions and does not sustain the permanent separation of anodic and cathodic reactions that would be required for localized corrosion to occur. As the repository environment becomes anaerobic, the $CuCl_2{\cdot}3Cu(OH)_2$ layer dissolves with further corrosion supported by the cathodic reduction of Cu(II).

In the absence of oxygen, corrosion would require a reaction with water to produce hydrogen gas (H_2):

$$2Cu + H_2O \rightleftarrows Cu_2O + H_2 \tag{5-17}$$

or

$$Cu + H_2O \rightleftarrows CuOH + \tfrac{1}{2}H_2 \tag{5-18}$$

Known thermodynamic relationships (Puigdomenech and Taxén 2000) indicate that the equilibrium shown in Reaction (5-17) is very strongly biased towards the reactants: metallic copper and water. Accordingly, upon formation of a very small amount of Cu_2O (i.e. a single layer), only a very small amount of hydrogen, with a partial pressure on the order of 10^{-11} mbar, is necessary to suppress the corrosion reaction; i.e., Reaction (5-17) becomes unfavourable in the forward direction. In addition, the corrosion product in Reaction (5-18) has not been shown to be stable. Therefore, Reactions (5-17) and (5-18) are considered very improbable in water.

Under anaerobic conditions, copper corrosion accompanied by the evolution of H_2 does occur in the presence of sulphide (Reaction (5-19)).

$$2Cu + H^+ + HS^- \rightleftarrows Cu_2S + H_2 \quad (5\text{-}19)$$

Sulphide is not widely found in groundwaters in sedimentary rock in Canada (INTERA 2011). In Sweden and Finland, however, deep groundwaters do contain small amounts of HS^- (typically ~1 mg/L, King et al. 2010, 2011a), resulting in corrosion rates of the order of nm/year due to the slow transport of sulphide to the container surface through the compacted bentonite buffer (SKB 2011).

Researchers from the Royal Institute of Technology (Sweden) have published experimental results that they claim indicate that copper can corrode in pure, oxygen-free water. Their research claims that water is reduced in the anaerobic corrosion process to form hydrogen atoms (Szakálos et al. 2007, Hultquist et al. 2009, 2011), and that a hydroxyl-containing copper corrosion product may be produced. Subsequent expert review (Swedish National Council 2010) concluded that it was necessary to demonstrate that the proposed corrosion product was thermodynamically stable before it could be justifiably claimed that copper could corrode in oxygen and sulphide-free water. An SKB review also concluded that there were possible errors in the original experiments (SKB 2010).

Further studies are underway in Sweden, as well as by NWMO, to address these topics. Preliminary results are reported in SSM (2011a) and Hultquist et al. (2013). These have found extremely small quantities of hydrogen in similar experiments, although the tests were not definitive. In addition, careful analysis of the thermodynamics of the reactions between copper, pure water, and sulphide (SSM 2011b) has indicated that copper-water interactions as described by (5-17) and (5-18) are theoretically possible, but would only produce very small quantities of hydrogen, and that reactions with sulphide species are much more important (SSM 2011b).

In summary, while this topic is still being studied, it appears that the hydrogen produced from a copper-water interaction would be self limiting, and not a significant corrosion mechanism within a repository. Assuming the corrosion mechanism via reaction (5-18) occurs, then at temperatures of 73°C and 45°C, hydrogen partial pressures of ~1 mbar (Szakálos et al. 2007) and 0.5 mbar (Hultquist et al. 2009), respectively, would suppress the corrosion reaction. This hydrogen could be present either from the copper-water reaction, if it occurs, or more likely from the anaerobic corrosion of steel components or reactions between copper or steel with trace levels of sulphides or from native hydrogen levels (SKB 2010). For example, measurements at depth within crystalline formations have demonstrated hydrogen concentrations between 2 and 1,600 µmol/L (Sherwood Lollar 2011), equivalent to partial pressures of 2.6 to 2,000 mbar.

The rate controlling process for the uniform corrosion of copper changes as the environmental conditions evolve. Under aerobic conditions, there is evidence that the transport of dissolved Cu away from the corroding interface is rate controlling (King et al. 2010, 2011a) (i.e., the corrosion reaction is anodically transport limited). As the repository environment becomes anoxic, the corrosion rate must eventually become cathodically transport limited as a result of the slow diffusion of oxidant to the container surface. In the presence of sulphide, if such species were to be found in Canadian groundwaters or produced from sulphates by microbes, then the corrosion rate is limited by the rate of transport of HS^- to the container surface (Chen et al. 2011, King et al. 2011b).

Overall, the uniform corrosion behaviour of copper in conditions expected for a deep geological repository in sedimentary rock is well understood. Both the mechanism of copper corrosion in oxygen-containing chloride (as high as 5 mol/L) and kinetic and thermodynamic parameters required for modelling are available.

In addition to the extensive experimental studies on which the mechanism in Figure 5-8 is based, a detailed reactive-transport model has been developed to predict the long-term uniform corrosion behaviour of copper containers in the repository. The model, referred to as the Copper Corrosion Model for Uniform Corrosion (CCM-UC), is based on the mechanism in Figure 5-8 and couples the corrosion behaviour of the container to the various processes occurring in the near- and far-fields of the repository, specifically the evolution of the environmental conditions. The corrosion behaviour is modelled using electrochemical mixed-potential principles. As a result, the model not only predicts the time-dependent corrosion rate (as a corrosion current density), but also the time-dependent corrosion potential (E_{CORR}). As discussed below, E_{CORR} is a useful parameter for assessing the probability of localized corrosion and stress corrosion cracking, as well as providing information about uniform corrosion.

Various methods have been developed to predict the rate or extent of the uniform corrosion of copper containers. Because uniform corrosion is limited by the availability of oxidant, the rate of corrosion is of less importance than the extent of corrosion. The maximum depth of corrosion can be assessed based on mass-balance principles (SKB 2011) or using the detailed mechanistically based CCM-UC model (King et al. 2008).

The total amount of O_2 trapped in the repository at the time of closure, expressed per unit area of the container surface, is of the order of 1-10 mol_{O2}/m^2. The exact amount depends on the volume and porosity of buffer and backfill materials and, crucially, the initial degree of saturation (since the majority of the trapped O_2 is present as gaseous O_2 in the air-filled pores of the buffer and backfill). If all of this oxygen is consumed by corrosion of the container, King et al. (2010) estimate that the maximum wall penetration for a copper container in a deep geological repository would be 0.17 mm. In reality, some of the O_2 will be consumed by aerobic microbial activity in the backfill material and the oxidation of ferrous species, so that the actual depth of uniform corrosion will be lower. Depending upon the relative rates of the different microbial and redox reactions, the model predictions suggest that more than 50% of the trapped O_2 could be consumed by processes other than corrosion. A consequence of the limited availability of oxidant is that once all of the O_2 (or the Cu^{2+} produced by the oxidation of $CuCl_2^-$ by O_2) has been consumed, and there is sufficient generation of H_2, corrosion of the container ceases.

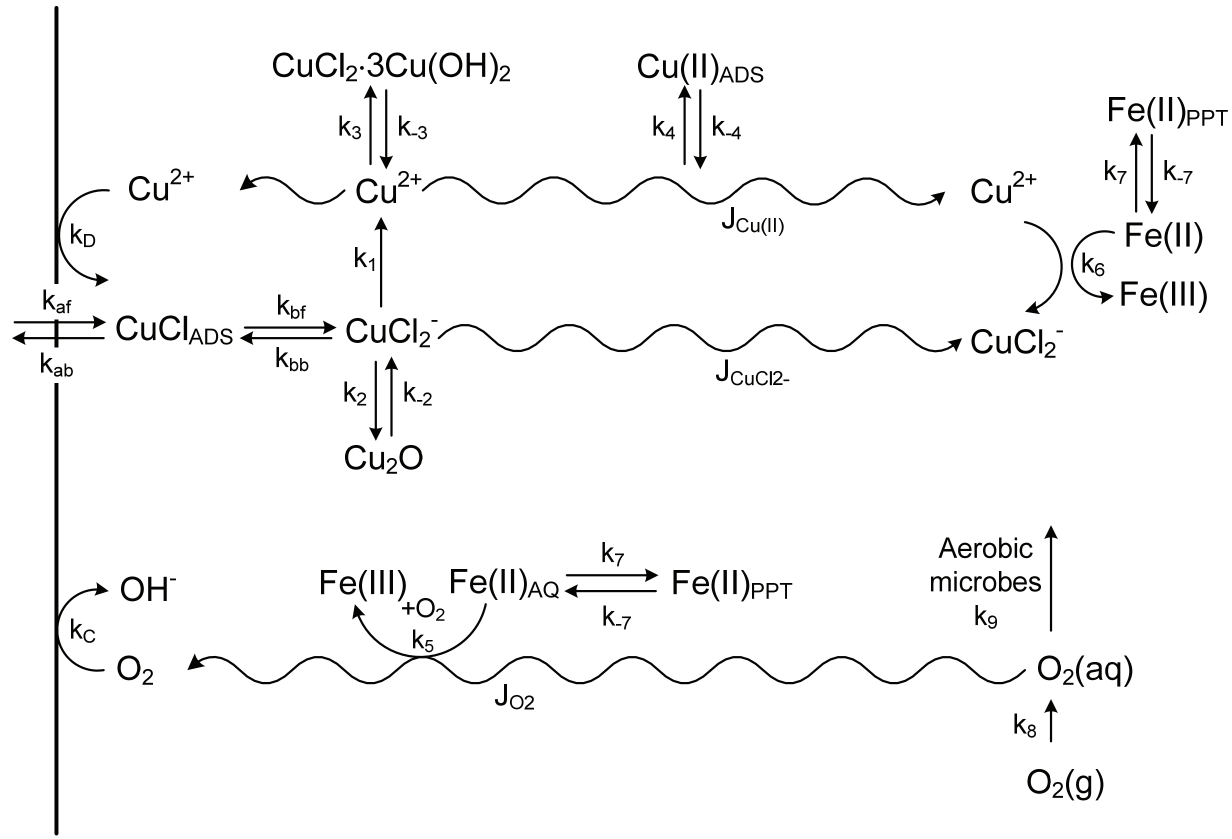

Notes: From King and Kolář (2000) and King et al. (2008, 2010, 2011a). The k's denote rate constants for the various interfacial electrochemical and homogeneous reactions and the J's denote diffusive fluxes.

Figure 5-8: Reaction Scheme for the Uniform Corrosion of Copper in Compacted Bentonite Saturated with O_2-Containing Chloride Solution

5.3.1.5.2 Localized Corrosion

Kwong (2011) and Scully and Edwards (2013) identify that studies designed to specifically examine the surface profile of copper corroded in groundwater-saturated, compacted buffer materials have been completed. Results showed that the copper will only undergo a form of surface roughening as a result of the non-permanent separation of anodic and cathodic processes. Evaluations of the distribution of precipitated corrosion products and surface morphology on the coupon surface (i.e., distribution of peaks and valleys on the surface) indicated an “under-deposit” corrosion. A mechanism to account for the observed surface profile, which involved the periodic separation of anodic and cathodic processes through the formation of temporary occluded cells has since been proposed (King and Kolář 2000).

Experiments were carried out to assess the possibility of localized corrosion of copper for the situation in which there are differences in the flux of O_2 to different parts of the container surface, for example, in the case where bentonite blocks of different density might be used around the container. In this situation, the temporary spatial separation of anodic and cathodic processes is possible. It was shown that the localized corrosion rates would decrease with decreasing oxygen concentration and decreasing container surface temperature. The corroded copper surface showed only general corrosion with minor surface roughening and no distinct pitting. It was concluded that the rate and extent of localized corrosion in a deep geological repository would be very small since there will only be a limited supply of oxygen. It was expected that the corrosion products on the container surface would further limit the rate and extent of localized corrosion.

The long-term localized corrosion behaviour of copper has also been extensively studied in the Swedish / Finnish nuclear waste management programs. They predicted the depth of localized corrosion based on pitting factors and an analysis of empirical pitting data from archaeological artifacts subject to long-term burial in natural environments. Extreme-value statistics developed by Ontario Power Generation for the Canadian program have also been applied to estimate the maximum pit depth on a container as a function of exposure time in the repository (King 2006). A pit propagation model was developed for reducing conditions assuming the pit growth was limited by the transport of HS^- to the copper surface.

Based on these various measurements and models, it was generally agreed that a copper container in a deep geological repository will not undergo classical pitting corrosion, but only a surface roughening or under-deposit corrosion. Corrosion occurs under deposits on the surface, with the resultant temporary spatial separation of the anodic and cathodic sites accounting for the roughened surface. Surface roughening, or under-deposit corrosion, may add a maximum of 0.1 mm to the depth of general corrosion.

5.3.1.5.3 Stress Corrosion Cracking

This section summarizes the considerations for stress corrosion cracking (SCC) of the copper shell that are explored in Kwong (2011). The occurrence of SCC requires a susceptible metal to be exposed to sufficient tensile stress and an active SCC agent. Copper is known to be susceptible to SCC in environments containing ammonia, nitrite ions, acetate, or, possibly, high concentrations of sulphide. Studies focussed on SCC have concluded that the SCC of copper requires the prior formation of a thin oxide or tarnish film. When this film does not form, SCC is not observed.

While SCC agents are not normally found in natural groundwater, they could be introduced by either mining activities or microbial activity. Numerous tests have, therefore, been performed to assess the SCC behaviour of copper in nitrite-, ammonia- and acetate-containing environments. Results indicate that copper SCC susceptibility would decrease with decreasing concentrations of the SCC agents. These studies also suggest a threshold concentration level for each agent below which SCC would not occur. Also observed in these studies is the inhibiting effect of chloride on copper SCC in nitrite, ammonia and acetate environments, the SCC susceptibility decreasing with increasing chloride concentration. The ability of chloride to inhibit SCC also appears to be enhanced by elevated temperatures, as exhibited in tests conducted at 100 to 130°C (in nitrite only and nitrite/chloride solutions). This effect can be attributed to the ability of chloride ions to promote general dissolution of copper, which results in more uniform corrosion at the expense of the formation of the required thin oxide film.

Surface defects on the used fuel container surface can act as stress concentrators (notch-like defects) or stress intensifiers (crack-like defects) and may increase the probability of crack initiation or growth, respectively. A literature review and engineering analyses were performed to assess the effect of surface discontinuities on the initiation and propagation of localized corrosion and SCC of copper welds. The findings indicate no evidence that weld discontinuities would adversely affect the localized corrosion and SCC behaviour of copper containers. The predicted service life of the containers is not affected by the presence of the surface discontinuities.

A number of mechanisms have been proposed for the SCC of copper, including film-rupture/anodic dissolution, tarnish rupture, film-induced cleavage, and surface mobility mechanisms. Taking into account the pre-requisites for crack initiation and crack growth, a conceptual SCC model was defined for copper containers in a repository based on predicting whether the necessary environmental conditions will exist or co-exist. The model is mechanistically based and defines various absolute and conditional criteria for SCC. This model also addresses each of the environmental parameters that control the initiation and growth of SCC.

Research results have suggested SCC under aerobic conditions in a deep geological repository is unlikely as the pre-requisite conditions of corrosion potential, interfacial pH, and concentration of SCC agents do not exist simultaneously at the container surface. According to mechanistic arguments, there is also no evidence to indicate that SCC of copper is possible under anaerobic conditions at the sulphide levels expected at the container surface. Based on the nature of the repository environment, SCC does not appear to be a threat to the integrity of a copper used fuel container.

Despite the low risk of SCC on copper, suitable engineering procedures can be effectively applied to further minimize the probability of SCC. For instance;

1. The level of airborne ammonia and nitrite formed during blasting operations can be controlled to below the threshold concentration in order to preclude the possibility of cracking;
2. The residual tensile stress following container shell and bottom manufacturing can be thermally relieved; and
3. The residual stress on the final closure weld can be controlled and/or reduced using a suitable welding technique.

With regard to the later, it is often good engineering practice to perform a post-weld stress relief of the final closure weld, regardless of the apparent SCC susceptibility of the material. The introduction of a surface compressive stress has proven to be an effective way of preventing the initiation of SCC on various industrial structures. Ambient temperature techniques, such as laser peening and low plasticity burnishing have been developed in the Yucca Mountain Project for this purpose (DOE 2008).

5.3.1.5.4 Microbiologically Influenced Corrosion

The microbiologically-influenced corrosion (MIC) program is summarized in Kwong (2011). Similar to other engineering materials, copper is susceptible to this type of corrosion. Microbial metabolic by-products may affect the SCC behaviour of copper as microbial activity may form SCC agents, namely ammonia, nitrite, and acetate ions. Ammonia and nitrite are produced (and also consumed) by different types of microbe as part of the nitrogen cycle. Acetate is produced by the fermentation of organic molecules. Another species often considered is HS^- produced by the reduction of sulphate by sulphate-reducing bacteria. This last reaction occurs under anaerobic conditions and requires the presence of simple organic molecules or H_2 as electron donors. Without the formation of biofilms on the container surface, the only form of MIC possible is that due to the diffusion of remotely-produced metabolic by-products through the bentonite to the container surface. Sulphide ions produced at a location away from the container surface must diffuse through the bentonite sealing materials to have any effect on container corrosion. The corrosion rate is, therefore, limited by the rate of diffusion of sulphide (HS^-) to the container surface, a continued supply of which is required to sustain MIC.

The Canadian microbial experimental program has demonstrated that a water activity of ≤ 0.96 will be readily achieved within the Canadian sedimentary system, as the pore-water salinity may approach 300 g/L total dissolved salts (see Table 2-4).

A reactive-transport corrosion model to predict the extent of MIC of copper containers has also been developed in the Canadian corrosion program. This model indicates that microbial activity in the repository will not result in shorter container lifetimes. The amount of sulphide ions provided by the microbial reduction of sulphate that reach the container surface is predicted to be insignificant over a million year timeframe. The amount of nitrite and acetate ions, both of which are associated with SCC of copper, are similarly insignificant. Although a higher maximum concentration of ammonia (another known SCC agent) of $\sim 10^{-6}$ mol/L is predicted at the container surface, cracking is unlikely because of the relatively low concentration and because ammonia is only formed after all oxidants in the repository have been consumed.

Based on the assumption that sulphate-reducing bacteria activity would occur in the host rock near the placement room wall and would, conservatively, produce a continuous concentration of 3 ppm of hydrogen sulphide, the corrosion rate was estimated at 1 nm per year and the corrosion allowance for MIC was estimated to be 1 mm after one million years.

5.3.1.6 Summary

Research work over the past 20 years has established a good understanding of the long-term performance of copper used fuel containers in a deep geological repository.

In the high salinity environments anticipated in sedimentary rock groundwater (i.e., > total dissolved solids of $\approx$ 300 g/L), copper will begin to corrode under early atmospheric conditions provided the relative humidity is above ~ 50 - 70%. The rate and mechanism of corrosion will be affected by the presence of atmospheric contaminants such as SO_2 and NO_2. Over time, as the repository environment evolves, the copper container will experience an initial aerobic period of uniform corrosion and some form of surface roughening, before establishing a long-term condition of thermodynamic stability. Uniform corrosion is associated with active copper dissolution in the presence of chloride, which causes the copper container to corrode uniformly, thereby avoiding localized corrosion. Stress corrosion cracking on the copper container is unlikely owing to the lack of the pre-requisite conditions for SCC; namely, the required threshold concentration of SCC agents, a suitable interfacial pH, and the required corrosion potential on the copper surface. Microbiologically influenced corrosion of copper will be controlled by the use of compacted bentonite around the copper container and the high salinity of native groundwater to suppress microbial activity in the near field and to limit the migration of any corrosive agents produced by microbial activity in the far field.

Although there have been measurements of water acting as an oxidant for copper, the available evidence is not entirely reproducible. Within experiments, early measurements are complicated by the presence of air-formed oxides, which may explain some reproducibility concerns; however, there appears to be a gradual coalescence among researchers. Within the most recent Hultquist work (Hultquist et al. 2013), corrosion rates below 10 nm/a have been observed in bulk solutions; this particular value presumes a significant, unproven loss of hydrogen during experimentation has occurred: up to three times what is detected. Without this factor, the Hultquist et al. (2013) corrosion rates are in the 3 nm/yr range in the absence of mass-transfer restrictions from bentonite; this would project to be much lower when the effects of bentonite and ambient hydrogen are included. It is expected that continued experimentation will also decrease uncertainty of such measurements. Regardless of such uncertainty, there is significant evidence that the hydrogen produced from a copper-water interaction or steel corrosion within the repository, would compel any such mechanism to be self limiting, and not a significant corrosion mechanism within a repository. In addition, any effects of water corroding copper would be overwhelmed by the corrosive interaction of copper and microbially produced sulphide, which allows for 1 mm corrosion in one million years.

The knowledge gained over the past 20 years from studies on the corrosion of copper has allowed improved and more realistic predictions to be made for the lifetime of a copper container in a deep geological repository. Under the expected saline groundwater conditions, a realistic estimate of the total extent of copper corrosion from all processes is a loss of wall thickness of about 1.27 mm, i.e., 0.17 mm (uniform corrosion) + 0.1 mm (under-deposit corrosion) + 1 mm (MIC) in one million years.

Therefore, the lifetime of a copper used fuel container is expected to exceed one million years in a deep geological repository in Canada. This finding is comparable with the predicted container lifetime for the Swedish deep geological repository in crystalline rock.

5.3.2 Evolution of a “Breached Used Fuel Container”

Containers for a repository would be manufactured according to a process that includes careful design, fabrication, closure welding, and a series of inspections to avoid significant defects.

Based on defect statistics for a variety of pressure vessels and nuclear components, it was estimated that the probability of a used fuel container having a undetected through-wall manufacturing or installation defect was on the order of 1 defect per 5000 containers (range 1:1,000 to 1:10,000) (Maak et al. 2001).

More recent SKB (2011) analysis of sample welded containers with a similar design but 50 mm thick copper shell, states that the likelihood of an undetected copper weld defect longer than 20 mm is negligible, and the likelihood of a 10-20 mm defect is one per 1,000 containers. As a result, they do not expect any initial through-wall defects within their 6,000 container repository. However, their weld defect statistics are roughly consistent with an estimate that, for a 25-mm thick container, the likelihood of an undetected through wall defect is somewhat less than 1 in 1,000 containers. In a Canadian repository with 12,800 containers, therefore it is statistically estimated that there would be about three containers emplaced with an undetected through-wall defect.

The defect size would be constrained by the fact that it must be large enough to penetrate a sheet of copper that is about 25 mm thick but small enough that it escapes detection. For example, the area exposed by a defect was assumed to be 5 mm^2 in early SKB models, and 0.07 to 7 mm^2 in AECL models associated with the Second Case Study. In the current study, the size of the assumed initial defect is approximately 3 mm^2.

5.3.2.1 Repository Conditions Prior to Saturation for a "Breached Container"

The pre-saturated period covers the time from when the containers are first placed in a repository until the time their exterior (copper) surface is in contact with fully saturated sealing materials (i.e., the time at which the buffer is saturated and is exerting a swelling pressure on the container surface). In low permeability rock, it is likely that this pre-saturated period would last at least 10,000 years.

At the time that the placement rooms are backfilled and sealed, they would contain partially saturated (moistened) buffer. Voids (porosity) in the sealing materials would contain trapped air. Heat from the container would cause the nearby bentonite to dry out. Condensation of the water vapour would occur in cooler portions of the sealing materials.

The relative humidity of the trapped air in the sealing materials near a container is of interest because corrosion of copper and iron in air is observed to be slow or nonexistent at relative humidities less than about 60%. Above this value, copper is subject to aerobic uniform corrosion. Corrosion of steel under the same conditions produces hydrated iron oxides ("rust").

In a breached container, air would initially be present in the narrow assembly gap between the copper and steel vessels (Figure 5-9). The void space in the interior of the steel vessel would be filled with an inert gas (i.e., helium), held in place by a gasket seal beneath the bolted-on lid of the steel vessel. By the end of the pre-saturated period, the gas in the interior of the steel vessel would consist mainly of a mixture of oxygen-depleted air (largely N_2) and helium (Figure 5-9).

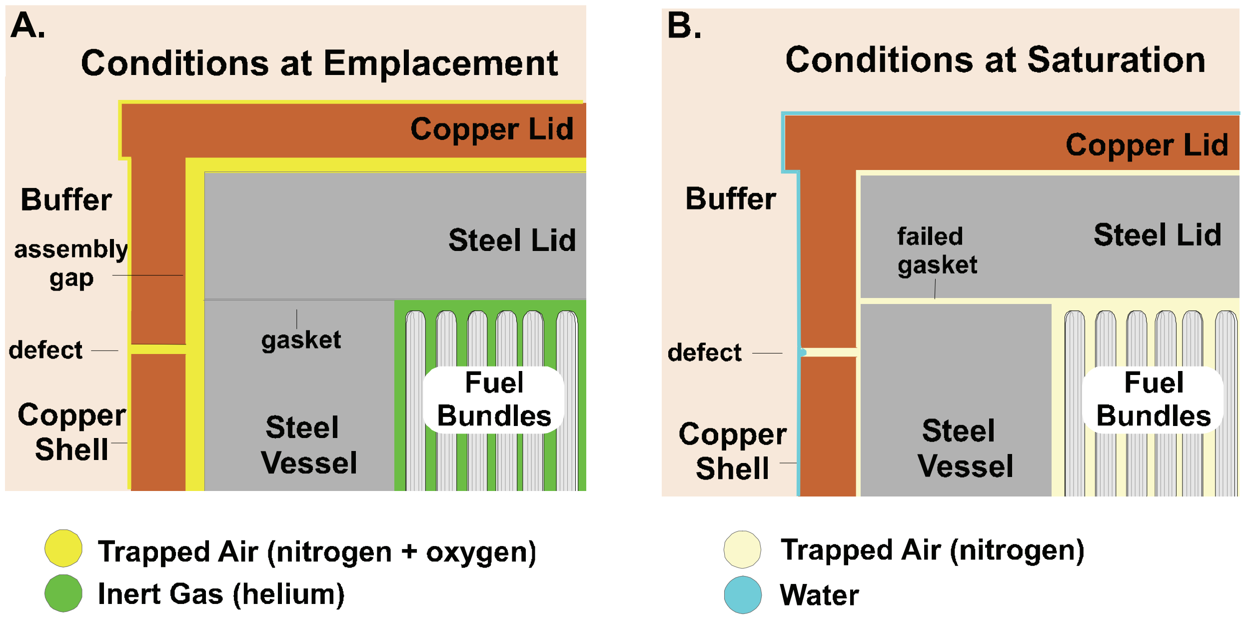

Note: Figure from McMurry et al. (2004).

Figure 5-9: Early Evolution of Conditions in a Container with a Small Defect in the Copper Shell

At saturation, the hydrostatic pressure in the water-filled pores of the sealing materials would be 6 MPa; however, it is likely that the air pressure inside a breached container at this point would be less. This is because the internal free volume (void space) of a container is approximately 1.58 m^3. Filling this volume to 6 MPa would require 75 m^3 of air at 0.1 MPa (i.e., atmospheric pressure); however, this volume is a significant fraction of all of the air that was originally trapped in the room. Given other constraining factors, such as the low permeability of saturated buffer, it is likely that a pressure differential will develop between the interior and exterior of the breached container. As a result, water vapour or liquid would be drawn from the wet buffer into the container interior via the defect in the copper shell.

5.3.2.2 Description of Post-Saturation Processes for a “Breached Container”

The description of post-saturation processes begins when the clay buffer surrounding the breached container is saturated, and liquid water is able to enter the defect in the container (Figure 5-9). A minimum of 10,000 years will have passed after placement of the container in the repository. The assembly gap between the copper and steel vessels (about 1 mm in the reference design) will be almost completely squeezed closed except near the corner of the copper lid and shell. The temperature of the container at this time would be likely in the range of 60 to 90°C.

5.3.2.3 Anaerobic Corrosion of the Steel Vessel

By the time that the repository is saturated, virtually all of the free oxygen in the sealing materials would have been consumed, and anaerobic conditions would prevail. A thin layer of corrosion products (mostly iron oxides or hydroxides from aerobic corrosion of the steel vessel) would be sandwiched between the copper and steel of the breached container. Compared to the metals, the corrosion products would be more porous and less dense. Gases may preferentially diffuse through them, and liquid water may be able to permeate them. Porewater would move from the buffer through the defect in the copper shell, and come into contact with the inner steel vessel. The copper itself would be chemically resistant under anaerobic conditions and would not be significantly affected by contact with water. In contrast, the steel vessel would undergo anaerobic corrosion as long as it was in contact with water; although the corrosion rate would be slower than under oxygenated conditions, and would also decrease as corrosion products were generated.

Where water is in contact with the steel, Reaction (5-6) will occur forming an iron corrosion product and, in the absence of oxygen, hydrogen.

An amorphous or poorly crystalline solid would be likely to form first, which would gradually transform into a more crystalline phase, likely magnetite, and possibly siderite, should sufficient carbonate be carried into the breached container, as discussed in Section 5.2.6.

Initially, iron corrosion products would form only on the outside surface of the steel. After water leaked into the interior of the steel vessel along the space between lid and body, anaerobic corrosion would also occur on the inside steel surfaces. Literature values for the anaerobic corrosion rate of steel vary over a wide range, between 0.1 and 50 μm/a. The corrosion rate in a breached container likely would be at the lower end of the range, given that the water would be chemically buffered by clay and given that the water would be supplied at a limited rate to the steel; this same limitation would likely mitigate any radiolysis reactions that could potentially impact corrosion. Among other factors, the water ingress would be restricted by the low permeability of the bentonite clay around the container, by the small aperture of the defect in the copper shell which may be blocked by swelling bentonite, by slow passage through the porous corrosion products in the narrow copper-steel gap, and possibly by blockage of the opening by the build-up of a hydrogen gas backpressure from the corrosion reaction inside the container. For a steel corrosion rate of 0.1 μm/a, the corresponding H_2 production rate would be about 0.1 to 1 mol/a for one container (equivalent to approximately 0.04 to 0.4 L/a at 6 MPa) depending on what fraction of the inner vessel surface was corroding.

5.3.2.4 Galvanic Corrosion

Although the design of the container puts the copper shell and inner steel container in physical contact, galvanic corrosion will not occur as long as the copper shell is intact. While this condition persists, corrosion reactions and rates will be defined by the outer copper shell. However, for a “breached container”, galvanic corrosion may exist, where one metal performs/catalyzes the cathodic electrochemical reactions, while the other metal performs/catalyzes anodic reactions. In the case of steel (iron) coupled to copper, oxidation of iron at the container breach would be enhanced if the very large intact copper surface could sufficiently support reduction reactions: either oxygen reduction during the aerobic period or hydrogen reduction during the long anaerobic period.

Experiments conducted by Smart et al. (2004, 2005) have examined both conditions and measured galvanic currents: with the copper behaving as a cathode and the iron behaving as an anode. In aerated conditions, galvanic corrosion rates of iron (coupled to copper) are as high as 100 µm/a. Other research has revealed that copper-steel couples in aerated seawater can cause an enhancement in corrosion of steel (Chen et al. 2007). However, the actual depth of corrosion from this process would be significantly limited by the repository oxygen volume, as described in Section 5.3.1.5. When their system was dearated, galvanic currents measured by Smart et al. were much lower: typically 0.1 µm/a at 30°C and 1 µm/a at 50°C (Smart et al. 2005). These values are no different from those measured on iron in dearated groundwater that is not coupled to copper; in effect, the copper couple does not alter the corrosion properties of iron in this medium. The interpretation of this result is that the couple between iron and copper does not sufficiently polarize the copper negatively to support enhanced water reduction (King et al. 2010). Accordingly, the copper shell would be largely inactive to the iron corrosion process, as well as having the additional benefit of protecting the remainder of the steel container from corrosion processes.

The low importance of galvanic corrosion is also supported by results from the SKB Minican experiment. Post-test examination of the first experiment after 4 years in-situ have indicated extensive corrosion by sulphide present in the groundwater, but no evidence of galvanic corrosion (Smart et al. 2012).

5.3.2.5 Deformation of the Copper Shell

As the iron exposed through the copper defect is corroded, it will form corrosion products. Iron corrosion products are less dense than the metal itself. Thus, the volume of Fe_3O_4 formed by Reaction (5-6) is about twice the volume of the Fe metal consumed in its formation (McMurry et al. 2004). As a result of this volume change, the formation of corrosion products in a confined space has the potential to exert a force on the adjacent solids. These stresses would have little preliminary effect on the steel vessel, due to its thick walls (100 mm) and high mechanical strength. However, the copper shell and the surrounding clay buffer would deform more easily. The build up of corrosion products could eventually cause the copper shell to open further around the defect. The opening of the copper shell at the defect site would allow more water to enter the container. Eventually, water also would begin to seep between the steel vessel and the steel lid and into the interior of the container.

This would be limited by the rate of water access through the defect and through the corrosion product. Furthermore, the iron corrosion reactions would also produce hydrogen. This could be at a rate exceeding the ability of the gas to diffuse into the buffer. In this case, hydrogen gas would accumulate in and around the container and form a pressure build-up that would block liquid water from moving into the container through the defect. Then, only water vapour could diffuse through the opening to sustain the steel corrosion. In these analyses, the “bubble” of hydrogen gas blanketing the steel vessel would slow the rate of steel corrosion and expansion of corrosion product thereby delaying rupture of the copper shell for time scales of the order of 200,000 years. The hydrogen blanketing scenario is plausible, but the long time delay requires that there be complete blanketing of the steel.

Experimental evidence shows that high stresses will not be produced by iron corrosion products (Smart et al. 2003, 2006). During analysis of stresses produced during anaerobic corrosion, no detectable expansion was observed over a two year period for bentonite-equililbrated groundwaters under compressive loads (Smart et al. 2006). In addition, the anaerobic corrosion products are easily deformable, and are incapable of producing expansion under simulated repository conditions. Only for aerobic conditions, and low applied loads were expansions measureable due to corrosion products. Similarly, observations from the first MiniCan experiment after 4 years in-situ indicates no expansion in the outer copper shell due to corrosion of the cast iron insert, and apparent extrusion of iron corrosion products through the defect (Smart et al. 2012). As a result, it is likely that the copper shell deformation/rupture described above would occur very slowly.

5.3.2.6 Deformation of the Steel Vessel

The container design for normal loading conditions (i.e., prior to glaciation) would have a significant margin of mechanical strength. For example, the reference container design with 100 mm of steel can meet the reference maximum 7 MPa external pressure with a safety factor of about six. At an anaerobic corrosion rate of 0.1 to 1 μm/a (including corrosion of inner, as well as outer surfaces of the steel vessel), it would take 10,000 to 100,000 years before a 20 mm thickness of steel would be consumed.

Another factor to consider is the additional stress from glacial loading, which would be expected to first occur in about 60,000 years (see Chapter 2, Figure 2-2). At the full design-basis glaciation load, there may be little margin for thinning of the steel vessel walls. If significant corrosion had occurred already, collapse or brittle fracture of the steel vessel would be likely in response to the glacial loading stresses. It is also plausible that the glaciation load would be less than the design basis. For example, if the ice thickness is less than the design-basis maximum, if the load transmitted to depth is less than the hydrostatic loading equivalent to the ice thickness, or if the container was full of water (which would provide hydrostatic balancing of the glacial load). In such cases, the container would be more likely to tolerate further corrosion before plastic deformation and buckling. Regardless of the specific timing and processes the key point is that at some point the steel vessel in a breached container would become sufficiently weakened by corrosion that it would cease to be load-bearing, and it would collapse by buckling inwards.

The stresses causing the steel vessel to collapse would produce a corresponding deformation of the copper shell around it. During this movement, the strain limit for copper would be exceeded in portions of the copper shell, and the copper would crack, but in a general sense the copper metal would continue to conform to the shape of the steel vessel. Similarly, as the copper and steel compressed inwards, the surrounding buffer would expand around the new configuration of deformed metal.

Even after the breached container collapsed, the overall change in its volume would not be substantial compared to the volume that was originally occupied by the container. Initially (at the time of placement), the open or void space in a container, into which the collapse would occur, would be roughly 1.58 m^3, which is about 30% of the container's total volume. Moreover, it is likely that much of this initially open volume would have become filled with iron corrosion products, further restricting the amount of collapse.

After the breached container buckled and the buffer around it expanded to conform to the change in shape, the copper shell would remain essentially unchanged in appearance for the remainder of the million-year timeframe. Complete corrosion of the copper is estimated to take several million years or longer, as indicated by sheets of natural copper that have persisted in sedimentary rocks for more than a hundred million years. In contrast to the copper, anaerobic corrosion of the steel vessel would continue in-situ until all of the steel was consumed.

5.3.2.7 Corrosion and Deformation of the Zircaloy Cladding

At the time of placement in a repository, virtually all of the used fuel elements would have intact Zircaloy cladding. A few of the cladding sheaths would have become defective during their use in a reactor (estimates of this number range from approximately 1 per 10,000 to 1 per 100,000 fuel elements) (Frescura and Wight 1979). Some others may have developed defects during post-reactor storage, during transportation, or during packaging into containers. In a breached container, one of the most significant changes in the used fuel bundles over time would be mechanical failure of the cladding, mainly in association with corrosion of the steel vessel. In addition, the cladding would be subjected to hydrogen embrittlement, corrosion, and creep, as described below.

Over time, hydrogen gas would be produced inside a breached container by two separate processes - the anaerobic corrosion of steel and the radiolysis of water. Hydrogen-induced cracking is a potential failure mechanism for Zircaloy cladding. Studies of the durability of used fuel bundles in dry or moist air have found no evidence of cladding failures (Lovazic and Gierszewski 2005). Given that significant partial pressures of hydrogen gas would not develop in a container until saturation of the repository had occurred, lifetimes of the Zircaloy cladding in a breached container could exceed thousands of years.

On observable time scales, the uniform corrosion of Zircaloy cladding is negligible, likely between 1 and 5 nm/a, and with an upper limit of 20 nm/a, even in contact with water, due largely to the corrosion resistance of a passive oxide film on the Zircaloy surface (Shoesmith and Zagidulin 2010). In a breached container, pitting and crevice corrosion of cladding would be inhibited by the rapid consumption of oxidizing agents (residual oxygen and radiolysis products) by the iron and copper container materials. In addition, iodine-induced stress corrosion cracking would be inhibited because most of the iodine in the fuel gap in CANDU fuel exists as cesium iodide, preventing it from forming the zirconium iodides that are thought to be the chemical precursors to stress corrosion cracking in Zircaloy. Using the above values, a general corrosion lifetime for a 0.5 mm cladding could be calculated to exceed 25,000 years presuming the highest corrosion rate of 20 nm/a, and with a more realistic expectation above 100,000 years for the expected corrosion rates at or below 5 nm/a.

Ultimately, any used fuel bundles that otherwise remained unruptured would be likely to fail during the corrosion-induced collapse of the steel vessel. As discussed previously, the timing of this event is uncertain, but a reasonable estimate would be within 10,000 to 100,000 years after a defect is created in the copper shell.

5.3.2.8 Dissolution of the Used Fuel Matrix

After the cladding is breached and the fuel pellets exposed to water, the next barrier against radionuclide release is the UO_2 fuel matrix, which contains most of the radionuclides and has a very low solubility. Dissolution of the UO_2 matrix of the used fuel would progress according to two general methods: oxidative dissolution (i.e., corrosion) and chemical dissolution. Radiolysis of water in contact with the fuel pellets would produce oxidizing conditions at or near the used fuel surface, contributing initially to oxidative dissolution of the UO_2. To the extent that water is able to contact the fuel while radiation fields are high, this process would tend to promote the dissolution of the used fuel at a higher rate than would be expected solely on the basis of the chemical solubility of UO_2 in the near-field porewater. The production rate of oxidants by radiolysis would decrease with time as the strength of the radiation field decreases (Gobien et al. 2013).

At the fuel-water interface, the alpha dose rate exceeds the gamma and beta dose rates for most of the fuel history (Figure 5-10) and is the main contributor to radiolysis, producing molecular oxidants such as H_2O_2. Other potential sources of oxidants, such as any O_2 trapped inside the container when it was sealed, would already have been consumed by Fe and Cu corrosion processes before the fuel cladding was breached because these corrosion reactions are much faster than the reaction with UO_2. In principle, the radiolytically produced oxidants also would be consumed by reaction with container materials rather than by reaction with used fuel; however, for alpha radiolysis, the oxidants would only be produced within 20 μm of the fuel-water interface and they would have difficulty diffusing through openings in the cladding to react with container materials.

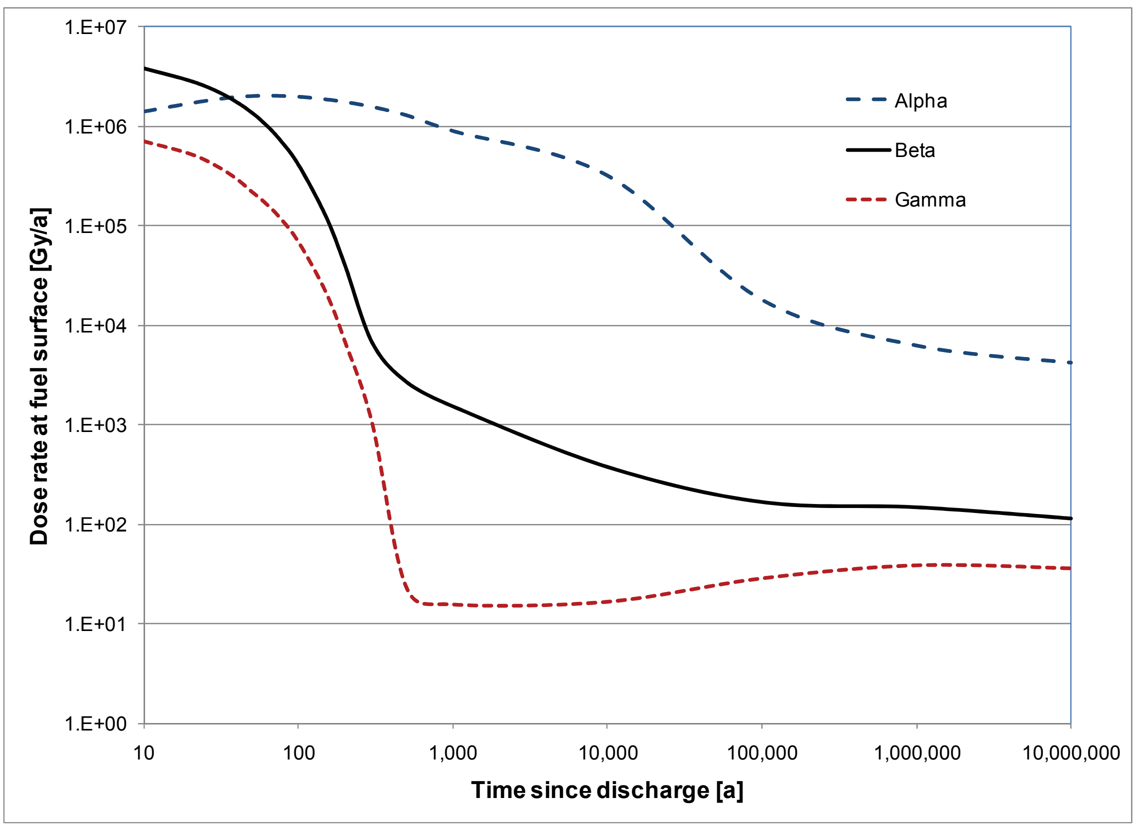

Figure 5-10: Radiation Dose Rate in Water at the Fuel Surface (220 MWh/kgU burnup)

Oxidative dissolution of the fuel continues as long as the alpha radiation field is sufficiently high. However, the actual dissolution rate decreases as the alpha field decreases due to decay. Experiments and mechanistic models have been developed to describe this corrosion rate, and indicate that the dissolution of the used fuel would take more than one million years (Gobien et al. 2013).

Furthermore, in UO_2 and used fuel dissolution experiments the dissolution rate dropped by several orders of magnitude in the presence of even modest pressures of hydrogen gas (Shoesmith 2008) that would certainly be present due to corrosion of the iron vessel. A number of mechanisms have been either demonstrated or proposed to explain these effects, all of which involved the activation of hydrogen to produce the strongly reducing $H^{\bullet}$ radical, which scavenges radiolytic oxidants and suppresses fuel oxidation and corrosion (Shoesmith 2008).

After the alpha radiation field has decreased substantially, chemical dissolution of the fuel, proceeds according to the reaction,

$$UO_2 + 2H_2O \rightarrow U(OH)_4 \qquad (5\text{-}20)$$

under the anaerobic conditions expected in the repository. This reaction occurs very slowly, as is illustrated by the age of uraninite ore (largely UO_2) deposits, including northern Saskatchewan.

5.3.2.9 Radionuclide Release from the Fuel Pellets

Extensive studies of the interactions between used fuel and groundwater have established that radionuclide release from the used fuel occurs by two main processes. Initially, there would be a comparatively rapid release of a small fraction (typically a few percent) of the inventory of a selected group of radionuclides, that are either very soluble (such as ^{137}Cs, ^{129}I, ^{14}C and ^{36}Cl) or gaseous (such as Xe), and that are residing in the fuel sheath gap or at grain boundaries which are quickly accessed by water. This release process is referred to as “instant-release”. The second and slower release process comprises release of radionuclides from the UO_2 fuel matrix as the matrix itself corrodes or dissolves (called "congruent dissolution").

The instant-release fractions for various important radionuclides in used CANDU fuel are given in Gobien et al. (2013) and typical values for selected radionuclides are presented in Table 5-5. Note that the use of the term “instant release” with reference to the gap and grain boundary inventories is a simplification. In reality, it would take a finite time for water to penetrate into the grain boundaries and for the radionuclides located there to diffuse out. However, compared to the much longer time required for dissolution of the UO_2 matrix itself, grain boundary releases are so much faster that they can be considered “instantaneous”. Therefore, in conceptual models of radionuclide release, both locations - the gap and grain boundary inventories - are considered to contribute to the instant-release fraction.

Table 5-5: Typical Instant-Release Fractions for Selected Radionuclides

Radionuclide	Instant-Release Fraction (% of Inventory)
Cs	4
I	4
Cl	6
Tc	1
Actinides (Pu, Am, etc.)	0

Note: From Gobien et al. (2013).

Ferry et al. (2008) have shown that the instant release fractions do not change with time due to, for example, athermal diffusion of radionuclides induced by alpha-particle recoil displacements.

In addition to the bulk of the radionuclides in the used fuel pellets, there would be a small quantity of radionuclides present in the irradiated Zircaloy cladding from neutron activation. These radionuclides are generally distributed uniformly through the cladding and would only be released as the cladding itself dissolves. (However, evidence suggests that some of the C-14 in the Zircaloy is present within the zirconium oxide film (Gobien et al. 2013). This C-14 is released as soon as water contacts the Zircaloy. Zircaloy is corrosion-resistant in water due to the stability of its oxide coating, as described in Section 5.3.2.7. The strong adherence of the ZrO_2 corrosion layer to the metal surface suggests that radionuclides would be incorporated into the ZrO_2 as it forms and would only be released to solution when the oxide itself dissolves. Given the low solubility of ZrO_2, the rate of dissolution of the oxide and hence the release rate of the nuclides in the Zircaloy can be described using a solubility-limited dissolution model in which the rate of dissolution of the ZrO_2 is determined by the rate of diffusion of Zr away from the cladding.

5.3.2.10 Fate of Released Radionuclides

As radionuclides are released to solution, some would become oversaturated and secondary radionuclide-bearing phases would precipitate (e.g., ThO_2) on the fuel surface or on other surfaces nearby, such as provided by the metal corrosion products. Besides the low overall amount of such nuclides in a container, it is expected that their concentration in a precipitate would be diluted by the co-precipitation of other elements. Precipitation of a large mass of fissile nuclides in particular would be hindered by the intergrowth of such mixed-isotope precipitates along with iron corrosion products or buffer clays.

The radionuclides that remained in solution as aqueous species, and solids suspended in colloidal form, would diffuse through the various metal corrosion products inside the container. The corrosion products would also provide a surface for sorption of many of the radionuclides. In some cases, the sorption would be irreversible because the radionuclides would be incorporated into the crystal lattice of the corrosion product if it undergoes a transformation to a more stable solid phase.

Dissolved radionuclides would diffuse by a tortuous path through what was left of the steel container, through the cracks in the copper shell, through the low-permeability sealing materials, and finally through the rock around the repository. Migration of radionuclides away from the repository and their transport rate through the geosphere as a whole would be controlled by the local hydrogeological conditions. For the current hypothetical geosphere, groundwater velocities are low and transport is diffusion controlled. Radionuclides in colloid form or sorbed to colloids would be filtered by the buffer and not reach the geosphere.

5.3.3 Confidence

Extensive corrosion experiments have been carried out to improve the confidence for predicting the corrosion behaviour and lifetime of copper used fuel containers in a deep geological repository in Canada.

Container Corrosion: Because of the extensive experimental database on the corrosion of copper, the level of mechanistic understanding that has been developed over the past 30 years, and the existence of natural and archaeological analogues (discussed in Chapter 10), there is a significant confidence in the prediction of the long-term corrosion behaviour of copper containers. Both the predictive models for corrosion processes that are expected to occur, such as uniform corrosion and localized surface roughening, and the reasoned arguments against those that are not thought to be possible, such as stress corrosion cracking, are robust. Where uncertainty exists, such as the mechanism and exact corrosion rate that describe copper corrosion in anaerobic water or brine solutions, the total corrosion possible from these processes is very small over the container design life.

The evidence from natural and man-made analogues builds confidence in the conclusions drawn from experimental and modelling studies. Man-made analogues, such as Bronze Age artifacts or more-recent anthropogenic objects (discussed in Chapter 10), also provide useful supporting evidence that copper corrodes slowly, even in near-surface aerobic environments. The existence of native metallic copper deposits indicates that, under certain environmental conditions, metallic copper is stable over geological time scales. The fact that the majority of copper deposits in the Earth's crust are in the form of sulphide minerals is also evidence of the potential role of HS^- species in the corrosion of copper containers. Although it is not a pre-requisite that the groundwater at repository depth be free of sulphide, as the programs in Sweden and Finland demonstrate, there are clear advantages to selecting a site with no or low sulphide groundwater levels, as appears to be the case in southern Ontario sedimentary rock.

Confidence in long-term predictions is also supported by the robustness of those predictions and on the underlying information on which they are based. This confidence can stem from achieving the same result from different modelling approaches. For example, the conclusion that the maximum depth of uniform corrosion is of the order of a few hundred micrometres is predicted by both simple mass-balance models (SKB 2011) and from detailed mechanistically based reactive-transport modelling (King et al. 2008). These detailed reactive-transport models have been validated against experimental data and evidence from archaeological analogues (King et al. 2001).

Confidence also results from having a sound mechanistic understanding of corrosion processes. For example, the proposed mechanism to explain observations discussed in Section 5.3.1.5.2 is strong evidence that under repository conditions the localized corrosion of copper containers will take the form of surface roughening rather than pitting. This understanding is equally important for processes that are not considered likely to occur, such as stress corrosion cracking. The approach for stress corrosion cracking provides multiple lines of argument against this behaviour and it is not considered feasible that all of the pre-requisite conditions for cracking would exist in the repository at the same time.

There are also multiple lines of argument for why microbiologically induced corrosion will have a minimal impact on the container (King 2009b, Sherwood Lollar 2011 and Wolfaardt and Korber 2012). However, uncertainties regarding the potential for microbial growth and activity under unsaturated conditions and at component interfaces requires further investigations. Since the possibility of remote microbial activity cannot be excluded, a corrosion allowance is made for this in lifetime assessments (Kwong 2011 and Scully and Edwards 2013).

The multi-barrier repository system represents a robust system that is capable of withstanding upset or unexpected conditions whilst still maintaining a high degree of containment. For example, the predicted container lifetimes are insensitive to the groundwater salinity and, in fact, higher Cl^- concentrations promote uniform rather than localized corrosion (King et al. 2010, 2011a). Information from site investigations in sedimentary rock in Canada suggest that the there is little or no sulphide in deep groundwaters (INTERA 2011). Experience from the Swedish and Finnish programs demonstrates that the combination of a copper container and dense bentonite buffer provides long-term containment even if sulphide were to be present. Similarly, there is no geological evidence that O_2-containing water has never reached repository depths even through glaciation events (see Chapter 2).

Copper Creep: Creep tests and modelling studies indicate that the copper creep deformation would stop once it has collapsed onto the inner steel vessel since the estimated creep deformation is extremely small. This also means that the amount of creep deformation of the copper vessel would depend on the gap width between the copper vessel and steel vessel. Recent analysis of data has revealed some uncertainty in the long-term creep fracture performance of oxygen-free phosphorus doped copper, and a need to supplement modelling capability with respect to creep ductility and mechanical integrity models. Accordingly, a long-term study is ongoing to improve confidence in these areas.

Container Temperature: The container surface temperature is affected by the container power, placement method, chemical composition, water content and thickness of sealing materials, distance between containers, distance between the placement rooms and tunnels, etc. The thermal responses were successfully modelled and there is good confidence that the evolution of temperatures of the container surface and surrounding bentonite buffer materials can be well estimated by existing computer models.

Container Structural Integrity: To maintain long-term structural integrity during its design life, the repository container is designed to withstand a load of 45 MPa. This includes an external isotropic pressure of up to 7 MPa during the pre-glaciation period, which accounts for the 6 MPa hydrostatic pressure up to a 500 m depth together with 1 MPa bentonite swelling pressure. The container could also withstand an external pressure load of 38 MPa during the glaciation period (which corresponds to a 3,800 m thick ice sheet) with full load applied as hydrostatic head (i.e., no load carried by the rock matrix). These are conservative assumptions. While glaciation would be a significant load, the earliest site coverage due to an ice sheet would be thousands of years in the future, probably at least another 60,000 years.

The copper container would be subjected to uneven bentonite swelling loads during the transient period before the completion of full water saturation and also, possibly, after saturation (though to a reduced extent) because of density differences that do not entirely homogenize because of internal friction. It is expected that the uneven swelling pressure loads would not cause container failure, based on the results of analyses for similar SKB and Posiva containers (Werme 1998, Raiko 2005). This will be verified by further engineering analyses.

Overall, there is high confidence in the structural integrity of the inner steel container for at least 100,000 years, and probably for as long as the copper shell maintains its integrity.

5.4 Long-Term Evolution of Buffer, Backfill and Seals

Each used fuel container along the centerline placement tunnel rests on a highly-compacted bentonite pedestal, with the remaining void spaces filled with gap-fill pellets. Bentonite is a type of clay that swells on contact with water, providing a natural self-sealing ability. Bentonite is a durable natural material that is expected to maintain its properties over the long term.

The safety strategy acknowledges that properties of the engineered barriers will allow safety functions to be fulfilled. This includes the design characteristics of surrounding the container by a buffer layer (approximately 60 cm) of dense bentonite-based clay pellets that will swell on contact with water. This clay layer will inhibit groundwater movement, has self-sealing capability, will inhibit microbial activity near the container, and retard contaminant transport.

The main processes with potential influence on the evolution of the sealing systems are listed in Table 5-6 and discussed in the following sections.

Table 5-6: Processes with a Potential Influence on the Evolution of Buffer/Backfill/Seals

PROCESS	POTENTIAL INFLUENCE
RADIATION	
None	• None
THERMAL	
Heat transport from container	• Change in temperature of sealing materials and rock • Redistribution of moisture prior to saturation • Temperature increases across gap or interface
HYDRAULIC & PNEUMATIC	
Saturation of repository	• Expansion of bentonite to close gaps • Chemical reactions between water and sealing materials • Development of swelling and hydrostatic pressure • Changes in thermal conductivity of buffer

PROCESS	POTENTIAL INFLUENCE
Groundwater flow	• Rate of water supply for saturation • Erosion/piping under excessive amounts of inflow in the preclosure period
MECHANICAL	
Swelling pressure	• Density redistribution in clay-based sealing materials • Sealing of cracks and gaps in clay • Stresses in concrete/bulkhead
Thermal strains in concrete	• Fracturing in concrete; increased permeability
CHEMICAL	
Diffusion of chemical species	• Changes in porewater composition/salinity
Ion exchange in clays	• Changes in porewater composition • Change in hydraulic conductivity and swelling pressure of clay-based seals
Reactions with redox-sensitive minerals	• Consumption of oxygen in repository
Increase in salinity	• Changes in hydraulic conductivity and swelling pressure of clay-based seals
BIOLOGICAL	
Aerobic microbial activity in backfill	• Consumption of oxygen in repository
Anaerobic microbial activity in backfill	• Generation of sulphide which is a potential corrosion risk to copper container

Notes: Processes listed are those that are most likely to have a notable effect on the buffer/backfill/seals, over a time scale of one million years.

5.4.1 Changes during Saturation

After the buffer pellets are installed, the water seeping into the repository would begin to wet them, and the bentonite in the buffer would expand. As this expansion progresses, it will fill the space between the pellets and restrict water movement. Moreover, the swelling pressure would in due course provide mechanical resistance to the local effects of large-scale flexing and crustal rebound processes associated with glacial loading, reducing the severity of damage to the near-field rock surrounding the backfilled openings of the repository. The swelling capacity of the bentonite decreases at high salinity, but the performance requirements for swelling pressures are met for salinities expected at 500 m depth, i.e., a total dissolved solids content of aroound 275 g/L (Figure 5-11).

The Effective Montmorillonite Dry Density (EMDD) is a parameter that allows a comparison of the behaviour of different types and densities of clay-based materials (Man and Martino 2009, Dixon et al. 2011) (see Table 4-4). For the reference gap fill material, using dense pellets of MX-80 clay and emplaced at an effective dry density of 1,410 kg/m^3, the EMDD will be around 1,260 kg/m^3.

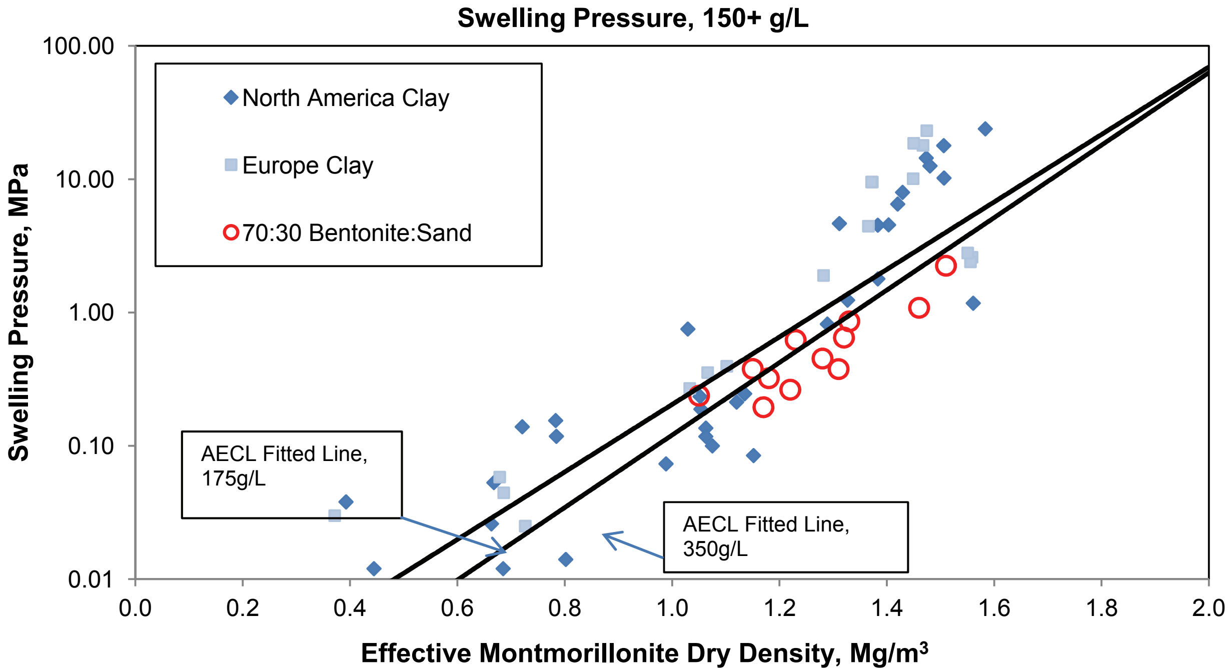

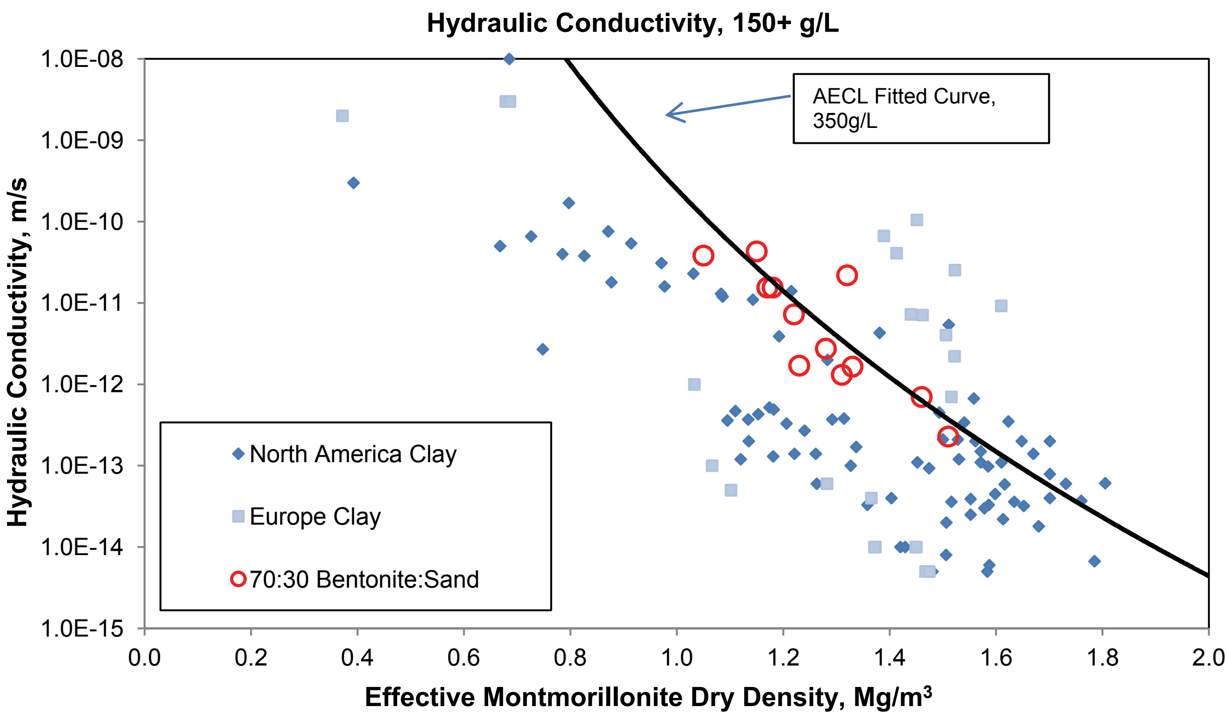

Note: Recent measurements of 70:30 Bentonite:Sand under relevant sedimentary rock conditions are shown in red circles.

Figure 5-11: Hydraulic Conductivity and Swelling Pressure under Saline Water Conditions: Variation with Effective Montmorillonite Dry Density

The timing and rate of saturation of a repository depends on a number of site-specific conditions. In the Cobourg Formation, the limestone has a very low hydraulic conductivity and porosity; as such, ingress of water into the repository will be very slow and the bentonite buffer will take a considerable amount of time to saturate. In addition, other factors such as the thermal gradient from the containers would counter the resaturation process. In order to estimate the saturation time of the repository, the saturation process was modelled using the coupled thermal-hydro-mechanical code T2GGM (Suckling et al. 2013). The minimum saturation time was estimated to be 10,000 years (Gobien et al. 2013, Section 5.2) accounting for the availability of water in the rock, the suction potential of the bentonite and the thermal gradient of the container.

5.4.2 Temperature Changes

The thermal conductivity of the various clay-based sealing system components changes with their degree of water saturation. Figure 5-12 illustrates this relationship for bentonite-only and bentonite-sand compositions. This figure illustrates the effects of sealing material composition and water content on its heat-transfer characteristics. Initially considered for use as the buffer material in the repository concept developed by AECL, a mixture of equal dry weight proportions of sand and bentonite was defined as the reference bentonite-sand buffer for use in filling the region between the container and the surrounding rock. Subsequent review identified bentonite-only clay as the preferred buffer material, such as the 100% bentonite gap fill pellets with a dry density of 1,410 kg/m^3.

From Figure 5-12, it can be seen that in the region nearest the containers, the thermal conductivity of the buffer will decrease as heat from the containers drives moisture away. In contrast, buffer thermal conductivity will gradually increase as the degree of saturation increases. Good agreement is obtained in modelling of thermal profiles in field experiments like the SKB Container Retrieval Test when the thermal conductivity characteristics provided in Figure 5-12 were used (Guo 2009).

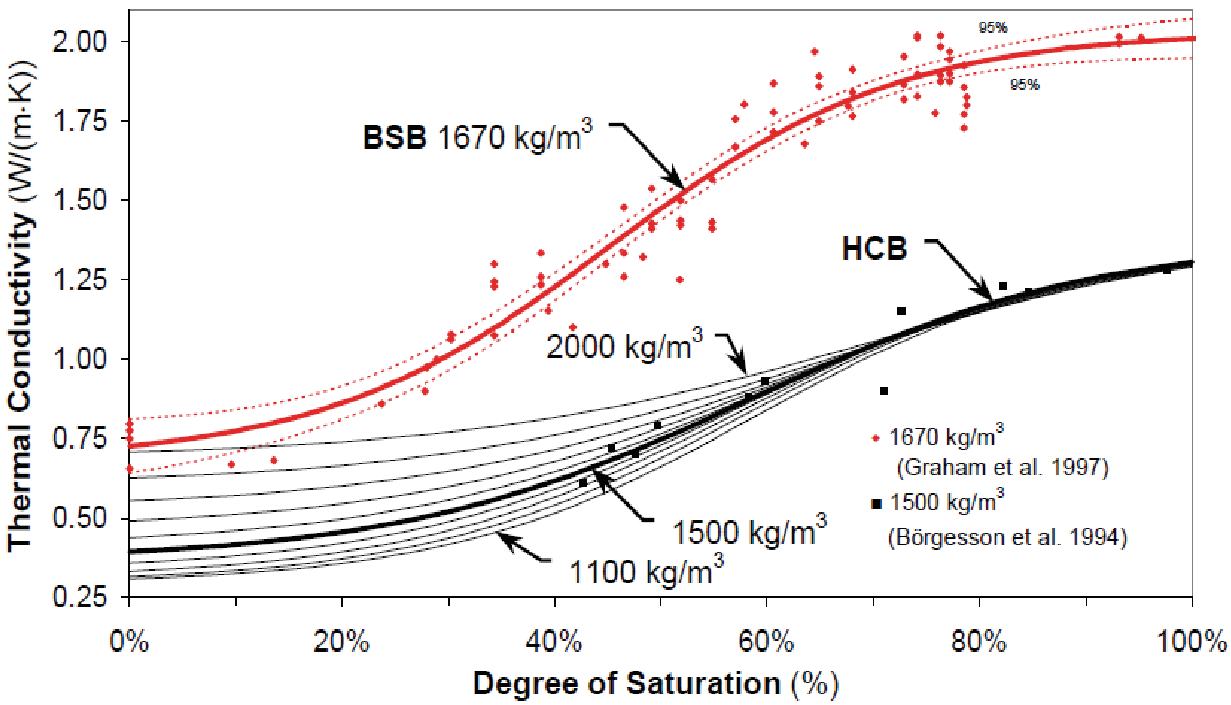

Notes: From Man and Martino (2009). Label units are dry densities.

Figure 5-12: Thermal Conductivity of 50:50 wt% Bentonite-Sand Buffer (BSB) and of 100 wt% MX-80 Bentonite

The maximum near-field temperature is predicted to occur within the first 30 years following placement as shown in Figure 5-5 (Guo 2010), when the buffer will be unsaturated.

The main sealing material that would potentially be affected by thermal expansion is the concrete bulkheads at the ends of placement rooms (Figure 4-15), which could also be affected by heat released during their curing process. These would be installed using low-heat concrete and in a manner that minimized contraction during the concrete curing process.

Later, as the temperature of the repository declines (Figure 5-5), thermal contraction of the concrete bulkhead is likely to cause some rejuvenation of cracks or the production of new cracks at the rock-concrete interface. This process was observed in the concrete seal portion of the AECL URL Tunnel Sealing Experiment (Chandler et al. 2002). The concept of using a composite HCB-concrete structure in a repository anticipates that by the time temperatures decrease significantly in this region, the clay gasket that was installed as part of the composite seal should be fully saturated. The clay would expand providing a tight contact with the concrete and rock and if water flow is occurring from the backfilled tunnel past the concrete it is expected that some of the clay will move/intrude into the open interface and reduce mass-transport along this feature.

5.4.3 Chemical Changes

An important function of the buffer is to produce/maintain a chemical environment in the repository, which will inhibit corrosion of the containers and, in the case of a breach in a container, would limit the solubility of the used fuel and the subsequent migration of radionuclides. Conversely, the composition of porewater in the repository will affect the mechanical and hydraulic properties of the buffer. The evolution of porewater chemistry in the sealing materials is complex as it is influenced by many parameters, including the compositions and proportions of minerals in the buffer and backfill, the composition of the saturating groundwater, the repository temperature, the relative rates of movement through the clay, the initial proportions of exchangeable cations in the clay minerals, and the composition of the water used during wetting and compaction of the sealing materials. Eventually the porewater in the buffer would resemble the groundwater entering the repository and the Na in the bentonite would have exchanged with Ca in the groundwater, potentially causing a reduction in the swelling pressue and an increase in the hydraulic conductivity of the buffer. However, such potential effects are accounted for in the design of the repository.

5.4.4 Changes due to Biological Processes

Aerobic biodegradation of concrete is a well-known microbial process (Humphreys et al. 2010). Initially, conditions in the vicinity of the concrete seals and floors in the deep geological repository may be moist and aerobic enough that pyrite or other sulphide minerals present in the sealing materials (as part of the concrete aggregate or as minor components in buffer or backfill) could be converted to sulphuric acid by sulphate-producing bacteria. The extent of this corrosion would be minor, however, given the relatively short duration of oxidizing conditions in the repository and the likely low abundances of sulphide accessory minerals in the sealing materials.

Clay-based materials have been shown to contain indigenous aerobic and anaerobic microorganisms. Microorganisms could also enter the sealing materials during the operating phase of a repository from the air and human activities in the short term and from the host rock in the long term. The current understanding of microbiology in the context of a repository is summarized by Wolfaardt and Korber (2012).

Specific biogeochemical processes in the buffer, backfill and seals pertain to:

1. Consumption of oxygen and creation of an anaerobic environment;
2. Gas production and consumption; and
3. Microbiologically-influenced corrosion (MIC).

As the geosphere of a deep geological repository is nutrient-poor, microbial activity at depth is limited compared to the near-surface environment.

During the time that a repository is open, the engineered barrier system and adjacent rock would be exposed to air. This would facilitate the growth of aerobic bacteria. After the repository is closed, the aerobic bacteria in this zone are expected to actively promote reducing conditions by consuming the remaining oxygen. Anaerobic bacteria, which were likely to have been the main forms of life in the deep subsurface environment prior to repository excavation, would eventually dominate again, and reducing groundwater conditions would be maintained far into the future. Upon establishment of anaerobic repository conditions, a variety of organisms with the capabilities to utilize alternate electron acceptors have the potential to become active. Anaerobic bacteria can both produce and consume gases, which have limited potential to impact both the physical and chemical aspects of the repository. Of particular interest, is the potential for microbial activity to cause microbiologically influenced corrosion, as discussed in Section 5.3.1.5.4. As a result, a substantial amount of research has been conducted on ability of clay buffer to inhibit microbial activity (e.g., Stroes-Gascoyne 2010).

In the current Canadian EBS design, 100% highly-compacted bentonite buffer material surrounding the waste containers is proposed to prevent or minimize potential negative consequences of microbial activity, such as damage to the container or barrier integrity. Numerous studies have evaluated the survival and activity of microorganisms in clay-based sealing materials under relevant environmental conditions, as summarized in Wolfaardt and Korber (2012). The activity and abundance of microbes in a repository are affected by three main factors: the supply of usable nutrients and energy sources, the availability of water, and elevated temperatures. Radiation fields are not expected to be significant due to the shielding provided by the thick-walled containers.

Sources of nutrients in the sealing materials would include organic matter associated with the clays, as well as nitrates and fuel oil from blasting residues, and hydrocarbons from diesel oils and exhaust gases, introduced during repository excavation and operation. As the organic matter in such clays has already persisted in the presence of indigenous microbial assemblages for thousands to millions of years, it is probably unrealistic to assume that all of the organic carbon would be accessible to microbes. It is likely, therefore, that “available” organic carbon would be the limiting nutrient for microbial activity in a repository.

The second factor that would have an important influence on microbes in clay-based sealing materials is the availability of water. Microbiologists generally use a thermodynamic parameter, water activity (a_w), to express water availability in a quantitative sense. This term corresponds to the ratio of a solution’s vapour pressure to that of pure water at a given temperature. The activity of porewater in sealing materials is affected in particular by the salinity of the water, as well as by the affinity of the clay for water. For example, while the water activity in pure water is 1, the water activity in a 2 mol/kg solution of $CaCl_2$ is about 0.85 within the buffer material (King and Stroes-Gascoyne 1997). Bacteria must expend extra effort to grow in a habitat with a low a_w because they must maintain a high internal solute concentration to retain water within their cells. Most bacteria flourish only at or above an a_w of approximately 0.98, the a_w for seawater (see Figure 5-13). In order for the buffer to inhibit bacterial growth, it has been established that bentonite would need to meet one or both of the following criteria:

- A water activity of less than or equal to 0.96, resulting from a bentonite dry density of at least 1,600 kg/m^3 or a porewater salinity greater than 60 g NaCl/L (Stroes-Gascoyne et al. 2006, 2007a, 2007b); or
- A swelling pressure of at least 2 MPa (Pusch 1999). Swelling of clay is expected to restrict the mobility of microbes and of nutrients, causing starvation.

The third major factor affecting the viability of microbes in the sealing materials is temperature, which would range from ambient (10 - 20^{o}C) to ~120^{o}C adjacent to the container. Temperatures within this range would have some impact on the viability of most microbes indigenous to the sealing materials. The bacteria in buffer closest to the container would be subjected to the most intense heat and also the related buffer desiccation. Experiments assessing the effect of temperature suggest that microbes were not particularly sensitive to a temperature of 60°C and some culturability remained after exposure to 80°C at all dry buffer densities studied (0.8 to 2.0 Mg/m^3), whereas at temperatures ≥ 121°C, culturability was reduced (Stroes-Gascoyne and Hamon 2010). Importantly, the effect of temperature on culturability in low dry density bentonite was reversible once the heat source was removed and re-saturation was allowed to occur, highlighting the importance of maintaining high dry density to keep microbial activity to a minimum (Stroes-Gascoyne and Hamon 2010).

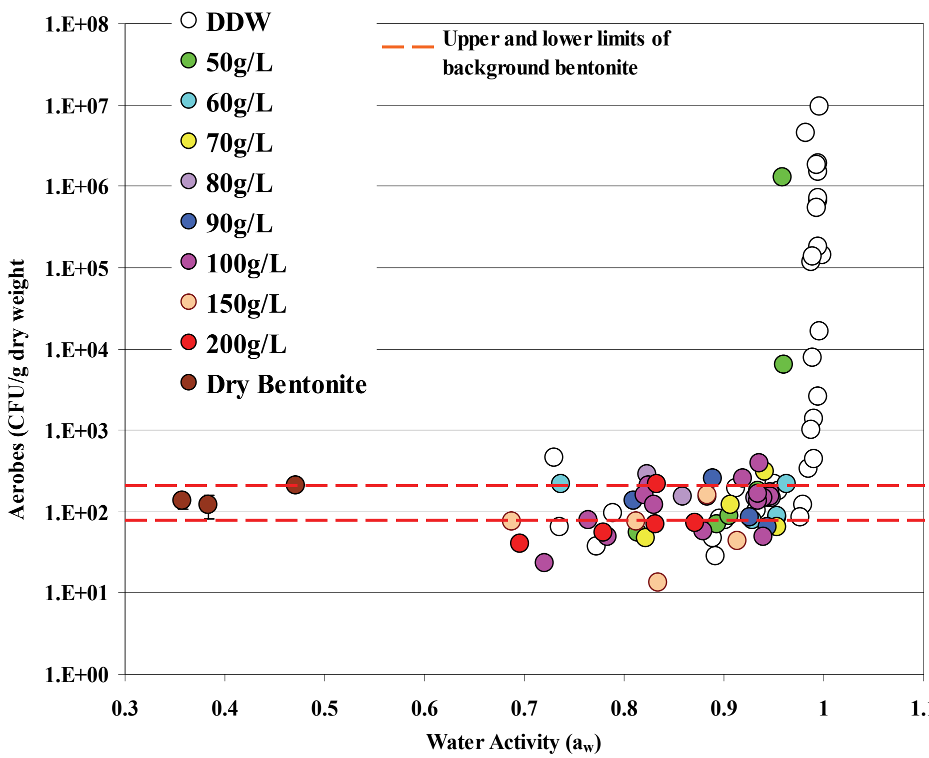

Notes: Stroes-Gascoyne and Hamon (2008). CFU – Colony Forming Units.

Figure 5-13: Effect of Water Activity on Aerobic Culturability in Compacted Bentonite

In summary, in a high-salinity repository environment, with porewater salinities ≥ 50 g/L, salinity will suppress microbial activity over a wider range of bentonite dry densities (~ 800 to 1,800 kg/m^3) (Stroes-Gascoyne et al. 2010a, 2011). In contrast, experimental evidence indicates that in a low-salinity environment, a highly compacted bentonite with a dry density of 1,600 kg/m^3 will suppress microbial aerobic culturability below background levels (Stroes-Gascoyne et al. 2010b).

5.4.5 Radiation

Radiation would have little effect on the sealing materials, even near the container surfaces, because the thick-walled containers are largely self-shielding. It was estimated that for the reference container, the initial surface gamma dose rate would be approximately 0.05 Gy/a.

Radiation may restrict biological processes in the immediate vicinity of the container, and it may result in minor chemical changes in gas and porewater composition due to radiolysis, but none of these effects are expected to be major (McMurry et al. 2003).

5.4.6 Sorption

An important function of the clay-based buffer is to provide a substrate for the sorption of contaminants if there is a breach of containment. Sorption is a general term for surface-related processes that involve the transfer of ions from a solution in which they have freedom of movement to a fixed position on a surface. In addition to ion exchange, sorption includes surface complexation, in which ions form a strong chemical bond with a reactive surface group at the mineral surface without the displacement of any other ions, and surface precipitation, in which a chemical reaction occurs on the surface because conditions there differ from those in solution. Under highly saline conditions, ion exchange will not be an important sorption mechanism, and only species that react through surface complexation will be significantly sorbed (Vilks 2009, Vilks et al. 2011).

5.4.7 Vertical Movement of Containers

In the horizontal tunnel placement concept, used fuel containers rest on a highly-compacted bentonite pedestal, with the remaining void space filled with gap-fill bentonite pellets. One of the design requirements of this buffer is to prevent containers from shifting from the centre of the placement tunnel, which would reduce the buffer thickness.

Upon closure, water is expected to slowly enter the placement rooms, wetting, swelling and compressing the blocks and pellets. The rate of resaturation will depend on the rate and location of water inflow and the actual evolution of the saturation and homogenisation of the buffer. Variability in resaturation is expected to lead to an uneven distribution of swelling pressures within the placement rooms. In addition, some upwards swelling is expected since the gap-fill pellets have a lower swelling pressure than the bentonite pedestal and a certain degree of compressibility. Such small movements of the containers would not affect repository evolution.

5.4.8 Buffer Erosion and Colloid Formation

Colloids are small solid particles between 1 nm and 1 μm in diameter that are suspended and dispersed in groundwater. Colloids may form by microbial activity or as precipitates due to a change in porewater chemistry. Colloids are of interest in a repository primarily because they have the potential to sorb radionuclides if containers have failed, at which point the transport of the contaminant is controlled by the mobility of the colloid, rather than by the chemical speciation of the radionuclide. These are not expected to be important due to the very low permeability host rock, such that transport is by diffusion not advection. Also, the high salinities will tend to minimize microbial activity (and potential colloid formation) as well as formation of bentonite colloids.

5.4.9 Confidence

The engineered sealing system components would be installed subject to design, manufacturing, and construction specifications, and so their properties would be known with a high degree of confidence. Nevertheless, there are uncertainties about the long-term behaviour of the materials and the processes that would affect them.

Temperature: There is confidence in the results of thermal models over long timeframes. Temperatures in the near-field are generally well-predicted in modelling of prototype repository design experiments over a range of repository saturation levels. Uncertainties would tend to be localized, and due to spatial variability in properties.

Repository Resaturation: Considerable confidence exists in the ability to describe repository performance in a saturated state, but there would exist a period of potentially thousands of years in which saturation has not yet been achieved in this very low permeability host rock. It is therefore during this pre-saturation stage of repository evolution that many of the interactions between repository components would occur. The resaturation of a repository involves coupling of thermal-hydraulic-mechanical processes. Current numerical models are able to broadly explain the evolution of saturation conditions.

Swelling Pressures and Stresses: The swelling pressures generated by the buffer would depend on the buffer composition, buffer density, and groundwater conditions. The swelling characteristics of a wide range of bentonite based sealing materials have been determined through testing but would need to be confirmed for site-specific conditions. The manner in which stresses develop within a repository would also influence the swelling pressure. Strains within one component of the repository sealing system may affect the density and hence the swelling pressure development of another component. The development of thermal stresses in conjunction with the hydraulic and swelling stresses within a multi-component system is complex. Numerical models are presently weakest in explaining the evolution of the stress field in the near-field.

Evolution of Material Properties: The properties of the pellet gap fill are not yet thoroughly characterized with respect to their performance under repository conditions. Further studies on the long-term evolution of these materials under interaction with adjacent materials and saline groundwater are warranted.

Mineralogical Stability of Montmorillonite: Under the expected repository conditions (temperatures less than 120°C, moderate pH levels, moderate potassium concentrations in groundwater), it is very unlikely that substantial conversion of montmorillonite to illite would occur over a million-year timeframe. The effect of high salinities, however, needs more assessment.

Microbial Processes: Although viable microbes would initally inhabit at least some portions of a deep geological repository, there are a number of uncertainties associated with the extent of changes that would result from their presence. For example, although experimental data indicate it is unlikely that bacteria would become active or able to recolonize saturated, highly compacted buffer material, their behaviour in gap fill material needs to be demonstrated. Nevertheless, in the long run, the salinity of the groundwater would limit microbial activity in the repository.

Redox Conditions: There is some uncertainty about when reducing conditions would be established in the sealing materials. It has also been noted that estimates of the time required to reach anaerobic conditions vary, depending on assumptions made in the calculations, from approximately tens of thousands of years to hundreds of thousands of years. Regardless of the amount of time required for oxygen in the repository to be consumed, the total amount of oxygen available for reaction is limited. There are no processes (including radiolysis) that are likely to introduce significant additional quantities of oxygen after closure.

5.5 Long-Term Evolution of the Geosphere

As noted in Chapter 1, the Geoscience program for a future candidate site will be designed to support the safety case. As part of geosynthesis activities, both regional and site-specific information from site characterization activites would be integrated to provide improved understanding of the natural processes that might affect the performance of a repository over one million years. These processes include climate change (specifically glaciation) and geologic processes such as glacial erosion, seismicity, fault rupture/reactivation and volcanism (Table 5-7). To capture the potential degradation of the rock mass, the long-term strength of the rock would be used to analyze the stability of the opening in the host rock at a future candidate site.

Table 5-7: Processes with a Potential Influence on the Geosphere

PROCESS	INFLUENCE
THERMAL	
Glaciation-related cooling	• Permafrost formation • Development of thick ice sheet
HYDRAULIC & PNEUMATIC	
Glaciation and permafrost formation	• Regional changes in groundwater flow pattern • Depth-related changes in groundwater composition
MECHANICAL	
Glacial loading and unloading	• Glacial erosion • Repository rock mass stability
CHEMICAL	
Glaciation-related changes in groundwater flow	• Depth-related changes in groundwater composition • Potential precipitation of secondary mineral phases due to depth-related changes in groundwater composition, and potential dissolution of soluble vein infilling minerals (e.g., gypsum, halite).
BIOLOGICAL	
Glaciation-related changes in groundwater flow	• Potential changes in microbial activity due to depth-related changes in groundwater composition

Notes: Glaciation is the most significant process likely to disturb the geosphere at repository depths over a time scale of one million years.

5.5.1 Geological Disturbances

The following sections describe, in general terms, the likely effects of seismicity, fault rupture/reactivation and volcanism on a repository located within the Michigan Basin.

5.5.1.1 Seismicity and Seismic Hazard Assessment

In general, the Michigan Basin is characterized by low levels of seismic activity as it is located within the tectonically stable center of the stable North America continent (Hayek et al. 2010). Most earthquakes in the regional area, although rare, are deep and occur in the Precambrian basement. Seismic events with focal depths in the Paleozoic sequence are not known to occur. During glaciation, an increase in the frequency of earthquakes is expected during a glacial retreat, however the magnitude of these events is expected to remain low. This is supported by the lack of apparent evidence for cross formational mixing of groundwaters and the lack of neotectonic deformation (NWMO 2011).

To further improve confidence in long-term stability regarding seismic hazards, there is a considerable body of evidence to show that earthquakes, in general, are less destructive at depth than at the surface, diminishing the impact of any seismic activity (including proximal events) on a deep geological repository (Bäckblom and Munier 2002, Atkinson and Kraeva 2011).

Although beyond the scope of the current study, it is noted that for an actual deep geological respository site (or sites), a probabilistic seismic hazard assessment would be conducted for the area as part of site characterization/geosynthesis activities. This assessment would be done following the guidance of the Senior Seismic Hazard Advisory Committee (SSHAC 1997). Seismic monitoring would also be conducted as part of site characterization activities to capture additional information on low-magnitude seismic events.

5.5.1.2 Fault Rupture and Reactivation

Seismicity within a sedimentary basin environment is expected to be confined to regions containing pre-existing features (e.g., faults, fractures) within the Precambrian basement. Damage to intact rock is not expected to occur because in-situ tectonic and glacially induced stresses are not considered sufficient to generate the forces required to create rupture (Lund 2006). For this case study, it is assumed that the repository is sited in an area where no faults have been observed, and it would require earthquakes to propagate faults into previously unfaulted rock. As previously stated, most earthquakes in the region are deep, occur on pre-existing basement faults, and are very rare in this area. There are no known seismic events in the region with a focal depth in the Paleozoic sequence.

5.5.1.3 Volcanism

Volcanoes are primarily found at plate boundaries. Because the Michigan Basin is located several thousands of kilometres from the nearest plate boundary, the risk to a repository from a volcano is considered insignificant. Another mechanism that might create a volcano is a mantle plume, or “hot spot”. The closest active “hotspot” is located in the Snake River Plain and Yellowstone area of the western United States, at a distance of over 3,000 km away.

The lack of active orogenic activity in southern Ontario under the currently stable tectonic regime suggests strongly that volcanic activity is not expected to influence the hypothetical repository site.

5.5.2 Climate Change (Glaciation)

The past 2 million years of Earth’s history has been marked by periods of glaciation. Ice coverage was not continuous over the Michigan Basin, but was marked by many cycles of glacial ice sheet advance and retreat, separated by ice-free periods of warmer climate (interglacials), lasting from thousands to hundreds of thousands of years. Nine glacial cycles occurred over the past million years. During the last glaciation, starting approximately 120,000 years before present, more than 97% of Canada was repeatedly covered by ice. The final retreat of the ice sheet occurred between about 9,000 and 6,500 years ago. Discussion on the current understanding of glaciation, and the processes that cause glaciations, can be found in Peltier (2002, 2011).

If a reglaciation of the Canadian land mass should occur again, it is most likely to occur 60,000 years from present (Peltier 2011). If, at that time, the concentration of carbon dioxide and other greenhouse gases in the atmosphere were similar to present levels, it is unlikely that a renewed episode of glaciation could occur. Because our ability to predict the CO_2 level that will exist at a time so far into the future is difficult, we cannot discount the possibility of a renewed glacial event and, therefore, must take glacial processes into account when developing the safety case for a used fuel repository.

The numerous characteristics of the glaciation process that are relevant to the understanding of repository performance include:

- Erosion, related to ice sheet movement across the land surface.
- Mechanical properties, such as the time dependence of the thickness of glacial ice that could develop over the site and the normal stress regime associated with the weight of the ice load. Also relevant is the evolution of temperature at the base of the ice sheet. Periods of thickest ice cover are associated with the warmest basal temperatures, which is a consequence of the degree of thermal insulation provided by the thick ice and the continuing flow of heat from the Earth's interior into the base of the ice sheet.

The subsurface thermal regime is important to repository performance as well, in particular the depth to which frozen ground (permafrost) may extend. This issue is important not only in the regions that are episodically ice-covered, but also in exterior regions where the influence of permafrost may be even more extreme. In regions within which the base of the ice sheet is temperate (i.e., having temperatures above the freezing point), meltwater is continually generated by the outflow of geothermal heat, and the rate of such generation is crucial to understanding the extent to which such meltwater may be forced to infiltrate into the subsurface and potentially impact deep groundwater systems.

The phenomena associated with glaciation potentially affecting a repository and/or the geologic setting at the repository site can be grouped into three broad categories: glacial erosion, glacial loading and permafrost formation. These are discussed under the headings below.

5.5.2.1 Glacial Erosion

The predominant geosphere process that will result in erosion over the next million years is glaciation. Glacial meltwater can erode sediment and rock by abrasion, quarrying, and mechanical erosion. Regardless of the mechanism, the rate of surface erosion can be limited by the ability of the meltwater to remove debris (e.g., due either to an insufficient hydraulic head gradient to carry debris-laden subglacial water out of the basin, or the lack of adequate subglacial pathways for water). In terms of erosion at a local level, the basal sliding velocity is the primary factor controlling the rate of erosion. However, rapid basal sliding velocity does not necessarily correlate with rapid erosion at the base of the glacier, as the glacier may be decoupled from the bedrock surface by a thin layer of basal melt water, or by a layer of deformable sediment.

Hallet (2011) conducted a glacial erosion assessment in which several independent types of geological evidence were examined to assess the magnitude of erosion which would likely occur over one glacial cycle at different scales, from regional to local. In total, thirteen estimates (eleven of which are independent of one another) were presented which support the conclusion that erosion would not exceed many tens of metres in the Bruce region of southern Ontario over one glacial cycle; no erosion and net deposition of sediments in the region is also possible. For the hypothetical site considered in this study, it is assumed that net erosion is likely on the order of tens of metres over one million years. This assumption is supported by local erosion estimates reported by Hallet (2011) for the Bruce nuclear site. As part of site characterization activities, an investigation would be conducted of topographic features or other known factors that might tend to localize erosion at a potential site.

5.5.2.2 Glacial Loading

Climate modelling of the late Quaternary ice advances and retreats has predicted ice thicknesses of up to 4 km of ice over northern Canada and approaching 2.5 km of ice in southern Ontario (Peltier 2002). The last glacial episode had a duration of approximately 120,000 years, and involved multiple glacial advances and retreats, resulting in loading and unloading cycles on the underlying rock with each advance and retreat.

The weight of the thick ice sheet acts to depress the Earth's crust and removal of the ice load by melting leads to crustal rebound, a process known as isostacy, which continues today. Peltier (2011) has predicted that the maximum crustal depression from the equilibrium level occurred at the Last Glacial Maximum (LGM) and reached values in excess of 500 m.

The University of Toronto Glacial Systems Model (UofT GSM), which is a model of continental-scale glaciation events, was used by Peltier (2011) to develop a description of glaciation of the Canadian landmass. A maximum glacial event time profile for ice loading was developed based on Peltier (2011), as shown in Figure 5-14, and indicates that the vertical stress reaches a maximum value of approximately 30 MPa. In addition to changing the vertical stress at depth, glaciation can also cause the horizontal stress to increase due to both Poisson's effect and plate bending. The horizontal stress increase due to Poisson's effect is:

$$\Delta\sigma_h = \frac{\nu}{1-\nu}\Delta\sigma_v \tag{5-21}$$

where... σ_h is the horizontal stress;
σ_v is the vertical stress; and
ν is the poisson's ratio.

The increase in the horizontal stress due to plate bending is also proportional to the increase in vertical stress, with the maximum increase assumed to be 2 MPa. Numerical analyses carried out by Lund et al. (2009) showed that shear stresses are relatively minor compared to the vertical and horizontal normal stresses.

Numerical modelling of the effects of stress changes associated with glacial advance and retreat (as described above) on a repository is beyond the scope of this study for a hypothetical site, but would be conducted in order to support a safety case for a candidate site.

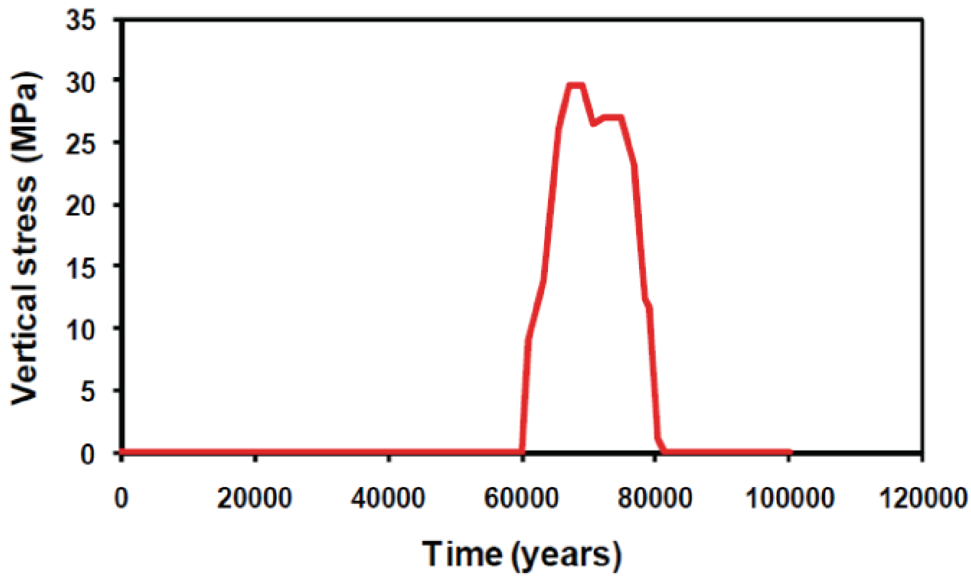

Notes: Time from present is for first event.

Figure 5-14: Simulated Evolution of Ice Sheet Load

5.5.2.3 Permafrost Formation (Changes in Groundwater Recharge)

Permafrost formation as a result of glaciation will impact the extent to which glacial meltwater will infiltrate into the subsurface. Future glacial conditions at the hypothetical repository site would be preceded by an extended period with widespread formation of permafrost. Under permafrost conditions, groundwater would freeze in the subsurface, decreasing the connected porosity and permeability and significantly decreasing recharge and altering flow system hydraulic gradients for up to tens of thousands of years.

In regions of permafrost, taliks are regions of perennially unfrozen ground that exist within otherwise continuous permafrost environments (Peltier 2004). The formation of taliks is dependent on site-specific thermal, chemical, geological and hydrological conditions (Peltier 2004). Heat emanating from the repository is unlikely to create a talik since periglacial conditions are not expected for several tens of thousands of years, after heat from the repository has already decreased.

Meltwater beneath glacial ice sheets can be pressurized, resulting in hydraulic heads far in excess of those found during interglacial periods. Two factors affecting the penetration of glacial water to depth are permafrost depth and distribution, as well as stress changes developed from the ice load.

When permafrost exists under the ice sheet (cold-based conditions), groundwater recharge to depth is inhibited, despite the high hydraulic head imposed at the ice sheet base. A warm-based ice sheet is one in which the free water at the base is at temperatures above the pressure freezing point beneath the ice (i.e., no permafrost), and enhanced recharge may occur. Subglacial groundwater flow patterns associated with warm-based conditions are likely to involve increased volumes of water and more rapid movement than pre-glacial or cold-based conditions, particularly in the shallow groundwater flow system.

Glaciation-related changes in groundwater chemistry are not expected to affect the redox or salinity conditions of groundwaters at repository depth. Paleohydrogeology and geochemical modelling studies can be used to evaluate changes associated with previous glaciation events. For example, isotopic evidence in the Michigan Basin indicates that recharge of glacial meltwater is constrained to formations above the Ordovician shales (NWMO 2011).

The depth of penetration of glacial waters into the deep groundwater system at the hypothetical sedimentary site was considered in this study. Paleohydrogeological modelling was completed for the Laurentide glacial episode (120,000 to 10,000 years before present) and presented in detail in Chapter 2 (Section 2.3.4.3). The key insights from the illustrative modelling are summarized.

A total of eleven paleohydrogeologic simulations were performed to investigate the role of varying paleoclimate boundary conditions. Details of the paleoclimate modelling scenarios can be found in Section 2.3.4.3. The performance measure of choice to compare the paleohydrogeologic simulations is the movement of a conservative unit tracer applied with a Cauchy boundary condition at the top surface of the model domain. This tracer represents the predicted migration of recharge waters into the groundwater system over the course of a 120,000 year simulation. The depth of the tracer is determined by the 5% isochlor, which is conservative in that it represents a pore fluid containing 5% recharge water. The 5% isochlor provides an indication of recharge water migration into the subsurface, which can be used to compare alternative paleohydrogeologic scenarios. The paleohydrogeologic simulations do not consider reactive transport; therefore, although the 5% isochlor provides an indication of the percentage meltwater, it does not take into account the consumption of oxygen. In addition to the tracer, Péclet numbers were estimated to assess changes in transport mechanisms during the paleohydrogeologic scenarios. The Péclet number is estimated by comparing rates of advection to diffusion.

The depth of penetration of the conservative tracer is shown in Figure 5-15. The penetration depths of surficial recharge are represented by the intercepts between a straight line at a concentration of 0.05 and tracer concentration profiles at the hypothetical repository footprint at 120 ka. As shown in Figure 5-15, the low permeability Ordovician shales and Silurian evaporites and dolostones prevent the migration of the tracer to the repository horizon. Thus, the downward migration of tracer is largely retarded by the low permeability Ordovician formations, which is indicative of low rates of mass transport in the Ordovician.

Plots of Péclet number at the repository horizon versus time are shown in Figure 5-16 for points bounding the repository, as well as at the repository centre. The glacial loading history is also included to reflect its impact on the groundwater system at the repository horizon. As illustrated by the plots, mass transport mechanisms within the repository during the 120,000 year paleohydrogeologic simulation are predicted to remain diffusive, even at the maximum ice thickness of almost 3 km.

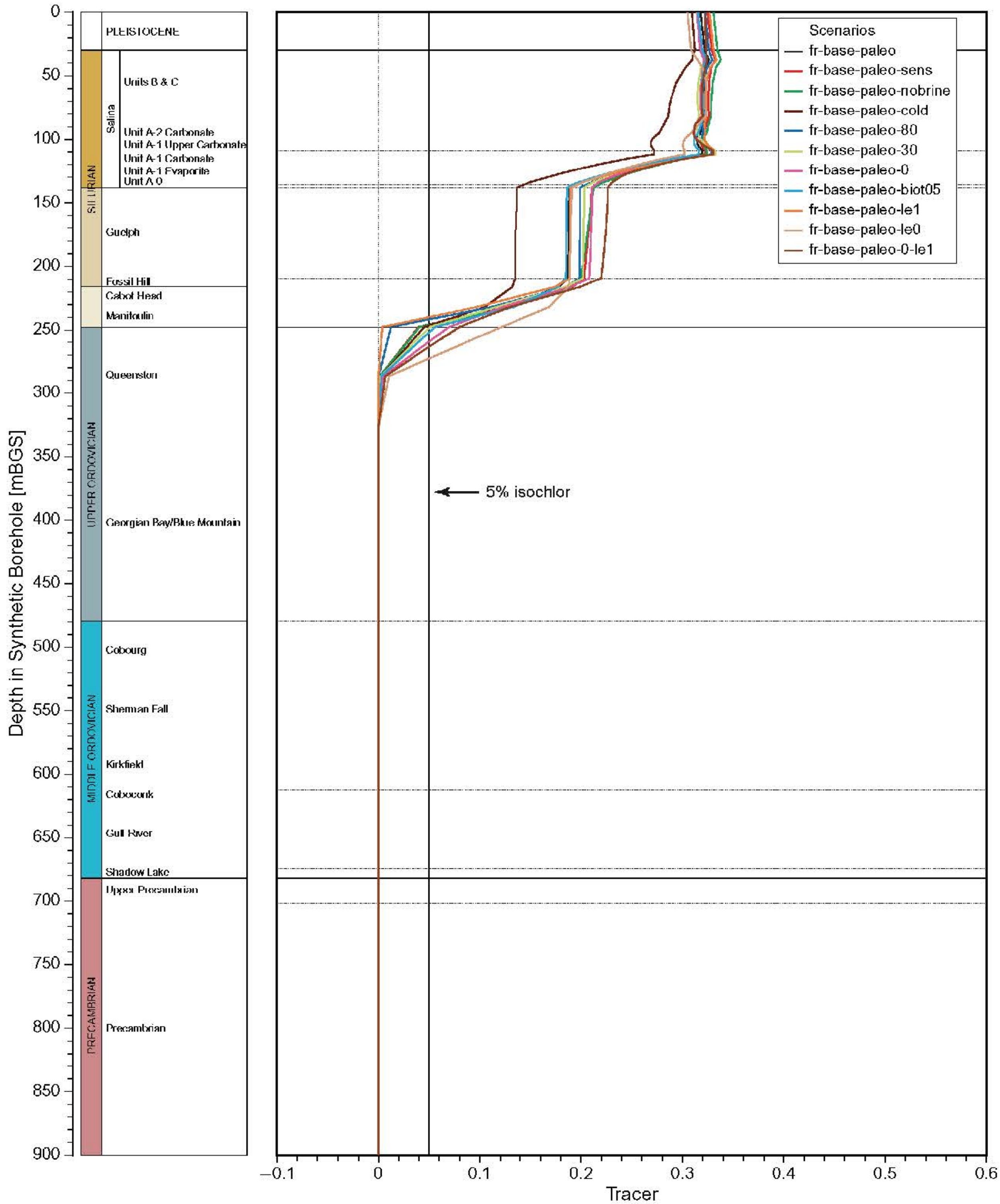

Figure 5-15: Vertical Profile Plots of Tracer Concentrations for the Paleohydrogeologic Simulations at the Location of the Hypothetical Repository Footprint at 120,000 Years

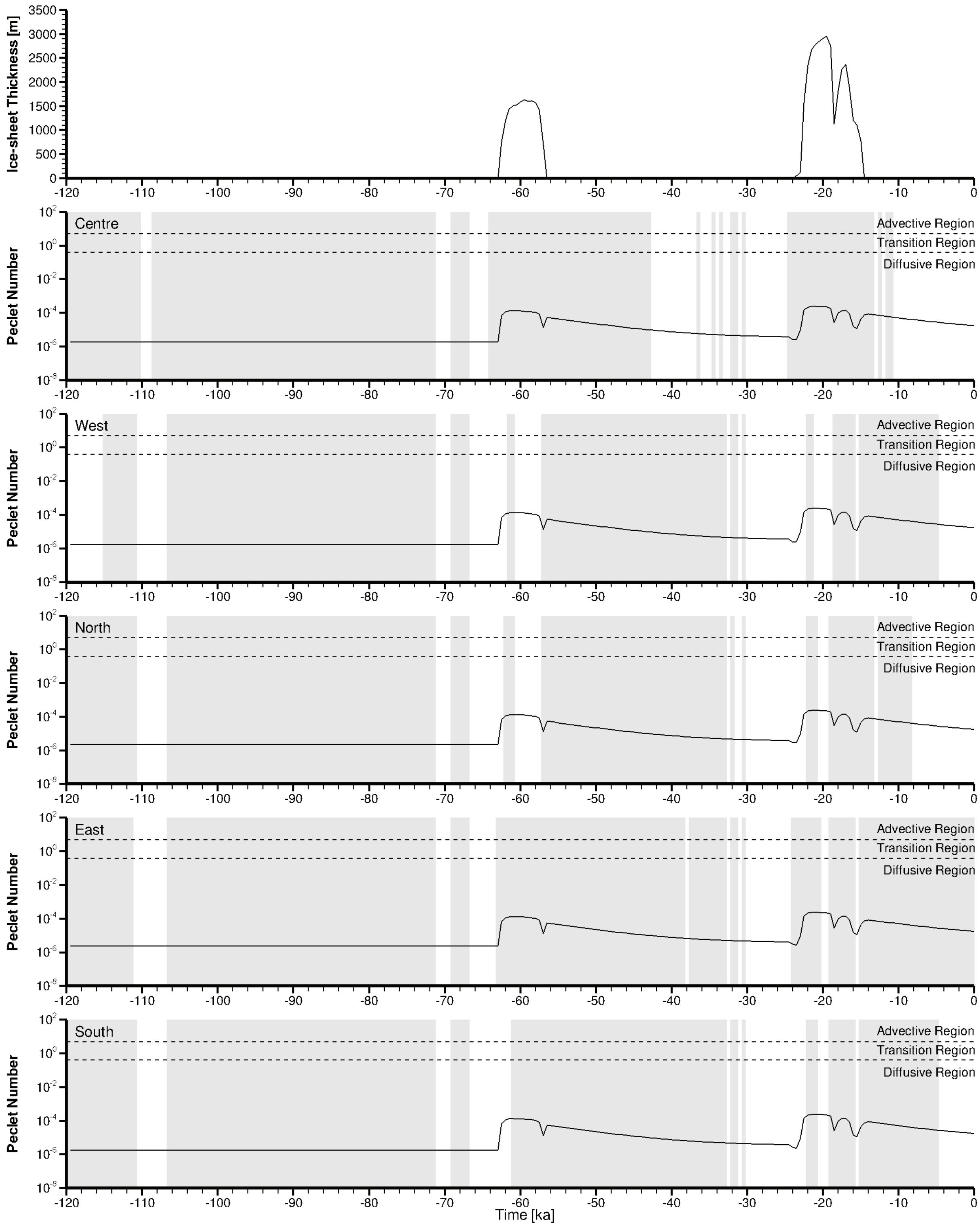

Note: grey regions represent upward flow and white regions represent downward flow

Figure 5-16: Péclet Number of Molecular Diffusion versus Time at the Hypothetical Repository Footprint for the Reference Paleohydrogeological Scenario (fr-base-paleo)

5.5.3 Confidence

As noted in Chapter 1, the geosciences program for a future candidate site will be designed to support the safety case. A site model and geosynthesis will be developed during a phased site characterization work program. The work program will allow for the iterative development, testing and refinement of a site-specific model that will contribute to managing uncertainties in scientific understanding, data and models.

Temperature: The thermal conductivity of sedimentary rock is primarily influenced by the rock composition and structure. Many of the uncertainties associated with estimates of heat transport in the geosphere would be resolved during site characterization activities. Temperature distributions in the geosphere would vary on a local scale as a result of details of repository design.

Fracture Development: A factor in repository siting is the geomechanical environment. The host rock would be demonstrably resilient to fracture development based on its history. The actual repository location would be chosen to avoid fracture zones or faults where future fracture movement or development is more likely.

Groundwater Mass Transport: Evidence gathered during site characterisation activities would attempt to minimize uncertainties through a synthesis of geologic, structural geologic, hydrogeochemical and physical hydrogeology to assess long-term groundwater system evolution and stability. Such efforts would be aided through the application of numerical methods that provide a systematic framework to integrate independent data sets. Such techniques, as supported by field data, can provide a basis to gain insight into trends (i.e., time rate of change and magnitude) of groundwater system response to external events and constrain uncertainty with regard to geosphere performance.

Glacial Processes: Peltier (2011) provides a review of what is currently known concerning the geologically recent history of long-term climate change, as background to the detailed analysis of the conditions that would be expected to develop at and below the surface of the Earth if the Canadian land mass were to be reglaciated. Results from an appropriately calibrated model of the most recent glaciation events that occurred in the Late Quaternary period of Earth history are used as a model of a future reglaciation event. The physical model employed for the purpose of this analysis is the University of Toronto Glacial Systems Model (UofT GSM).

The analyses that have been performed using the UofT GSM, for the purpose of contributing to the development of the required future glacial event predictions, are explicitly based upon the fact that it is impossible to provide a unique description of the detailed characteristics of such an event. The approach used is to apply Bayesian methods to examine the range of models that would be compatible with the constraints that can be brought to bear upon the detailed characteristics of the most recent North American glaciation event of the Late Quaternary ice-age. It is thereby shown that the spread of model characteristics is rather broad, sufficiently broad, it is believed, to encompass the characteristics of any similar event that could occur in the future (Peltier 2011).

Geochemistry: Uncertainties in the future evolution of groundwater compositions are coupled to uncertainties about the movement of groundwater. Similarly, impacts of glaciation at repository depth will be dependent on site-specific conditions. The age of, and potential influence of glaciation on, groundwaters and porewaters cannot be determined directly; instead, they are inferred from paleohydrogeological evidence such as fluid inclusion data and stable water isotope ratios. Together with numerical tools, such as reactive transport modelling, this information can be used to illustrate the potential evolution of geochemical conditions at repository depths.

5.6 Summary

This discussion in this chapter describes changes that would occur in the multi-barrier repository system during its lifetime. The discussion is based on reasonable expectations for conditions that are likely to be encountered in sedimentary rock.

Many properties of the repository components and the processes that would affect them are well-characterized. The system is based on durable materials and passive natural processes. Natural and archaeological analogues help to support the descriptions of system behaviour into the far future. Of the uncertainties that remain, some questions would be resolved during the site characterization. Other uncertainties about the future evolution of the system arise from the recognition that simplifying assumptions and simple models may not in all cases adequately represent the complexity or heterogeneity of an actual repository over long periods of time. These uncertainties would be addressed by further analyses, by additional experimental or field studies (including extended monitoring in the repository itself), and by using conservative or bounding assumptions in the safety assessment models.

5.7 References for Chapter 5

Akiyama, E., K. Matsukado, M. Wang and K. Tsuzaki. 2010. Evaluation of hydrogen entry into high strength steel under atmospheric corrosion. Corrosion Science 52, 2758-2765.

Atkinson, G. and N. Kraeva. 2011. Polaris Underground Project at Sudbury Neutrino Observatory (P.U.P.S.). Nuclear Waste Management Organization Report TR-2009-02. Toronto, Canada.

Bäckblom, G. and R. Munier. 2002. Effects of Earthquakes on the Deep Repository for Spent Fuel in Sweden based on Case Studies and Preliminary Model Results. Swedish Nuclear Fuel and Waste Management Company Report TR-02-24. Stockholm, Sweden.

Bock, H., B. Dehandschutter, C.D. Martin, M. Mazurek, A. De Haller, F. Skoczylas and C. Davy. 2010. Self-Sealing of Fractures in Argillaceous Formations in the Context of Geological Disposal of Radioactive Waste. Nuclear Energy Agency No. 6184. Paris, France.

Börgesson, L., A. Fredrikson and L-E. Johannesson. 1994. Heat Conductivity of Buffer Materials. Swedish Nuclear Fuel and Waste Management Company Report 94-29. Stockholm, Sweden.

Chandler, N.A, A. Cournut, D.A. Dixon, C. Fairhurst, F. Hansen, M. Gray, K. Hara, Y. Ishijima, E. Kozak, J. Martino, K. Masumoto, G. McCrank, Y. Sugita, P. Thompson, J. Tillerson and B. Vignal. 2002. The Five-year Report of the Tunnel Sealing Experiment: An International Project of AECL, JNC, ANDRA and WIPP. Atomic Energy of Canada Limited Report AECL-12727. Pinawa, Canada.

Chen, J., Z. Qin and D.W. Shoesmith. 2011. Rate controlling reactions for copper corrosion in anaerobic aqueous sulphide solutions. Corrosion Engineering, Science and Technology 46, 138-141.

Chen, Y., X.H. Wang, J. Li, J.L. Lu, F.S. Wang. 2007. Polyaniline for corrosion prevention of mild steel coupled with copper. Electrochimica Acta 52, 5392-5399.

CNSC. 2006. Regulatory Guide G-320: Assessing the Long Term Safety of Radioactive Waste Management, Canadian Nuclear Safety Commission, Ottawa, Canada.

Crowe, R., K. Birch, J. Chen, D. Doyle, F. Garisto, M. Gobien, N. Hunt, S. Hirschorn, M. Hobbs, P. Keech, L. Kennell, E. Kremer, P. Maak, J. McKelvie, C. Medri, M. Mielcarek, A. Murchison, A. Parmenter, R. Ross, E. Sykes and T. Yang. 2013. Technical Program for Long-Term Management of Canada's Used Nuclear Fuel – Annual Report 2012. Nuclear Waste Management Organization Report NWMO TR-2013-01. Toronto, Canada.

Dixon D., T. Sandén, E. Jonsson and J. Hansen. 2011. Backfilling of Deposition Tunnels: Use of Bentonite Pellets. Swedish Nuclear Fuel and Waste Management Company Report SKB P-11-44. Stockholm, Sweden.

DOE. 2008. Final Supplemental Environmental Impact Statement for a Geologic Repository for the Disposal of Spent Nuclear Fuel and High-Level Radioactive Waste at Yucca Mountain, Nye County, Nevada. Department of Energy Report DOE/EIS-0250F-S1. Nevada, USA.

Dutton, D. 2006. Preliminary Evaluation of the Creep Behaviour of the Inner Steel Vessel of a Used-fuel Container. Ontario Power Generation Report 06819-REP-01300-10108-R00. Toronto, Canada.

Ferry, C., J.-P. Piron, A. Poulesquen and C. Poinssot. 2008. Radionuclides release from the spent fuel under disposal conditions: Re-evaluation of the instant release fraction. Materials Research Society Symposium Proceedings 1107, 447-454.

Fracture Systems. 2011. Excavation Damaged Zones Assessment. Nuclear Waste Management Report NWMO DGR-TR-2011-21. Toronto, Canada.

Freire-Canosa, J. 2011. Used Fuel Integrity Program: Summary Report. Nuclear Waste Management Organization Report NWMO TR-2011-04. Toronto, Canada.

Frescura, G.M. and A.L. Wight. 1979. Fuel Management & Reactor Operation Review of Operating Experience. From Canteach Website at: https://canteach.candu.org/Content%20Library/20042116.pdf.

Garisto, F. 2013. Fifth Case Study: Features, Events and Processes. Nuclear Waste Management Organization Report NWMO TR-2013-06. Toronto, Canada.

Gobien, M., F. Garisto and E. Kremer. 2013. Fifth Case Study: Reference Data and Codes. Nuclear Waste Management Organization Technical Report NWMO-TR-2013-05. Toronto, Canada.

Graham, J., N.A. Chandler, D.A. Dixon, P.J. Roach, T. To and A.W.L Wan. 1997. The Buffer/Container Experiment: Results, Synthesis, Issues. AECL Report 11746, COG-97-46-I.

Guo, R. 2009. Coupled Thermal-Hydraulic-Mechanical Modelling of the Canister Retrieval Test. Nuclear Waste Management Organization Report NWMO TR-2009-31. Toronto, Canada.

Guo, R. 2010. Coupled Thermal-Mechanical Modelling of a Deep Geological Repository using the Horizontal Tunnel Placement Method in Sedimentary Rock using CODE_BRIGHT. Nuclear Waste Management Organization Report NWMO TR-2010-22. Toronto, Canada.

Hallet, B. 2011. Glacial Erosion Assessment. Nuclear Waste Management Organization Report NWMO DGR-TR-2011-18. Toronto, Canada.

Hayek, S.J., J.A. Drysdale, J. Adams, V. Peci, S. Halchuk and P. Street. 2010. Seismic Monitoring near the DGR - Annual Report 2009. Nuclear Waste Management Organization Report DGR-TR-2010-03. Toronto, Canada.

Hultquist G., P. Szakálos, M.J. Graham, A.B. Belonoshko, G.I. Sproule, L. Gråsjö, P. Dorogokupets, B. Danilov, T. AAstrup, G. Wikmark, G.-K. Chuah, J.-C. Eriksson and A. Rosengren. 2009. Water corrodes copper. Catalysis Letters 132, 311-316.

Hultquist G., M.J. Graham, P. Szakálos, G.I. Sproule, A. Rosengren and L. Gråsjö. 2011. Hydrogen gas production during corrosion of copper by water. Corrosion Science 53, 310-319.

Hultquist, G., M.J. Graham, O. Kodra, S. Moisa, R. Liu, U. Bexell and J.L. Smialek. 2013. Corrosion of Copper in Distilled Water without Molecular Oxygen and the Detection of Produced Hydrogen. SSM Technical Note 2013:07. Stockholm, Sweden.

Humphreys, P.N., J.M. West and R. Metcalfe. 2010. Microbial Effects on Repository Performance. Prepared by Quintessa Limited for the Nuclear Decommissioning Authority Report No. QRS-1378Q-1. Oxfordshire, United Kingdom.

INTERA. 2011. Descriptive Geosphere Site Model. Nuclear Waste Management Organization Report NWMO DGR-TR-2011-24. Toronto, Canada.

Jensen, K.A. and R.C. Ewing. 2001. The Okélobondo natural fission reactor, southeast Gabon: Geology, mineralogy, and retardation of nuclear-reaction products. Geological Society of America Bulletin 113, 32-62.

King, F. 2006. Review and Gap Analysis of the Corrosion of Copper Containers under Unsaturated Conditions. Ontario Power Generation Report 06819-REP-01300-10124-R00. Toronto, Canada.

King, F. 2009a. Hydrogen Effects on Carbon Steel Used Fuel Containers. Nuclear Waste Management Organization Report NWMO TR-2009-29. Toronto, Canada.

King, F. 2009b. Microbiologically influenced corrosion of nuclear waste container. Corrosion 65, 233-251.

King, F. 2013. Consequences of the General Corrosion of Carbon Steel Used Fuel Containers for Gas Generation in a DGR. Nuclear Waste Management Organization Report NWMO TR-2013-16. Toronto, Canada.

King, F. and S. Stroes-Gascoyne. 1997. Predicting the effects of microbial activity on the corrosion of copper nuclear waste disposal containers. Eds. J.H. Wolfram, R.D. Rogers and L.G. Gazso in Microbial Degradation Processes in Radioactive Waste Repository and in Nuclear Fuel Storage Areas. Volume 11 of NATO ASI Series. Kluwer Academic Publishers, Netherlands. 149-162.

King, F. and M. Kolář. 2000. The Copper Container Corrosion Model Used in AECL's Second Case Study. Ontario Power Generation Report 06819-REP-01200-10041-R00. Toronto, Canada.

King, F., L. Ahonen, C. Taxén, U. Vuorinen and L. Werme. 2001. Copper Corrosion under Expected Conditions in a Deep Geologic Repository. Swedish Nuclear Fuel and Waste Management Company Report SKB TR-01-23. Stockholm, Sweden.

King, F., M. Kolář and P. Maak. 2008. Reactive-transport model for the prediction of the uniform corrosion behaviour of copper used fuel containers. Journal of Nuclear Materials 379, 133-141.

King, F. and D. Shoesmith. 2010. Nuclear waste canister materials, corrosion behaviour and long-term performance in geological repository systems. Eds. J. Ahn and M.J. Apted in Geological Repository Systems for Safe Disposal of Spent Nuclear Fuel and Radioactive Waste. Woodhead Publishing, Cambridge, United Kingdom.

King, F., C. Lilja, K. Pedersen, P. Pitkänen and M. Vähänen. 2010. An Update of the State-of-the-Art Report on the Corrosion of Copper under Expected Conditions in a Deep Geologic Repository. Swedish Nuclear Fuel and Waste Management Company Report SKB TR-10-67. Stockholm, Sweden.

King, F., C. Lilja, K. Pedersen, P. Pitkänen and M. Vähänen. 2011a. An Update of the State-of-the-art Report on the Corrosion of Copper under Expected Conditions in a Deep Geologic Repository. Posiva Oy Report POSIVA 2011-01. Olkiluoto, Finland.

King, F., M. Kolář, M. Vähänen and C. Lilja. 2011b. Modelling long term corrosion behaviour of copper canisters in KBS-3 repository. Corrosion Engineering, Science and Technology 46, 217-222.

Kwong, G.M. 2011. Status of Corrosion Studies for Copper Used Fuel Containers Under Low Salinity Conditions. Nuclear Waste Management Organization Report NWMO TR-2011-14. Toronto, Canada.

Lovasic, Z. and P. Gierszewski. 2005. CANDU Fuel Long-Term Storage and Used Fuel Integrity. Paper at 9th International Conference on CANDU Fuel. Canadian Nuclear Society Bulletin Vol. 26, No. 4.

Lund B. 2006. Stress Variations during a Glacial Cycle at 500 m Depth in Forsmark and Oskarshamn: Earth Model Effects. Swedish Nuclear Fuel and Waste Management Company Report R-06-95. Stockholm, Sweden.

Lund, B., P. Schmidt and C. Hieronymus. 2009. Stress Evolution and Fault Stability during the Weichselian Glacial Cycle. Swedish Nuclear Fuel and Waste Management Company Report TR-09-15. Stockholm, Sweden.

Maak, P., M. Saidfar and P. Gierszewski. 2001. Early Failure Probability of Used-Fuel Containers in a Deep Geologic Repository. Ontario Power Generation Report 06819-REP-01300-10022 R00. Toronto, Canada.

Man, A. and J.B. Martino. 2009. Thermal, Hydraulic and Mechanical Properties of Sealing Materials. Nuclear Waste Management Organization Technical Report NWMO TR-2009-20. Toronto, Canada.

McMurry, J., D.A. Dixon, J.D. Garroni, B.M. Ikeda, S. Stroes-Gascoyne, P. Baumgartner and T.W. Melnyk. 2003. Evolution of a Canadian Deep Geologic Repository: Base Scenario. Ontario Power Generation Report 06819-REP-01200-10092-R00. Toronto, Canada.

McMurry, J., B.M. Ikeda, S. Stroes-Gascoyne, D.A. Dixon and J.D. Garroni. 2004. Evolution of a Canadian Deep Geologic Repository: Defective Container Scenario. Ontario Power Generation Report 06819-REP-01200-10127-R00. Toronto, Canada.

NWMO. 2011. Geosynthesis. Nuclear Waste Management Organization Report NWMO DGR-TR-2011-11. Toronto, Canada.

OPG. 2002. Pickering Waste Management Facility Safety Report. Ontario Power Generation Report 92896-SR-01320-10002-R02. Toronto, Canada.

Pedersen K. 2000. Microbial Processes in Radioactive Waste Disposal. Swedish Nuclear Fuel and Waste Management Company Report SKB TR 00-04. Stockholm, Sweden.

Peltier, W.R. 2002. A Design Basis Glacier Scenario. Ontario Power Generation Report 06819-REP-01200-10069-R00. Toronto, Canada.

Peltier, W.R. 2004. Permafrost Influences Upon the Subsurface. Ontario Power Generation Report 06819-REP-01200-10134-R00. Toronto, Canada.

Peltier, W.R. 2011. Long-term Climate Change. Nuclear Waste Management Organization Report NWMO DGR-TR-2011-14 R000. Toronto, Canada.

Poon, G., M. Saiedfar and P. Maak. 2001. Selection of a Primary Load-Bearing Component Conceptual Design for Used-fuel Containers. Ontario Power Generation Report 06819-REP-01200-10051-R00. Toronto, Canada.

Posiva. 2010. EDZ09 Project and related EDZ Studies in ONKALO 2008-2010. Posiva Working Report 2010-27. Olkiluoto. Finland.

Puigdomenech, I. and C. Taxén. 2000. Thermodynamic Data for Copper: Implications for the Corrosion of Copper under Repository Conditions. Swedish Nuclear Fuel and Waste Management Company Report SKB TR 00-13. Stockholm, Sweden.

Pusch, R. 1999. Mobility and Survival of Sulphate-reducing Bacteria in Compacted and Fully Water Saturated Bentonite – Microstructural Aspects. Swedish Nuclear Fuel and Waste Management Company Report SKB TR 99-30. Stockholm, Sweden.

Raiko, H. 2005. Disposal Canister for Spent Nuclear Fuel – Design Report. Posiva Oy Report POSIVA 2005-02. Olkiluoto, Finland.

Raiko H., R. Sandström, H. Rydén and M. Johansson. 2010. Design Analysis Report for the Canister. Swedish Nuclear Fuel and Waste Management Company Report SKB TR-10-28, Stockholm, Sweden.

Saiedfar, M. and P. Maak. 2002. Preliminary Assessment of the Deformation and Stresses of Copper Used-fuel Containers in a Hypothetical Deep Geologic Repository. Ontario Power Generation Report, 06819-REP-01300-10049-R00. Toronto, Canada.

Scully, J. and M. Edwards. 2013. Review of the NWMO Copper Corrosion Allowance. Nuclear Waste Management Report NWMO TR-2013-04. Toronto, Canada.

Sherwood Lollar, B. 2011. Far-Field Microbiological Considerations Relevant to a Deep Geological Repository – State of Science Review. Nuclear Waste Management Organization Report NWMO TR-2011-09. Toronto, Canada.

Shoesmith, D.W. and F. King. 1999. The Effects of Gamma Radiation on the Corrosion of Candidate Materials for the Fabrication of Nuclear Waste Packages. Atomic Energy of Canada Limited Report AECL 11999. Pinawa, Canada.

Shoesmith, D.W. 2008. The Role of Dissolved Hydrogen on the Corrosion/Dissoluton of Spent Nuclear Fuel. Nuclear Waste Management Organization Report NWMO TR-2008-19. Toronto, Canada.

Shoesmith, D.W. and D. Zagidulin. 2010. The Corrosion of Zirconium under Deep Geological Repository Conditions. Nuclear Waste Management Organization Report NWMO TR-2010-19. Toronto, Canada.

Simmons, G. R. 1992. The Underground Research Laboratory Room 209 Excavation Response Test - A Summary report. Atomic Energy of Canada Limited. Report AECL-10564, COG-92-56. Chalk River, Canada.

SKB. 2010. Critical Review of the Literature on the Corrosion of Copper by Water. Swedish Nuclear Fuel and Waste Management Company Report SKB TR-10-69. Stockholm, Sweden.

SKB. 2011. Long-term Safety for the Final Repository for Spent Nuclear Fuel at Forsmark. Main Report of the SR-Site Project. Volume I. Swedish Nuclear Fuel and Waste Management Company Report SKB TR-11-01. Stockholm, Sweden.

Smart N., A. Rance, P. Fennell and L. Werme. 2003. Expansion due to anaerobic corrosion of steel and cast iron: experimental and natural analogue studies. Eds. D. Féron and D.D. Macdonald in Prediction of Long Term Corrosion Behaviour in Nuclear Waste Systems: Proceedings of the International Workshop. Cadarache, France. London: Maney Pub. (European Federation of Corrosion Publications 36), paper 19, pp 280–294.

Smart N., P. Fennell, A. Rance and L. Werme. 2004. Galvanic corrosion of copper-cast iron couples in relation to the Swedish radioactive waste canister concept. Ed. D. Féron in Prediction Of Long Term Corrosion Behaviour in Nuclear Waste Systems: Proceedings of the 2nd International Workshop. European Federation of Corrosion, pp 52–60. Nice, France.

Smart N.R., A.P. Rance and P.A.H. Fennell. 2005. Galvanic Corrosion of Copper-Cast Iron Couples. Swedish Nuclear Fuel and Waste Management Company Report SKB TR-05-06. Stockholm, Sweden.

Smart N.R., A.P. Rance and P.A.H. Fennell. 2006. Expansion due to the Anaerobic Corrosion of Iron. Swedish Nuclear Fuel and Waste Management Company Report SKB TR-06-41. Stockholm, Sweden.

Smart N., A. Rance, B. Reddy, P. Fennell and R. Winsley. 2012. Analysis of SKB MiniCan Experiment 3. Swedish Nuclear Fuel and Waste Management Company Report SKB TR-12-09. Stockholm, Sweden.

SSHAC. 1997. Recommendations for Probabilistic Seismic Hazard Analysis. Guidance on Uncertainty and Use of Experts. Senior Seismic Hazard Advisory Committee, U.S. Nuclear Regulatory Commission, NUREG/CR-6372. Washington, USA.

SSM. 2011a. Evolution of Hydrogen by Copper in Ultrapure Water without Dissolved Oxygen. Strål Säkerhets Myndigheten Report 2011:34. Stockholm, Sweden.

SSM. 2011b. Is Copper Immune to Corrosion when in Contact with Water and Aqueous Solutions? Strål Säkerhets Myndigheten Report 2011:09. Stockholm, Sweden.

SSM. 2012a. 2012. A Review of the Creep Ductility of Copper for Nuclear Waste Canister Application. Strål Säkerhets Myndigheten Technical Note 2012:13. Stockholm, Sweden.

SSM. 2012b. A Review of the Mechanical Integrity of the Canister. Strål Säkerhets Myndigheten Technical Note 2012:15. Stockholm, Sweden.

Stroes-Gascoyne, S. 2010. Microbial occurrence in bentonite-based buffer, backfill and sealing materials from large-scale experiments at AECL's Underground Research Laboratory. Applied Clay Science 47, 36-42.

Stroes-Gascoyne, S., C.J. Hamon, C. Kohle and D.A. Dixon. 2006. The Effects of Dry Density and Porewater Salinity on the Physical and Microbiological Characteristics of Highly Compacted Bentonite. Ontario Power Generation Report 06819-REP-01200-10016 R00. Toronto, Canada.

Stroes-Gascoyne, S., C.J. Hamon, D.A. Dixon and J.B. Martino. 2007a. Microbial analysis of samples from the tunnel sealing experiments at AECL's Underground Research Laboratory. Physics and Chemistry of the Earth: Parts A/B/C 32, 219-231.

Stroes-Gascoyne, S., P. Maak, C.J. Hamon, and C. Kohle. 2007b. Potential Implications of Microbes and Salinity on the Design of Repository Sealing System Components. Nuclear Waste Management Organization Report NWMO TR-2007-10. Toronto, Canada.

Stroes-Gascoyne, S. and C.J. Hamon. 2008. The Effect of Intermediate Dry Densities (1.1-1.5 g/cm^3) and Intermediate Porewater Salinities (60-90 g NaCl/L) on the Culturability of Heterotrophic Aerobic Bacteria in Compacted 100% Bentonite. Nuclear Waste Management Organization Report NWMO TR-2008-11. Toronto, Canada.

Stroes-Gascoyne, S. and C.J. Hamon. 2010. The Effects of Elevated Temperatures on the Viability and Culturability of Bacteria Indigenous to Wyoming MX-80 Bentonite. Nuclear Waste Management Organization Report NWMO TR-2010-08. Toronto, Canada.

Stroes-Gascoyne, S., C.J. Hamon, D.A. Dixon and D.G. Priyanto. 2010a. The Effect of $CaCl_2$ Porewater Salinity (50-100 g/L) on the Culturability of Heterotrophic Aerobic Bacteria in Compacted 100% Bentonite with Dry Densities of 0.8 and 1.3 g/cm^3. Nuclear Waste Management Organization Technical Report NWMO TR-2010-06. Toronto, Canada.

Stroes-Gascoyne, S., C.J. Hamon, P. Maak and S. Russell. 2010b. The effects of the physical properties of highly compacted smectitic clay (bentonite) on the culturability of indigenous microorganisms. Applied Clay Science 47, 155-162.

Stroes-Gascoyne, S., C.J. Hamon and P. Maak. 2011. Limits to the Use of Highly Compacted Bentonite as a Deterrent for Microbiologically Influenced Corrosion in a Nuclear Fuel Waste Repository. Physics and Chemistry of the Earth 36(17-18), 1630-1638.

Suckling, P., J. Avis, N. Calder, P. Humphreys, F. King and R. Walsh. 2012. T2GGM Version 3.1: Gas Generation and Transport Code. Nuclear Waste Management Organization Report NWMO TR-2012-23. Toronto, Canada.

Suckling, P., J. Avis, N. Calder, P. Humphreys, F. King and R. Walsh. 2013. T2GGM Version 3.1: Gas Generation and Transport Code – Supporting Documentation. Quintedda Limited Report QRS-1335B-TR6. Henley-on-Thames, UK.

Swedish National Council. 2010. Nuclear Waste State-of-the-Art Report 2010 – Challenges for the Final Repository Programme. Swedish Government Official Reports SOU 2010:6. Stockholm, Sweden.

Szakálos P., Hultquist G., Wikmark G. 2007. Corrosion of copper by water. Electrochemical and Solid-State Letters 10, C63–C67.

Tait, J.C., H. Roman and C.A. Morrison. 2000. Characteristics and Radionuclide Inventories of Used Fuel from OPG Nuclear Generating Stations. Ontario Power Generation Report 06819-REP-01200-10029-R00. Toronto, Canada.

Tsuru, T., Y. Huang, Md.R. Ali and A. Nishikata. 2005. Hydrogen entry into steel during atmospheric corrosion process. Corrosion Science 47, 2431-2440.

Vilks, P. 2009. Sorption in Highly Saline Solutions – State of the Science Review. Nuclear Waste Management Organization Report NWMO TR-2009-18. Toronto, Canada.

Vilks, P., N.H. Miller and K. Felushko. 2011. Sorption Experiments in Brine Solutions with Sedimentary Rock and Bentonite. Nuclear Waste Management Organization Report NWMO TR-2011-11. Toronto, Canada.

Villagran, J., M. Ben Belfadhel, K. Birch, J. Freire-Canosa, M. Garamszeghy, F. Garisto, P. Gierszewski, M. Gobien, S. Hirschorn, N. Hunt, A. Khan, E. Kremer, G. Kwong, T. Lam, P. Maak, J. McKelvie, C. Medri, A. Murchison, S. Russell, M. Sanchez-Rico Castejon, U. Stahmer, E. Sykes, A. Urrutia-Bustos, A. Vorauer, T. Wanne and T. Yang. 2011. RD&D Program 2011 – NWMO's Program for Research, Development and Demonstration for Long-Term Management of Used Nuclear Fuel. Nuclear Waste Management Organization Report NWMO TR-2011-01. Toronto, Canada.

Werme, L. 1998. Design Premises for Canister for Spent Nuclear Fuel. Swedish Nuclear Fuel Waste Management Company Report SKB TR-98-08. Stockholm, Sweden.

Wersin, P., M. Birgersson, S. Olsson, O. Karnland and M. Snellman. 2007. Impact of Corrosion-Derived Iron on the Bentonite Buffer within the KBS-3H Disposal Concept – the Olkiluoto Site as Case Study. Posiva Oy Report POSIVA 2007-11. Olkiluoto, Finland.

Wolfaardt, G.M. and D.R. Korber. 2012. Near-Field Microbiological Considerations Relevant to a Deep Geological Repository for Used Nuclear Fuel – State of Science Review. Nuclear Waste Management Organization Report NWMO TR-2012-02. Toronto, Canada.

6. SCENARIO IDENTIFICATION AND DESCRIPTION

Postclosure safety is assessed through consideration of a set of potential future scenarios, where scenarios are descriptions of alternative possible evolutions of the repository system. However, scenarios can also be designed with the aim of illustrating the properties of natural or engineered barriers (IAEA 2012). For that purpose, it can be instructive to assign parameter values such that the barrier under consideration is influenced in an exaggerated way so that the robustness of the barriers can be more clearly exhibited. Scenarios of this sort are often called “what-if” scenarios to distinguish them from realistic scenarios.

The purpose of scenario identification is to develop a comprehensive range of possible future evolutions against which the performance of the system can be assessed. Consistent with the specification of CNSC Guide G-320 (CNSC 2006), both Normal Evolution and Disruptive Event Scenarios are considered. The Normal Evolution Scenario represents the normal (or expected) evolution of the site and facility, while Disruptive Event Scenarios examine the effects of unlikely events that might lead to penetration of barriers and abnormal degradation and loss of containment.

Scenarios of interest are identified through consideration of the various factors (see Table 6-1) that could affect the repository system and its evolution (IAEA 2012). These factors can be further categorized into Features, Events and Processes (FEPs) as shown in Table 6-1. FEPs are organized in a hierarchical structure with up to 4 levels. The finest discretization of the FEPs occurs at the lowest level. This is illustrated in Table 6-2 where the FEPs are listed down to level 3, the lowest level for these FEPs.

FEPs can be characterized as either “external” or “internal”, depending on whether they are outside or inside the spatial and temporal boundaries of the repository system domain, which here includes the repository, the geosphere and the affected biosphere. The external factors originate outside these boundaries; whereas, waste package, repository, geosphere, biosphere and contaminant factors can be considered as “internal" factors. Hence, the waste package, repository, geosphere, biosphere and contaminant factors will be referred to as Internal FEPs and the external factors will be referred to as External FEPs.

The External FEPs provide the system with boundary conditions and include influences originating outside the repository system that might cause change. Included in this group are decisions related to repository design, operation and closure since these are outside the temporal boundary of the postclosure behaviour of the repository system. If these External FEPs can significantly affect the evolution of the system and / or its safety functions of isolation and containment, they are considered scenario-generating FEPs in the sense that whether or not they occur (or the extent to which they occur or the form that they take) could define a particular future scenario that should be considered.

The External FEPs are listed in Table 6-2. Those that are likely to affect the repository system and its evolution are discussed in Section 6.1. The effects of less likely External FEPs and certain Internal FEPs that might lead to abnormal degradation and loss of containment are discussed in Section 6.2.

Table 6-1: FEP List Showing FEPs Down to Level 2

FEP Number and Title	
1.	**EXTERNAL FACTORS**
1.1	Repository Issues
1.2	Geological Factors
1.3	Climatic Factors
1.4	Future Human Actions
1.5	Other External Factors
2.	**WASTE PACKAGE FACTORS**
2.1	Waste Package Characteristics
2.2	Waste Form Processes
2.3	Waste Container Processes
2.4	Contaminant Transport – Waste Package
3.	**REPOSITORY FACTORS**
3.1	Repository Characteristics
3.2	Repository Processes
3.3	Contaminant Transport – Repository
4.	**GEOSPHERE FACTORS**
4.1	Geosphere Characteristics
4.2	Geosphere Processes
4.3	Contaminant Transport - Geosphere
5.	**BIOSPHERE FACTORS**
5.1	Surface Environment
5.2	Human Behaviour
5.3	Contaminant Transport - Biosphere
5.4	Exposure Factors
6.	**CONTAMINANT FACTORS**
6.1	Contaminant Characteristics

Note: From Garisto (2013).

6.1 The Normal Evolution Scenario

The Normal Evolution Scenario is based on a reasonable extrapolation of present day site features and receptor[1] lifestyle. It includes the expected evolution of the site and repository.

[1] The receptor is a person (or persons) who may be exposed to contaminants potentially released from the repository.

6.1.1 External FEPs

The External FEPs have been reviewed to identify those that are likely to occur and could potentially affect the repository and, therefore, should be included in the Normal Evolution Scenario. The resulting list of included / excluded items is shown in Table 6-2 together with a brief justification for their inclusion / exclusion. Further details are provided in Garisto (2013).

Table 6-2 shows that the repository is largely unaffected by many External FEPs, primarily due to its depth and associated geological characteristics. The main External FEPS that are likely to have an impact are:

- Placement of some containers with undetected defects (FEP 1.1.03);
- Glaciation and its effects (FEPs 1.2.02, 1.2.03, 1.2.07, 1.3.01, 1.3.02, 1.3.04, 1.3.05, 1.3.08 and 1.3.09);
- Earthquakes (FEP 1.2.03);
- Human influence on global climate (FEP 1.4.01) delaying onset of the next glaciation; and
- Social and institutional developments leading to changes of land use at the repository site (FEP 1.4.02), and associated drilling, site development and water management (FEPs 1.4.04, 1.4.08 and 1.4.10).

The containers are robust and there are multiple inspection steps to ensure they are fabricated and placed correctly (Chapter 4). However, with the large number of containers, it is possible that some containers could be placed in the repository with defects. Consequently, for the assessment of the Normal Evolution Scenario, it is assumed that some containers with undetected defects are present in the repository.

An important external influence is glaciation. Although glaciation is likely to cause major changes in the surface and near-surface environment, as discussed below, the repository itself is intentionally isolated by its depth from these changes.

Glacial erosion at the hypothetical repository site, although slow, could progressively remove a fraction of the rock overlying the repository in the first one million years. Hence, glacial erosion is considered in the Normal Evolution Scenario; however, deep erosion is assumed not to be likely within this time frame for this hypothetical site and repository depth.

For the hypothetical repository site, the paleohydrogeologic simulations described in Chapter 2 indicate that glacial meltwaters will not reach the repository horizon, as illustrated in Figure 2-24. This is due to the low hydraulic conductivity of the overlaying shales, dolostones and Salina Group evaporites. The glacial recharge penetrating below the shallow groundwater system (i.e., depths greater than 215 m) is not expected to be oxygenated or influence the redox conditions at the repository horizon (see Section 2.4). Furthermore, for the paleohydrogeologic sensitivity cases performed, the glacial perturbations did not materially change mass transport rates at the repository depth (i.e., diffusion remains the dominant transport mechanism (see Section 2.3.4.3, particularly Figures 2-31 to 2-34)). These characteristics of the repository site are used in the scenario identification.

Table 6-2: Status of External FEPs for the Normal Evolution of the Repository System

External FEP			Status*	Remark
1.1	***Repository Issues***			
	1.1.01	Site Investigation	Included	The sedimentary rock site is hypothetical. The topography, stratigraphy and hydrological properties are typical of those found on the Michigan Basin in Southern Ontario. The site is described in Chapter 2. It is assumed that there are no fractures or faults at or near the repository site (as per Chapter 2), there are no undetected geological features at the site, and there are no identified commercially viable mineral resources at the site (as per Chapter 1).
	1.1.02	Excavation and Construction	Included	The repository is built consistent with the design basis, as described in Chapter 4. Controlled drill and blast excavation is used, which reduces but does not avoid formation of an excavation damaged zone (see Chapter 4).
	1.1.03	Placement of Wastes and Backfill	Included	The in-room container placement method is used. Rooms are backfilled as containers are placed, as described in Chapter 4. Due to the large number of containers, it is assumed that some containers are placed with initial defects that are not detected during the fabrication, inspection and placement processes.
	1.1.04	Closure and Repository Sealing	Included	The repository is closed and sealed as described in Chapter 4. This includes sealing of the shafts.
	1.1.05	Repository Records and Markers	Included	Repository records and markers (and passive societal memory) are assumed sufficient to ensure that inadvertent intrusion would not occur for at least a few hundred years.
	1.1.06	Waste Allocation	Included	The repository holds 4.6 million CANDU fuel bundles. There is no placement of other radioactive or chemically hazardous material at the site.
	1.1.07	Repository Design	Included	The repository design concept is described in Chapter 4.

External FEP			Status*	Remark
	1.1.08	Quality Control	Included	Construction, operation, monitoring and closure of the repository are all undertaken under a project quality plan that ensures that the design and safety basis is met (see Chapter 10). However, due to the large number of containers, it is assumed that some containers are placed with initial defects that are not detected during the fabrication, inspection and placement processes.
	1.1.09	Schedule and Planning	Included	The assumed schedule is ~40 years operation, 70 years extended monitoring and 30 years for decommissioning and closure.
	1.1.10	Repository Administrative Control	Included	Administrative controls ensure proper operation and closure of the repository. Institutional controls (e.g., land use restrictions) will be implemented on closure, which, while they remain effective, will prevent inadvertent human intrusion and the drilling of wells.
	1.1.11	Monitoring	Excluded	The postclosure monitoring program will not compromise the safety of the repository.
	1.1.12	Accidents and Unplanned events	Excluded	The likelihood of preclosure accidents or unplanned events that could impact the long-term safety of the repository will be minimized by good engineering practice and quality control; and the effects of any that do occur will be mitigated before the repository is closed.
	1.1.13	Retrieval of Wastes	Excluded	The repository schedule includes an extended period of monitoring after rooms have been filled but before the access tunnels and shaft are sealed, which would facilitate retrieval if required. However, retrieval after closure is not expected and is not included in this safety assessment.
1.2	***Geological Factors***			
	1.2.01	Tectonic Movement and Orogeny	Excluded	The hypothetical site is in a tectonically stable region away from plate margins, with no tectonic activity over the time scale of interest (i.e., 1,000,000 years).

External FEP			**Status***	**Remark**
	1.2.02	Deformation (Elastic, Plastic or Brittle)	Included	The repository site is assumed to be tectonically stable; hence, deformation due to tectonic movement and orogeny is unlikely over the timescales on interest. Thus, over the next million years, the only significant deformation force is that due to ice sheet advance over the site. This could cause crustal depression in excess of 500 m, but would occur on a continental scale (Peltier 2011). Ice sheet weight could also cause local movement along existing faults or fractures zones but would not lead to creation of new fractures. As per Chapter 2, it is assumed there are no fractures or faults intersecting the repository.
	1.2.03	Seismicity (Earthquakes)	Included	Earthquakes will occur over the time scale of interest; however, since the site is assumed located in a seismically inactive region, the likely magnitude, frequency and distance of earthquakes would limit their impact at the repository location. Larger earthquakes are more likely during retreat of ice sheets. Earthquakes are in general less destructive at depth than at the surface, diminishing the impact of any seismic activity on a deep repository. Since the repository is backfilled, preventing rock fall, the main concern would be shearing along an existing fracture plane intercepting the repository, providing either a groundwater pathway or damaging containers. However, it is assumed for the Normal Evolution Scenario that, consistent with Chapter 2, there are no fracture zones or faults at or near the site and that there are no undetected geological features at the repository site.
	1.2.04	Volcanic and Magmatic Activity	Excluded	No volcanic or magmatic activity over the time scale of interest due to the site location.
	1.2.05	Metamorphism	Excluded	No processes occur over the time scale of interest that will cause metamorphism.
	1.2.06	Hydrothermal Activity	Excluded	The hypothetical repository is assumed located in a geologically stable sedimentary basin in Ontario with a low geothermal flux. Hydrothermal processes therefore act too slowly to be of concern over the time scale of interest.

External FEP			Status*	Remark
	1.2.07	Regional Erosion and Sedimentation	Included	The area is topographically relatively flat and not high above sea level so there is limited potential for large-scale denudation. However, over the past 1,000,000 years, ice-sheet erosion and deposition has shaped the topography and could continue to do so in the future. Erosion is accounted for in the definition of the Normal Evolution Scenario.
	1.2.08	Diagenesis	Excluded	Would have negligible effect on repository safety over the timescale of interest (1,000,000 years).
	1.2.09	Salt Diapirism and Dissolution	Excluded	No significant salt deposits are assumed to be located in the vicinity of the site. Historically, there could have been salt deposits but these have already been dissolved in the distant past.
	1.2.10	Hydrological Response to Geological Changes	Excluded	A severe seismic event could potentially change fracture zone permeabilities or activate a fault and therefore change local hydrology. However, it is assumed for the Normal Evolution Scenario that site characterization has not identified any fracture zones or faults at or near the hypothetical repository site. At the hypothetical site, it is assumed that the hydraulic pressure is hydrostatic - there is no pattern of over- and under-pressures in the different rock formations (see Chapter 2). Also, none of the other included geologic processes identified above are able to cause significant hydraulic changes on relevant timescales.
1.3	***Climate Factors***			
	1.3.01	Global Climate Change	Included	After a period of global warming, it is assumed that glacial / interglacial cycling will eventually resume since the solar insolation variation driving this cycling will continue.
	1.3.02	Local and Regional Climate Change	Included	In the near term, global warming is likely to cause temperature and precipitation changes, although the local / regional climate is likely to remain generally temperate due to its northerly latitude location. In the long-term, it will respond to global climate change, and in particular will cool or warm with glacial cycles.

External FEP			Status*	Remark
	1.3.03	Sea-level Change	Excluded	Changes in sea level do not affect the site due to its assumed mid-continental location.
	1.3.04	Periglacial Effects	Included	These will occur during colder climate states experienced during the glacial cycles that are likely to occur at the site over a one million year timeframe. In particular, this would include permafrost development (see Chapter 2).
	1.3.05	Local Glacial Effects	Included	Ice sheets will cause a range of local effects. These include change in rock stress (FEP 1.2.02), earthquake initiation (FEP 1.2.03), change in surface and near-surface hydrology (FEP 1.3.07), penetration of glacial waters to depth, changes in ecosystems (FEP 1.3.08) and human behaviour (FEP 1.3.09).
	1.3.06	Warm Climate Effects (Tropical and Desert)	Excluded	Climate change is unlikely to result in development of tropical or hot desert conditions at the site due to its northerly latitude. An initial period of human-induced global warming is not expected to result in extreme temperature rise resulting in tropical or desert conditions in this region.
	1.3.07	Hydrological Response to Climate Change	Excluded	Surface and near-surface groundwater systems could be altered by a climatic change to wetter or drier conditions. However, the deep groundwater system at the site would not be significantly altered by climatic change to wetter or drier conditions (within expected variation, see FEP 1.3.06), due to its low-permeability and depth (see Chapter 2). Changes in hydrology due to glaciation are discussed separately under Periglacial Effects (1.3.04) and Local Glacial Effects (1.3.05).
	1.3.08	Ecological Response to Climate Changes	Included	Flora and fauna at the site change in response to glacial / interglacial cycling.
	1.3.09	Human Behavioural Response to Climate Change	Included	Human behaviour changes in response to glacial / interglacial cycling.

External FEP			Status*	Remark
1.4	***Future Human Actions***			
	1.4.01	Human Influences on Climate	Included	Human actions are a possible cause of global climate change, which is included in expected evolution (see FEP 1.3.01, Global Climate Change).
	1.4.02	Deliberate Human Intrusion	Excluded	Deliberate human intrusion into the repository is not considered. It is assumed that any future society choosing to recover materials from the repository would have the technology to understand and manage the hazards. Note that unauthorized deliberate intrusion is unlikely due to the infrastructure needed to excavate to repository depth.
	1.4.03	Non-Intrusive Site Investigation	Excluded	Non-intrusive site investigations would not have any effect because of the repository depth.
	1.4.04	Drilling Activities (Human Intrusion)	Excluded	The drilling of deep exploration boreholes that penetrate to the repository is excluded from the expected evolution due to the repository depth (around 500 m), the relatively small repository footprint (~6 km^2), and the assumed lack of commercially viable natural resources at the site. Note that this FEP does not include drilling of shallow wells which are considered under FEP 1.4.07.
	1.4.05	Mining (Human Intrusion)	Excluded	It is assumed that there are no commercially viable mineral resources present at the site.
	1.4.06	Surface Environment, Human Activities	Excluded	Unlikely to have any direct impact on repository due to the repository depth.

External FEP			Status*	Remark
	1.4.07	Water Management (Wells, Reservoirs Dams)	Included	The drilling of shallow water wells in the area is considered once institutional controls are no longer effective (see FEP 1.1.10). Wells in the deeper groundwater zones are excluded since the groundwater in these zones is not potable. This is consistent with present-day practice in Ontario for extraction of water from shallow groundwater systems. Construction of dams and reservoirs is unlikely to have significant effects on the deep groundwater system due to the generally low topography around the site and the low permeability of the rock.
	1.4.08	Social and Institutional Developments	Included	Institutional controls ensure appropriate use and control of the site in the near term, but it is assumed that this institutional control is eventually lost. Thereafter, the site is assumed to return to land use typical of the region and the site is occupied, including drilling of wells (see FEP 1.4.07).
	1.4.09	Technological Developments	Excluded	It is assumed that the capabilities of future humans will largely resemble present-day capabilities, consistent with the International Commission on Radiological Protection's (ICRP 2000) recommendations and CNSC (2006). Thus, there is no credit taken for advances that might reduce the risk from the repository.
	1.4.10	Remedial Actions	Excluded	Remedial actions are not expected following closure of the repository.
	1.4.11	Explosions and Crashes	Excluded	Most surface explosions and crashes would have no direct impact on the repository due to its depth. Explosions large enough to affect repository depth would likely have large direct consequences that would be much more significant than any additional harm caused by damage to the repository.

External FEP			Status*	Remark
1.5	***Other External Factors***			
	1.5.01	Meteorite Impact	Excluded	Excluded due to low probability (due to relatively small repository footprint) and / or low consequence (due to depth of repository). See FEP 1.5.01 in Garisto (2013). Furthermore, meteorites large enough to affect the repository would likely have large direct consequences that would be much more significant than any additional harm caused by damage to the repository.
	1.5.02	Species Evolution	Excluded	No evolution of humans assumed, consistent with the ICRP recommendation to apply the concept of (present-day) Reference Man to the management of long-lived solid radioactive waste (ICRP 2000). Similarly, no evolution of non-human biota assumed. General characteristics of biota are assumed to remain similar to current biota.
	1.5.03	Earth Tides, Reversal of Earth's Magnetic Poles, Polar Wander and other Unusual FEPs	Excluded	Consideration of unusual FEPs such as earth tides, reversal of earth's magnetic poles, polar wander, etc. are excluded because of their low probability or because they have no significant effect on the repository.

Note: * Status – *Included* means this factor is considered in the Normal Evolution Scenario. *Excluded* means this factor is not considered in the Normal Evolution Scenario.

6.1.2 Internal FEPs

Internal FEPs are important aids in defining the expected evolution of the repository. They assist in determining which features and processes are important to include in the conceptual model and related computer codes.

The significant FEPs are accounted for in the description of the Normal Evolution Scenario which appears in the following section.

The internal FEPs are reviewed in Garisto (2013).

Internal FEPs are not usually scenario generating; however, they are considered with respect to Disruptive Scenarios in Section 6.2.1.

6.1.3 Description of the Normal Evolution of the Repository System

From consideration of the External FEPs and the Internal FEPs, the following high-level narrative of the expected evolution of the repository system can be developed. This understanding is based on many years of study, including laboratory studies, underground research studies, and observations of analogous natural and long-lived human-made structures and materials. This narrative is used to guide both the subsequent development of the conceptual model for the safety assessment and the variations to this model considered in alternative calculation cases.

The narrative summarizes the main events in the evolution of the repository in broad terms, including the long-term changes in the geosphere and biosphere due to glaciation. It is based on the reference design concept where used fuel is placed in the repository in long-lived copper-and-steel containers. These containers are designed not to fail and will be carefully fabricated and inspected. Most of these containers do not fail in the relevant time scale; however, as noted earlier there could be some containers with undetected defects in the copper shell, potentially leading to early releases of radioactivity. Since defective containers behave differently than intact containers, they are described separately in the following sections.

The possibility of failure of the copper shell at long times due to creep deformation under expected repository conditions is presently an open issue. Because of this uncertainty and others, the All Containers Fail Scenario is included as a Disruptive Event Scenario in Section 6.2. This creep failure mechanism is assumed not to occur in the Normal Evolution Scenario.

Most of the processes identified are well understood as discussed in Chapter 5. Key points are that the geosphere isolates the repository from the surface, that the groundwater around the repository level remains within its natural chemistry range and low oxygen state, and that the load-bearing capacity of the containers is sufficient to withstand the effects of glaciation and earthquakes at repository depth.

6.1.3.1 Events Occurring for Intact Containers

0-100 years

The repository is assumed to be open and actively monitored for a period of about 100 years. The 100 year period consists of the reference design assumption of ~40 years of operation and up to 70 years of monitoring during which access tunnels are kept open. Decommissioning and closure will take a further 30 years. In the operation period, 12,778 containers (containing about 4.6 million used fuel bundles, or about 90,000 Mg of uranium) are placed in the repository with the placement rooms backfilled with clay-based sealing materials. The initial radioactivity in a full repository (assuming 30 year old fuel on average) is about 10^{20} Bq and the initial thermal load is about 16 MW (Figure 6-1).

During the first 100 years after placement:

- Radioactivity drops by a factor of 10 and the thermal output drops by a factor of four. Radionuclides with short half-lives such as tritium (H-3) and Co-60 decay to negligible levels.
- Peak temperatures are reached within the repository, with values of about 120°C at the container outer surface and values less than 100ºC at distance greater than 20 cm from the container (Guo 2010).
- The copper container reacts with oxygen from the buffer to form a very thin corrosion layer.
- Recent experiments indicate that it may be possible for copper to corrode in pure, oxygen-free water (see Section 5.3.1.5). However, the hydrogen gas generated by this copper corrosion reaction suppresses further corrosion (e.g., at 73ºC, a hydrogen partial pressure of ~1 mbar (Szakálos et al. 2007) is sufficient to suppress the copper-water reaction).
- Thermal expansion and contraction of the rock and concrete combine to create near-field stresses within the low-permeability rock and the concrete bulkhead at the ends of the placement rooms, and a limited amount of microcracking occurs.
- In the rock around the repository, groundwater flow and heads are influenced by the presence of the open tunnels and the high-suction clay, which draw water towards the repository. This is countered by the container thermal power, which redistributes water away from the containers.
- Microbes in the buffer material near the containers die or become dormant because of heat, desiccation, lack of nutrients or space to be viable.

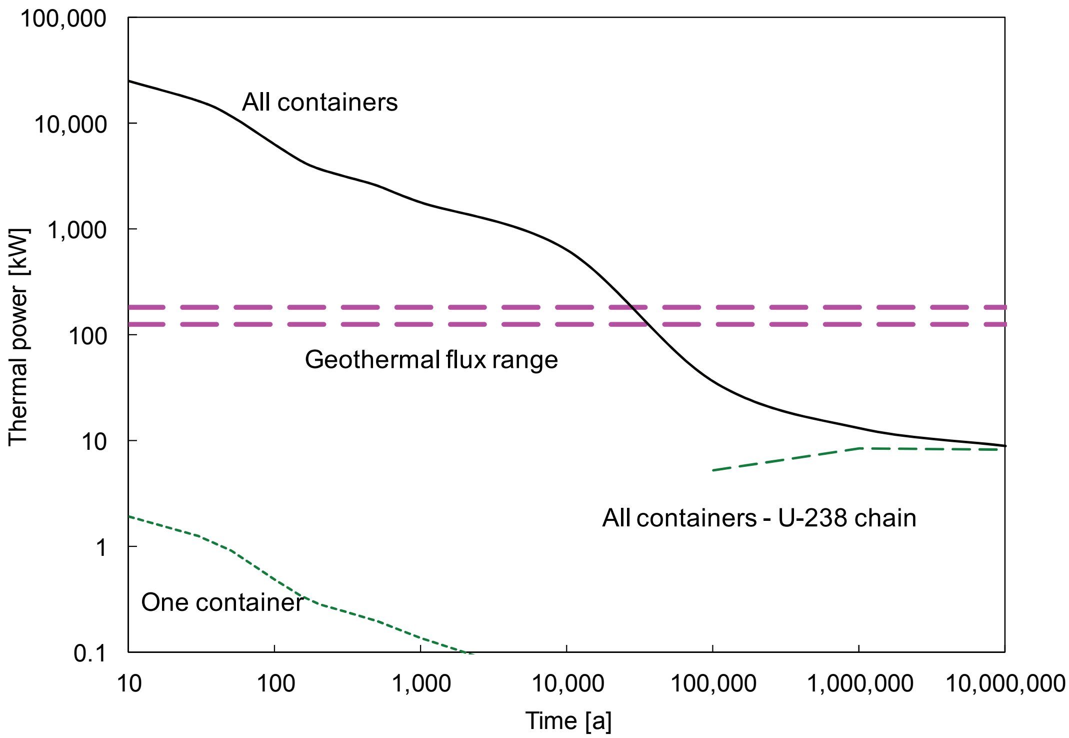

Notes: The power is similar to the natural geothermal flow (Perry et al. 2010) through the repository area after about 30,000 years. After about 1 million years, the residual power is due to radioactive decay of the decay products of uranium.

Figure 6-1: Total Thermal Power of the Repository (Average 220 MWh/kgU Burnup)

<u>100-1,000 years</u>

Shortly after the beginning of this time period, all access tunnels and shafts are backfilled and sealed, with particular attention paid to sealing the shafts. All intrusive monitoring systems and deep boreholes are removed or closed. For several hundred years thereafter, distinct physical and chemical differences (e.g., temperature, porewater composition) will exist between the various components of the repository, and between the repository and the geosphere. Many of the changes that occur within this timeframe are driven by these gradients. During this period:

- Radioactivity drops by a factor of 30. Most fission products decay to insignificant levels, including Sr-90 and Cs-137.
- Container thermal power drops to around 120 W per container. Residual heat comes from decay of the remaining actinides.
- Temperatures in the buffer material around the container drop to about 75°C.
- The oxygen initially present in the sealing materials (as trapped air) is consumed.
- Groundwater from the geosphere enters the repository. As the clay materials begin to saturate, they start to swell and exert pressure on adjacent materials. The swelling process proceeds slowly and perhaps non-uniformly.
- Climate change may have occurred. Global warming with higher average temperatures could lead to more or less precipitation at the site. This would affect the surface waters

(lakes and rivers) and shallow groundwaters, and also the local ecosystem around the site, but deep groundwaters are unaffected.

<u>1,000-60,000 years</u>

- Radionuclides like C-14 have decayed.
- Thermal power drops to 6 W per container. The temperatures in and around the repository drop to approximately 10ºC above ambient rock temperatures.
- By the end of this time, the repository is saturated and anaerobic, conditions typical of deep rock environments. Peak swelling loads of clay-based seals are 0.6 to 0.7 MPa under the high salinity conditions in the repository. The swelling clay fills cracks and voids. The EDZ properties are assumed unaffected by swelling of the clay-based seals.
- Hydrostatic loads and some of the rock mechanical loads are transmitted through the clays onto the container. The copper shell is compressed onto the inner steel vessel, which is rigid and maintains its shape.
- The repository components gradually achieve equilibrium with the surrounding geosphere.
- Corrosion of the container has essentially stopped since the lack of oxygen prevents both uniform and localized corrosion.
- A fraction (< 5%) of the montmorillonite in the buffer is converted to illite due to the high potassium concentration (0.32 mol/L) in groundwater and the elevated temperatures experienced by the buffer over this period.
- The main microbial activity occurring in the repository is due to anaerobic bacteria, including sulphate-reducing bacteria, located mainly at the interfaces with the rock and in the backfill. The buffer remains largely inhospitable because of the high salinity, and high clay density and pressure, which creates adverse conditions of low water activity and small pore size.
- Locally near concrete surfaces, a more alkaline porewater develops in the clay-based sealing materials, resulting in an altered layer of clay, several centimetres thick, with a reduced swelling capacity near the interface.
- Changes continue to occur in the surface environment. Climate change due to natural or human influences would likely occur. In particular, the climate might start to cool as part of a long-term glacial cycle with possible formation of permafrost and initiation of glaciation at the site.

<u>60,000-1,000,000 years</u>

- Over this timeframe, the perturbations to the system will be driven by external events. The most important events will be glaciation cycles, which are likely to occur over this time period. These are likely to repeat on a period of roughly every 120,000 years.
- The residual radioactivity is dominated by the decay of actinides. By the end of this period, all plutonium has decayed.
- The onset of a glacial cycle will start with a cooling period, with mean surface temperatures over the sedimentary basin (in Ontario) dropping to approximately 0^{o}C. Permafrost develops, disrupting groundwater flow down to about 60 metres (see Chapter 2).
- Eventually, an ice sheet will form and extend across the site. The hydrological conditions at the edge of the glacier cause major perturbations to the near-surface groundwater flow system. The hydraulic heads at depth also change, but groundwater response is muted due to the low permeability of the deep rock.

- In some areas, glacially driven recharge may penetrate deeper, but reactions with minerals and microbes along the flow path of recharging meltwaters consume dissolved oxygen. Conditions at repository depth remain reducing.
- At its maximum development, the glacial ice sheet could be 2 to 3 kilometres thick above the repository, potentially increasing the hydrostatic pressure at repository depth by 20 to 30 MPa (possibly much less, depending on the rock properties and the nature of the ice sheet). This value is within the design tolerance of the containers.
- During glaciation, the land mass flexes vertically in excess of 500 m in response to the weight of the ice sheets. During glacial retreat, earthquakes may occur. Existing fracture zones may be reactivated in these locations although there is little change in terms of new fracture development.
- The advancing and retreating ice sheets and their associated meltwater both erode and deposit rock and till. The amount of additional bedrock erosion could be up to tens of metres over a one million year timeframe, but this would not adversely impact the isolation of the repository.
- The chemistry of the porewater within the sealing materials slowly changes to resemble that of the groundwater.
- Along with the porewater chemistry change, the montmorillonite component of the bentonite has lost Na and gained Ca, Mg, and Fe but has still retained its swelling capacity. Due to the lower temperatures, very little additional montmorillonite has converted to illite.
- Microbial activity in the repository is limited in general by the salinity of the groundwater (see Chapter 5). It is limited in terms of mobility by the impermeability of the dense buffer around the containers and host rock; and it is also limited metabolically by the requirement for nutrients to diffuse through the clay-based sealing materials.

<u>Beyond 1,000,000 years</u>

Virtually all the reactor-generated radioactivity has decayed, and most of the residual radioactivity in the used fuel comes from its natural uranium content. The amount of uranium in the repository is comparable to the large uranium ore bodies in north-central Canada. These natural deposits of uranium oxide have been stable for billions of years. Similarly, many ore deposits of metallic copper and sedimentary deposits of bentonite are known that range in age from millions to hundreds of millions of years. The ultimate fate of the repository and the materials it contains will be largely indistinguishable from these natural analogues.

6.1.3.2 Events Occurring for Defective Containers

The evolution of any defective containers will be different from that of intact containers. This evolution is summarized below (see Chapter 5 for a more detailed description).

Only the additional events that may occur in the evolution of these containers are summarized here, since most of the events occurring for the intact containers (e.g., radiation-related changes, thermal changes, etc.) also occur for defective containers. For this discussion, it is assumed that some containers are placed in the repository with small undetected defects that penetrate the copper shell. The inner steel container is therefore exposed to evolving conditions in the repository.

<u>0-100 years</u>

Over this period the repository is not fully saturated. Atmospheric corrosion of the steel next to the defect may occur but only to a very limited extent because the relative humidity near the copper container is low and oxygen is consumed by other processes.

<u>100-1,000 years</u>

As the repository saturates, water may enter the defect and contact the steel vessel. Anaerobic corrosion of the steel vessel begins, generating iron oxides and hydrogen gas. The most likely iron corrosion product is magnetite.

<u>1,000-60,000 years</u>

- During this period the repository becomes saturated and the buffer may swell into the defect in the container.
- Water leaks into the interior of the steel vessel through the bolted lid and the inside of the steel vessel also starts to corrode.
- Corrosion of the steel vessel continues and the hydrogen gas pressure increases near the defective container. The timing of events depends on the behaviour of the hydrogen. The corrosion rate of the steel may be limited by the availability of water due to the low hydraulic conductivity of the host rock.
- Iron corrosion products build up on the steel vessel near the defect. The build up of corrosion products causes local deformation of the copper shell and the initial defect enlarges. Formation of iron oxides however also covers the surface and inhibits the corrosion reaction.
- Hydrogen gas generated by steel corrosion forms a bubble or blanket that also inhibits water contact with the container. Once the hydrogen pressure is high enough (on the order of the hydrostatic pressure plus swelling pressure), the gas will create a channel through the buffer, and move to the interface with the rock and into the EDZ. Here, the gas would move along the interface until the gas pressure decreases sufficiently that there is no driving force for advective gas movement. The pathway through the buffer re-seals after the gas passes so the effectiveness of the buffer is not impaired.
- Water in the steel vessel contacts the fuel bundles. Local failure or corrosion of the Zircaloy cladding allows water to contact the used fuel in places. The more soluble radionuclides (typically a few percent) in the fuel / cladding gap and grain boundaries are released into the water inside the steel vessel.
- A small amount of the used fuel dissolves, releasing other radionuclides into the water. The presence of hydrogen gas from corrosion of the steel container sustains conditions that significantly decrease the rate of fuel dissolution.
- Most radionuclides have decayed, or are trapped within the used fuel. Dissolved radionuclides diffuse out of the container and into the buffer surrounding the container.

<u>60,000-1,000,000 years</u>

- The steel vessel continues to corrode until all of the steel is consumed.
- Corrosion of the copper vessel continues but only a small fraction of the copper corrodes over this time period.
- Hydrogen gas from steel corrosion present within the excavation damaged zone slowly dissolves in groundwater and slowly diffuses away from the repository. Hydrogen gas remaining in the container also slowly dissolves allowing full saturation of the container.

- At some point, the steel vessel is sufficiently weakened by corrosion that it is no longer load bearing and collapses. Any remaining intact fuel bundles are damaged and exposed to water.
- Most of the UO_2 is fractured but intact. About 20% of the fuel has dissolved by the end of this period.
- Some radionuclides migrate out of the container, through the buffer, and into the nearby rock. Most radionuclides decay within or near the repository and surrounding rock. Slow migration of the more mobile, soluble and long-lived species (such as I-129) through the geosphere and eventually into the shallow groundwater system and the biosphere can occur.

6.2 Disruptive Event Scenarios

Disruptive Event Scenarios postulate the occurrence of unlikely events leading to possible penetration of barriers and abnormal loss of containment.

6.2.1 Identification of Disruptive Scenarios

A set of Disruptive Scenarios has been identified by evaluating the potential for the External FEPs (Table 6-2) to compromise the safety of the repository system. Specifically, the repository system safety attributes and features identified in Chapter 1 are checked to see if they could be significantly compromised by any of the External FEPs, with the results of this assessment summarized in Table 6-3.

As a further check, the potential for the Internal FEPs to compromise the long-term safety features is also considered, and summarized in Table 6-4. Note that the FEPs considered under the “Biosphere Factors” and “Contaminant Factors” categories are not capable on their own of modifying the repository system to an extent that results in a fundamentally different evolution to that considered in the Normal Evolution Scenario. These are therefore not scenario generating and their effects can be evaluated through different calculation cases for the Normal Evolution Scenario rather than through the development of Disruptive Event Scenarios.

The failure mechanisms identified in Table 6-3 and Table 6-4 can be grouped into eight Disruptive Scenarios as discussed below and summarized in Table 6-5. Since the long-term safety of the repository is based on the strength of the geosphere and engineered barriers (including the container and the shaft seals), the scenarios focus on events in which these can be bypassed.

Table 6-3: External FEPs Potentially Compromising Arguments Relating to the Long-Term Safety

Safety Feature	Potentially Compromised by	Consider as Failure Mechanism
1. The depth of the host rock formation should be sufficient for isolating the repository from surface disturbances and changes caused by human activities and natural events.	Near-surface design adopted (FEP 1.1.02).	**No,** only a deep design is being considered for the repository.
	Meteorite impact (FEP 1.5.01).	**No,** due to low probability of meteor impact capable of compromising safety due to the relatively small repository footprint (~6 km^2) and depth of repository (~500 m). See Garisto (2013) for further discussion of probabilities.
	Exploration borehole penetrates into repository providing enhanced permeability pathway to surface environment and potential for direct exposure to waste (FEP 1.4.04).	**Yes,** although the absence of economically exploitable resources, and the depth (~500 m) and relatively small repository footprint (~6 km^2) mean that the probability of such a borehole intruding into the repository would be very low during the period of greatest potential hazard.
	Mining and other underground activities resulting in excavation in the vicinity of the repository (FEP 1.4.05).	**No,** due to assumption of the absence of commercially viable mineral resources near or below repository level. Shallow quarrying or tunnelling activities are unlikely to affect the repository because of repository depth (~500 m). Also, most underground activities would likely be preceded by exploration boreholes, as addressed above.
	Deliberate human intrusion into repository (FEP 1.4.02).	**No,** exclude deliberate human intrusion since it is expected that the intruders would take appropriate precautions. Note that unauthorized deliberate intrusion is unlikely due to the infrastructure needed to excavate to repository depth.

Safety Feature	Potentially Compromised by	Consider as Failure Mechanism
	Could discover resources that were not identified during site investigations (FEP 1.1.01) or exploit existing rocks that have become a commercially viable resource. These new resources are exploited by drilling or mining at or below repository level (FEP 1.4.04 and FEP 1.4.05).	**No,** the lack of resources at the site is assumed to be consistent with regional information. Even if the existing rocks became commercially viable, the repository site is unlikely to become a mine site because of the uniformity and large lateral extent of the host rocks that extend to shallower depths elsewhere. Also, deep mining activities would likely be preceded by an exploration borehole, which is considered under FEP 1.4.04.
	Repository and shafts not properly sealed at time of closure providing an enhanced permeability pathway to the surface environment (FEP 1.1.04).	**Yes,** although NWMO quality control and regulatory oversight will ensure that poor sealing is very unlikely. Alternatively, due to some severe societal disruption, the repository is not closed as planned but remains open and unsealed but not maintained.
	Site investigation / monitoring borehole not properly sealed at time of closure providing an enhanced permeability pathway to the surface environment (FEP 1.1.01 and FEP 1.1.11).	**Yes,** although NWMO quality control and regulatory oversight will ensure that poor sealing is very unlikely. Alternatively, due to some severe societal disruption, the repository is not closed as planned but remains open and unsealed but not maintained.
	Poor construction techniques affect the performance of the repository and shaft excavation disturbed zones providing an enhanced permeability pathway to the surface environment (FEP 1.1.02).	**Yes,** although NWMO quality control and regulatory oversight will ensure that poor sealing is very unlikely.

Safety Feature	Potentially Compromised by	Consider as Failure Mechanism
	Site investigations do not identify a permeable fracture zone or fault that provides a connection between the repository horizon and shallow groundwater system (FEP 1.1.01).	**Yes,** although very unlikely, such a feature cannot be categorically ruled out due to the limits of current technologies to identify all fracture zones, and so is considered in a "what-if" scenario.
	High magnitude seismic event results in reactivation of undetected existing structural discontinuity and / or failure of shaft seals which provides an enhanced permeability pathway to higher horizons (FEP 1.2.03).	**Yes,** the assessment time scales are such that a significant event may occur even though the annual probability is low. Even then, the probability that the earthquake could actually reactivate a nearby fracture or fail the shaft seals is very small since it would take a significant amount of energy.
	Ice sheet erosion removes a significant thickness of rock above repository (FEPs 1.2.07, 1.3.01, 1.3.02, and 1.3.05).	**Yes,** the impact of realistic rates of glacial erosion is addressed as part of the Normal Evolution Scenario; whereas, severe erosion is considered as a disruptive event scenario.
	Advance / retreat of ice sheets generate large hydraulic gradients which affect groundwater flow velocities in the deep groundwater zone (FEP 1.3.05).	**No,** the changing hydraulic head due to ice sheet advance and retreat over the repository site may affect groundwater flow at the repository level, but advective flows will remain low due to the low permeability of the deep rock (see Chapter 2, particularly the discussion of the paleohydrogeologic sensitivity cases).
	Other external geological processes disrupt the repository system, i.e., Tectonic Movement (FEP 1.2.01), Volcanic and Magmatic Activity (FEP 1.2.04), Metamorphism (FEP 1.2.05), Hydrothermal Activity (FEP 1.2.06), Diagenesis (FEP 1.2.08) and Salt Diapirism and Dissolution (FEP 1.2.09).	**No,** since precluded by site's location and assessment time scales.

Safety Feature	Potentially Compromised by	Consider as Failure Mechanism
2. The volume of available competent rock at repository depth should be sufficient to host the repository and provide sufficient distance from active geological features such as zones of deformation or faults and unfavourable heterogeneities.	Site investigations do not identify a permeable fracture zone or fault that provides a connection between the repository horizon and shallow groundwater system (FEP 1.1.01).	**Yes,** although very unlikely, such a feature cannot be categorically ruled out and so is considered in a “what-if” scenario. A nearby fracture zone could be missed due to the limits of current technologies to identify all such features in the rock.
	High magnitude seismic event results in reactivation of undetected existing structural discontinuity and / or failure of shaft seals which provides an enhanced permeability pathway to higher horizons (FEP 1.2.03).	**Yes,** the assessment time scales are such that a significant event may occur even though the annual probability is low. Even then, the probability that the earthquake could actually reactivate a nearby fracture or fail the shaft seals is very small since it would take a significant amount of energy.
	Other external geological processes disrupt the repository system, i.e., Tectonic Movement (FEP 1.2.01), Volcanic and Magmatic Activity (FEP 1.2.04), Metamorphism (FEP 1.2.05), Hydrothermal Activity (FEP 1.2.06), Diagenesis (FEP 1.2.08) and Salt Diapirism and Dissolution (FEP 1.2.09).	**No,** since precluded by site’s location and assessment time scales.
3. The hydrogeological regime within the host rock should exhibit low groundwater velocities.	High magnitude seismic event results in reactivation of undetected existing structural discontinuity and / or failure of shaft seals which provides an enhanced permeability pathway to higher horizons (FEP 1.2.03).	**Yes,** the assessment time scales are such that a significant event may occur even though the annual probability is low. Even then, the probability that the earthquake could actually reactivate a nearby fracture or fail the shaft seals is very small since it would take a significant amount of energy.

Safety Feature	Potentially Compromised by	Consider as Failure Mechanism
	Advance / retreat of ice sheets generate large hydraulic gradients which affect groundwater flow velocities in the deep groundwater zone (FEP 1.3.05).	**No,** for the paleohydrogeologic sensitivity cases examined in Chapter 2, the glacial perturbations did not materially change groundwater flow rates at repository depth and diffusion remains the dominant transport mechanism in the host rock zone. Note that it is assumed that there are no fracture zones or faults at or near the site, which is consistent with Chapter2, and, furthermore, there are no undetected geological features at the repository site.
	A pattern of over- and underpressure in the groundwater and porewater hydraulic heads at the site is observed during site investigation or forms in the future due to, for example, glaciation. Such pressures would represent a state of disequilibrium.	**Yes,** such patterns have been observed at some sites in the Michigan Basin in Ontario. However, the hypothetical site is assumed to not include any significant over- or underpressure, and this would be readily detected during site characterization. No future geological mechanisms are identified that would cause this behavior on relevant timescales. Glaciation would cause pressure changes, but these are evaluated in Chapter 2 and are temporary and not significant. Nonetheless, the possibility of an overpressure forming at the boundary with the Precambrian basement is considered as a conservative sensitivity case for the Normal Evolution Scenario, even though the low hydraulic conductivity of the rock means advective flows would remain low for realistic overpressures.
	Other external geological processes disrupt the repository system, i.e., Tectonic Movement (FEP 1.2.01), Volcanic and Magmatic Activity (FEP 1.2.04), Metamorphism (FEP 1.2.05), Hydrothermal Activity (FEP 1.2.06), Diagenesis (FEP 1.2.08) and Salt Diapirism and Dissolution (FEP 1.2.09).	**No,** since precluded by site's location and assessment time scales.

Safety Feature	Potentially Compromised by	Consider as Failure Mechanism
4. The mineralogy of the rock, the geochemical composition of the groundwater and rock porewater should not adversely impact the expected performance of the repository multi-barrier system.	Infiltration of glacial meltwater (without oxygen) into the repository modifies the hydrogeochemical conditions, affecting, for example, the stability of the buffer and backfill materials (i.e., leads to erosion of these materials due to colloid formation) (FEP 1.3.05).	**No,** the paleohydrogeologic simulations described in Chapter 2 suggest that glacial meltwaters will not reach the repository horizon. This is due to the low hydraulic conductivity of the overlaying shales, dolostones and Salina Group evaporites. Note that, consistent with Chapter 2, it is assumed that there are no fracture zones (or faults) at the repository site.
5. The mineralogy of the host rock, the geochemical composition of the groundwater and rock porewater should be favourable to retarding radionuclide movement.	Infiltration of oxygenated glacial meltwater into the repository leads to oxidizing conditions in the repository, causing relatively rapid corrosion of copper containers, rapid corrosion of used fuel in any defective containers, and enhanced mobility of redox sensitive nuclides such as U and Tc.	**No,** glacial recharge penetrating below the shallow groundwater system (i.e., depths greater than 215 m) is not expected to be oxygenated or influence the redox conditions at the repository horizon (see Chapter 2).
	Other external geological processes disrupt the repository system, i.e., Tectonic Movement (FEP 1.2.01), Volcanic and Magmatic Activity (FEP 1.2.04), Metamorphism (FEP 1.2.05), Hydrothermal Activity (FEP 1.2.06), Diagenesis (FEP 1.2.08) and Salt Diapirism and Dissolution (FEP 1.2.09).	**No,** since precluded by site's location and assessment time scales.
6. The host rock should be capable of withstanding mechanical and thermal stresses induced by the repository without significant structural deformation or fracturing that could compromise the containment and isolation functions of the repository.	Presence of repository weakens rock near repository, potentially making it susceptible to fracturing during earthquakes which could be caused by ice sheet loading / unloading (FEP 1.2.02).	**Yes,** an unknown fault or fracture zone could be reactivated due to seismic activity.

Safety Feature	Potentially Compromised by	Consider as Failure Mechanism
7. Current and future seismic activity at the repository site should not adversely impact the integrity of the repository during operation and in the very long-term.	High magnitude seismic event results in reactivation of undetected existing structural discontinuity and / or failure of shaft seals which provides an enhanced permeability pathway to higher horizons (FEP 1.2.03).	**Yes,** the assessment time scales are such that a significant event may occur even though the annual probability is low. Even then, the probability that the earthquake could actually reactivate a nearby fracture or fail the shaft seals is very small since it would take a significant amount of energy.
	Large seismic event results in shearing along an existing fracture zone that passes through a placement room of the repository. The shearing load causes failure of a used fuel container.	**Yes,** the assessment time scales are such that a significant seismic event may occur even though the annual probability is low. However, the probability that an earthquake would cause failure of a container in a placement room due to a shear load is very small due to the low seismicity, as assumed in Chapter 1; the lack of fractures in the host rock at the repository site, which is consistent with Chapter 2; and the tolerance of the design to some extent of shearing.
8. The expected rates of land uplift, subsidence and erosion at the repository site should not adversely impact the containment and isolation of the repository.	Ice sheet erosion removes a significant thickness of rock above repository (FEPs 1.2.07, 1.3.01, 1.3.02, and 1.3.05).	**Yes,** the impact of realistic rates of glacial erosion is addressed as part of the Normal Evolution Scenario; whereas, severe erosion is considered as a disruptive event scenario.
	Land uplift decreases depth of repository.	**No,** land uplift occurs on a continental scale so relative depth of repository does not change. Land uplift and large-scale erosion are also not significant factors in affecting repository depth on assessment time scale.

Safety Feature	Potentially Compromised by	Consider as Failure Mechanism
9. The repository should not be located within rock formations containing economically exploitable natural resources such as minerals and other valuable commodities as known today. 10. The repository is not located within geological formations containing groundwater resources at repository depth that could be used for drinking, agriculture or industrial uses.	Mining and other underground activities resulting in excavation in the vicinity of the repository (FEP 1.4.05).	**No,** due to the assumption of the absence of commercially viable resources near or below repository level. Other underground activities are unlikely to affect the repository (e.g., rock quarry) because of repository depth (~500 m). Also, such activities would likely be preceded by exploration boreholes, as addressed above. Even if the host rock itself became commercially viable, the repository site is unlikely to become a mine site because of the uniformity and large lateral extent of the host rock that extends to shallower depths elsewhere.
	Deliberate human intrusion into repository (FEP 1.4.02).	**No,** exclude deliberate human intrusion since it is expected that the intruders would take appropriate precaution.
	Could discover resources that were not identified during site investigations (FEP 1.1.01) or exploit existing rocks that have become a commercially viable resource. These new resources are exploited by drilling or mining at or below repository level (FEP 1.4.04 and FEP 1.4.05).	**No,** the lack of resources at the site is assumed to be consistent with regional information. Even if the host rock itself became commercially viable, the repository site is unlikely to become a mine site because of the uniformity and large lateral extent of the host rock that extends to shallower depths elsewhere. Also, the impact of drilling is already considered under exploration borehole (FEP 1.4.04).

Safety Feature	Potentially Compromised by	Consider as Failure Mechanism
11. The used nuclear fuel is a durable uranium oxide (UO_2); it will dissolve very slowly under the chemical conditions within a failed container. 12. Most of the initial radioactivity is held within the UO_2 grains, where it can only be released as the used fuel dissolves.	Infiltration of oxygenated glacial meltwater into the repository leads to oxidizing conditions in the repository, causing relatively rapid corrosion of copper containers, rapid corrosion of used fuel in any defective containers, and enhanced mobility of redox sensitive nuclides such as U and Tc.	**No,** glacial recharge penetrating below the shallow groundwater system (i.e., depths greater than 215 m) is not expected to be oxygenated or influence the redox conditions at the repository horizon (see Chapter 2).
13. The used fuel container has a design life of at least 100,000 years under the geomechanical and chemical repository conditions expected to exist within the repository.	Poor manufacturing techniques or unanticipated material problems / interactions impact on the durability of the used fuel containers (FEP 1.1.03, 1.1.07) significantly reducing the expected lifetime of some containers.	**Yes,** although application of NWMO's quality control will make it very likely that poorly manufactured containers would be discovered and not used.
	Used fuel containers fail due to increase in the isostatic load caused by a thick ice sheet passing over the repository site.	**Yes,** although the containers are designed to withstand the isostatic load from buffer swelling, hydrostatic load and a 3 km thick ice sheet over the repository site, the possibility that the design load of the container could be exceeded due to the passage of a thicker ice sheet needs to be considered. Also, given the uncertainty regarding the long-term creep behaviour of copper, container failures could occur due to this mechanism.
	Infiltration of oxygenated glacial meltwater into the repository leads to oxidizing conditions in the repository, leading to relatively rapid corrosion of the copper containers (FEP 1.3.05).	**No,** glacial recharge penetrating below the shallow groundwater system (i.e., depths greater than 215 m) is not expected to be oxygenated or influence the redox conditions at the repository horizon (see Chapter 2).

Safety Feature	Potentially Compromised by	Consider as Failure Mechanism
14. The container is surrounded by a layer (approximately 60 cm) of dense bentonite-based clay that inhibits groundwater movement, has self-sealing capability, inhibits microbial activity near the container, and retards contaminant transport.	Bentonite buffer layer not properly installed and, therefore, the density of the buffer around the container is lower than design requirement.	**Yes,** although application of NWMO's quality control will ensure that poor sealing is very unlikely.
	Infiltration of glacial meltwater (without oxygen) into the repository modifies the hydrogeochemical conditions in the repository, affecting, for example, the stability of the buffer and backfill materials (i.e., leads to erosion of these materials due to colloid formation) (FEP 1.3.05).	**No,** the paleohydrogeologic simulations described in Chapter 2 suggest that glacial meltwaters will not reach the repository horizon. This is due to the low hydraulic conductivity of the overlaying shales, dolostones and Salina Group evaporites.
	A large seismic event causes rock shear along an undetected fracture intersecting the repository at a container location, reducing the buffer thickness between the container surface and the rock.	**Yes,** the assessment time scales are such that a significant seismic event may occur even though the annual probability is low. Even then, the probability that the earthquake could actually reactivate a nearby fracture is very small since it would take a significant amount of energy.
15. Institutional Controls will limit the potential for human encounter with the repository in the near term after closure	Institutional controls on the development of the site are ineffective (FEP 1.4.08). This allows development of the site (FEP 1.4.06) and human intrusion into the repository to occur by drilling (FEP 1.4.04) and / or mining (FEP 1.4.05)	**No,** Measures are assumed to be taken in the near term to ensure that information regarding the purpose, location, design and contents of the repository is preserved so that future generations are made aware of the consequences of any actions they may choose to take. With these institutional measures as well as general societal memory, and with the absence of commercially viable natural resources at depth, inadvertent intrusion in the near term after closure is not considered. However, Human Intrusion is considered in the long-term.

Table 6-4: Internal FEPs Potentially Compromising Arguments Relating to Long-Term Safety*

Safety Feature	Potentially Compromised By	Consider as Failure Mechanism
1. The depth of the host rock formation should be sufficient for isolating the repository from surface disturbances and changes caused by human activities and natural events.	No Internal FEP could result in a significant change in the depth of the repository. Note that FEP 5.1.10 relates to the erosion of surficial deposits and not bedrock.	**No.**
2. The volume of available competent rock at repository depth should be sufficient to host the repository and provide sufficient distance from active geological features such as zones of deformation or faults and unfavourable heterogeneities.	An undetected feature (e.g., a fracture zone) in the geosphere provides a relatively high permeability connection between the repository horizon and higher horizons (FEP 4.1.02 and FEP 4.1.03)	**Yes,** a nearby fracture zone or other feature could be missed during site investigation due to the limits of current technologies to identify such features.
3. The hydrogeological regime within the host rock should exhibit low groundwater velocities.	An undetected feature (e.g., a fracture) in the geosphere provides a relatively high permeability connection n between the repository horizon and higher horizons (FEP 4.1.02 and FEP 4.1.03)	**Yes,** a nearby fracture zone or other feature could be missed due to the limits of current technologies to identify such features.
	The failure of most of the containers in the repository, due to an unexpected mechanism, leads to generation of a significant amount of hydrogen gas due to corrosion of the iron inner vessel. The hydrogen pressure could, in theory, exceed the lithostatic pressure leading to rock fracture.	**Yes,** mechanisms have been identified by which most of the containers in the repository fail (see Table 6-3). For such a scenario, it will be necessary to determine the magnitude of the peak hydrogen pressure and its impact on the repository and host rock.

Safety Feature	Potentially Compromised By	Consider as Failure Mechanism
4. The mineralogy of the rock, the geochemical composition of the groundwater and rock porewater at repository depth should not adversely impact the expected performance of the repository multi-barrier system. 5. The mineralogy of the host rock, the geochemical composition of the groundwater and rock porewater should be favourable to retarding radionuclide movement.	Various repository FEPs (e.g., FEPs 3.1.02, 3.2.01 to 3.2.05), such as temperature rise in the repository, groundwater salinity and groundwater-buffer interactions, and geosphere FEPs (e.g., FEPs 4.2.01 to 4.2.05), such as geothermal gradient and karst formation, have the potential to modify the hydrological, mechanical and chemical conditions at repository depth, affecting seal properties and / or radionuclide movement.	**No,** the effects are likely to be localized to the immediate vicinity of the repository and these FEPs can be evaluated through considering different calculation cases for the Normal Evolution Scenario (e.g., no sorption and no solubility sensitivity cases) rather than through the development of alternative Disruptive Scenarios. For conservatism, concrete seals are assumed degraded from the time of repository closure.
	Various waste package FEPs (e.g., FEPs 2.3.01 to 2.3.04) can influence the durability of the used fuel containers, potentially leading to container failures.	**Yes,** poor local conditions (e.g., low buffer density) might cause a limited number of container failures due to, for example, biofilm formation on the copper surface. Note that the Normal Evolution Scenario already includes a number of containers with pre-existing defects (e.g., welding defects) which lead to early container failures.
	Various repository FEPs (e.g., FEPs 3.2.01 to 3.2.05), such as temperature rise and groundwater interactions, and geosphere FEPs (e.g., FEPs 4.3.01 to 4.3.08), such as sorption and diffusion, can affect the rate at which contaminants are released from the repository and migrate through the shafts and geosphere.	**No,** the effects of these FEPs can be evaluated through considering different calculation cases for the Normal Evolution Scenario rather than through the development of alternative Disruptive Scenarios (e.g., no sorption and no solubility sensitivity cases). The repository and shaft excavation damaged zones are considered in the Normal Evolution Scenario. Also, concrete seals are assumed degraded from the time of repository closure.

Safety Feature	Potentially Compromised By	Consider as Failure Mechanism
	Changes in porewater chemistry in the repository due to, for example, temperature rise in the repository and presence of concrete adversely affects clay seals (FEP 3.1.02 and FEP 3.2.04).	**No,** use of low-temperature, low pH concrete in the repository minimizes interactions with clay seals. Also, the amount of concrete in the repository is small compared to the amount of clay sealing materials. Note that the Normal Evolution Scenario already includes a number of containers with pre-existing defects (e.g., welding defects) which lead to early container failures.
6. The host rock should be capable of withstanding mechanical and thermal stresses induced by the repository without significant structural deformation or fracturing that could compromise the containment and isolation functions of the repository.	Mechanical and thermal stresses induced by presence of repository are underestimated and cause greater than expected fracturing within the repository, the host rock and shaft excavation damaged zones, providing an enhanced permeability pathway to the surface environment (e.g., FEP 3.2.01 and FEP 3.2.03).	**Yes,** although application of NWMO's quality control will ensure that stresses are not underestimated and engineering calculations include safety factors.
7. Current and future seismic activity at the repository site should not adversely impact the integrity of the repository during operation and in the very long-term.	Relates to External FEPs only (see Table 6-3).	
8. The expected rates of land uplift, subsidence and erosion at the repository site should not adversely impact the containment and isolation of the repository.	Relates to External FEPs only (see Table 6-3).	

Safety Feature	Potentially Compromised By	Consider as Failure Mechanism
9. The repository should not be located within rock formations containing economically exploitable natural resources such as minerals and other valuable commodities as known today. 10. The repository is not located within geological formations containing groundwater resources at repository depth that could be used for drinking, agriculture or industrial uses.	Relates to External FEPs only (see Table 6-3).	
11. The used nuclear fuel is a durable uranium oxide (UO_2); it will dissolve very slowly under the chemical conditions within a failed container.	Various waste package FEPs (e.g., FEP 2.1.02, and FEP 2.2), such as radiation and temperature effects, and rates of used fuel dissolution in groundwater, can affect the rate at which contaminants are released from the used fuel.	**No,** the effects of these FEPs can be evaluated through considering different calculation cases for the Normal Evolution Scenario rather than through the development of alternative Disruptive Scenarios (e.g., sensitivity cases with a faster fuel dissolution rate or larger instant release fractions).
12. Most of the initial radioactivity is held within the UO_2 grains, where it can only be released as the used fuel dissolves.	Release due to criticality accident.	**No**, the used fuel is natural uranium based. . The fissile content of the used fuel is too low.

Safety Feature	Potentially Compromised By	Consider as Failure Mechanism
13. The used fuel container has a design life of at least 100,000 years under the geomechanical and chemical repository conditions expected to exist within the repository.	Containers are not fabricated to specifications and so are placed in the repository with defects (FEPs 2.3.01 to 2.3.04).	**Yes**, although the fabrication method is designed to be robust, and there would be multiple methods of inspection, there is statistically some probability of initial defects not being detected such that a few containers are placed with initial defects. The Normal Evolution Scenario assumes some containers with undetected defects are present in the repository at the time of closure, leading to early container failures.
	Various waste package and repository FEPs (e.g., FEPs 2.3.03, 2.3.04, 3.1.02, 3.2.01 to 3.2.05), such as uniform corrosion, buffer properties, temperature, and groundwater chemistry, can influence the durability of the used fuel containers, potentially leading to container failures.	**Yes,** although evidence suggests that the copper container would be thermodynamically stable under the reducing conditions expected in the repository, poor local conditions might cause a limited number of container failures. The Normal Evolution Scenario assumes some containers with undetected defects are present in the repository at the time of closure, leading to early container failures.
14. The container is surrounded by a layer (approximately 60 cm) of dense bentonite-based clay that inhibits groundwater movement, has self-sealing capability, inhibits microbial activity near the container, and retards contaminant transport.	Various repository FEPs (e.g., FEPs 3.1.02, 3.2.01 to 3.2.05), buffer properties, temperature, and groundwater chemistry, can influence the durability of the used fuel containers, potentially leading to container failures.	**Yes,** although evidence suggests that the copper container would be thermodynamically stable under the reducing conditions expected in the repository, poor local conditions might cause a limited number of container failures. The Normal Evolution Scenario assumes some containers with undetected defects are present in the repository at the time of closure, leading to early container failures.

Safety Feature	Potentially Compromised By	Consider as Failure Mechanism
	Various repository FEPs (e.g., FEPs 3.1.02, 3.1.03, 3.2.01 to 3.2.05), such as temperature, hydrothermal alteration of the buffer, and buffer-groundwater interactions, have the potential to modify the hydrological, mechanical and chemical conditions at the repository depth, affecting properties of clay-based materials.	**No,** the effects are likely to be localized to the immediate vicinity of the repository (particularly near the container surface) and these FEPs can be evaluated through considering different calculation cases for the Normal Evolution Scenario (i.e., no sorption and no solubility sensitivity cases) rather than through the development of alternative Disruptive Scenarios.
15. Institutional Controls will limit the potential for human encounter with the repository in the near term after closure	Affected by External FEPs relating to Future Human Actions (see Table 6-3) rather than the Internal FEPs relating to human behaviour that responds to the Future Human Actions.	

Note: * - the Internal FEPs are shown in Garisto (2013).

Table 6-5: Potential Failure Mechanisms and Associated Scenarios

Failure Mechanism	Associated Disruptive Scenario
Exploration borehole penetrates into the repository providing an enhanced permeability pathway to the surface environment and potential for direct exposure to waste	Human Intrusion
Poor construction techniques lead to a large excavation damaged zone around shaft seals, which provides an enhanced permeability pathway to the surface environment	Shaft Seal Failure
Repository and shafts are not properly sealed at the time of closure, providing an enhanced permeability pathway to the surface environment	Shaft Seal Failure
Long-term performance of shaft seals and excavation damaged zone deviates from that expected, due to some unexpected internal processes, resulting in an enhanced permeability pathway to the surface environment	Shaft Seal Failure
Site investigation / monitoring borehole is poorly sealed at time of closure providing an enhanced permeability pathway to the surface environment	Poorly Sealed Borehole
Long-term performance of site investigation / monitoring borehole seal deviates from that expected, due to some unexpected internal processes, resulting in an enhanced permeability pathway to the surface environment	Poorly Sealed Borehole
The repository is not closed as planned after the monitoring period and tunnels and shafts remain open.	Abandoned Repository
Site investigations do not identify a relatively high permeability fracture zone or fault that provides a connection between the repository horizon and higher horizons	Undetected Fault
Seismic event results in reactivation of an existing fracture zone and / or failure of shaft seals that provides an enhanced permeability pathway to higher horizons	Undetected Fault and Shaft Seal Failure
Glacial erosion is much more extensive than expected at the repository site over a one million year period.	Severe Erosion
Seismic event results in shearing along an existing fracture zone passing through a placement room, resulting in failure of some container(s) due to the shear load.	Container Failure
Manufacturing defect in steel vessel or unexpected high local loads lead to mechanical failure of some containers.	Container Failure
Unexpected corrosion of some copper containers due to, for example, initial defects in the copper shell, or unanticipated interaction of the copper container with groundwater in the repository.	Container Failure
Unexpected poor mechanical or chemical performance of the copper shell under repository conditions leads to failure of a significant number of containers in the repository.	All Containers Fail
Passage of thicker than expected ice sheet over repository site causes isostatic load on all containers to exceed design load of containers, resulting in failure of all containers.	All Containers Fail

The repository siting process will ensure that there are no known commercially viable natural resources near or below repository depth. Also, the repository has a relatively small footprint (~6 km^2) and the repository is at a depth of around 500 m. These factors limit the range of human activities that could directly affect the closed repository to a borehole unintentionally drilled into the repository as part of a future geological exploration program[2]. Even this situation has a low probability of occurrence. Nevertheless, once controls on the use of the site are no longer effective, the possibility of inadvertent human intrusion by this method cannot be ruled out over long time scales[3]. Such a borehole could provide an enhanced permeability pathway to the surface environment and potential for direct exposure to waste. This scenario is referred to as the **Human Intrusion Scenario**.

A second scenario by which the geosphere barrier can be bypassed is via the shafts (main, service and ventilation shafts). These are ~8 m diameter holes that penetrate the geosphere, but are placed away from the waste panels and carefully sealed in the design. The **Shaft Seal Failure Scenario** considers the possibility that the shaft seals are not fabricated or installed appropriately, or that the long-term performance of the shaft seals and shaft / repository Excavation Damaged Zones (EDZs) is poor due to unexpected physical, chemical and / or biological processes, or the shaft seals are damaged by a seismic event. While these situations could result in an enhanced permeability pathway to the surface, they are very unlikely due to quality control measures that will be applied during shaft seal closure and due to multiple durable material layers in the shaft.

In the Shaft Seal Failure Scenario, it is assumed that the other repository engineered barriers (i.e., the tunnel and room seals, and the backfill and buffer), are not degraded relative to their design properties except for the concrete component of the seals, for which degraded properties are used throughout the simulations, as in the Normal Evolution Scenario.

The geosphere barrier is also bypassed via the shafts in the “what-if” **Abandoned Repository Scenario** in which the repository is assumed not to be sealed following the monitoring period (i.e., after all containers are deposited and placement rooms are sealed), and therefore both the access tunnels and shafts remain open but not maintained at least for an extended period. Since closing the repository is clearly important and funds would have been set aside for this purpose, this scenario would require a societal collapse or abandonment of the site for other unknown reasons. The likelihood of such a scenario is unknown but is probably low.

Another way in which the geosphere barrier can be bypassed is through the site characterization / monitoring boreholes. These boreholes are located in the vicinity of the repository down to and below repository depth. These boreholes will be appropriately sealed on completion of site investigation / monitoring activities so they will have no effect on repository performance. However, if a deep borehole were not properly sealed or were to extensively degrade, then it could provide a small but relatively permeable pathway for the migration of contaminants from the repository horizon. The scenario is termed the **Poorly Sealed Borehole**

[2] The assessment excludes deliberate human intrusion since it is expected that the intruders would take appropriate precaution.

[3] The repository might appear as an anomaly in a surface / air-borne survey of the area, and this could encourage drilling at the site if all records had been lost. However, the absence of interesting minerals or geologic features in the area would argue against deliberate surveys of the area. Furthermore, a cautious approach to drilling might be used if such unexpected anomalies were identified that would minimize the consequences of any intrusion into the repository.

Scenario. Like the Shaft Seal Failure Scenario, such a situation is very unlikely due to the adoption of good engineering practice and quality control.

For the Normal Evolution Scenario, it is assumed that site investigation and geosynthesis would detect the occurrence of transmissive vertical faults / fracture zones which could provide an enhanced permeability pathway from the repository horizon to the overlying aquifer within the footprint or vicinity of the repository. However, it is possible that site characterization does not identify all existing significant fractures at the site and, therefore, a "what-if" scenario is defined to investigate the safety implications of a hypothetical transmissive fault that is either undetected or formed by the displacement of an existing structural discontinuity. The hypothetical fault is assumed to be in close proximity to the repository and to extend from below the repository level to the shallow groundwater system. This scenario is termed the **Undetected Fault Scenario**.

Glacial erosion is considered in the Normal Evolution Scenario. At this hypothetical site, a realistic amount of glacial erosion over a one million year time frame is considered as part of the Normal Evolution Scenario. However, a more severe glacial erosion rate is assessed in the **Severe Erosion Scenario**. Such a scenario is considered highly unlikely because of the absence of topographic features or other known factors that would tend to localize erosion by ice or water in the Michigan Basin (Hallet 2011). Furthermore, future glaciations would tend to repeat the actions of their predecessors, by funneling into lake basins and deepening them, and maintaining the topographic highs where the ice flow velocities and erosion rates are relatively low and where sediments tend to accumulate.

While the copper used fuel containers have a design requirement for a minimum functional life of not less than 100,000 years, they are expected to last much longer based on thermodynamic, experimental and natural analogue evidence that copper is stable for very long periods under deep geological repository conditions. Nevertheless, there are several mechanisms by which the containers could fail some time after they are installed in the repository. These container failures would be more severe than the small defects considered in the Normal Evolution Scenario (which could arise be due to, for example, undetected welding defects.) Possible failure mechanisms include the following:

- After the repository attains reducing conditions, the copper containers should be immune to further corrosion. However, unexpected interactions between the groundwater and copper container (e.g., due to higher than expected sulphide concentrations) could damage the copper container sufficiently over the time frame of interest that the steel vessel would be exposed to water, leading to weakening of the vessel due to corrosion and / or seepage of water into the container.
- A container could be damaged by a sufficiently large shear load. A large seismic event that causes the rock to slip along an undetected fracture zone intersecting a placement room could produce such a shear load. The probability of such an event depends on the likelihood of an earthquake of a sufficient magnitude, the likelihood that a placement room is intersected by a fracture zone and that a container is near the fracture zone and, finally, how the shear load is transmitted through the buffer material, which depends on the buffer thickness and density. The analysis in SKB (2011) indicates that, for their repository, less than 0.2 containers would fail due to shear load over one-million years.

The specific failure mode is not defined here, but the consequences are evaluated in the **Container Failure Scenario**. The key characteristics of this scenario are that only a few containers are affected, that the container damage is significant, but also that the failure occurs at least 10,000 years and possibly 60,000 years after closure.

The containers are designed to be corrosion resistant and to be robust. As noted in Chapter 4, the inner steel vessel is designed to sustain an external isostatic load of 45 MPa, (i.e., the maximum load experienced by the container during passage of a 3 km thick ice sheet above the repository site). Thus, the containers are expected to have a long lifetime. However, it is possible that some unexpected event or process may occur in the future such that there are multiple container failures in the repository. For example, the copper shell of the container could fail at long times due to creep deformation. Also, the design load of the container could be exceeded if, for example, the thickness of the ice sheet passing over the repository is greater than the design basis ice sheet.

Consequently, an **All Containers Fail Scenario** is considered in which all the containers in the repository fail at 60,000 years (i.e., there are no initially defected containers), the time of the assumed first passage of an ice sheet over the site (see Chapter 2). The probability of such a scenario is likely low since, for example, the ice sheet would have to be substantially thicker than 3 km for the load exerted on the container to exceed 45 MPa, given the low buffer swelling pressure. Further, the creep behaviour of copper under repository conditions is an open issue.

Other potential Disruptive Scenarios were considered but ruled out on various grounds as discussed further in the FEPs report (Garisto 2013). No volcanic activity is anticipated in the area over the next one million years. The probability of being hit by a large meteor capable of damaging the repository is remote and the consequences of the impact itself would likely be more significant than those from the repository. Seismic activity is possible, and likely earthquakes are included in the Normal Evolution Scenario. Such seismic activity will not cause rockfall because the repository is backfilled. Large earthquakes are unlikely since it is assumed that the hypothetical site is located in a low-seismicity area. The main effects on the repository are represented by the Shaft Seal Failure, the Undetected Fault and the Container Failure Scenarios, so there is no need to consider an additional earthquake scenario. Glaciation, which could affect the repository system, is considered within the Normal Evolution Scenario.

Further confidence that an appropriate set of Disruptive Scenarios has been identified can be obtained by examining the scenarios (or sensitivity cases) considered in the postclosure safety assessments of deep repositories in other countries. The results of such an examination, summarized in Table 6-6, show that most assessments have identified a limited number of additional scenarios that consider the degradation / failure of engineered and natural barriers by natural processes (e.g., earthquakes, climate change) and human actions (e.g., drilling, poor quality control). Although there are some scenarios that are not considered in the current study, these are either not relevant for the hypothetical site (e.g., volcanic activity, sea-level rise, mining of resources) or have been included in the Normal Evolution Scenario (e.g., climate change, container failure).

Table 6-6: Additional Scenarios Considered in Other Safety Assessments

Assessment	Reference	Additional Scenarios Considered
SR-Site (Sweden)	SKB (2011)	• Canister failure due to corrosion or shear load • Disrupted buffer (due to erosion, advection) • Extended greenhouse effects • Exploratory drilling • Rock facility (e.g., quarry) • Incompletely sealed (or abandoned) repository
Olkiluoto (Finland)	POSIVA (2012)	• Defective canister (early and delayed penetration) • Earthquake/rock shear • Disrupted buffer • Exploratory drilling
Dossier Argile (France)	ANDRA (2005)	• Seal failure and defective plug • Defective waste and spent fuel containers • Borehole penetrating repository • Functioning of repository greatly degraded
H12 (Japan)[1]	JNC (2000)	• Climate and sea-level change • Exploitation drilling (water well) • Engineering defects, including poorly sealed repository
Opalinus (Switzerland)	NAGRA (2002)	• Gas pathways • Exploratory drilling • Poorly sealed repository
GPA (UK)	NIREX (2003)	• Exploratory drilling
WIPP (USA)	DOE (2004)	• Mining • Exploratory drilling
Yucca Mountain (USA)[2]	DOE (2002)	• Exploratory drilling • Seismicity • Volcanic event
SAFIR 2 (Belgium)	ONDRAF/NIRAS (2001)	• Exploratory drilling • Greenhouse effect • Poor sealing of repository • Fault activation • Severe glacial period • Failure of engineered barriers • Gas-driven transport

Notes:

[1] Isolation Failure Scenarios that involve penetration of the repository (including magma intrusion, human intrusion and meteorite impact) were also considered but screened out on the grounds that they are extremely unlikely to occur. Some 'what if' calculations were carried out instead.

[2] The term 'scenario' is used in a way that differs from the other assessments reviewed. Three Thermal Load Scenarios are discussed that are design variants, while two No-action Scenarios refer to futures in which the Yucca Mountain facility does not go ahead.

6.2.2 Description of Disruptive Event Scenarios

The identified Disruptive Event Scenarios are described below. These scenarios are evaluated separately rather than in combination since they have low probability and independent causes, and so the likelihood of simultaneous occurrence is even lower.

6.2.2.1 Inadvertent Human Intrusion Scenario

The Inadvertent Human Intrusion Scenario considers the impact of human intrusion sometime in the future. In this scenario, an exploration borehole is drilled through the geosphere and into the repository with the drill bit intersecting a used fuel container.

It is assumed that the drill crew is unaware of the facility (i.e., the intrusion occurs after institutional controls are no longer effective and societal memory of the site is lost). The investigators will most likely collect samples or conduct measurements at the repository level, due to the unusual nature of the materials. This would identify significant residual radioactivity (e.g., gamma logging is a standard borehole measurement) and the investigators would likely take precautions to prevent further exposure, including appropriate management of any materials released at the surface and sealing of the borehole. Therefore, under normal drilling, there would be little impact after the initial drill crew exposure.

Nevertheless, the Inadvertent Human Intrusion Scenario assumes:

- It is not recognized that the drill has intercepted a waste repository so no safety restrictions are applied; and
- The borehole and drill site are not managed and closed to current standards, and material from the borehole is released onto the surface around the drill site.

Contaminants can be released and humans and biota exposed via:

- Retrieval and examination of drill core contaminated with waste; and
- Uncontrolled dispersal of contaminated drill core debris on the site.

This could result in the exposure of the drill crew or other people at the time of intrusion, and people who might occupy the site subsequent to the intrusion event.

If the borehole is not properly sealed, it could provide an enhanced permeability pathway to the surface environment or even be used as a well by a future site resident. The impact of this open borehole on the future residents of the site is examined as part of the Inadvertent Human Intrusion Scenario.

6.2.2.2 Shaft Seal Failure Scenario

The shafts represent a potentially important pathway for contaminant release and therefore the repository design includes specific measures to provide good shaft seals, taking into account the characteristics of the geosphere. The Shaft Seal Failure Scenario considers the consequences of rapid and extensive shaft seal degradation. This scenario, like the other Disruptive Event Scenarios, is a bounding scenario designed to investigate the robustness of the repository system.

The groundwater transport exposure pathways are the same as those considered in the Normal Evolution Scenario.

6.2.2.3 Abandoned Repository Scenario

Another scenario by which the geosphere barrier can be bypassed via the shafts is the “what-if” Abandoned Repository Scenario. The basic assumption in the Abandoned Repository Scenario is that the repository is abandoned during the monitoring phase (i.e., after all containers are placed in the repository and all placement rooms are backfilled and sealed), but the main access tunnels and the shafts are still open. This is consistent with normal operations, in which the placement rooms are successively filled with containers and backfilled, and sealed as soon as they are filled.

Abandonment of the repository would require a significant societal breakdown because of the known importance of properly closing the repository.

The groundwater transport exposure pathways are the same as those considered in the Normal Evolution Scenario.

6.2.2.4 Poorly Sealed Borehole Scenario

Multiple deep site investigation / monitoring boreholes will be drilled in the vicinity of the repository during the site investigation phase. The Poorly Sealed Borehole Scenario considers the consequences of one of the boreholes not being properly sealed or having a seal that extensively degrades. The poorly sealed borehole provides an enhanced permeability connection between the level of the repository, the overlying groundwater zones and the biosphere, thereby bypassing some of the natural geological barriers to contaminant migration from the repository. The exposure pathways are the same as those considered in the Normal Evolution Scenario.

6.2.2.5 Undetected Fault Scenario

The Undetected Fault Scenario considers the impact of an undetected or new transmissive fault extending from around the repository level into the shallow groundwater system in close proximity to the repository. Such a fault could provide an enhanced permeability pathway that bypasses the deep groundwater system.

The groundwater transport exposure pathways are the same as those considered in the Normal Evolution Scenario.

6.2.2.6 Severe Erosion Scenario

The Severe Erosion Scenario considers the impact of severe glacial erosion on the performance of the used fuel repository.

The groundwater transport exposure pathways are the same as those considered in the Normal Evolution Scenario.

6.2.2.7 All Containers Fail Scenario

The long-lived used fuel containers are an important feature of the multi-barrier repository concept in this conceptual design. The copper containers are expected to last for a long time because copper is stable under anticipated conditions in a deep geological repository; however, the All Containers Fail Scenario considers the unlikely and hypothetical case in which all the containers simultaneously fail (i.e., water enters all containers and contacts the fuel) at 60,000 years. This timeframe corresponds to the approximate time scale for glacial cycles to resume and an ice sheet to first cover the site (see Chapter 2), which could be assumed to cause multiple container failures if the isostatic load on the containers is higher than expected. For simplicity, in this scenario, there are no initially defected containers as in the Normal Evolution Scenario

A variant case in which all containers are assumed to fail at 10,000 years is also investigated to determine the sensitivity to the assumed failure time.

The groundwater transport exposure pathways are the same as those considered in the Normal Evolution Scenario. However, the failure of all containers also leads to the generation of significant amounts of hydrogen gas due to corrosion of the inner steel vessel. Consequently, the impact of gas generation on the performance of the repository and the transport of contaminants is also addressed.

6.2.2.8 Container Failure

The Container Failure Scenario considers the impact of container failure due to several possible mechanisms.

- Corrosion of the container due to unexpected chemical interactions with the groundwater or installation of a defective (i.e., low density) buffer which allows formation of biofilms on the copper surface.
- A large seismic event (earthquake) in the vicinity of the repository that causes slip along a fracture zone that intersects a placement room. The rock slip along the fracture zone is assumed to be so large that it causes complete failure of a container. The shear is also assumed to significantly increase the transmissivity of the fracture. Although the shear movement should not affect the buffer properties, the amount of buffer between the container and the shearing fracture zone would likely be reduced.

The exposure pathways are the same as those considered in the Normal Evolution Scenario.

6.3 References for Chapter 6

ANDRA. 2005. Dossier 2005 Argile Tome Evaluation de Sûreté du Stockage Géologique. Paris, France.

CNSC. 2006. Regulatory Guide G-320: Assessing the Long Term Safety of Radioactive Waste Management. Canadian Nuclear Safety Commission. Ottawa, Canada.

DOE. 2002. Final Environmental Impact Statement for a Geologic Repository for the Disposal of Spent Nuclear Fuel and High-level Radioactive Waste at Yucca Mountain, Nye

County, Nevada. United States Department of Energy, Office of Civilian Radioactive Waste Management, DOE/EIS-0250. Nevada, USA.

DOE. 2004. 2004 WIPP Compliance Recertification Application (CRA) - Main Volume. US Department of Energy Report DOE/WIPP 04-3231. Available at: http://www.wipp.energy.gov/library/CRA/CRA_Index.htm. Accessed January 2011.

Garisto, F. 2013. Fifth Case Study: Features, Events and Processes. Nuclear Waste Management Organization Report NWMO TR-2013-06. Toronto, Canada.

Guo, R. 2010. Coupled Thermal-Mechanical Modelling of a Deep Geological Repository using the Horizontal Tunnel Placement Method in Sedimentary Rock using CODE_BRIGHT. Nuclear Waste Management Organization Technical Report NWMO TR-2010-22. Toronto, Canada.

Hallet, B. 2011. Glacial Erosion Assessment. Nuclear Waste Management Organization Report NWMO DGR-TR-2011-18 R000. Toronto, Canada.

IAEA. 2012. The Safety Case and Safety Assessment for the Disposal of Radioactive Waste. IAEA Safety Standards. Specific Safety Guide No. SSG-23. International Atomic Energy Agency. Vienna, Austria.

ICRP. 2000. Radiation Protection Recommendations as Applied to the Disposal of Long-lived Solid Radioactive Waste. International Commission on Radiological Protection Publication No. 81, Annals of the ICRP 28(4).

JNC. 2000. H12: Project to Establish the Scientific and Technical Basis for HLW in Japan. Japan Nuclear Cycle Development Institute Report JNC TN1410 2000-004. Tokai, Japan.

NAGRA. 2002. Project Opalinus Clay: Safety Report, Demonstration of the Disposal Feasibility for Spent Fuel, Vitrified HLW and Long-lived ILW. Nagra Technical Report 02-05. Wettingen, Switzerland.

NIREX. 2003. Generic Repository Studies: Generic Post-closure Performance Assessment. Nirex Report N/080. Harwell, United Kingdom.

ONDRAF/NIRAS. 2001. SAFIR 2: Safety Assessment and Feasibility Interim Report 2. ONDRAF/NIRAS Report NIROND 2001-06E. Brussels, Belgium.

Perry, C., C. Rosieanu, J.-C. Mareschal and C. Jaupart. 2010. Thermal Regime of the Lithosphere in the Canadian Shield, Canadian Journal of Earth Sciences 47, 389-408.

Peltier, W.R. 2011. Long-Term Climate Change. Nuclear Waste Management Organization Technical Report NWMO DGR-TR-2011-14 R000. Toronto, Canada.

POSIVA. 2012. Safety Case for the Disposal of Spent Nuclear Fuel at Olkiluoto – Synthesis 2012. Posiva Report 2012-12. Olkiluoto, Finland.

SKB. 2011. Long-term Safety for the Final Repository for Spent Nuclear Fuel at Forsmark, Main Report of the SR-Site Project. Swedish Nuclear Fuel and Waste Management Report SKB TR-11-01. Stockholm, Sweden.

Szakálos, P., G. Hultquist, and G. Wikmark. 2007. Corrosion of Copper by Water. Electrochemical and Solid-State Letters, 10, pp C63–C67.